Katedra vodního hospodářství a environmentálního modelování

Česká zemědělská univerzita v Praze
Fakulta životního prostředí

Vliv sněhové pokrývky na odtok během dešťových srážek

Effect of snowpack on runoff generation during rain on snow event

Disertační práce

Dissertation thesis

Ing. Roman Juras

školitel: doc. Ing. Petr Máca, Ph.D.

školitel specialista: Ing. Jiří Pavlásek, Ph.D.

Praha 2016

Prohlášení

Prohlašuji, že jsem předloženou dizertační práci vypracoval samostatně pod vedením doc. Ing. Petra Máci, Ph.D., a že jsem použil prameny, které jsou uvedeny v seznamu použité literatury.

V Praze, dne 20. 11. 2016

.....

Poděkování

Na tomto místě bych rád poděkoval školiteli Petrovi Mácovi. Především bych chtěl poděkovat Jiřímu Pavláskovi, bez kterého by tato práce nevznikla, a který mě inspiroval svými inovativními myšlenkami jak v teoretické rovině, tak při měření v terénu a připomínkami při psaní publikací. Dále bych velmi rád poděkoval Tobiasu Jonasovi, Sebastianu Würzerovi, Tomáši Vitvarovi a Martinu Šandovi za výbornou spolupráci při výzkumu a při psaní publikací. Velké díky patří také FŽP, DBU a SCIEX za finanční podporu při namáhavém výzkumu.

Na závěr bych také rád poděkoval své manželce Vladimíře Jurasové za její morální podporu v průběhu celého studia.

Obsah

Souhrn

V zimním období, kdy leží na povodí sněhová pokrývka, stále přibývá výskytu dešťových srážek. Déšť dopadající na sníh (ROS) má často za následek vznik povodní a mokrých lavin. Predikce vlivu ROS záleží především na lepším pochopení mechanismů vzniku a složení odtoku ze sněhové pokrývky. Spojení simulace deště na sněhovou pokrývku a využití stopovačů bylo testováno jako vhodný nástroj pro tento účel. Celkem bylo provedeno 18 experimentů na sněhovou pokrývku s různými počátečními vlastnostmi v horských podmínkách střední a západní Evropy.

Pro určení charakteru proudění bylo použito barvivo brilliant blue (FCF), pomocí kterého je možné vizualizovat preferenční cesty, ale i určit rozhraní dvou vrstev o různých hydraulických vlastnostech. Zastoupení jednotlivých složek odtékající vody na výtoku bylo stanoveno pomocí metody separace hydrogramu, která poskytuje dobré výsledky s přijatelnou nejistotou. Z technických důvodů nebylo možné obě metody použít současně během jednoho experimentu, i když by to ještě více rozšířilo znalosti o dynamice proudění dešťové vody ve sněhové pokrývce. Množství tavné vody bylo vypočteno pomocí rovnice energetické bilance. Použití této rovnice je poměrně přesné, ale zároveň náročné na vstupy. Z toho důvodu bylo tání vypočteno pouze u jednoho experimentu.

Rychlost vzniku odtoku roste v první řadě intenzitou srážky. Počáteční vlastnosti sněhové pokrývky, jako hustota a vlhkost, ovlivňují rychlost vzniku odtoku až druhotně. Na druhou stranu při stejné intenzitě srážky vykazovala nevyzrálá sněhová pokrývka s malou hustotou rychlejší hydrologickou odpověď, než vyzrálá pokrývka s větší hustotou. Velikost odtoku je závislá, především na počátečním nasycení. Vyzrálá sněhová pokrývka s vyšším počátečním nasycením generovala vyšší celkový odtok, kde dešťová voda přispívala maximálně z 50ti %. Proti tomu protekla dešťová voda nevyzrálou sněhovou pokrývkou poměrně rychle a do odtoku se propagovala přibližně z 80ti %.

Pro predikci odtoku během ROS byla použita Richardsova rovnice v rámci modelu SNOWPACK. Tento model byl upraven tak, že byla sněhová matrice rozdělena pro lepší simulaci preferenčního proudění. Tento přístup přinesl zlepšení výsledků oproti klasickému přístupu, kdy se uvažuje pouze matricové proudění.

Summary

During a winter season, when snow covers the watershed, the frequency of rain-on-snow (ROS) events is still raising. ROS can cause severe natural hazards like floods or wet avalanches. Prediction of ROS effects is linked to better understanding of snowpack runoff dynamics and its composition. Deploying rainfall simulation together with hydrological tracers was tested as a convenient tool for this purpose. Overall 18 sprinkling experiments were conducted on snow featuring different initial conditions in mountainous regions over middle and Western Europe.

Dye tracer brilliant blue (FCF) was used for flow regime determination, because it enables to visualise preferential paths and layers interface. Snowpack runoff composition was assessed by hydrograph separation method, which provided appropriate results with acceptable uncertainty. It was not possible to use concurrently these two techniques because of technical reasons, however it would extend our gained knowledge. Snowmelt water amount in the snowpack runoff was estimated by energy balance (EB) equation, which is very efficient but quality inputs demanding. This was also the reason, why EB was deployed within only single experiment.

Timing of snowpack runoff onset decrease mainly with the rain intensity. Initial snowpack properties like bulk density or wetness are less important for time of runoff generation compared to the rain intensity. On the other het when same rain intensity was applied, non-ripe snowpack featuring less bulk density created runoff faster than the ripe snowpack featuring higher bulk density. Snowpack runoff magnitude mainly depends on the snowpack initial saturation. Ripe snowpack with higher saturation enabled to generate higher cumulative runoff where contributed by max 50 %. In contrary, rainwater travelled through the non-ripe snowpack relatively fast and contributed runoff by approx. 80 %.

Runoff prediction was tested by deploying Richard's equation included in SNOWPACK model. The model was modified using a dual-domain approach to better simulate snowpack runoff under preferential flow conditions. Presented approach demonstrated an improvement in all simulated aspects compared to the more traditional method when only matrix flow is considered.

1. Úvod

Sněhová pokrývka představuje zásobu vody v pevném skupenství na povodí. Z hydrologického hlediska její důležitost roste především v období tání, kdy se pevná forma začne měnit na kapalnou vodu. Pro hydrology je tedy velmi zásadní informace kolik vody po roztání sněhové pokrývky můžeme očekávat ve vodních tocích. Rychlé tání sněhové pokrývky však může představovat nebezpečí v podobě nadlimitních průtoků až povodní.

Specifickou roli hraje sněhové pokrývka v případě, když se setká s kapalnou srážkou ve formě deště. Tuto srážku následně transformuje do odtoku. Transformace dešťové srážky může probíhat dvěma způsoby (Obr. 1). V prvním případě plní sněhová pokrývka ochrannou retenční funkci, kdy část srážky v sobě na určitou dobu zadrží a odtok je malý nebo nemusí nastat vůbec. V druhém případě může být odtok ještě zvýšen, protože dešťová voda proteče a celkový odtok je navýšen o množství vody z tání. Přítomnost dešťové vody ve sněhové pokrývce může celkové tání ještě urychlit a tím ještě zvýšit celkový odtok z pokrývky a potenciální riziko povodní.

Odpověď na otázku, zda se sněhová pokrývka bude chovat prvním nebo druhým způsobem není jednoduchá. Pro určení chování kapalné vody ve sněhové pokrývce jsou klíčové především její fyzikální vlastnosti. V poslední době je věnována velká pozornost povodním z tání sněhu v kombinaci s deštěm jak v Evropě, tak i ve světě. Možnosti předpovídání následků takových událostí jsou spojené především se znalostí chování dešťové vody ve sněhové pokrývce a dynamikou jejího odtoku, které jsou stále omezené. Tato disertační práce se proto snaží tuto problematiku více přiblížit pomocí několika experimentálních studií a využitím stávajících matematických modelů.

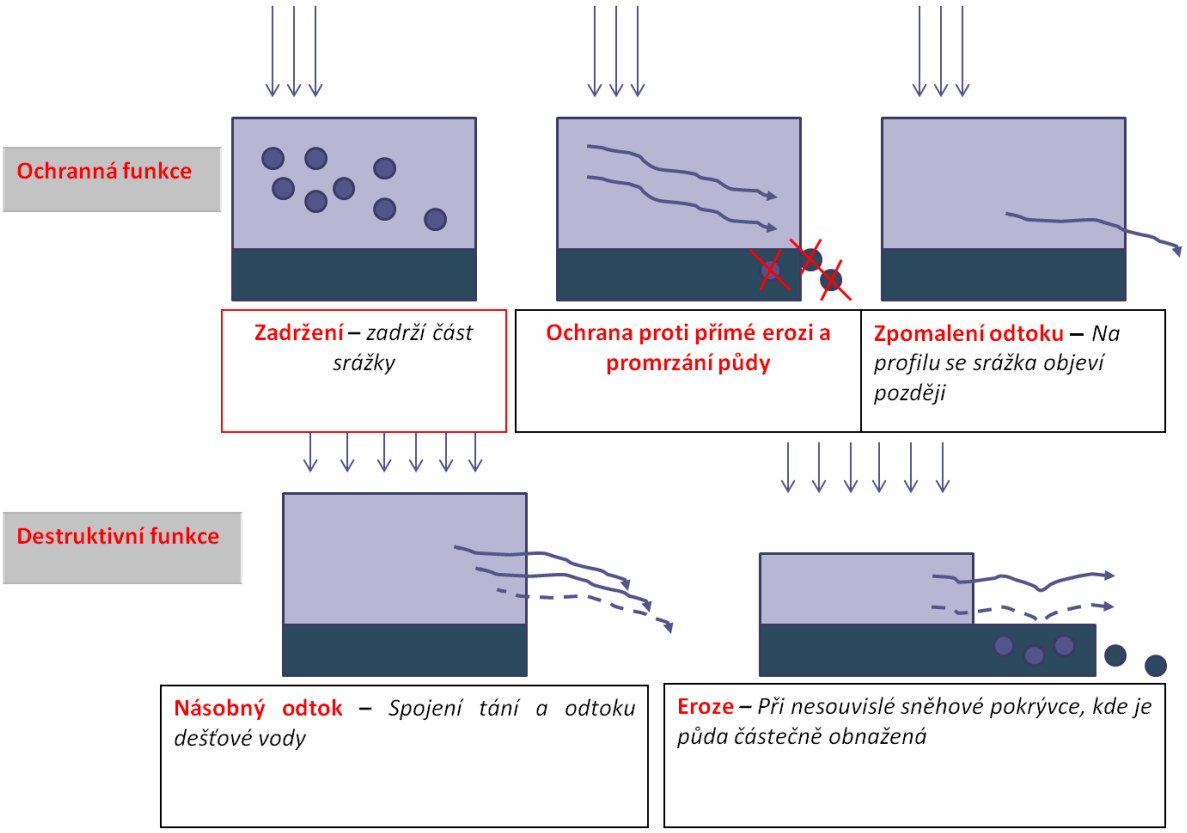

Obr. 1 – Základní funkce sněhové pokrývky během deště.

2. Přehled studované problematiky

2.1. Úvodní poznámka

V textu jsou některé termíny uvedeny jak v české, tak v anglické verzi. Tato dvojí terminologie je zavedena především kvůli často neustáleným českým výrazům a mohlo by dojít k nedorozumění a případné záměně termínů. U některých termínů nebyl nalezen žádný český ekvivalent, a proto je uveden pouze anglický výraz.

2.2. Definice a význam deště na sněhovou pokrývku

Události, kdy déšť přichází do kontaktu se sněhovou pokrývkou, se v anglické literatuře označují jako „Rain-on-snow“, zkráceně ROS. Jelikož v české terminologii zatím není pro tento fenomén ustálený výraz, tak je v této práci používána anglická zkratka ROS.

ROS se mohou vyskytovat prakticky všude, kde leží sněhová pokrývka. Freudiger et al. (2014) definuje ROS jako srážkovou událost, při které spadne alespoň 3mm deště na sněhovou pokrývku s minimálním vodním ekvivalentem (SWE) 10mm a odtok ze sněhové pokrývky obsahuje alespoň 20% tání. Pokud se dešťová voda dostane do sněhové pokrývky, tak se zpravidla chová dvěma způsoby: (1) Část infiltrovaného objemu dešťové vody zůstane ve sněhové pokrývce a dočasně se neúčastní odtoku (Hirashima et al., 2010; Kattelmann, 1987a; Singh et al., 1997). (2) Infiltrovaná voda dále vytéká a rovnou se účastní odtoku, případně se infiltruje do půdy (Laudon et al., 2004). V každém případě sněhová pokrývka vstupní dešťovou vodu částečně zpomalí. Dinçer et al. (1970) uvádí, že voda infiltrovaná do půdy ze sněhu může tvořit až dvě třetiny z celkové zásoby podzemní vody během jarního tání. Odtok ze sněhové pokrývky během ROS záleží především na intenzitě deště a vlastnostech sněhové pokrývky, které mohou být použity jako základní prediktory vzniku odtoku (Würzer et al., 2016). Tato problematika je v dostupné literatuře však řešena spíše okrajově.

Pozornost si ROS zasluhují především proto, že jsou často příčinou různých přírodních ohrožení. V minulých letech byla zaznamenána řada povodní způsobených ROS v Severní Americe (Ferguson, 2000; Kattelmann, 1997; McCabe et al., 2007), ale i v Evropských státech jako Německo (HND Bayern, 2011; Sui et Koehler, 2001), Švýcarsko (Badoux et al., 2013; Rössler et al., 2014) nebo Česká republika (Čekal et al., 2011). Akumulovaná dešťová voda způsobuje nižší soudržnost sněhové pokrývky což má také za následek vznik mokrých lavin (Ambach et Howorka, 1966; Conway, 1994; Kattelmann, 1987a; Marshall et al., 1999) nebo břečkotoků (Gude et Scherer, 1999; Hestnes et Setersen, 1987; Tomasson et Hestnes, 2000). Oba tyto jevy byly pozorovány i v České republice (Kociánová et Štursová, 2008; Spusta et Kociánová, 1998). Dešťová voda také ovlivňuje transport rozpuštěných látek a iontů (Feng et al., 2001a; Harrington et Bales, 1998; Lee et al., 2008a; Waldner et al., 2004), což následně ovlivňuje chemické složení a pH vodních toků (Casson et al., 2014; Dozier et al., 1989; MacLean et al., 1995).

ROS nemusí být spojené pouze se zimním nebo jarním obdobím tání. Pokud se sněhová pokrývka vyskytne již na podzim, případně přetrvá do léta, tak se mohou vyskytnout i ROS. Např. Badoux et al. (2013) popisuje výskyt ROS ze švýcarských Alp z první poloviny října a Pomeroy et al. (2016) doplňuje výskyt ROS v kanadských Rocky Mountains během června. S probíhající změnou klimatu a zvyšující se globální teplotou můžeme také očekávat zvýšení frekvence kapalných srážek v zimním období na úkor srážek sněhových (Safeeq et al., 2016). Ye et al. (2008) uvádí růst ročního výskytu dní s ROS o 0.5 – 2.5 dne na zvýšení teploty vzduchu o 1°C. Můžeme také očekávat snížení frekvence ROS v nižších nadmořských výškách a posun do vyšších nadmořských výšek (Safeeq et al., 2016; Ye et al., 2008). Vliv na výskyt ROS mají také oscilace v NAO indexu, které mohou v budoucnu zvyšovat četnosti výskytu ROS v Eurasii (Ye et al., 2008).

Z výše uvedeného je patrné, že v budoucnosti můžeme očekávat vyšší výskyt ROS, a proto si tento fenomén zasluhuje vyšší pozornost. Budoucí výzkum by se tedy měl zaměřit především na možnosti modelování následků ROS, především výskytu povodní a mokrých lavin.

2.3. Kapalná voda ve sněhové pokrývce

2.3.1. Hydraulické a hydrologické vlastnosti sněhové pokrývky

Ve sněhové pokrývce se voda vyskytuje ve všech svých skupenstvích. Důležitou vlastností sněhové pokrývky je obsah kapalné vody (*liquid water content - LWC*). Množství kapalné vody ve sněhové pokrývce představuje její vlhkost (θ), která je definována jako podíl celkového objemu tekuté vody (V_w) ve sněhu k celkovému objemu vzorku sněhu (V_s). Můžeme ji definovat jako:

$$\theta = \frac{V_w}{V_s}. \qquad (1)$$

Zdrojem kapalné vody ve sněhu je nejčastěji voda z tání nebo voda z deště.

Kapalná voda se ve sněhové pokrývce vyskytuje jen, pokud je její teplota kolem 0°C. Můžeme rozlišit tři formy tekuté vody: adsorbční voda, kapilární voda a gravitační voda (Singh et Singh, 2001).

- **Adsorbční voda** je neoddělitelná na povrchu jednotlivých zrn a je téměř nepohyblivá. Tato voda se neúčastní odtoku, dokud sněhová zrna neroztají. Během tání se objem adsorbční vody začne zvětšovat, až se z ní stane voda kapilární nebo gravitační.
- **Kapilární voda** je držena povrchovým napětím v kapilárních pórech mezi jednotlivými sněhovými zrny. Pohyb je způsoben rozdílem kapilárního tlaku v různých místech sněhové pokrývky. Tato voda se také zpočátku neúčastní odtoku. Na odtoku se podílí až při určitém stupni nasycení sněhové pokrývky.
- **Gravitační voda** se pohybuje ve sněhové pokrývce především vlivem gravitační síly a není již vázaná v pórech kapilárními silami.

Pokud obsah kapalné vody ve sněhu (LWC) přesáhne cca 3 %, tak se voda stává mobilní (Singh et Singh, 2001). Do té doby je voda ve sněhové pokrývce držena převážně adsorpčními a kapilárními silami se sníženou schopností pohybu. Na začátku svého vývoje neobsahuje studená nevyzrálá pokrývka žádnou vlhkost a označujeme ji jako suchou. Obsah kapalné vody roste, jak sněhová pokrývka zraje během sezóny.

Podle stupně nasycení sněhové pokrývky rozlišujeme pendulární a funikulární režim (Colbeck, 1974). V **pendulárním** režimu dosahuje vlhkost sněhu hodnot od 3-8 % z celkového objemu. Póry jsou převážně vyplněny vzduchem a tekutá voda se vyskytuje především v blízkosti dotyku jednotlivých zrn (Obr. 2a). Obsah vody je však malý a voda je vázaná kapilárními silami a je jen těžko pohyblivá. Ve **funikulárním** režimu se postupně lemy adsorbční vody spojují a voda začíná vyplňovat většinu pórů a zabírá již více než 14% jejich objemu. Z hlediska celkové vlhkosti je to 8-15% z celkového objemu sněhu. Vzduch je uvězněn v bublinách mezi jednotlivými sněhovými zrny (Obr. 2b). Stále ale dochází ke kontaktu mezi jednotlivými sněhovými zrny a kapilární síla již hraje podstatnou roli při pohybu vody.

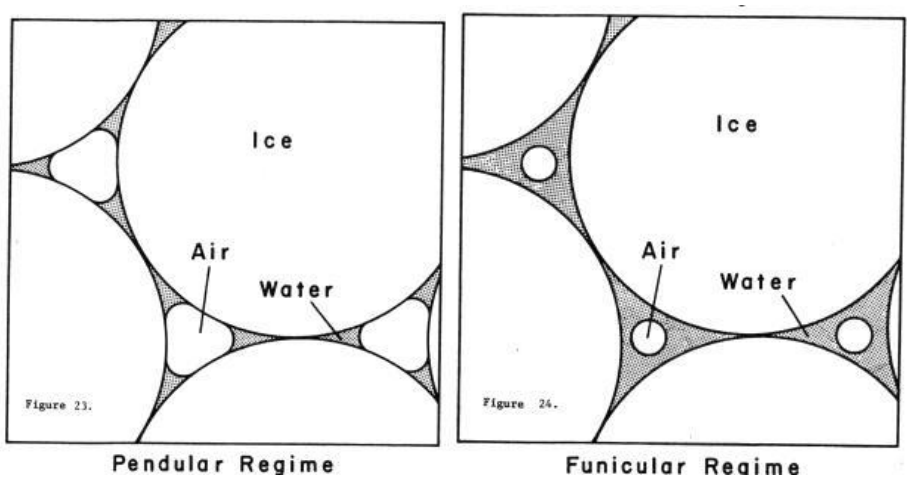

Obr. 2 – Výskyt vody ve sněhu v pendulárním a funikulárním režimu (Colbeck, 1974).

Pokud sníh dosahuje po delší dobu stupně nasycení přes 15 % - supersaturace (Tab 1), tak voda obklopuje celá ledová zrna, která se již vzájemně téměř nedotýkají. Vzduchové bubliny se skoro nevyskytují (Obr. 3). V takovém případě je již sněhová pokrývka velmi nestabilní a tento stav označujeme jako tzv. **břečku** – *slush* (Fierz et al., 2009). V této fázi se ve sněhu vyskytuje velké množství gravitační vody, která nemůže vlivem níže položené nepropustné vrstvy odtéct (např. ledová vrstva, skalní podloží). Takto nasycená masa sněhu se snadno uvolní a začne téct po svahu dolů. Tento jev označujeme jako **břečkotok** – *slushflows* (Hestnes et Setersen, 1987; Tomasson et Hestnes, 2000). Postupné sycení sněhové pokrývky a následný vznik břečkotoku je znázorněn na Obr. 4.

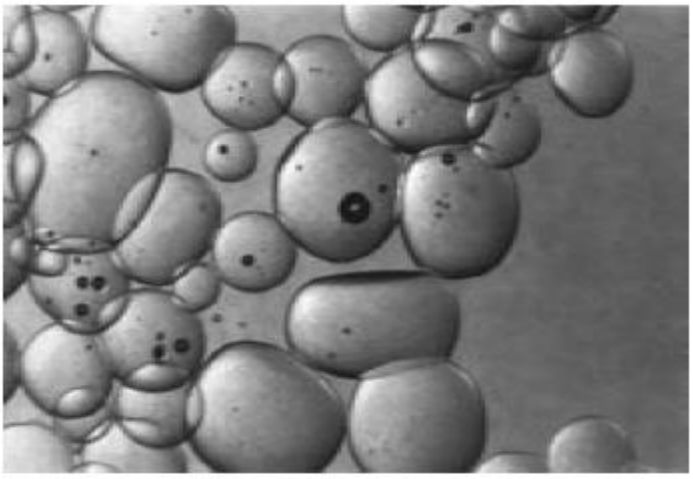

Slush MFsl, ∘, grain size E 0.5-1 mm (Colbeck) #52

Obr. 3 – Detailní pohled na uspořádání sněhových krystalů v břečce (podle Fierz et al. (2009)).

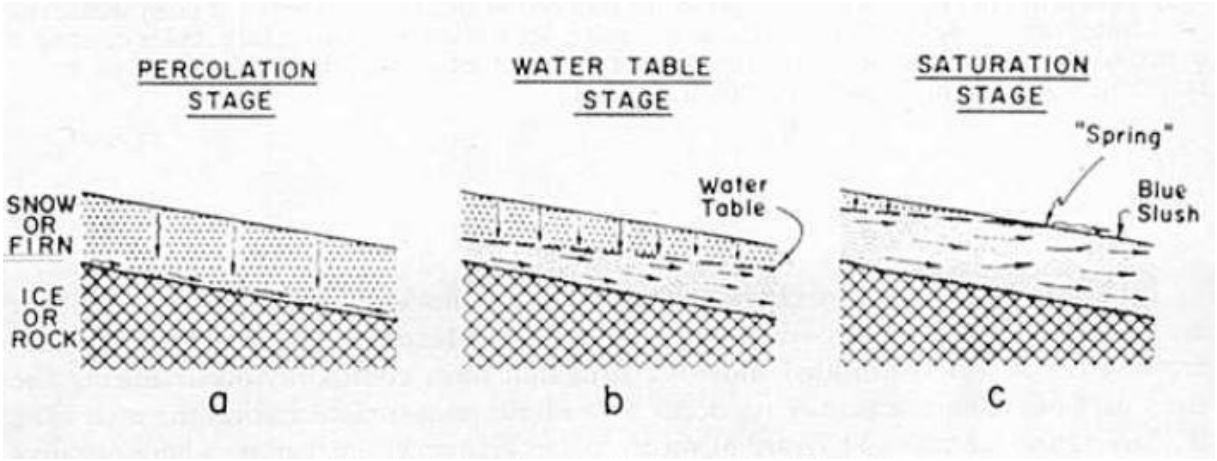

Obr. 4 – Sycení sněhové pokrývky na nepropustném podkladu, které vede ke spuštění břečkotoku (Nobles, 1966).

Pokud ve vlhkém sněhu poklesne obsah vody, tak zároveň vzroste kapilární tlak v pórech mezi zrny. Pokud obsah vody poklesne pod 7%, tak se zrna zformují do slepenců a vytvoří shluk. Kapalná voda ve sněhu může přes noc také zmrznout a to společně s vytvořenými ledovými shluky sněhovou vrstvu zpevňuje (McClung and Schaerer, 2006).

2.4. Měření obsahu kapalné vody ve sněhu

Aktuální obsah kapalné vody ve sněhové pokrývce můžeme měřit několika způsoby. Základní používané techniky rozdělujeme na kalorimetrické, zřeďovací a kapacitní.

Kalorimetrické metody jsou založeny na stanovení přijatého nebo uvolněného tepla z rozpuštění – *melting calorimetry* (Akitaya, 1985) nebo zmrznutí – *freezing calorimetry* (Jones et al., 1983) celého

sněhového vzorku. Tyto metody jsou však poměrně náročné na provedení a v porovnání s ostatními nejsou tak přesné.

Zřeďovací techniky využívají rozpuštění sněhového vzorku ve slabém roztoku kyseliny (Davis et al., 1985) nebo alkoholu (Fisk, 1986).

V současné době se nejčastěji ke stanovení obsahu kapalné vody ve sněhu používá **měření permitivity sněhu (ε)**. Permitivita je charakterizována vztahem mezi intenzitou elektrického pole a elektromagnetickou indukcí v daném materiálu. Nejčastěji používaná zařízení jsou „*Denoth meter*“ (Denoth, 1994), TDR sonda (Waldner et al., 2004) nebo „*Snow fork*“ (Sihvola et Tiuri, 1986; Techel et Pielmeier, 2011). Pro stanovení vlhkosti pomocí těchto přístrojů je nutné znát také hustotu sněhu v místě měření.

Přímou empirickou závislost ε na hustotě sněhu (ρ_s) a obsahu kapalné vody (θ) uvádí Denoth (1994):

$$\varepsilon = 1 + 1{,}92\rho_s + 0{,}44\rho_s^2 + 0{,}187\theta + 0{,}0045\theta^2. \qquad (2)$$

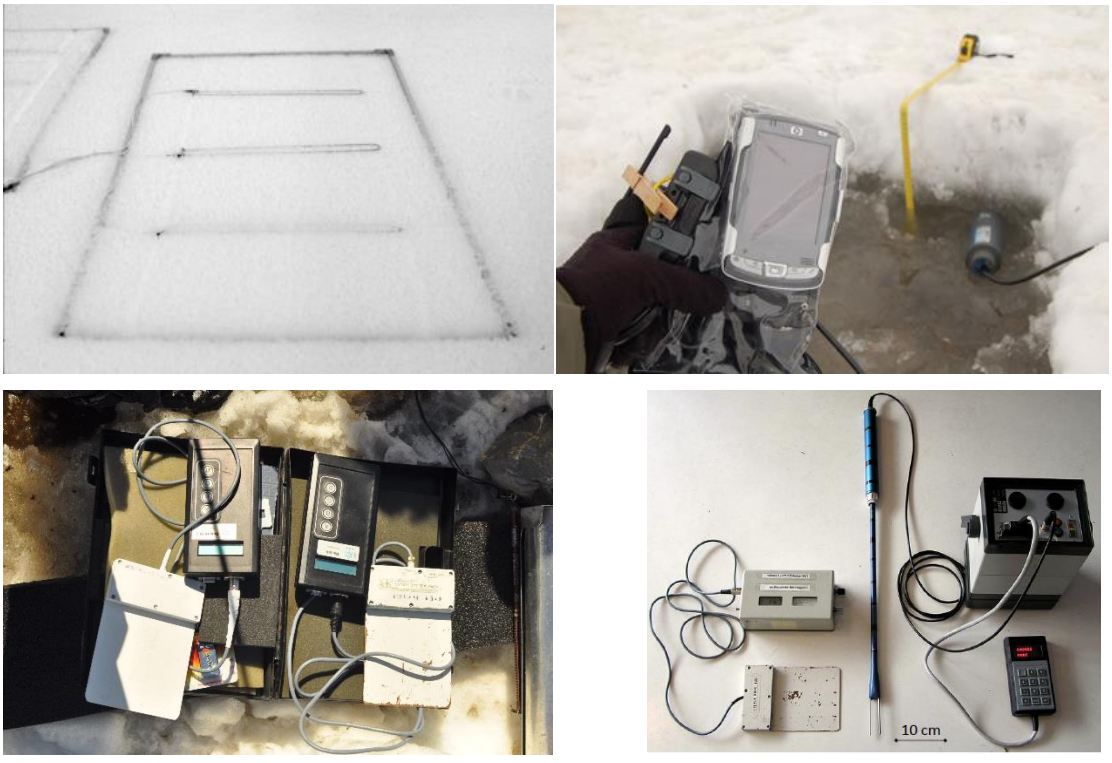

Obr. 5 – ***A:*** *Použití TDR pro kontinuální měření* (převzato z Waldner, 2002), ***B:*** *Použití TDR pro bodové měření (foto autor),* ***C:*** *„Denoth meter“ (foto autor),* ***D:*** *Srovnání „Denoth meter“ a „Snow Fork“* (převzato z Techel et Pielmeier, 2011)

2.5. Proudění ve sněhové pokrývce

2.5.1. Obecné principy

Sněhová matrice je porézní prostředí, a proto se pro popis proudění používají stejné charakteristiky, jako pro ostatní porézní prostředí (např. půda). Sníh se však od ostatních porézních prostředí liší tím, že jeho hydraulické vlastnosti se v čase relativně rychle mění vlivem zrání sněhové pokrývky. Hydraulická vodivost a propustnost jsou jedny z nejdůležitějších parametrů ovlivňujících proudění vody ve sněhové pokrývce. **Hydraulická vodivost** *K* ($m.s^{-1}$) určuje, jak snadno se může voda pohybovat v porézním prostředí. Rychlost vertikálního proudění sněhovou matricí lze popsat pomocí Darcy-Buckinghamova zákona jako funkce nenasycené hydraulické vodivosti *K* a gradientu hydraulické výšky (Hirashima et al., 2010; Jordan, 1983) jako:

$$q = K\left(\frac{dh}{dz} + 1\right), \tag{3}$$

kde *q* je makroskopická rychlost proudění sněhovou pokrývkou ($m.s^{-1}$), *h* je hydraulická výška (m), *z* je geodetická výška (m), derivace *dh/dz* určuje hydraulický gradient. Tlaková výška je závislá na kapilárním tlaku P_c ($N.m^{-2}$):

$$h = \frac{P_c}{\rho_w g}, \tag{4}$$

kde ρ_w je hustota vody ($kg.m^{-3}$) a *g* je gravitační zrychlení ($m.s^{-2}$).

Hydraulická vodivost je závislá nejen na velikosti a propojenosti pórů, velikosti a křivosti sněhových zrn ale také jejich rozložení v celém profilu a na objemové vlhkosti (Hirashima et al., 2010; Kuroiwa, 1968). Kromě toho závisí hydraulická vodivost také na stupni nasycení celého sněhového profilu (Singh et Singh, 2001).

Propustnost – *k* (m^2) je vlastnost porézního prostředí charakterizující jeho prostupnost bez ohledu na vlastnosti proudící kapaliny.

Při nasycení sněhové pokrývky vodou, kdy voda vyplňuje všechny póry, je možné pohyb vody popsat pomocí Darcyho zákona, který můžeme zapsat jako závislost rychlosti proudění na propustnosti (Waldner, 2002):

$$q = -k\frac{\rho_w g}{\mu}\frac{dh}{dz}, \tag{5}$$

kde μ je dynamická viskozita vody ($m^2.s^{-1}$). Nenasycená hydraulická vodivost *K* a propustnost *k* jsou na sobě lineárně závislé:

$$K = -k\frac{\rho_w}{\mu}g. \tag{6}$$

Shimizu (1970) uvádí vztah závislosti propustnosti na hustotě sněhu a průměru sněhových zrn:

$$k = 0.077 \cdot d^2 \cdot \exp\left(-7.8 \cdot \frac{\rho_s}{\rho_w}\right), \quad (7)$$

kde d je průměr zrna (mm) a ρ_s je hustota sněhu. Tento vztah ale platí pouze pro zrna do průměru 1 mm. Hustota sněhu (ρ_s) je pak funkcí jeho pórovitosti (Φ):

$$\rho_s = \rho_i(1 - \Phi), \quad (8)$$

kde ρ_i představuje hustotu ledu.

Detailně se závislostí propustnosti na hustotě sněhu zabýval také Calonne et al. (2012), který zahrnul také velikost zrn. Došel k závěru, že firnový sníh s velkou hustotou a velkými zakulacenými zrny je charakteristický malou propustností. Nejvyšší propustnost naopak pozorujeme u nového nevyzrálého sněhu (Obr. 6).

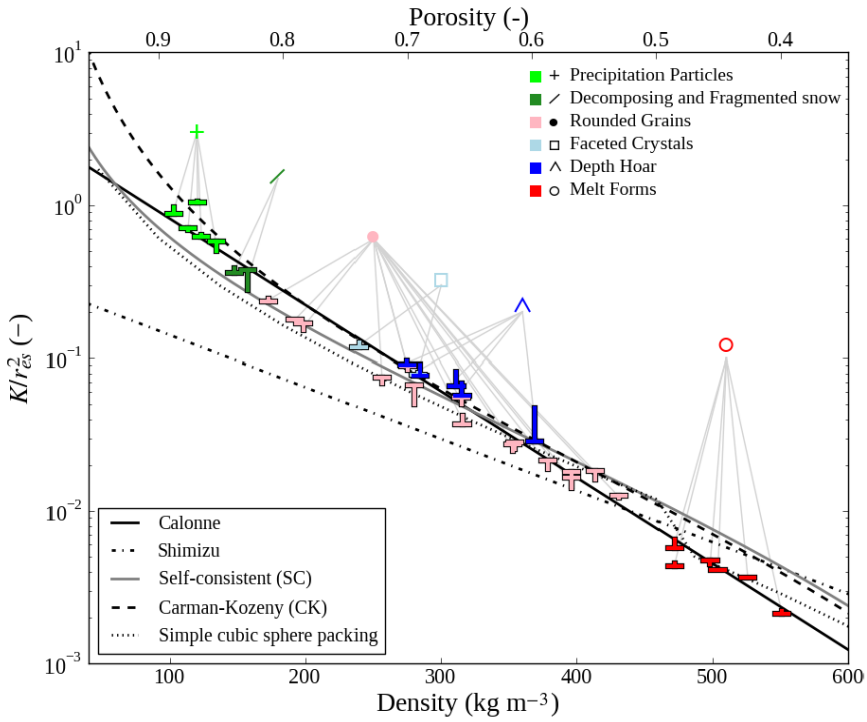

Obr. 6 – Závislost propustnosti (bezrozměrná) na pórovitosti a hustotě sněhu. Výsledky byly získány na základě numerického modelování (Calonne et al., 2012).

2.5.2. Typy proudění ve sněhové pokrývce

Jak již bylo řečeno v předchozích kapitolách, tak charakter proudění vody ve sněhové pokrývce nejvíce ovlivňuje hydraulická vodivost a také kapilární síly, které jsou závislé především na pórovitosti v jednotlivých sněhových vrstvách (Hirashima et al., 2010). Conway et Benedict (1994) rozlišují **suché zóny** (*dry snow zone*), kde se nevyskytuje žádná kapalná voda a teplota je pod bodem mrazu. Teplo se přenáší především vedením (kondukcí) a jeho tok je řízen teplotním gradientem. Naopak **vlhké zóny**

(wet snow zone) jsou charakteristické přítomností kapalné vody a teplotou kolem 0°C, existuje zde však stále malý tepelný gradient. Hranice mezi těmito zónami se nazývá čelo zvlhčení (*wetting front*).

Podle charakteru pohybu vody ve sněhové pokrývce rozlišujeme několik typů proudění.

Matricové proudění (*matrix flow*) je charakteristické rovnoměrným čelem zvlhčení, které postupuje podobnou rychlostí v celé sněhové matrici. V zóně matricového proudění má sníh podobnou vlhkost (Techel et al., 2008). Proudění lze popsat pomocí Darcy-Buckinghamovy rovnice pro nenasycené proudění v porézním prostředí (Waldner et al., 2004).

Preferenční proudění (*preferential flow, finger flow*) je nejčastější způsob pohybu tekuté vody sněhovou pokrývkou (Waldner et al., 2004). Tento typ proudění je charakteristický nerovnoměrným čelem zvlhčení a voda proudí v preferenčních cestách. Tyto preferenční cesty se vyznačují relativně větší hydraulickou vodivostí vůči okolnímu prostředí (Hirashima et al., 2010; Waldner et al., 2004). Hydraulická vodivost závisí na prostorové heterogenitě hustoty a velikosti sněhových krystalů (Calonne et al., 2012). Velikost preferenčních cest roste s intenzitou proudění kapalné vody na vstupu (Hirashima et al., 2014). Pokud jsou preferenční cesty již zvlhčeny, tak v nich bude voda proudit s větší pravděpodobností, než v suchých částech sněhu (Conway et Raymond, 1993). Na druhou stranu trvání preferenčních cest je omezeno. Pokud v nich delší dobu neproudí voda, tak zanikají (Waldner et al., 2004).

Horizontální proudění

Na rozhraní vrstev, kde se spodní vrstva vyznačuje menší hydraulickou vodivostí oproti horní vrstvě, dochází často ke změně proudění z vertikálního (typické pro nenasycenou zónu) na horizontální (typické pro nasycenou zónu). Rozlévání vody do stran je způsobeno především větší lokální heterogenitou ve velikosti sněhových zrn, což zároveň způsobuje i větší heterogenitu v kapilárním tlaku (Hirashima et al., 2014). Typicky nastává tato situace nad ledovou vrstvou nebo na rozhraní jemnozrnné vrstvy nad hrubozrnnou (Avanzi et al., 2015; Waldner et al., 2004). V takovém případě dojde k částečnému nasycení horní vrstvy a postupnému rozlévání do stran. Takto nasycená vrstva může poté zmrznout, což je mechanizmus vzniku ledových vrstev (Wever et al., 2016).

Typy proudění se mohou samozřejmě v rámci sněhové pokrývky měnit a podle charakteristik sněhu v daném místě přecházet z jednoho typu na druhý (Singh et Singh, 2001). Jednotlivé typy proudění jsou zobrazeny na Obr. 7 - 9. Z hlediska předpovídání odtoku ze sněhové pokrývky nebo vzniku lavin je klíčové vědět, kdy můžeme očekávat jaký charakter proudění. To umožňuje odhadnout, za jak dlouho voda sněhem proteče. Současné studie se však zabývaly většinou prouděním tavné vody a proudění dešťové vody nebyl věnován takový prostor.

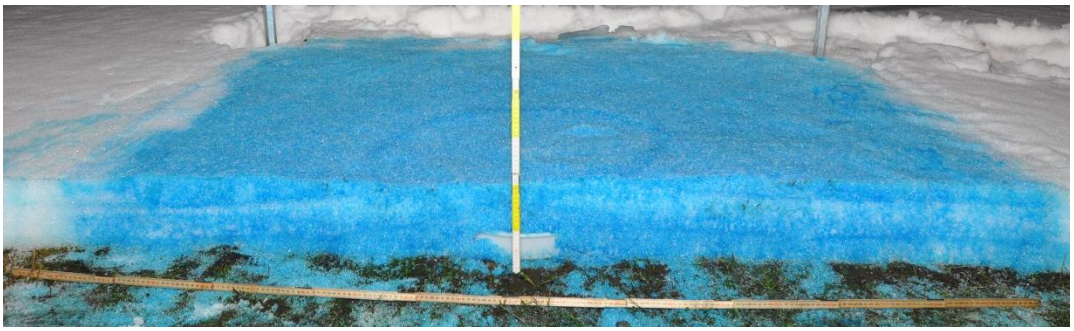

Obr. 7 – Matricové proudění ve sněhu je charakteristické kompletním zvlhčením celého objemu v dané části sněhové pokrývky. Na obrázku je znázorněn izotermální firnový sníh v období tání s velkým stupněm nasycení (foto autor).

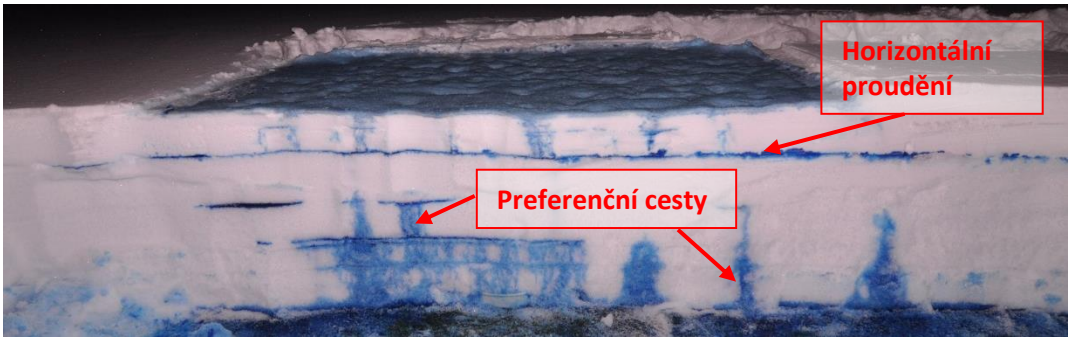

Obr. 8 – Preferenční proudění v nevyzrálé sněhové pokrývce. Horizontální proudění nastalo na rozhraní dvou vrstev, kdy těsně nad tímto rozhraním došlo k nasycení sněhu o mocnosti několik milimetrů (foto autor).

Obr. 9 – Přechod počátečního matricového proudění na preferenční proudění (foto autor).

2.6. Reakce sněhové pokrývky na déšť

ROS mají často za následek povodně (Böhm et al., 2011; Čekal et al., 2011; Ferguson, 2000; HND Bayern, 2011; Singh et al., 1997; Sui et Koehler, 2001). Vznik povodní bývá mimo jiné zapříčiněn tím, že se dešťová voda ve sněhové pokrývce pohybuje několikanásobně rychleji, než voda z tání (Singh et Singh, 2001), a proto může celkový odtok rychle zesílit. Toto zesílení odtoku je způsobené především kombinací srážkové a tavné vody. Dešťová voda má také vliv na rychlejší odtávání sněhové pokrývky. Teplá voda z deště působí jako významný energetický vstup a sněhovou pokrývku zahřívá. Odtok ze sněhové pokrývky během ROS ovlivňuje také charakter povodí. Kattelmann (1987b) pozoroval v povodí Sierra Nevady, že během několika ROS byl přibližně 2x vyšší odtok z otevřených ploch, než z ploch zalesněných. V několika případech lesní plochy dešťovou vodu zcela pohltily, aniž by odtok z povodí nastal. Z lesních ploch byly větší odtoky způsobeny spíše táním.

Pro předpověď povodní je velmi důležitá doba zpoždění odtoku od začátku deště. Tato doba je závislá na výšce sněhové pokrývky (Conway, 1994; Wever et al., 2014a). Zároveň je to klíčový faktor pro vznik případné povodně. Conway (1994) uvádí vzorec pro výpočet času zpoždění odtoku od počátku deště (v hodinách):

$$t_z = V_w \cdot \theta \cdot HS/\mathrm{PI}, \qquad (9)$$

kde V_w je podíl objemu vlhkého sněhu v čase odtoku, θ je průměrná vlhkost sněhu, HS je výška sněhu (m) a PI je průměrná intenzita deště (m/hod). Dále můžeme zavést pojem **kombinovaný odtok**, což je součet odtoku z tání spolu s odtokem způsobeným deštěm (Singh et Singh, 2001).

Zpoždění výtoku je větší u nevyzrálého sněhu, než u sněhu vyzrálého (Singh et Singh, 2001). Tzn., že voda proudí poměrně rychle skrze vyzrálý sníh, ale je zpomalena zmrzlými nebo suchými jemnozrnnými vrstvami. Na druhou stranu Calonne et al., (2012) uvádí, že vysoká propustnost sněhu odpovídá nízkým hustotám, které jsou typické spíš pro nevyzrálý sníh. Singh et Singh, (2001) porovnává čerstvý, vyzrálý a přemrzlý sníh a udává, že vyzrálý sníh v sobě nezadrží téměř žádnou vodu (tedy pokud není výrazněji stratifikován ledovými vrstvami a tvrdým firnem), ale zbylé dva typy v sobě zadrží přibližně stejné množství (Singh et Singh, 2001).

Mezi hlavní faktory ovlivňující odtok ze sněhové pokrývky patří především: povrchové tání, metamorfóza sněhu, pohyb vody skrze mokrou sněhovou pokrývku, interakce mezi tající vodou a půdou pod pokrývkou a přízemní tok v nejnižší vrstvě sněhové pokrývky (Singh et Singh, 2001).

Déšť mimo jiné urychluje i sesedání sněhu, protože je do pokrývky přidána další hmotnost vody (Conway et Raymond, 1993). Akumulace dešťové vody způsobuje zvýšení obsahu tekuté vody ve sněhové pokrývce, což následně může snížit její stabilitu (Conway et Raymond, 1993; McClung et Schaerer, 2006). Tato nestabilita často způsobuje vznik mokrých lavin (Ambach et Howorka, 1966; Conway et Benedict, 1994; Kattelmann, 1987b; Marshall et al., 1999). Načasování lavinové aktivity

během deště závisí především na vývoji mechanických vlastností sněhové pokrývky, které jsou částečně řízeny celkovým objemem a intenzitou srážky.

Zmiňovanou ztrátu pevnosti sněhové pokrývky kvůli přítomnosti kapalné vody způsobují tyto faktory:

- Voda způsobuje tání na spojích zrn a tím snižuje tření mezi jednotlivými zrny.
- U nového sněhu kapalná voda velmi urychluje metamorfózu způsobující změnu velikosti a tvaru zrn a tím celkovou strukturu sněhové pokrývky.

Na druhou stranu může sněhová pokrývka po dešti zůstat stabilní. To nastane většinou tehdy, když je vytvořen systém perkolačních kanálků a voda se v pokrývce neakumuluje, ale rychle odteče. Sněhová pokrývka časem zvětší svou hustotu a celkově se zpevní (Conway et Raymond, 1993).

Na základě pozorování meteorologických podmínek a načasování a počtu lavin rozlišují Conway et Raymond (1993) tři typy lavinové aktivity následkem deště: 1) okamžitý odtrh několik minut po začátku deště, 2) zpožděný odtrh, více než hodinu po začátku deště a 3) stabilizace sněhové pokrývky, která nastane 10 – 20 hodin po začátku deště.

2.7. Studium chování dešťové vody ve sněhu

Chováním kapalné vody ve sněhové pokrývce se v minulosti zabývala řada prací. Především se jednalo o laboratorní pokusy, kdy byl zvlhčován vzorek sněhu (Avanzi et al., 2015; Katsushima et al., 2013) nebo terénní experimenty (Conway et Benedict, 1994; Eiriksson et al., 2013; Feng et al., 2001a; Singh et al., 1997). Tyto experimenty se např. zaměřovaly na transport rozpuštěných látek ve sněhu (Lee et al., 2008, 2010b; Taylor et al., 2001; Waldner et al., 2004), tvorbu odtoku (Singh et al., 1997) nebo mechanismus infiltrace vody do sněhu (Conway et Benedict, 1994; Kattelmann, 1987a; Techel et al., 2008).

Pro detekci dešťové vody se využívají různé stopovače jako barvivo (Eiriksson et al., 2013; Techel et Pielmeier, 2011), vzácné prvky (Taylor et al., 2001), stabilní izotopy (Herrmann et al., 1981) nebo změny teploty v rámci celého profilu (Conway et Benedict, 1994).

Conway et Raymond (1993) uvádějí, že pokud byl sníh vlhký už před vstupem vody, tak voda prošla celým profilem (2 m) za několik málo minut. Autoři dále popisují pokus, kdy voda proudila čerstvým sněhem a za hodinu se dostala pouze do horních 5 – 10 cm. Ve větších hloubkách začala proudit preferenčními kanálky (*flow fingers*), které se ze šířky 1cm postupně rozšířily do 20 – 30 cm.

Pokud déšť trvá dostatečně dlouho, tak voda dokáže penetrovat i skrze několik slabších (0,5 – 1 cm) ledových vrstev (Conway et Benedict, 1994). Voda potom penetruje do sněhu skrze preferenční kanálky, které mohou zabírat i 50 % celkového objemu sněhové pokrývky. Celková vlhkost sněhu může v těchto

případech dosahovat kolem 6 % z celkového objemu a celková vlhkost v mokrých částech je při infiltraci dokonce 8 – 10 % (Conway et Benedict, 1994).

2.8. Modelování odtoku ze sněhové pokrývky

Modelování odtoku ze sněhové pokrývky souvisí především se stanovením množství tavné vody a modelování proudění kapalné vody, která odtéká ze sněhové pokrývky. Pro stanovení tavné vody se používají především dva základní koncepty modelů. Jedná se o koncept **energetické bilance**, která uvažuje energetické toky ovlivňující sněhovou pokrývku. Model energetické bilance je poměrně komplexní a přesný, ale má velké nároky na kvalitu a množství vstupů. To je často také hlavním omezujícím faktorem pro používání těchto modelů. Druhým přístupem je koncept **teplotního indexu** neboli **degree-day modelů**. Tyto typy modelů pracují převážně se vstupy teploty vzduchu, které bývají většinou k dispozici. Pro modelování proudění vody ve sněhové pokrývce se používá především Richardsova rovnice (RE).

V následujících kapitolách je popsán koncept energetické bilance a možnosti modelování proudění ve sněhové pokrývce.

2.8.1. Energetická bilance

Rovnice energetické bilance popisuje tok energií, které ovlivňují vývoj sněhové pokrývky a tím i proces tání. Základní rovnici energetické bilance můžeme vyjádřit:

$$Q_M = Q_{NR} + Q_H + Q_E + Q_P + Q_G + Q_I, \qquad (10)$$

kde Q_M je celková energie získaná sněhovou pokrývkou (kJ.m^{-2}), Q_{NR} je bilance záření (čistá energie – *net radiation*, (kJ.m^{-2}), Q_H je tok zjevného tepla (*sensible heat flux*) nebo konvektivního tepla získaného ze vzduchu (kJ.m^{-2}), Q_E je tok latentního tepla (*latent heat flux*) evaporace, kondenzace nebo sublimace (kJ.m^{-2}), Q_P je tepelný tok, způsobený deštěm (kJ.m^{-2}), Q_G je tepelný tok z půdy (kJ.m^{-2}), Q_I je tepelný tok způsobený změnami vnitřní energie sněhu (kJ.m^{-2}).

Nejvýznamněji ovlivňuje tání celková bilance záření, tok zjevného tepla, tok latentního tepla a tepelný tok způsobený deštěm. **Bilance záření** představuje rozdíl záření směřujícího ze sněhové pokrývky a ke sněhové pokrývce. V bilanci jsou zahrnuty toky dlouhovlnné i krátkovlnné radiace. Během deště je obecně celková bilance záření malá kvůli silné vrstvě oblačnosti.

Bilanci záření můžeme tudíž rozepsat:

$$Q_{NR} = Q_{ln} + Q_{sn}\,, \qquad (11)$$

kde Q_{ln} je tepelný tok dlouhovlnné radiace a Q_{sn} je tok krátkovlnné radiace.

Radiace dopadá na zemský povrch a zároveň je z něj také vyzařována. Z hlediska směru působení na zemský povrch jí můžeme tedy rozdělit na příchozí, odchozí a odraženou. Odraženou radiaci dále můžeme rozdělit na odraženou od zemského povrchu a odraženou od mraků. Schematický přehled toků záření ovlivňující zemský povrch je znázorněn na Obr. 11. Z hlediska vlnové délky můžeme radiaci dělit na:

- Krátkovlnná radiace – (λ = 0,3 – 3 μm)
  Součet krátkovlnného přímého a odraženého záření od mraků označujeme jako **globální radiaci**.
- Dlouhovlnná radiace (λ = 6,8 – 100 μm)

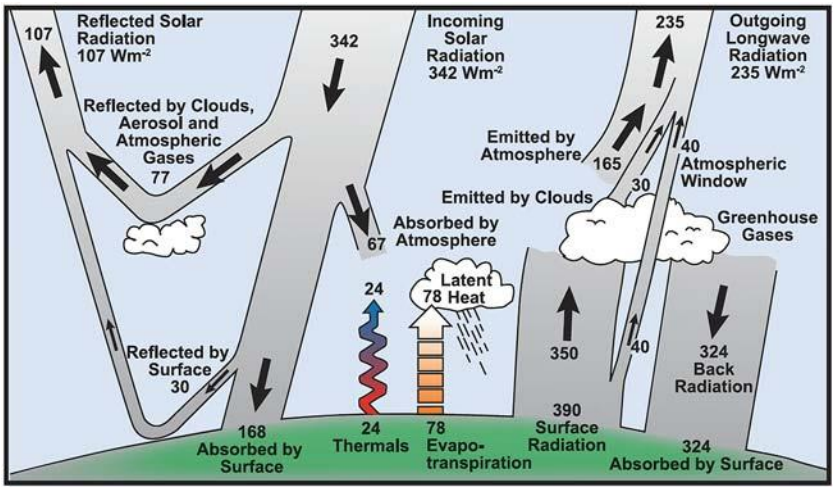

Obr. 10 – Přehled toků záření, které dopadá na zemský povrch a zároveň je z něho vyzařováno (http://www.optocleaner.com).

Sněhová pokrývka také neustále vyzařuje dlouhovlnné záření, což jí celkové ochlazuje. Proto se v zimě během jasných dnů dá předpokládat, že jižní svahy budou teplejší, protože vstup záření převyšuje jeho vyzařování. Na severních svazích dochází k opačnému efektu (McClung et Schaerer, 2006).

Jiný příklad je vznik mokrých lavin. Pod tenkou vrstvou nízkých mraků se sluneční záření nemůže dostat skrze mraky a emitované záření ze sněhu se od mraků odráží zpět (skleníkový efekt). Výsledkem je velké oteplení a zintenzivnění tání na povrchu sněhu. Toto jsou ideální podmínky pro vznik mokrých lavin (McClung et Schaerer, 2006).

Bilanci krátkovlnného záření vyjádříme:

$$Q_{sn} = S_{n\downarrow} - S_{n\uparrow}\,, \qquad (12)$$

kde S_n je krátkovlnná radiace a šipky v indexu naznačují směr záření. Odraženou krátkovlnnou radiaci pak vyjádříme:

$$S_{n\uparrow} = \alpha S_{n\downarrow} , \quad (13)$$

kde α je albedo sněhu, které můžeme odhadnout (DeWalle et Rango, 2008):

$$\alpha \cong 0{,}892 + 0{,}417.\rho_s - 2{,}99.{\rho_s}^2 . \quad (14)$$

Pokud není k dispozici měření, tak můžeme příchozí dlouhovlnnou radiaci vypočítat jako:

$$L_n = \sigma(eT_a^4 - T_s^4), \quad (15)$$

kde σ je Stefan-Boltzmannova konstanta (5.67 x 10^{-11} kW.m^{-2}.K^{-4}), T_s je teplota sněhu (°C) a e je emisivita sněhu (většinou se udává mezi 0,97 – 1) nebo se dá vyjádřit jako:

$$e = (0{,}72 + 0{,}005.T_a).(1 - 0{,}84C) + 0{,}84C, \quad (16)$$

kde T_a je průměrná teplota vzduchu a C je oblačnost.

Tok **zjevného tepla** je přenášen pomocí turbulentní výměny. Závisí především na rozdílu teploty mezi vzduchem a povrchem sněhové pokrývky a na rychlosti větru (Levia et Leathers 2011):

$$Q_h = \rho_a C_h C_a.(T_a - T_s), \quad (17)$$

kde ρ_a je hustota vzduchu, C_h je přenosový koeficient pro zjevné teplo, C_a je tepelná kapacita vzduchu (1,29 kJ.m^{-3}.°C^{-1}) a T_a je průměrná denní teplota vzduchu (°C).

Teplo spotřebované na fázovou přeměnu neboli **latentní teplo** závisí především na teplotě rosného bodu a na rozdílu hustoty vodních par vzduchu při povrchu sněhové pokrývky. Čím vyšší je teplota rosného bodu, tím větší je rozdíl hustoty vodních par. Latentní teplo se vypočítá:

$$Q_E = E_v C_E ws(q_a - q_v), \quad (18)$$

kde E_v je latentní teplo výparu (2500 kJ.kg^{-1}), C_E je přenosový koeficient pro latentní teplo, ws je rychlost větru, ρ_v je hustota nasycených vodních par při povrchu (kg.m^{-3}) a ρ_a je hustota vodních par ve vzduchu (kg.m^{-3}).

Během ROS představují energetické toky specifického a latentního teplo nejvýznamnější zdroj energie pro tání na otevřených prostranstvích (Garvelmann et al., 2014; Würzer et al., 2016). Význam bilance dlouhovlnného záření roste především v lesním prostředí (Garvelmann et al., 2014). Zatímco během jasných dnů má největší energetický přínos z hlediska tání především bilance krátkovlnného záření (Garvelmann et al., 2014).

Ke kondenzaci vodních par při povrchu sněhové pokrývky dochází, pokud je teplota rosného bodu nad 0°C (teplota sněhu bude tím pádem vždycky nižší, a proto vodní pára bude kondenzovat). Během kondenzace se opět uvolní latentní teplo, které podporuje tání (Levia et Leathers, 2011).

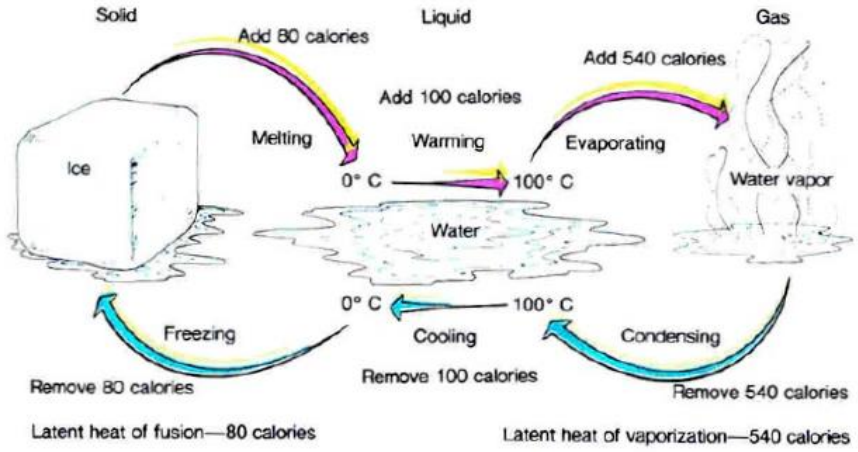

Obr. 11 – Energetická náročnost fázové přeměny (http://www.alchemical.org/thermo/latentheat.html).

Dešťová voda také velmi výrazně přispívá přenosem tepla do sněhové pokrývky. Nejvíce **tepla je z deště** dodáno při velkých teplotních rozdílech mezi deštěm a sněhem. Teplo dodané deštěm se vypočítá jako:

$$Q_P = C_w . R_p . (T_r - T_s), \qquad (19)$$

kde C_w je specifické teplo vody (4,2 kJ.kg^{-1}.°C^{-1}), R_p je množství dešťové srážky (m), T_r je teplota deště (°C) a T_s je teplota sněhu (°C).

Pokud se dešťová voda dostane do sněhu, který má teplotu pod bodem mrazu, tak zmrzne a tím uvolní latentní teplo, které dále oteplí sněhovou pokrývku. Tento proces pokračuje, dokud nezačne sněhová pokrývka tát. Pokud se dešťová voda dostane do sněhu s teplotou kolem 0°C (izotermální), tak je veškeré teplo spotřebováno rovnou na tání.

Teplo dodané z půdy je ve srovnání s ostatními složkami rovnice během zimní sezóny zanedbatelné. Sněhová pokrývka také působí jako výborný izolant, a proto se teplo z půdy na povrch sněhové pokrývky přenáší pouze velmi pomalu. Tento stav samozřejmě není stejný po celou sezónu. Významnější energetické toky půdy mohou nastat na začátku sezóny, kdy ještě není půda promrzlá a často způsobí tání prvního sněhu. Na konci sezóny, kdy se již nevyskytuje souvislá sněhová pokrývka, může obnažená prohřátá půda také významně ovlivňovat tání.

Na začátku a v průběhu sezóny je teplota ve vertikálním profilu sněhové pokrývky značně diverzifikovaná. Jak ale sněhová pokrývka postupně dozrává, tak se tepelný gradient snižuje a teplota se v celé mase sněhové pokrývky blíží 0°C – nulová izoterma. Podle období můžeme v celkové energetické bilanci tuto složku zanedbat nebo se vypočítá jako (Singh et Singh, 2001):

$$Q_G = k_g . \frac{dT_g}{dz}, \qquad (20)$$

kde k_g je tepelná vodivost půdy (W.m^{-2}) a dT_g/dz je teplotní gradient kolmý na povrch půdy.

Tepelná vodivost zmrzlé půdy je vyšší, než vodivost nezmrzlé půdy. Tání vlivem tepelného toku z půdy bývá zpravidla kolem 0.5 mm za den. Často se však zavádí konstanta Q_G = 173 kJ.m^{-2}den^{-1} (U.S. Army Corps of Engineers, 1998).

Vnitřní změny energie (Q_i) závisí především na množství uvolněného nebo pohlceného zjevného a latentního tepla. Tyto změny se projevují především změnou teploty sněhu a tvoří významnou složku energetické bilance. V období ohřívání přijímá sněhová pokrývka velké množství energie a tyto vnitřní energetické změny hrají důležitou roli. Jakmile je pokrývka ohřátá na 0°C, jsou tyto změny velmi malé. Více se začnou projevovat, pokud přes noc sněhová pokrývka zmrzne (uvolní teplo) a přes den opět rozmrzne (přijme teplo) (DeWalle et Rango, 2008). Pro výpočet vnitřní energie uvádí Singh et Singh (2001) vzorec:

$$Q_i = Q_{IL} + Q_{IK} + Q_{IV}, \qquad (21)$$

kde Q_{IL} je vnitřní energie ledu, Q_{IK} je vnitřní energie kapaliny a Q_{IV} je vnitřní energie výparu. Vnitřní energie se uvažuje často také jako konstanta 2.1 kJ.kg^{-1}.°C^{-1} (Walter et al., 2005), podobně jako energie dodané z půdy.

Pro výpočet výšky vodního sloupce celkového tání uvádí řada autorů různé vzorce. Singh et Singh (2001) uvádí jednoduchý vztah se zavedením konstanty:

$$M_d = 0{,}0031 Q_M, \qquad (22)$$

kde M_d (mm.den^{-1}) je množství tavné vody. DeWalle et Rango (2008) uvažují ve výpočtu i latentní teplo přeměny a tepelnou kvalitu sněhové pokrývky:

$$M_s = Q_M \left(\rho_w L_f \beta\right)^{-1}, \qquad (23)$$

kde M_S je množství tavné vody (mm.s^{-1}), L_f (J.kg^{-1}) je latentní teplo fázové přeměny a β (-) je tepelná kvalita sněhu.

2.8.2. Modelování proudění ve sněhové pokrývce

Pro modelování odtoku ze sněhové pokrývky se používá řada předpovědních modelů založených na modelování vývoje sněhové pokrývky. Mezi nejznámější patří např. CROCUS (Brun et al., 1989), SNTHERM (Jordan, 1991) nebo SNOWPACK (Lehning et al., 1999). Tyto modely se využívají pro operativní předpovídání odtoku ze sněhové pokrývky, případně pro predikci vzniku lavin. Pro výpočet tání používá většina modelů koncept energetické bilance, který byl popsán výše.

Pohyb vody ve sněhové pokrývce se popisuje jako proudění v nenasycené zóně. Základní model gravitačního proudění vody skrze sněhovou pokrývku představil (Colbeck, 1971), který byl různými autory dále modifikován. Modely CROCUS a SNTHERM používají pro řešení proudění vody ve sněhové pokrývce koncept kinematické vlny. Všechny tyto modely však zanedbávají vliv kapilárních sil, které zvláště ve stratifikované pokrývce mohou hrát při pohybu kapalné vody důležitou roli (Avanzi et al., 2015; Jordan, 1995). Vliv kapilarity zahrnují autoři modelů až později (Hirashima et al., 2010; Jordan, 1995). Model SNOWPACK k řešení proudění ve sněhu používá několik konceptů, které zahrnují numerické řešení Darcy-Buckinghamova zákona (Hirashima et al., 2010) nebo Richardsovy rovnice v 1D a také řeší infiltraci tavné vody do přilehlého půdního horizontu (Wever et al., 2014b). Model SNOWPACK byl využit i pro modelování odtoku během přírodních ROS (Würzer et al., 2016). Přesto by bylo vhodné provést pro kalibraci tohoto modelu více studií jak za přírodních, tak za kontrolovaných podmínek.

Pro doplnění výčtu existujících modelů lze uvést ještě hydrologický konceptuální model XINSNOBAL (Qu et al., 2013), který předpovídá celkový odtok na povodí.

2.9. Využití izotopů pro detekci dešťové vody

Určení zdrojů a velikost jednotlivých složek odtoku z povodí je klíčová otázka pro hydrology již několik desetiletí. Pro separaci hydrogramu na jednotlivé komponenty se využívá především rozdílného izotopového složení jednotlivých zdrojů. Pro analýzu se využívají přirozené stálé izotopy molekuly vody jako deuterium ^{2}H nebo ^{18}O, případně nestálé izotopy jako tritium ^{3}H. Celkový odtok se zpravidla separuje na vodu pocházející z hydrologické události – událostní voda („*event water"*) a na vodu vyskytující se v odtoku před touto událostí – předudálostní voda („*pre-event water"*).

Konečná separace na jednotlivé složky se provádí pomocí soustavy bilančních rovnic:

$$Q_{celkový}.\delta_{celkový} = Q_1.\delta_1 + Q_2.\delta_2 + \cdots Q_n.\delta_n, \quad (24)$$

$$Q_{celkový} = Q_1 + Q_2 + \cdots Q_n, \quad (25)$$

kde Q je průtok a δ deuteriový deficit daného izotopu vůči V-SMOW. Index *celkový* znamená celkový měřený průtok respektive deficit a indexy *1,2,…n* značí počet jednotlivých separovaných zdrojů. Platí, že neznámé jsou většinou jednotlivé průtoky Q_1, Q_2, …Q_n. Pro úspěšnou separaci hydrogramu musí být tedy vždy odebraný referenční vzorek z daných zdrojů, které chceme separovat. Pokud separujeme dva zdroje, tak po úpravě obou rovnic dostáváme konečný tvar pro stanovení dílčích průtoků:

$$Q_2 = \frac{Q_{celkový}.\delta_1 - Q_{celkový}.\delta_{celkový}}{(\delta_1 - \delta_2)}, \quad (26)$$

$$Q_1 = Q_{celkový} - Q_2, \quad (27)$$

Při separaci více, než dvou zdrojů musíme použít také více stopovačů. Kromě uvedených stabilních izotopů se ke stopování jednotlivých složek používají ionty Si^{4+}, Na^{+} , Cl^{-} (Rice et Hornberger, 1998; Suecker et al., 2000; Uhlenbrook et Hoeg, 2003).

Z hlediska hydrologie sněhu se tradičně v celkovém odtoku z povodí separuje tavná voda jako událostní od základního odtoku. Roli tavné vody v celkovém odtoku popsal pomocí analýzy deuteria a tritia jako jeden z prvních Dinçer et al. (1970). Studie uvádí, že v povodí Modrého potoka se přibližně 2/3 tavné vody infiltrují do půdy, kde vytlačí podzemní vodu do odtoku. Tímto způsobem se také doplňují v horských povodích zásoby podzemní vody. Hloubka infiltrace tavné vody je však omezena. Laudon et al. (2004) uvádí, že tavná voda se v povodí severního Švédska infiltrovala maximálně do hloubky 90 cm.

Separace tavné vody s sebou však přináší řadu komplikací, protože koncentrace stabilních izotopů ^{2}H a ^{18}O ve sněhové pokrývce a v odtékající tavné vodě se v průběhu sezóny zvyšuje (Hashimoto et al., 2002; Taylor et al., 2002). Toto zvyšování je mimo jiné způsobeno i kontaktem s izotopicky těžší dešťovou vodou (Unnikrishna et al., 2002). Vlivem frakcionace se izotopické složení vytékající tavné vody, respektive kapalné vody ve sněhu a pevného sněhu liší přibližně o 2 ‰ ^{18}O (Hashimoto et al., 2002; Unnikrishna et al., 2002), což odpovídá 16 ‰ ^{2}H (Feng et al., 2002). Z toho důvodu není vhodné používat při separaci tání v rovnici 26 jako referenční hodnotu (δ) izotopovou koncentraci pevného sněhu (Feng et al., 2002).

Sněhová pokrývka se na začátku svého vývoje vyznačuje izotopovou heterogenitou a v průběhu sezóny se postupně homogenizuje (Lee et al., 2010a). Tato homogenizace probíhá především pomocí redistribuce tavné vody napříč sněhovou pokrývkou (Taylor et al., 2001).

Během ROS však z dešťové pokrývky odtéká kombinace vody z tání a dešťové vody. Pouze několik málo studií se věnovalo této problematice v měřítku povodí. MacLean et al. (1995) stanovil na dvou kanadských povodích, že dešťová voda tvořila 30 % respektive 50 % celkového odtoku. Nicméně detailní studie zaměřující se na dynamiku a tvorbu odtoku dešťové vody ze sněhové pokrývky chybí. Z toho důvodu si tato studie klade za cíl přispět k lepšímu pochopení této problematiky s využitím separace dešťové a nedešťové vody ze sněhové pokrývky různých vlastností.

3. Cíle práce a základní předpoklady

Hlavním cílem disertační práce je posouzení vlivu sněhové pokrývky na transformaci dešťových srážek. Zároveň si tato práce klade za cíl přiblížit mechanismus vzniku a složení kombinovaného odtoku ze sněhové pokrývky během deště. Splnění těchto základních cílů zahrnuje dva základní úkoly:

I. Navrhnout vhodnou metodiku simulace deště v terénu, která umožňuje i následný monitoring odtoku ze sněhové pokrývky. Kromě toho by měla metodika zahrnovat analýzu změn vlastností sněhové pokrývky následkem deště.

   Navržená metodika by dále měla umožňovat vizualizaci proudění dešťové vody ve sněhové pokrývce s různými fyzikálními vlastnostmi, ale i možnosti stanovení dešťové vody na výtoku pomocí separace hydrogramu. Určení jednotlivých složek v celkovém odtoku by mělo umožňovat stanovení:

   a. Okamžitého procentuálního zastoupení dešťové vody na celkovém odtoku a v jednotlivých fázích deště.
   b. Za jak dlouho se dešťová voda objeví na výtoku, tj. doba zdržení.

II. Množství vody z tání pomocí energetické bilance.

   Pomocí navržené metodiky charakterizovat dynamiku proudění dešťové vody ve sněhové pokrývce a mechanismus vzniku odtoku v různých typech sněhu. Tato metodika bude doplněna o výsledky modelování z modelu SNOWPACK, který popisuje chování kapalné vody ve sněhu pomocí Richardsovy rovnice. Na základě předložené rešerše literatury bylo formulováno několik výzkumných otázek a předpokladů:

   a. Jak ovlivňují vlastnosti sněhové pokrývky charakter proudění a transport dešťové vody ve sněhové pokrývce?

      Předpoklad 1: *Velký specifický povrch krystalů u nevyzrálé pokrývky umožňuje větší interakci mezi srážkovou vodou a sněhovou pokrývkou.*

   b. Jaká je rychlost hydrologické odezvy na ROS v závislosti na charakteristikách zasažené sněhové pokrývky a intenzitě deště?

      Předpoklad 2a: *Vyzrálá sněhová pokrývka se vyznačuje rychlejší hydrologickou odezvou, než nevyzrálá pokrývka.*

      Předpoklad 2b: *Při vyšší intenzitě deště dochází k rychlejší hydrologické odezvě.*

   c. Jak se podílí dešťová voda na celkovém výtoku ze sněhové pokrývky s různými vlastnostmi?

      Předpoklad 3: *Dešťová voda je více zastoupena v odtoku z vyzrálé sněhové pokrývky, než z nevyzrálé sněhové pokrývky.*

   d. Jak se mění vlastnosti sněhové pokrývky vlivem deště?

      Předpoklad 4: *Déšť ve sněhové pokrývce způsobuje značné změny, především zvýšení hustoty, teploty, obsahu kapalné vody a obsahu deuteria.*

4. Výsledky

4.1. Článek I - A portable simulator for investigating rain-on-snow events

Juras, R., Pavlásek, J., Děd, P., Tomášek, V. and Máca, P.: A portable simulator for investigating rain-on-snow events, Zeitschrift für Geomorphol. Suppl. Issues, 57(1), 73–89, doi:10.1127/0372-8854/2012/S-00088, 2013.

Zeitschrift für Geomorphologie, Supplementary Issue
Published online June 2012

Fast Track Article

A portable simulator for investigating rain-on-snow events

R. Juras, J. Pavlásek, P. Děd, V. Tomášek and P. Máca

with 9 figures and 3 tables

Abstract. This paper deals with ways of simulating rain-on-snow events caused by high-intensity, short-duration precipitation. A low-cost rainfall simulator was developed for the purposes of this experiment. This device enables rainfall of varying intensity and duration to be simulated, and automatically monitors some components of the mass and energy balance, consisting of the outflow rate, the temperature of the inflow and outflow water, the air temperature, and the temperature in various positions in the snow cover. Artificial rain intensities ranging from 40 mm h^{-1} to 100 mm h^{-1} produced by a single nozzle under water pressure ranging from 0.7 bar to 1.65 bar were tested. The results of a field test revealed a limited retardation and transformation function of ripe snow cover during extreme rainfall events.

Keywords: Rainfall simulation, snow, outflow, water behaviour in snow

1 *Introduction*

Rainfall simulators have been employed for simulating rainfall-runoff processes for many years (e.g., Kincaid et al. 1964). These devices are used not only for investigations of rainfall-runoff processes, but also for making physical models of infiltration, irrigation, erosion (DeLima et al. 2002, Gonzales-Hidalgo et al. 2004) and nutrient movement (Withers et al. 2007). They provide a very powerful tool. Soil moisture can be measured simultaneously using Time Domain Reflectometry (TDR) during a rainfall simulation (Gonzales-Hidalgo et al. 2004). Rainfall simulators can be divided into several groups. The first category comprises laboratory simulators (e.g., DeKlerk 1992, Hignett 1995) and portable field simulators (e.g., Covert & Jordan 2009, Martinez-Zavala et al. 2008). Rainfall simulators can also be categorized according to the type of raindrops that are generated: a) drop-forming simulators, where the droplets start at zero velocity (Blanquies et al. 2003, Dimoyannis et al. 2001), and b) pressurized nozzle simulators, which need higher water pressure (Blanquies et al. 2003, Covert & Jordan 2009, Erpul et al. 1998), which is in most cases provided by a water pump; the initial raindrop velocity created by simulators of this type is greater than zero (Blanquies et al. 2003). Simulators with moving nozzles (oscillating, waggling) (e.g., DeKlerk 1992, Hamed et al. 2002) and with stable nozzles having the same position during the whole rainfall process (e.g., Arnáez et al. 2004, 2007, Covert & Jordan 2009) can also be distinguished. Some authors also include wind force in the rainfall simulating process. These experiments require a rainfall simulator placed in a wind tunnel (DeLima 2002, Erpul et al. 1998, Fister et al. 2012, Fister et al. 2011). However, some authors try to minimize the wind effect by placing wind protection along the structure of simulator (Arnáez et al. 2004, Martinez-Zavala et al. 2008). This approach enables a pure study of the effect of rain on the ground (Covert & Jordan 2009). Fister et al. (2011) carried out a comparison between a combined wind & rainfall simulator and a small portable rainfall wind protected simulator.

www.borntraeger-cramer.de
DOI: 10.1127/0372-8854/2012/S-00088
0372-8854/12/S-00088 $ 4.00

Rainfall simulators can also be used for investigating rainfall-runoff processes in snow covered areas, especially the behaviour of liquid water in snow. These simulators are quite rare. Two devices were constructed by Singh et al. (1997) and were used in the Austrian Alps, where the rainfall was generated by two horizontally moving pipes with holes fitted with nozzles. The possible simulated rainfall intensity varied from 20 mm h^{-1} to 200 mm h^{-1}, but only intensities from 48 mm h^{-1} to 100 mm h^{-1} were simulated during field experiments. During the simulations, measurements were also made of the rate of the surface outflow below the snowpack, and the infiltration rate to the soil was estimated by changes in soil moisture measured using TDR equipment.

Simulations of rain-on-snow events are useful mainly for understanding infiltration into the snowpack or the water flow rate in snow – a very important feature especially for forecasting natural hazards (Kobayashi & Motoyama 1985). Infiltration of water into the snowpack was mainly studied by spreading water on the snow surface (Conway & Benedickt 1994, DeWalle & Rango 2008) or through changes of temperature inside the snowpack (Conway & Benedickt 1994). When constructing rain-on-snow simulators, it is necessary to take into consideration the differences between the behaviour of water on snow and water on soil. The snow cover can contain water from a rain event, or it can contain liquid water caused by snow melting (Decaulne & Sæmundsson 2006). In most cases, these two processes act together (Decaulne & Sæmundsson 2006). Rain water moves several times faster in a snowpack than natural snowmelt water under no-rain conditions (Singh et al. 1997). For this reason there is a higher flood risk from rain-on-snow events than from snowmelt alone. (Kattelmann 1997, Singh et al. 1997, Sui & Koehler 2001). In January 2011, there were large floods caused by rain-on-snow events in Germany (HND Bayern 2011, Böhm et al. 2011) and in the Czech Republic (Čekal et al. 2011). Highest flood alerts were announced during these events. Spring floods with a return period higher than 100 years were observed in the Czech Republic in 2006 (Kašpárek et al. 2006).

However, the snowpack can act as a retarding element, and it delays water runoff from a watershed (Kobayashi & Motoyama 1985). Newly fallen snow can store a significantly higher volume of liquid water than ripe snow (Singh & Singh 2001).

Water flux in the snowpack depends on the precipitation rate and on the rate of freezing, as determined by the thermal conditions in the snowpack (Conway & Benedickt 1994). The holding capacity of the snowpack is driven by temperature, stratigraphy, grain size and snow age (Singh et al. 1997, Singh & Singh 2001). If the snow temperature is below zero, the water will freeze. Water can also be accumulated above the impermeable layer (ice, frozen ground) (Singh 1997, Singh & Singh 2001). The presence of water in the snowpack accelerates the snow metamorphism and coarsening of the snow grains (Singh 1997, Tusima 1985) and can cause instability, often leading to the formation of avalanches (Conway & Raymond 1993, Singh & Singh 2001) or slushflows (Smart et al. 2000, Tómasson & Hestnes 2000).

The theory of possible water behaviour in the snowpack is well described, but there is still lack of an appropriate field data for evaluating and quantifying the water behaviour in the snowpack with various properties. Simulation of rain-on-snow events requires improved rainfall simulators in order to monitor the mass and energy balance components, which are needed for an evaluation of the complicated processes in the snowpack during these events. The objective of this paper is to describe the development and a field test of a low-cost portable rain-on-snow simulator that enables monitoring of the water balance components (water inflow and outflow) and also of the

energy balance components (inflow and outflow water temperature, air temperature, and changes of temperatures inside the snowpack).

This leads to the first research question, which is: Is it possible to provide a detailed study of processes inside the snowpack using low-cost equipment that measures only water flow and temperature? The second question is: Is it possible to evaluate the role of the snowpack during extreme rainfall-runoff events using this type of rain-on-snow simulator?

2 *Materials and methods*

The rain-on-snow experiment included several processes: constructing a simulator with appropriate improvements, calibrating the simulator, a field test, and an evaluation of the results. When the simulator was being constructed, the limited budget available for the whole experiment was at all times an important consideration.

2.1 *Rainfall simulator*

The design of the rainfall simulator presented here was inspired by the classical portable nozzle-type simulators used for studying erosion and rainfall-runoff processes. The required rainfall simulator has to meet criteria similar to those for the rainfall simulators used in studies of erosion. The simulator must: 1) be able to generate multiple and uniform rainfall intensity, 2) be able to provide reproducible measurements and 3) be a portable and compact device. The device for simulating rain-on-snow events has in addition several improvements over widely-used simulators: 1) an adjustable nozzle and frame height according to snow depth, 2) automatic runoff measurement, and 3) multichannel temperature measurement.

2.1.1 *Structure*

The frame of the device is made of steel. The components of the frame can slide inside each other. The size of the rainfall simulator is adjustable, and the frame can hold up to nine nozzles. The position of the nozzles above the snow cover can be adjusted according to the requirements for the measurements. The main dimensions are displayed in Table 1. It must always be borne in mind that the vertical position of the nozzle affects the kinetic energy of droplets that penetrate the snow cover.

Table 1. Dimensions of the rainfall simulator.

Min frame height [cm]	100
Max frame height [cm]	250
Min nozzle height [cm]	30
Max nozzle height [cm]	250
Min number of nozzles	1
Max number of nozzles	9
Side length [cm]	120
Coverage area [m^2]	1

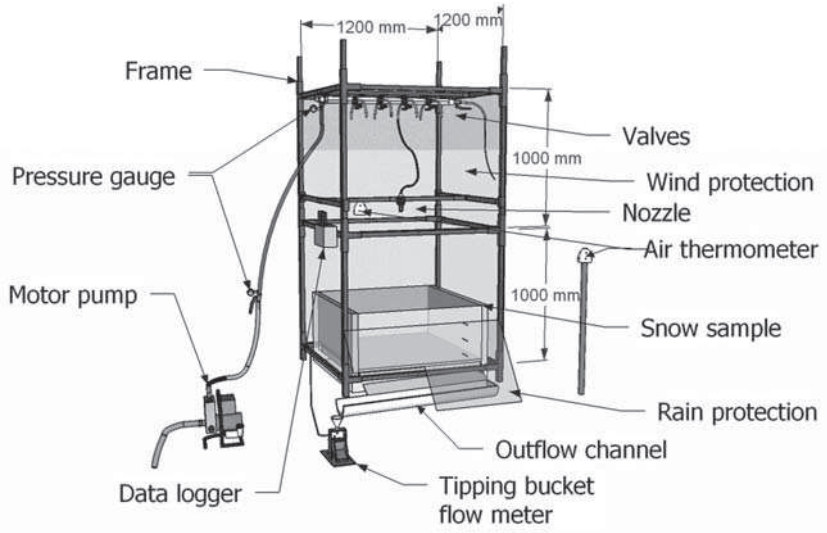

Fig. 1. Design of the rainfall simulator. The vertical position of the nozzle above the snow sample can be adjusted to different levels. The picture shows only one FullJet 1/8 GG3 6SQ nozzle, but the device can hold up to nine nozzles.

The structure and the measurement principle are presented in the sketch (Fig. 1). The height of the frame can be increased with the aid of four legs on the bottom corners. The legs are designed to get the simulator into a levelled horizontal position if the rainfall simulation runs on uneven terrain. The height of the nozzle must be adjustable, and it must be possible to increase the height by the legs on the corners, so that various depths of the snowpack can be sprayed from 15 cm to 150 cm, even on comparatively steep slopes. A tarpaulin wind barrier should be placed along the structure, because even a gentle wind can affect the trajectory of the rain droplets (DeLima et al. 2002) and this makes it complicated to determine the amount of rain on the plot (Covert & Jordan 2009).

2.1.2 *Rainfall generation*

The main purpose of the rainfall simulator presented here is to generate high-intensity short-duration rainfalls, usually lasting from 15 minutes to 45 minutes (but other durations can also be used). During natural events with similar properties, only small changes in snow structure and snow water equivalent (SWE) have been observed (Hanková et al. 2008), so these events are suitable for evaluating rainwater behaviour in the snowpack with only a small contribution of snowmelt water. The device was developed to produce rain intensities from 40 mm h^{-1} up to more than 400 mm h^{-1}. However, practical simulations should be carried out for lower intensities (e.g., up to 100 mm h^{-1}) according to the maximum natural values in the area of interest. The simulated intensities (40–98 mm h^{-1}) were estimated according to Němec (1964) for the location of Kvilda (Šumava Mts. in the Czech Republic) for duration 15 min and return period 1–15 years. Singh et al. (1997) used similar intensities in experiments ranging from 48 mm h^{-1} to 100 mm h^{-1}. The

simulator presented here generates these intensities with by a single FullJet 1/8 GG3 6SQ nozzle with a squared coverage of more than 1 m^2. The showered area can be enlarged by employing more nozzles. Thanks to their interchangeability, nozzles with a round area of coverage can also be employed. The vertical and horizontal position of the nozzles can be adjusted according to the requirements of a specific simulation. Each nozzle is switched on/off by a ball valve. The main ball valve behind the motor pump can switch the whole simulation process on/off, and ball valves can also be used to adjust the water pressure in the system. The maximum pressure in the system is controlled by a removable 1.8 bar safety valve. The water pressure is not measured directly on the nozzle (Fig. 1), but in front of the nozzle on the income piping. This system enables the same simulating pressure conditions to be set for each event. The rainfall intensity is driven by the water pressure and by the rain coverage on the plot, which depends on the water pressure and on the vertical position of the nozzle above the snow cover. The nozzles were calibrated by the manufacturer. The producer guarantees for droplets from 5 % to 95 % percentile diameters from 0.74 mm to 2.90 mm at 0.7 bar and 0.56 mm to 2.20 mm at 2.8 bar. Even area distribution is also guaranteed. The kinetic energy was not estimated.

Water is supplied by a Gardena 9000/3 classic motor pump, which is connected to the simulator by a garden hose 1" in diameter. The system uses water from a local source. If no natural water source is available, any water tank with water recirculation can be used, and the outflow water is reused for sprinkling. Up to 20 % of water losses during water recirculation were estimated, mainly due to droplets landing outside the plot.

The experiment was designed to simulate rain-on-snow events, which usually occur at temperatures around freezing point or higher. For this reason, the system does not deal with problems of water freezing in the pipes or nozzles, the incoming water being warmed up by about 2 °C by the heat generated by the pump.

2.1.3 *Outflow measurement*

Accurate measurement of the outflow water provides some of the most important information for estimating the mass balance. The water drained within the snow matrix is collected on a 100 × 100 cm metal sheet, placed above the surface of the ground. This kind of water flow measurement provides an accurate estimate of the water outflow from the snowpack as a part of the mass balance. To monitor the changes in soil moisture used by SINGH et al. (1997), it is necessary to install soil moisture sensors in the soil below the snow sample. This can be difficult when the soil is frozen, and it can also disturb the sample. The collected water goes to the tipping bucket flow meter (Fig. 2), which is connected to the data logger, which counts the number of tips every minute operated by a reed switch with contact resistance of 150 mΩ. Automatic outflow measurement is required, because it enables long-term outflow monitoring for various experimental designs, and it is also much more comfortable and less time-consuming for operating an experiment. Below the tipping bucket, the outflow water can be collected for the laboratory analyses.

2.1.4 *Temperature measurement*

Digital programmable 1-wire thermometers DS18B20 were used for all temperature measurements. These thermometers cover the range from -55 °C to +125 °C; resolution 0.0625 °C, and ac-

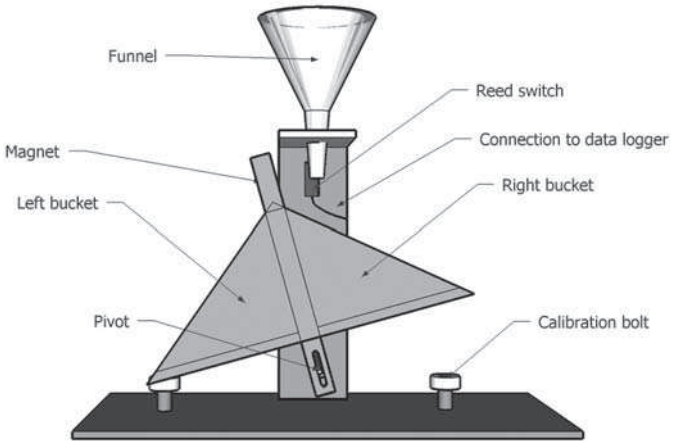

Fig. 2. Tipping bucket flow meter connected to the data logger.

curacy to ± 0.5 °C is guaranteed over the range from -10 °C to +85 °C. The temperature drift after a 1000-hour stress test at +125 °C is 0.2 °C. This range is wide enough, because the simulation is designed mainly for the melting period, when the air temperature is usually not far below zero. The measurement has to be set by the software prior to each experiment. Up to 16 thermometers can be connected to the data logger. During the simulation, the following temperatures are measured: 1) snow, 2) water, and 3) air.

It is important to measure the snow temperature in several points to determine the extent of the influence that the rain has had on the snow cover. CONWAY & BENEDICKT (1994) conducted an extensive study of the influence of rain on the temperature of the snow. Up to 12 thermometers can be used to measure the snow temperature in various positions. For more accurate measurement, the sensors are placed inside an aluminium tube, which helps the sensors to penetrate into the hard snow. The tubes also minimize the heat flux in cables heated by solar radiation or by the temperature of the air outside the sample. The distance of the thermometers inside the snowpack should be at least 10 cm to avoid the preferential pathways in the snowpack.

The inflow and outflow water temperature must also be measured in order to assess the amount of latent heat transferred from the water to the snow. The thermometers for the input and output water temperature are placed under the nozzle and under the outflow edge of the metal sheet, respectively.

For an estimation of the potential natural snow melt, the air temperature has to be measured. Two thermometers are used to estimate the air temperature inside and outside the rainfall simulator. The air temperature close to the snow surface can also be measured.

2.1.5 *Data logger*

A special tailor-made data logger was developed for the purposes of outdoor measurements (Fig. 3). The data logger was constructed as a simple and resistant device that can be used for recording temperature and flow rate data. The energy is supplied by a 6 V to 12 V battery, and the

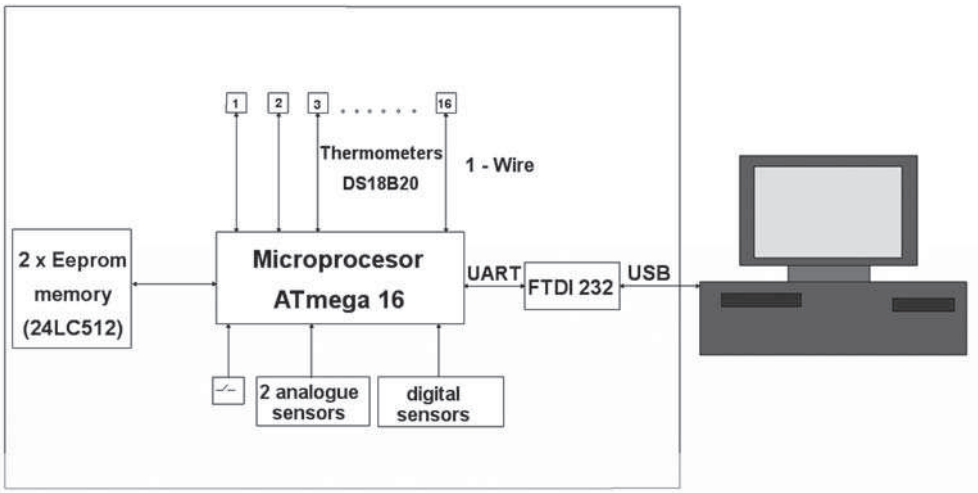

Fig. 3. Block diagram of a data logger.

energy consumption is 10 mA in active mode and 2 mA in standby mode. The data logger has 16 digital inputs for thermometers and one digital input for the flow meter. Not all the thermometers have to be used, and the number of connected thermometers is determined by the user. Two analogue inputs for 0–2.5 V with 256 bit resolution are also available. These analogue inputs can be used for a random sensor, for example for a photoresistor to determine the solar radiation. The data logger is driven by an ATmega 16 microprocessor. Two EEPROM memories are available for data storage, each with a capacity of 64 kB. A maximum of 32,000 records can be stored in one memory. The data recording frequency can be set from one minute to one day. Data download to a PC is enabled by a USB interface; the data download and the data logger setting prior to the measurement is software-driven. Several settings have to be made prior to the measurement: date, frequency of data input and selection of active sensors.

The status of the data logger is indicated by colour diodes. A blue diode blinks to indicate measurement in progress; activation of the digital flow meter is signalled by a green diode. The status of the control buttons is indicated by a yellow diode, and a red diode signals an alert for an active measurement or data transfer by a single blink; constant light of the red diode indicates a measurement error.

2.2 *Calibration*

Before the field test, the rainfall simulator was calibrated. The calibration focused on the nozzles and the tipping bucket used for outflow measurement.

2.2.1 *Calibration of the nozzles*

The rainfall intensities produced by the nozzles were calibrated on site under various water pressures and in two different vertical positions. The nozzle was placed at a height of 102.5 cm and

then 144.5 cm above the snow cover. The minimum rainfall intensity provides water pressure of 0.7 bar. It is important to set up the minimum rainfall intensity in order to determine the limits of the simulator. During the calibration rainfalls, pressures between 0.7 bar and 1.65 bar were simulated. The rainfall intensity was determined by the volume of the outflow from the calibrating plot 100 × 100 cm in area, which was showered with artificial rain. A calibrating plot made of a metal sheet was covered with a layer of soft foam 1 cm in thickness, which minimizes the effect of the kinetic energy of rain, causing back reflection of rain drops. When the soft foam was fully saturated, the inflow was equal to the outflow, and then the rainfall intensity was measured. The outflow water was measured directly by a calibrated vessel.

2.2.2 *Tipping bucket calibration*

The tipping bucket was calibrated in the laboratory. For accurate determination of the volume of water, the water was poured from a burette (static calibration) until the bucket tipped. The position of the two buckets can be set by two bolts placed under each of them. When the right position is found, the bolts have to be fixed. The volume of each of the buckets was measured 50 times at the time of tipping.

2.3 *Field test*

The design of the snow plot was inspired by Singh et al. (1997). An undisturbed and even snow cover was selected prior to experiment and then an isolated snow plot was prepared. Next, a snow cube was isolated with only three sides bared at first. The upper area of the cube was at least 150 × 150 cm. When three sides of the cube were ready, the metal sheet was pushed into the snow matrix at an angle of about 5° to provide a gentle hydraulic gradient. The whole experiment set up is shown in the sketch (Fig. 4). With one side not bared during the installation of the metal sheet, the snow matrix was more stable and the metal sheet could be pushed without any disturbance to the snow matrix. Vertical position of sheet metal was selected in respect to the required depth of the snow pack for the purposes of the simulation. Snow sample (30 cm in depth) was showered during the field test.

When the metal sheet was positioned correctly, the fourth side of the cube was also excavated. The size of the snow sample was then carefully reduced to 120 × 120 cm above the metal sheet and 100 × 100 cm under the metal sheet. The upper part of the snow matrix was made larger to avoid the edge effect. In order to simplify the measurements, only the vertical water flow through the snow matrix was considered. After reduction of the snow sample, a drainage channel leading the outflow water to the flow meter was connected to the outflow edge of the metal sheet. The flow meter had to be placed at least 35 cm below the outflow edge of the metal sheet. Next, the frame of the rainfall simulator was set up. The nozzles were connected to the water supply and their vertical position was adjusted. The nozzle was placed in a vertical position at a height of 144.5 cm above the snow plot, which ensured that the shower would cover the whole area of the snow plot (120 × 120 cm).

To analyze the condition of the snow, a snow pit was excavated and the snow profile was analysed prior to the experiment in the proximity of the rainfall simulator. Measurements of snow

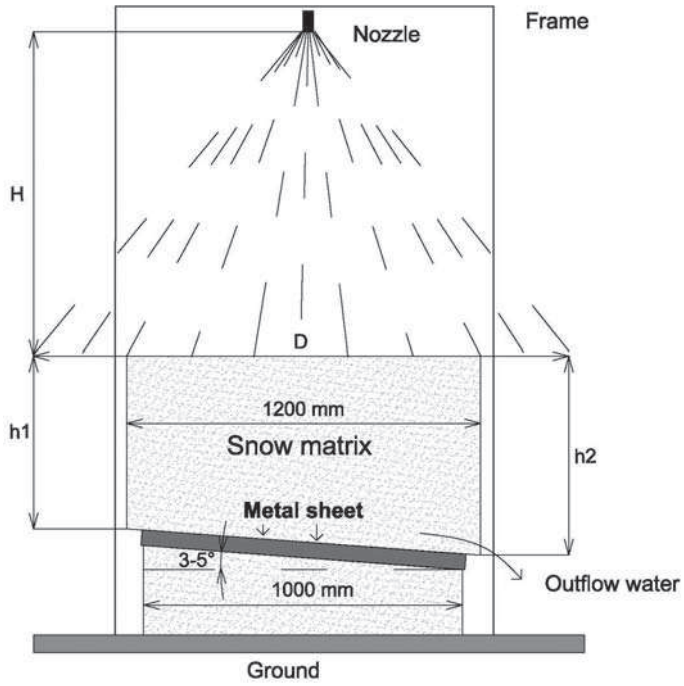

Fig. 4. Field test set up. H – vertical position of the nozzle above the snow surface; h1/h2 – upper/lower snow depth, D – width of the shower.

density [kg m^{-3}], SWE [mm], grain size [mm], snow layer depth [cm], hardness [N] and temperature [°C] were carried out. Similar measurements were also made after the rainfall experiment on the showered snow sample, in order to estimate the reaction of the snow cover to the artificial rain event. The changes in the size of the snow sample cube were also analysed. The amount of stored liquid water was computed by comparing the snow density before and after the experiment.

During the field test, only 7 thermometers were used for measuring the temperature in different positions. Three thermometers were placed inside the snow matrix at various levels to obtain information about the changes in the snow temperature conditions caused by the water flow inside the snow matrix. This is only appropriate for observations of 0 °C isotherm detecting the wetting front, because liquid water can only be contained by snow at a temperature of 0 °C (Conway & Benedickt 1994). The air temperature was measured in two positions – inside and outside the rainfall simulator. The two air thermometers were placed 1.5 m above the ground. Because the structure was protected by a tarpaulin during the simulation, the inside and outside air temperatures differed. The air temperature sensors were protected against direct solar radiation. The temperatures of the inflow water and the outflow water were also measured.

The inflow [mm h^{-1}] and outflow [L min^{-1}] intensities and their cumulative values [L] were measured, and the changes were compared with the changes in SWE during the experiment. From these values, the mass balance was computed and the amount of the rainwater stored in the snowpack during the experiment was estimated.

3 *Results and discussion*

This chapter presents the first results and experiences with the simulator during calibration and the field test.

3.1 *Nozzle calibration results*

The results from calibrating the nozzles under various pressure conditions and the regression of rainfall intensity estimation on the basis of the water pressure in the system are shown in the graph in Fig. 5, and in Table 2. The rainfall intensities used for the pressure conditions in the test ranged from 64 mm h^{-1} up to 98 mm h^{-1}. As these results show, the higher the pressure the greater the rainfall intensity is. This is also confirmed by the calibration provided by the producer. The dependence of rainfall intensity on the pressure in the system is well described by formulas with high R^2 coefficient values.

The stability of the simulated rainfall intensity was tested on the cumulative rainfall depth under various pressure conditions. The results of the calibration test for pressures of 0.75 bar, 1.0 bar and 1.5 bar are shown in Fig. 6. These results indicate a linear relationship with a high R^2 coefficient value, and also confirm higher intensity under higher generated pressure.

3.2 *Tipping bucket calibration results*

Fifty volume measurements were carried out for each bucket during the calibration. The tip volume was determined as 0.075 L throughout the measurements (Fig. 7). A statistical overview is

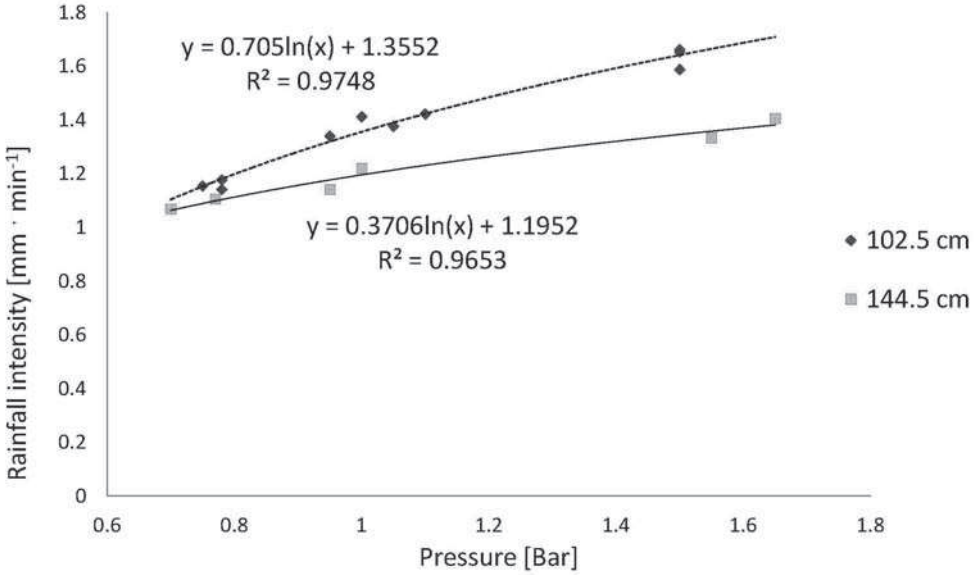

Fig. 5. Dependence of rainfall intensity on water pressure in the system for nozzle position 102.5 cm and 144.5 cm above the surface of the snow.

Table 2. Results of measured rainfall intensities for two different vertical positions of the nozzles with square coverage in different pressure conditions.

Hight above plot [cm]	Nozzle FullJet 1/8 GG3 6SQ						
102.5	0.75	0.78	0.95	1.00	1.10	1.50	Pressure [bar]
	69.23	69.51	80.36	84.71	85.90	98.04	Intensity [mm h^{-1}]
144.5	0.70	0.77	0.95	1.00	1.55	1.65	Pressure [bar]
	64.06	66.30	68.44	73.17	80.00	84.31	Intensity [mm h^{-1}]

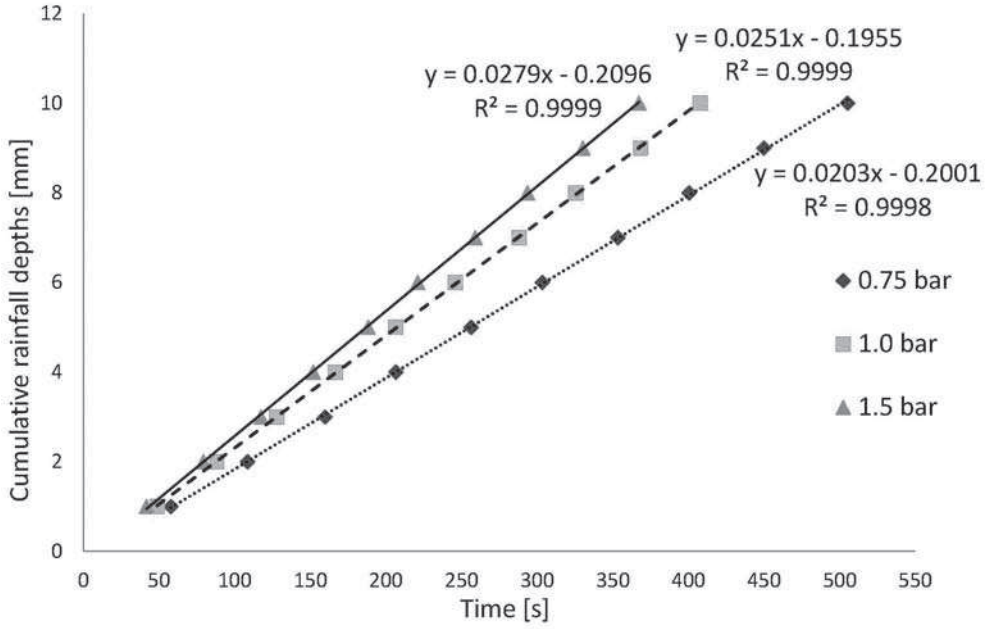

Fig. 6. Stability test of simulated rainfall intensity on cumulative rainfall depth under various water pressure conditions in the system. The nozzle was placed 102.5 cm above the plot.

Table 3. Statistical parameters of the tipping bucket flow meter.

	Mean [ml]	Standard deviation [ml]	Mode [ml]	Median [ml]	Number of measurements
Left bucket	74.0	2.2	72.0	74.0	50
Right bucket	75.5	2.6	74.0	75.5	50
Total	74.8	2.6	74.0	75.0	100

presented in Table 3. This table reveals that the bucket on the right is slightly bigger, but the mean value of the two buckets is more significant for the runoff estimation. The tipping bucket flow meter is constructed to measure outflow ranging from 0.075 L min^{-1} up to 2 L min^{-1}, but a higher

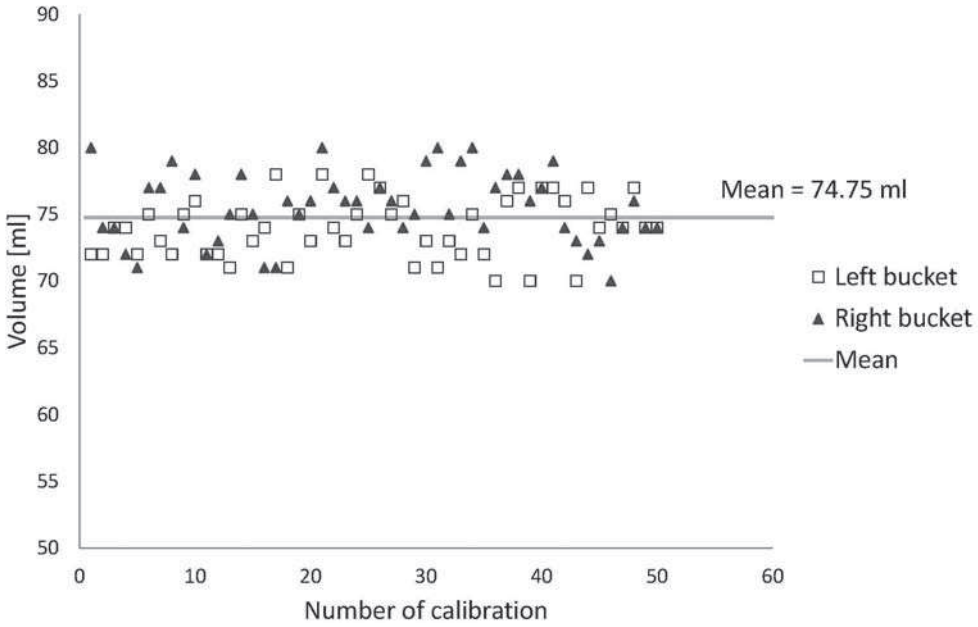

Fig. 7. Tipping bucket calibration results.

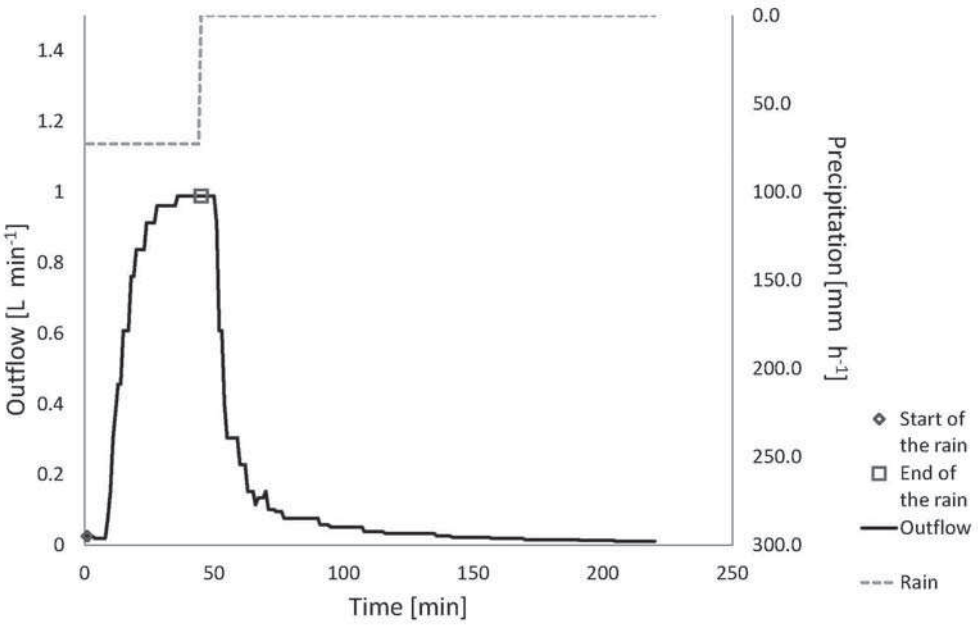

Fig. 8. An example of the outflow from the snowpack during a simulation of a rain-on-snow event.

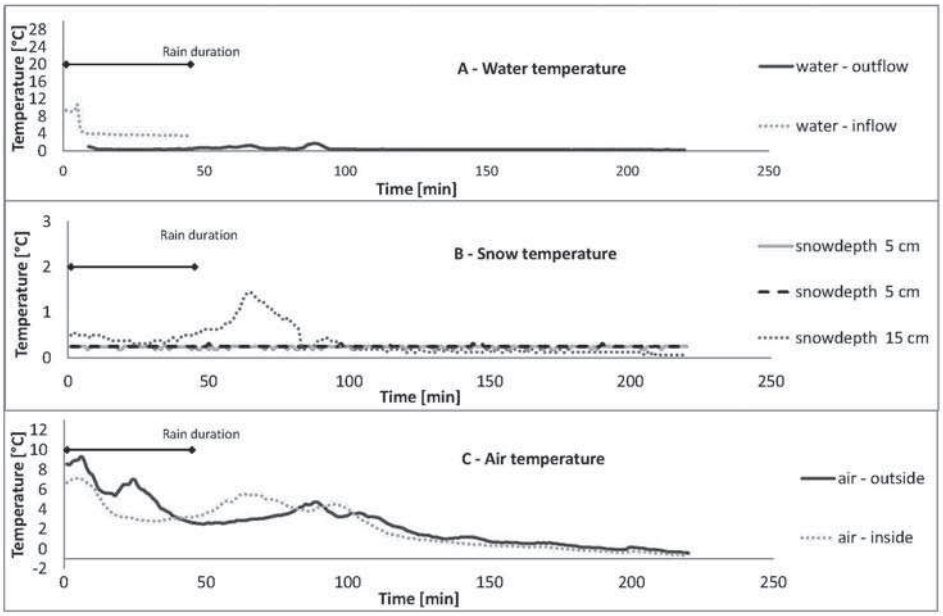

Fig. 9. An example of snow, air and water temperature measurements during the field test. Sensors were placed in three positions inside snow (the snowdepth means the vertical position of the sensors above the metal sheet).

outflow rate can probably also be measured. Some improvements in the accuracy of the tipping buckets are recommended for future work.

3.3 *Field test results*

Examples of outflow measurements and temperature measurements are shown in the Fig. 8 and Fig. 9 respectively. A ripe, homogeneous snow sample with starting density 444 kg m^{-3} and depth 39 cm was showered for 44 minutes by artificial rain with intensity 73 mm h^{-1}.

Several important characteristics according to KATTELMANN (1987) were observed after the field test. The onset lag, i.e., the time gap between the beginning of the rain event and the beginning of the outflow, was 8 minutes, and the peak lag, i.e., the time lag until the outflow peak was measured as 14 minutes. These results might seem to be quite a quick outflow reaction, but it should be taken into consideration that the infiltration into the soil was avoided, and this is probably also a very important factor affecting the outflow rate and the outflow time. This experiment investigated only the behaviour of liquid water in snow without the influence of soil. Another very important characteristic is the time when all the liquid water drains out. This time was estimated to be 96 minutes. Only the total amount of outflow water was measured. This amount consisted of rainfall water, natural melt water and melt water caused by rain. The constant natural snowmelt was measured for 8 minutes before the beginning of the outflow of rainfall water, and was estimated at 0.024 L min^{-1}.

The field test showed that the positioning and the number of thermometers are important parameters. The best results were obtained with the sensors penetrating at least 40 cm horizontally into the snow matrix. The field test results showed that placing thermometers in the snowpack can also affect the water movement. For this reason, the vertical difference between the sensors should be at least 10 cm. The sensor placed 15 cm above the metal sheet shows a temperature higher than 0 °C. This was probably caused by drainage of cold water from the surroundings of the sensor and a subsequent inflow of warmer air from above the snow into the snowpack, which was afterwards gradually cooled down almost to 0 °C. This can play an important role in the subsequent snow melt after a rain event. The higher temperature on the other two sensors is probably caused by the accuracy limits of the thermometers.

Changes were also observed in the stratigraphy and properties of the snowpack. The differences in grain diameter ranged from 0.5 to 1 mm, the hardness mostly decreased, but within the upper layer the hardness increased and some layers merged together. The snow density increased from 444 kg m^{-3} to 452 kg m^{-3} (2 %), and SWE increased from 17.3 cm to 18.1 cm (4 %). From a comparison of the volume of the rainfall and the changes in SWE it was estimated that approximately 15 % (8 mm) of the rainwater was stored in the snow cover during the experiment. These results show the retardation and accumulation function of snow cover during rains of high intensity and relatively short duration.

The energy balance results from the temperature measurement indicate a higher amount of snow melt due to the input of energy from the rainwater with an average temperature of around 4.5 °C, which was cooled down almost to 0 °C in the output.

The resulting outflow from the snow sample is the product of three processes in the snowpack: natural melting caused by higher air temperature, melting of the snow grains caused by warmer rainwater, and the rainwater itself flowing through the snowpack. For a more accurate estimate of the energy balance and of the ratio of these three components in the snowpack, additional monitoring of other components of the energy balance needs to be carried out. This monitoring should include components such as net radiation, latent heat transfer to or from the soil, etc.

4 *Conclusions*

A rainfall simulator for simulating rain-on-snow events was constructed, calibrated and subsequently tested on site. This device enables measurements not only of rainfall intensity, but also of some components of the energy and mass balance, which were used for describing the processes in the snow cover. The mass balance was estimated by comparing the input and output water volumes, and the simple energy balance was assessed from the temperatures of the inflow and outflow water and from the temperature changes inside the snowpack.

The mass balance and the simple energy balance can be calculated for a description of processes in the snowpack, but more components of the energy balance need to be taken into consideration for an accurate description of the processes in snow cover. The temperature of the water and snow should be measured, and an estimate should also be made of the sensible and latent heat. The presented data from monitoring the temperatures enables only a lower-accuracy estimation of the energy balance and for higher-accuracy estimation of energy balance more components are needed to be measured (global radiation, etc.).

The field test results indicate that a ripe snowpack (firn) plays a limited role during extreme rainfall events. The snow cover caused a lag of the peak discharge in the range of minutes, and the amount of input water stored in the snowpack was 8 mm, i.e., 4 % of SWE.

The whole testing system, which cost less than EUR 4 000, is a suitable device for simulating extreme rain-on-snow events. Nevertheless, further tests and measurements are highly recommended. In the future, more components of the energy balance of the system need to be included in order to obtain more accurate information about the temperature changes caused by water flow in snow.

Acknowledgements

The authors would like to thank many people and institutions without which the simulator could not have been made. The project was funded by Czech University of Life Sciences (CIGA ČZU v Praze) grant No. 20104203. In addition, we would like to thank Deutsche Bundesstiftung Umwelt, Deutscher Alpenverein, the Pavlásek family and the Gruber family for their support, Prof. Wolfgang Fellin, Dr. Achim Heilig, Dr. Wilfried Hagg, Mrs. Lisa Mayr for consulting the design of the device, Mr. Šnejdar, Mr. Beneš, Mr. Karas and Mr. Jošt for their help during the construction. We owe our special thanks to Horská služba Šumava, Kvilda Department, for the incredible support provided during the field test. Finally, we would like to thank Mr. Zbyněk Klose for his help during testing.

References

Arnaez, J., Larrea, V. & Ortigosa, L. (2004): Surface runoff and soil erosion on unpaved forest roads from rainfall simulation tests in northeastern Spain. – Catena **57:** 1–14.

Arnaez, J., Lasanta, T., Ruiz-Flano, P. & Ortigosa, L. (2007): Factors affecting runoff and erosion under simulated rainfall in Mediterranean vineyards. – Soil & Tillage Res. **93:** 324–334.

Blanquies, J., Scharff, M. & Hallock, B. (2003): The design and construction of a rainfall simulator. – International Erosion Control Association (IECA), 34th Annual Conference and Expo, Las Vegas, Nevada, February 24–28, 2003. Available on-line at: (www.owp.csus.edu/research/papers/papers/PP044.pdf); accessed 15.10.11.

Böhm, U., Fiedler, A., Machui-Schwanitz, G., Reich, T. & Schneider, G. (2011): Hydrometeorological analysis of the snow and thaw situation in December 2010/January 2011 in Germany – German Weather Service, Department of Climate and Environment. Available online at: (http://www.dwd.de/bvbw/generator/DWDWWW/Content/Wasserwirtschaft/Unsere__Leistungen/Schneeschmelzvorhersage/KU4__Tauwetter__2010__11__lang__pdf,templateId = raw,property=publicationFile.pdf/KU4_Tauwetter_2010_11_lang_pdf.pdf); accessed 27.12.2011 (in German).

Conway, H. & Benedickt, R. (1994): Infiltration of water into snow. – Water Resour. Res. **30:** 641–649.

Conway, H. & Raymond, C.F. (1993): Snow stability during rain. Journal of Glaciology 39: 635-642.

Covert, A. & Jordan, P. (2009): A portable rainfall simulator: Techniques for understanding the effects of rainfall on soil erodibility. – Streamline Watershed Manag. Bull. **13:** 5–9.

Čekal, R., Ryglewicz, M., Fryč, T., Bořík ová, L., Suchá, M., Přibyl, J. & Kotek, R. (2011): A report about a flood in January 2011. – Czech Hydrometeorol. Inst., available online at: (http://portal.chmi.cz/files/portal/docs/hydro/ohp/povoden_01_2011.pdf); accessed 27.12.2011 (in Czech).

Decaulne, A. & Sæmundsson, Þ. (2006): Meteorological conditions during slushflows release and their geomorphological impact in northwestern Iceland: A case study from the Bíldudalur Valley. – Geograf. Ann. **88** A (3): 187–197.

DeKlerk, F.R. (1992): The programmable rainfall simulator. – Department of Irrigation and Soil & Water Conservation, Wageningen Agricultural University, 25 pp.

DeLima, J.L.M.P., Torfs, P.J.J.F. & Singh, V.P. (2002): A mathematical model for evaluating the effect of wind on downward-spraying rainfall simulators. – Catena **46:** 221–241.

DeWalle, D.R. & Rango, A. (2008): Principles of snow hydrology. – Cambridge University Press, New York, 410 pp.

Dimoyiannis, D.G., Valmis, S. & Vyrlas, P. (2001): A rainfall simulation study of erosion of some calcareous soils. – Global Nest **3:** 179–183.

Erpul, G., Gabriels, D. & Janssens, D, (1998): Assessing the drop size distribution of simulated rainfall in a wind tunnel. – Soil & Tillage Res. **45:** 445–463.

Fister, W., Iserloh, T., Ries, J.B. & Schmidt, R.-G. (2012): A portable wind and rainfall simulator for in situ soil erosion measurements. – Catena **91:** 72–84, doi: 10.1127/0372-8854/2011/0055S3-0054.

Fister, W., Iserloh, T., Ries, J.B. & Schmidt, R.-G. (2011): Comparison of rainfall characteristics of a small portable rainfall simulator and portable wind and rainfall simulator. – Z. Geomorph. **55:** 109–126.

Gonzales-Hidalgo, J. C., De Luíz, M., Raventóz, J., Cordina, J. & Sánchez, J.R. (2004): Hydrological response of Mediterranean gorse shrubland under extreme rainfall simulation event. – Z. Geomorph. **48:** 293–304.

Hamed, Y., Albergel, J., Pépin, Y., Asseline, J., Nasri, S., Zante, P., Berndtsson, R., El-Niazy, M. & Balah, M. (2002): Comparison between rainfall simulator erosion and observed reservoir sedimentation in an erosion-sensitive semi-arid catchment. – Catena **50:** 1–16.

Hanková, R., Klose, Z., Pavlásek, J. & Skalská, P. (2008): Quantitative and qualitative development of snow cover on experimental catchment Modrava 2. – In: Kyselová, D., Hrušková, K. & Slivka, M.: International snow meeting 2008, conference proceedings, SHMI Bratislava, ISBN 978-80-88907-62-6, 39–46 (in Czech).

Hignett, C.T., Gusli, S., Cass, A. & Besz, W. (1995): An automated laboratory rainfall simulation system with controlled rainfall intensity, raindrop energy and soil drainage. – Soil Technology **8:** 31–42.

HND Bayern (2011): Hydrological monthly report January 2011 – Flood. – Available online at: (http://www.hnd.bayern.de/ereignisse/monatsberichte/md_fghw_0111.pdf); accessed 27.12.2011 (in German).

Kašpárek et al. (2006): Evaluation of Spring Flood 2006 in the Area of the Czech Republic. – VUV Prague (in Czech).

Kattelmann, R. (1987): Water release from a forested snowpack during rainfall. Forest Hydrology and Watershed Management (Proceedings of the Vancouver Symposium, August 1987). – IAHS-AISH Publication **167:** 265–272.

Kattelmann, R. (1997): Flooding from rain-on-snow events in the Sierra Nevada. – Destructive Water: Water-Caused Natural Disasters, their Abatement and Control (Proceedings of the Conference held at Anaheim, California, June 1996). – IAHS Publication **239:** 59–65.

Kincaid, D.R., Gardner, J.L. & Schreiber, H.A. (1964): Soil and vegetation parameters affecting infiltration under semiarid conditions. – IASH Publication **65:** 440–453.

Kobayashi, D. & Motoyama, H. (1985): Effect of snow cover on time lag of runoff from a watershed. – Ann. Glaciol. **6:** 123–125.

Martinez-Zavala, L., López Jordán, A. & Bellinfate, N. (2008): Seasonal variability of runoff and soil loss on forest road backslopes under simulated rainfall. – Catena **74:** 73–79.

Němec, J. 1964: Engineering hydrology. – SNTL Prague, 236 pp. (in Czech).

Singh, P., Spitzbart, G., Hübl, H. & Weinmeister, H.W. (1997): Hydrological response of snowpack under rain-on-snow events: a field study. – J. Hydrol. **202:** 1–20.

Singh, P. & Singh, V.P. (2001): Snow and Glacier Hydrology. – Kluwer Academic Publisher Group, Netherlands, 764 pp.

Smart, C.C., Owens, I.F., Lawson, W & Morfia, A.L. (2000): Exceptional ablation arising from rainfall-induced slushflows: Brewster Glacier, New Zealand. – Hydrol. Proc. **14:** 1045–1052.

Sui, J. & Koehler, G. (2001): Rain-on-snow induced flood events in Southern Germany. – J. Hydrol. **252:** 205–220.

Tómasson, G.G. & Hestnes, E. (2000): Slushflow Hazard and Mitigation in Vesturbyggd, Northwest Iceland. – Nordic Hydrol. **31** (4/5): 399–410.

Tusima, K. (1985): Grain coarsening of snow particles immersed in water and solutions. – Ann. Glaciol. **6:** 126–129.

Withers, P.J.A., Hodgkinson, R.A., Barberis, E., Presta, M., Hartikainen, H., Quinton, J., Miller, N., Sisák, I., Strauss, P. & Mentler, A. (2007): An environmental soil test to estimate the intrinsic risk of sediment and phosphorus mobilization from European soils. – Soil Use and Manag. **23:** 57–70.

Addresses of the authors:

R. Juras, J. Pavlásek, PhD and P. Máca, PhD, Department of Water Resources and Environmental Modeling, Faculty of Environmental Sciences, Czech University of Life Sciences, Prague, Czech Republic, juras@fzp.czu.cz, pavlasek@fzp.czu.cz, maca@fzp.czu.cz.

P. Děd, PhD, Department of Electrical Engineering and Automation, Faculty of Engineering, Czech University of Life Sciences, Prague, Czech Republic, ded@tf.czu.cz

V. Tomášek, Department of Ecology, Faculty of Environmental Sciences, Czech University of Life Sciences, Prague, Czech Republic, tomasekv@fzp.czu.cz

4.2. Článek II - Isotopic tracing of the outflow during artificial rain-on-snow event

Juras, R., Pavlásek, J., Vitvar, T., Šanda, M., Holub, J., Jankovec, J. and Linda Miloslav: Isotopic tracing of the outflow during artificial rain-on-snow event, J. Hydrol., 1, 1145–1154, doi:http://dx.doi.org/10.1016/j.jhydrol.2016.08.018, 2016.

Journal of Hydrology 541 (2016) 1145–1154

Contents lists available at ScienceDirect

Journal of Hydrology

journal homepage: www.elsevier.com/locate/jhydrol

Research papers

Isotopic tracing of the outflow during artificial rain-on-snow event

Roman Juras [a], Jirka Pavlásek [a,*], Tomáš Vitvar [a,b], Martin Šanda [b], Jirka Holub [a], Jakub Jankovec [b], Miloslav Linda [c]

[a] Faculty of Environmental Sciences, Czech University of Life Sciences Prague, Kamýcká 129, 165 21 Prague – Suchdol, Czech Republic
[b] Faculty of Civil Engineering, Czech Technical University in Prague, Thákurova 7, 166 29 Prague 6, Czech Republic
[c] Faculty of Engineering, Czech University of Life Sciences Prague, Kamýcká 129, 165 21 Prague – Suchdol, Czech Republic

ARTICLE INFO

Article history:
Received 21 March 2016
Received in revised form 1 July 2016
Accepted 11 August 2016
Available online 16 August 2016
This manuscript was handled by L. Charlet, Editor-in-Chief, with the assistance of Jesús Mateo-Lázaro, Associate Editor

Keywords:
Deuterium tracer
Rainfall simulator
Snowmelt
Water retention of snow
Hydrograph separation

ABSTRACT

The frequency of rain-on-snow (ROS) occurrence is increasing and this natural phenomenon is beginning to play an important role in temperate climate regions. Present knowledge of outflow generation mechanisms and rainwater dynamics during ROS is still insufficient. The study introduces a combined method of artificial ROS, isotopic tracing and energy balance to partition the event rainwater and the pre-event non-rainwater in the outflow. A rainfall simulator and water enriched with deuterium were used for identifying event rainwater and pre-event non-rainwater during an ROS event.

The ROS experiment was conducted in the Krkonoše Mountains in the Czech Republic. An experimental snow block consisting of ripe and isothermal snow was sprayed with deuterium enriched water. The outflow from the snowpack was continuously monitored to gain quantitative and qualitative information about outflow water. The isotopic deuterium content was further analysed from the samples by means of laser spectroscopy in order to separate the hydrograph components. The deuterium content was also analysed from the snow samples gathered before and after the experiment to identify the retention of event rainwater in the snowpack.

Isotopic hydrograph separation revealed that although high rain intensity was applied, the event rainwater represented one half (52.7%) of the total outflow volume. The ripe snowpack retained about one third of the rainwater input (33.6%). Significant changes in the outflowing water quality can therefore be expected during ROS events. This experiment also shows that rainwater during ROS firstly pushes-out the non-rainwater and then contributes to the outflow. These results show that the presented technique allows us to gain sufficient information about rainwater dynamics during ROS.

1. Introduction

Rain-on-snow (ROS) events with associated snowmelt and snowpack transformation are important natural phenomena in temperate climate regions. Event rainwater can be either stored in the snowpack or flow through the snowpack toward the soil surface. Released water from the snowpack reaches the stream through the soil environment, by the surface runoff, or via the lateral flow in the snowpack (Eiriksson et al., 2013). ROS events can significantly increase the risk of floods, especially during snowmelt (Böhm et al., 2011; Čekal et al., 2011; Ferguson, 2000; HND Bayer, 2011; Singh et al., 1997; Sui and Koehler, 2001).

The pioneering study of Ambach and Howorka (1966) and numerous later studies have examined the ROS-induced wet avalanches (Carran et al., 2000; Conway and Raymond, 1993; Conway, 1994; Kattelmann, 1987a; Marshall et al., 1999) and slushflows (Gude and Scherer, 1999; Hestnes and Sandersen, 1987; Tomasson and Hestnes, 2000).

ROS events also affects the water quality in the adjacent streams, because rainwater mostly has a different chemical composition compared to stream water. Whereas Jones et al. (1989) found that up to 20% of the ionic mass in snow may be released by the ROS, significant oscillation of solutes concentration or pH values were observed in the stream water during natural ROS events (Casson et al., 2014; Dozier et al., 1989; Maclean et al., 1995).

Understanding of the processes in the snowpack during ROS is very important for hydrological modelling, natural hazards forecasting and prediction of water quality and chemical composition of the streams. The need to properly understand rainwater

* Corresponding author.
E-mail addresses: juras@fzp.czu.cz (R. Juras), pavlasek@fzp.czu.cz (J. Pavlásek), vitvartom@gmail.com (T. Vitvar), martin.sanda@fsv.cvut.cz (M. Šanda), jholub@fzp.czu.cz (J. Holub), linda@tf.czu.cz (M. Linda).

http://dx.doi.org/10.1016/j.jhydrol.2016.08.018
0022-1694/

behaviour in the snowpack increases with higher ROS frequencies in higher altitudes which are expected in the temperate areas under changed climate conditions (Surfleet and Tullos, 2013).

During ROS events, the rain adds additional volume and energy to the snowpack, which subsequently affects the snowmelt, the snow metamorphism and the snow structure. Rainwater supports additional snowmelt during the warm-up of the snowpack (Kattelmann, 1987a). Liquid water also causes grain coarsening (Conway, 1994; Tusima, 1985), snow settlement and further densification (Marshall et al., 1999). These processes often lead to a weakening of the grain bonds, which can subsequently cause avalanche formation (Conway and Raymond, 1993). The water flow and storage in the snowpack are controlled by several factors, such as snow temperature, snow stratigraphy, grain size and snow ripeness (Colbeck and Davidson, 1973; Kattelmann, 1987b; Singh and Singh, 2001). Previous studies have also shown that new snow can hold much more water than ripe snow (Colbeck and Davidson, 1973; Martinec, 1987; Singh and Singh, 2001). Previous artificial ROS experiments revealed that ripe stratified snow can hold around 7% liquid water and this volume can double near the ice layer surface (Singh et al., 1997). Flowing velocity in the snowpack also affects the hydrological response of the snowpack under heavy rain. Kattelmann (1987a) mentions that this transmission rate is very variable and can reach up to 3 cm min^{-1} during natural ROS events. Several field sprinkling experiments have shown that, in extreme cases, the vertical water flow velocity reaches 10 cm min^{-1} (Kattelmann, 1987a; Singh et al., 1997).

Previous research of snowmelt-dominated ROS events has often been focused on partitioning the hydrograph into the meltwater component and the pre-event (subsurface water) component in the outflow within the catchment scale. This task has often been carried out by use of environmental tracers such as stable isotopes $\delta^{18}O$ and $\delta^{2}H$ (Buttle et al., 1995; Casson et al., 2014; Dinçer et al., 1970; Laudon et al., 2002; Maclean et al., 1995; Suecker et al., 2000). One of the first applications of isotopic tracers was conducted by Dinçer et al. (1970) in the Modrý Důl basin in the Krkonoše Mts, Czech Republic. This pioneering study revealed that two thirds of the total outflow from the catchment during the melting period originated from the subsurface storages. Another analysis of two natural ROS events in Canadian catchments established that rainwater contributed to the total outflow volume by 33% and 50% (Maclean et al., 1995). Nevertheless these studies (Dinçer et al., 1970; Maclean et al., 1995) were focused on the catchment scale, which usually leads to uncertainties in the runoff component separation caused by process heterogeneities at larger scales. However, the assessment of the rainwater ratio contributing to the outflow from the snowpack across scales is critical for understanding of runoff generation processes (Holko et al., 2015) and runoff modelling (Viviroli et al., 2009) up to catchment scale.

In the past decades, the impact of rain on the processes within the snowpack during ROS events has often been addressed using rainfall simulations or artificial snow wetting (Conway and Benedict, 1994; Eiriksson et al., 2013; Feng et al., 2001; Juras et al., 2013; Lee et al., 2010a; Marshall et al., 1999; Singh et al., 1997; Taylor et al., 2001). The most relevant studies are compiled in Table 1. The main focus of these studies addressed the investigation of ROS influence on solute transport through a snowpack (Feng et al., 2001; Lee et al., 2010a, 2008), runoff generation (Eiriksson et al., 2013; Singh et al., 1997), and particular mechanisms of water infiltration into the snowpack (Avanzi et al., 2015; Conway and Benedict, 1994; Kattelmann, 1987b). Some studies also focused on isotopic changes of water flowing through the snow, for instance pouring of isotopically enriched water to a snow-filled column in a cold laboratory environment (Herrmann et al., 1981). In this context, an increase in the $\delta^{18}O$ isotopic content of the outflow water was observed.

However, none of these experimental studies have partitioned the snowpack outflow hydrograph into event rainwater and pre-event non-rainwater in the natural snowpack during the rain event. Our study fills this gap and presents an innovative combination of a rainfall simulation technique with outflow partitioning. The expected main contribution of the experimental facility includes a better understanding of snowpack mass balance and rainwater propagation to the outflow during ROS events. It is assumed that the point scale approach brings more detailed insights into the process of runoff generation in contrast to catchment scale (Dinçer et al., 1970; Maclean et al., 1995) or the wetting of non-natural snow column approach (Herrmann et al., 1981). This paper addresses the main scientific question, whether the presented technique is suitable for investigation of rainwater interaction with snowpack and rainwater dynamics in the outflow.

2. Study site

The experiment was carried out on April 14th and 15th, 2012 near the Labská bouda chalet (50°46′13″N, 15°32′45″E), in the crystalline Krkonoše Mountains (Giant Mountains) in the Czech Republic at an elevation of approximately 1300 m (Fig. 1). The site of the experiment is located in the headwaters of the river Labe catchment, approximately 800 m southeast from the source of the Labe river. This part of the headwaters is oriented southwest-southeast, and the elevation ranges from 1270 m to 1465 m. The weather station, operated by the Czech Hydrometeorological Institute, is located 300 m southwest from the study site. This station monitors: air temperature, precipitation, snow depth, wind speed, wind direction, relative air humidity and global radiation. The mean April air temperature at Labská bouda is 0.6 °C and the mean precipitation sum from November until May is 795.7 mm (1962–2005). The mean duration of snow cover during the same period at the weather station is 161 days. During the 2011–2012 winter season (November–May), the weather station has recorded 944.5 mm of precipitation. The maximum snow depth at the weather station reached 260 cm in February 2012. The catchment is also significantly affected by the west and northwest winds that transport substantial portions of the snow on the leeward slopes and cause uneven snow depth distribution (Janásková, 2006). This fact was supported by the snow depth records from April 14th, 2012, when the snow depth was 144 cm near to the weather station and over 300 cm at the site of the experiment.

3. Material and methods

3.1. Experimental setup

A specially-tailored rainfall simulator (Fig. 2) was used for the experiment which was described by Juras et al. (2013). Water was sprayed on the snow block through a nozzle and the rain intensity was driven by water pressure in the system. The outflow was measured continuously by a tipping bucket flow meter (Fig. 3). The whole experiment lasted 734 min, from the beginning of the snow melt water recording (April 14th 2012 at 12:45) until the end of the discharge recording (April 15th 2012 at 0:59). Stable weather prevailed during the entire experiment. The air temperature varied between +0.8 °C at the beginning of the experiment and −0.3 °C at the end of the experiment. The temperature of the artificial rainwater varied between 7.2° and 10.7 °C during 61 min of the simulation. Natural snowmelt rate of approximately 0.05 L min^{-1} was observed prior to sprinkling.

Table 1
Comparison of relevant artificial rain-on-snow experiments.

	Eiriksson et al. (2013)	Feng et al. (2001)	Lee et al. (2010a, 2008)	Kattelmann (1987a)	Singh et al. (1997)	Conway and Benedict (1994)
Locality	Boise National Forest, Idaho, USA	Sierra Nevada, near Soda Springs, USA	Sierra Nevada, near Soda Springs, USA	Sierra Nevada, near Soda Springs, USA	Glatzbach watershed, Grossglockner, Austria	Cascade Mts., near Snoqualmie Pass
Elevation (m a.s.l.)	850	2100	2100	2100	2640	915
Nr. of events	8	3	4	3	6	2
Input (mm)	9.5 (per event)	240 (total)	460 (total)	2.5 (per event)	49.2–201	19; 100
Duration (min)	30	90–270	306–330	5	60–120	600; 2160
Tracer	Rhodamine WT, NaCl	Tm, Yb, Lu	F- (KF), Br- (LiBr)	Dye tracer	No tracer	Temperature
Affected area	1.5 × 0.5 m	6 × 3 m	6 × 3 m	1 m^2	2 × 1 m; 2 × 2 m	1.5 × 1 m
Snowpack depth (cm)	47–138	135	210	50–100	108	120; 135
Time lag (min)	120–1290	45–90	110–130	–	10–15	NA, 660
Total discharge (mm)	–	330	336	–	3.1–203.8	Not recorded
Grain size/Snow type	0.25–1 mm	Well ripe, isothermal	Subfreezing	Fresh, subfreezing snow	5 ice layers, isothermal	0.1–1 mm, stratified with two ice crusts
Infiltration front speed (cm min^{-1})	1.9–11.5	1.4–2.9	1.6–1.9	1.5–9.8	10.0	0.2
Bulk density (g cm^{-3})	0.209–0.398	0.42 ± 0.044	0.35 ± 0.14 (before 1. event) 0.39 ± 0.1 (after 1. event) 0.43 ± 0.07 (after 2. event)	–	–	–
Purpose	Lateral flow generation	Solute transport in snow	Solute transport in snow	Water infiltration	Runoff generation	Water infiltration

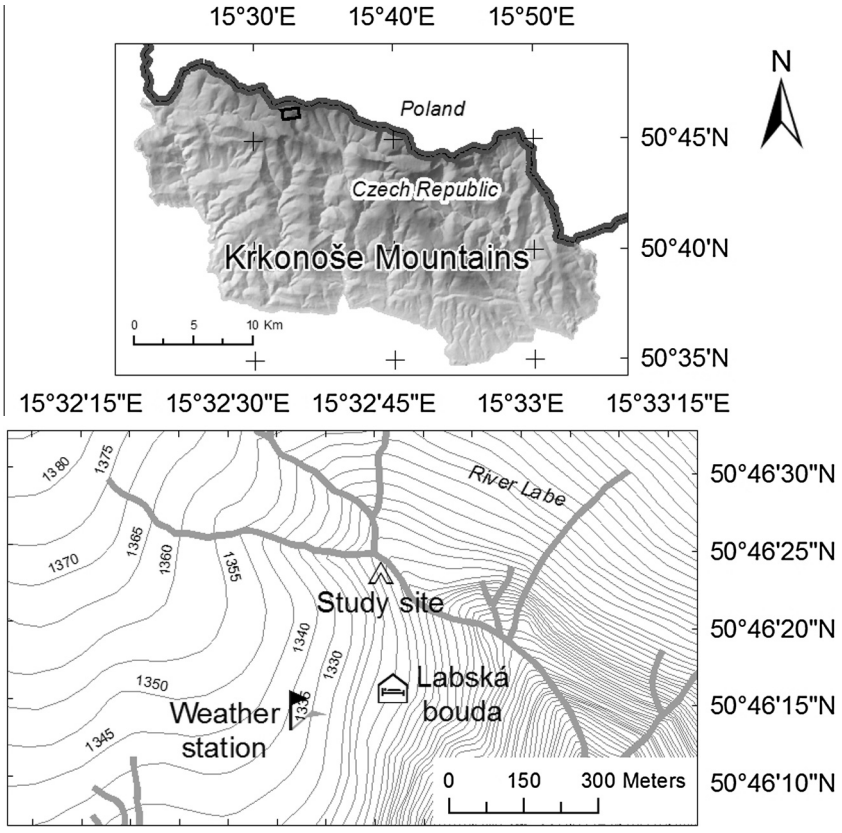

Fig. 1. Location of the experimental site. *Data source:* Krkonoše National Park Administration.

3.2. Rainfall simulation

The deuterium-enriched water was pumped into the spraying system. The spraying nozzle (FullJet 1/8 GG3 6SQ) was placed 60 cm above the experimental snow block surface, and the artificial rain covered an area of 50 × 50 cm (Fig. 3). The producer guarantees (from 5% to 95% percentile) droplet diameters from 0.74 mm to 2.90 mm at 0.7 bar and 0.56 mm to 2.20 mm at

Fig. 2. Photo of experiment device.

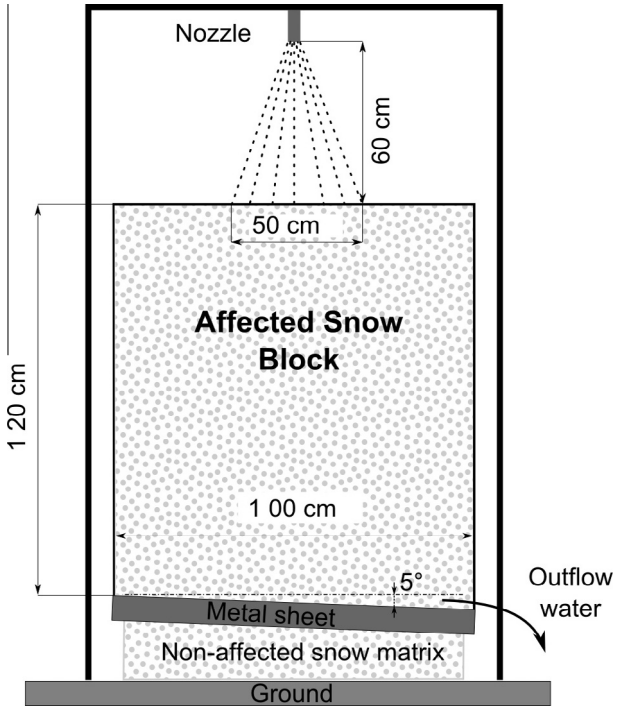

Fig. 3. Experiment setup.

2.8 bar, which is realistic compared to natural raindrops. The affected area was smaller than the total experimental snow block area (100 × 100 cm) in order to minimize the edge effect. The artificial rain event started at 14:41 on April 14th, and a volume of 72.7 ± 1.8 L of water enriched with deuterium was sprayed on the snow block in the course of the next 61 min. The applied volume was derived from the calibration curve and the water pressure setting in the system during the experiment. The applied rain intensity was higher as compared to the natural rainfall intensity during ROS events described in the literature (Colbeck, 1975; Osterhuber, 1999; Sui and Koehler, 2001; Würzer et al., 2016). This extreme rain amount guarantees sufficient outflow for an effective separation of outflow components.

Sprinkling water originated from the nearby stream of the River Labe was at first pumped to the barrel, where the natural deuterium concentration δ^2H was artificially raised from −73.1‰ (min = −74.1‰, max = −72.7) to +82.6‰ (min = +82.5‰, max = +82.7‰) V-SMOW. The reference samples for the event rainwater were collected from the barrel with deuterium-enriched water that was used for the rain simulation.

3.3. Experimental snow block

The investigated snowpack was isothermal, well ripe with coarse grains, and stratified by two significant hard layers, both 0.5 cm thick. A part of the snow cover was isolated as a snow block for the purpose of the experiment. The surface area of this snow block was 100 × 100 cm, and 120 cm beneath the snow surface was the snow block isolated by the metal plate (100 × 100 cm). A snow water equivalent (SWE) of 689 mm was measured prior to the experiment, using a snow tube next to the experimental snow block. The estimated bulk snow density was 574 kg m^{-3}.

Snow samples were taken every 5 cm throughout the experimental snow block to estimate the vertical snow isotopic composition before and after the experiment. Pre-experimental snow samples were collected from adjacent snow next to the experimental snow block. After the experiment, snow samples were collected close to the centre of the experimental snow block below the area of 50 × 50 cm affected by the artificial rain. All collected snow samples were stored under room temperature until melt and subsequently filled into 10 ml plastic bottles and maintained frozen until lab analysis. The vertical variation of the deuterium pre-experiment concentration (average δ^2H = −69.6‰, min = −102.97‰, max = −40.44‰ V-SMOW) shows a distinct isotopic heterogeneity of the snow block. Minimum and maximum values of deuterium content in the snowpack were used to assess the rainwater outflow uncertainties in the hydrograph according to Eqs. (1) and (2). These extreme values are reported in the results.

The four-sided excavation and the metal plate positioned under the snow block formed a hydraulic barrier to prevent lateral flow out from the investigated snow block and further percolation through the snow cover towards the soil surface. This setup enables to detect all outflowing water through the tipping bucket. The setup allowed mainly the vertical flow of the rainwater through the experimental snow block take into the consideration. This simplification also provides a more accurate calculation of the mass balance because it is possible to measure the total outflow water at the outlet using a tipping bucket flow meter.

The input and output water temperature before and after the experimental snow block was monitored during the experiment to evaluate the heat transfer from the rainwater into the snow. This heat exchange influences the temperature of the snow and cools the rainwater. A wind barrier was placed along the structure of rain simulator since even a gentle wind can have a very significant effect on the direction of the falling raindrops. This barrier also prevents additional melting caused by the wind-induced sensible heat.

3.4. Outflow measurement and sampling

A tipping bucket flow meter was attached to the metal plate to measure the outflow from the snow cube with a 1% accuracy. This setup enables instant water sampling above the tipping bucket with variable sampling frequency. The measurements of the snowmelt rate commenced two hours before the artificial rain began. The outflow from the snowpack was continuously monitored for 557 min after the rain had stopped. The outflow water samples were collected manually during the experiment and analysed for the deuterium isotope content in order to separate the hydrograph. The sampling intensity varied according to the flow rate from one minute during the rising limb and peak discharge to 30–90 min during the snowmelt and the falling limb phase. The reference snowmelt water deuterium content ($\delta^2H = -70.0‰$ [min = −71.7‰, max = −68.7‰] V-SMOW) was determined as the arithmetic mean of the five samples collected during the snow melt phase, prior to the application of the enriched rain. Extreme deuterium content values of melt water were used to assess uncertainties in volumes of the outflow components.

Deuterium content of the gathered samples was analysed by laser spectrometry. This approach was completed by using the LGR Inc. LWIA v2 facility of the Czech Technical University in Prague (Penna et al., 2010). The standard deviation of the results is $\delta^2H = 0.58‰$ V-SMOW.

3.5. Data interpretation

The data interpretation included the assessment of the hydrological response and the proportion of event rainwater in the total runoff. In addition, the portion of additional melt in the pre-event non-rainwater was calculated.

The proportions of event rainwater and pre-event non-rainwater in the total runoff from the snowpack were determined according to the mixing equations (Eqs. (1) and (2)):

$$Q_{total} \times c_{total} = Q_{rain} \times c_{rain} + Q_{non\text{-}rain} \times c_{non\text{-}rain}, \quad (1)$$

$$Q_{total} = Q_{rain} + Q_{non\text{-}rain}, \quad (2)$$

where Q [L min^{-1}] is the discharge rate, c [δ^2H ‰ V-SMOW] is the deuterium concentration and the subscripts *total*, *rain* and *non-rain* represent the measured total, the event rainwater, and the pre-event non-rainwater component, respectively. The pre-event non-rainwater represents the pre-event liquid water content in the snowpack and the additional snowmelt water within the experimental snow block:

$$Q_{non\text{-}rain} = Q_{melt} + Q_{pre\text{-}LWC}, \quad (3)$$

where Q_{melt} represents additional melt water volume produced during the experiment and $Q_{pre\text{-}LWC}$ represents volumetric pre-event liquid water content in the snowpack.

The additional snowmelt water volume (Q_{melt}) was estimated from the energy balance (EB) introduced by Walter et al. (2005). Single energy balance components were calculated according to DeWalle and Rango (2008) and Walter et al. (2005). Snow albedo (0.6) and snow emissivity (0.98) were estimated according to DeWalle and Rango (2008).

The isotopic value of the pre-event non-rainwater was derived from the sampling of the pre-experiment melt (5 samples) and the entire snowpack (24 samples).

The artificial ROS event has also assessed the changes in the snow water equivalent (SWE) and the deuterium concentration in the snowpack. They were measured vertically every five cm before and after the experiment.

The rainwater storage in the snowpack was calculated in two ways: first, as a difference between rain input and outflow, and second, from changes in deuterium concentrations and the SWE estimated after the experiment. This is described by following equations:

$$P = 1 - \frac{c_{SA} - c_{rain}}{c_{SB} - c_{rain}} \quad (4)$$

$$V_{rain} = SWE_A \times A \times P, \quad (5)$$

where the symbols represent: P – portion of rainwater in the affected snow cube volume [-], c – deuterium concentration [δ^2H ‰ V-SMOW], subscripts *SA*, *SB* and rain – snow after experiment, snow before experiment and rain water respectively, V_{rain} – volume of rainwater stored in the affected snow cube volume [L], SWE_A – snow water equivalent after experiment [mm], A – affected area [m^2].

4. Results

Table 2 summarizes the results and conditions of our study as compared to previous ROS artificial experiments (Table 1).

4.1. Outflow characteristics

The first noticeable increase in the discharge was observed 18 min after the commencement of the artificial rain. The speed of the wave front computed after (Kattelmann, 1987b) was estimated at 6 cm min^{-1}. Two flow peaks appeared in the hydrograph during the experiment (Fig. 4). The first flow peak (1.00 L min^{-1}) appeared 28 min after the commencement of the artificial rain, and the second (1.18 L min^{-1}) appeared between the 64th and 67th minute after the artificial rain commencement. The second flow peak was thus observed 3 min after the artificial rain had stopped. Although the air temperature was −0.3 °C at the end of the experiment, water was still leaking from the experimental snow block with a flow rate of 0.014 L min^{-1}. The total outflow water volume measured from the beginning of the artificial rain to the end of the experiment was 91.7 ± 1 L, which was 19 ± 2.8 L more than the rain input (Table 3).

4.2. Distribution of snowpack outflow components

The first noticeable increase in the deuterium concentration indicated the first substantial rainwater contribution to the outflow (Fig. 4). This situation was observed approximately one minute after an increase in the total flow rate, and is also documented in the deuterium mass flow (Fig. 5) and in the changes in deuterium concentration in the outflowing water (Fig. 6). The deuterium concentration then increased very rapidly (Fig. 6). The hydrograph separation of the event rain and the pre-event

Table 2
Conditions and results of the presented ROS.

Locality	Krkonoše Mts. Czech Republic
Elevation (m)	1340
Nr. of events	1
Input (mm)	72.7
Duration (min)	61
Tracer	Deuterium
Affected area	0.5 × 0.5 m
Snowpack depth (cm)	120
Time lag (min)	19
Total discharge (mm)	91.7
Snow type	Well riped, 2 hard layers
Infiltration front speed (cm min^{-1})	6
Bulk density (g cm^{-3})	0.574 (before event) 0.502 (after event)
Purpose	Hydrograph separation

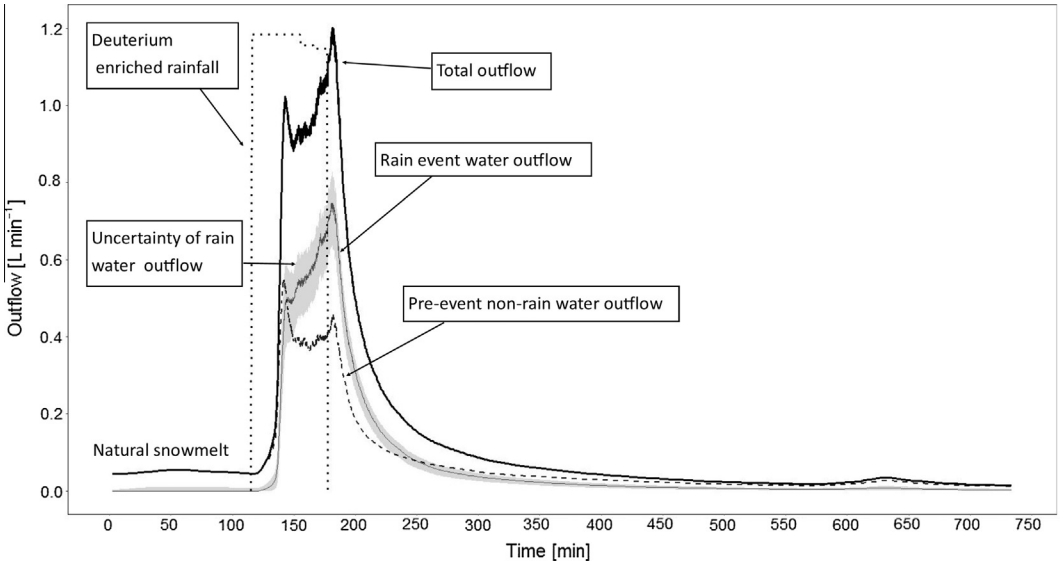

Fig. 4. The total outflow hydrograph separation into event rain water and pre-event non-rain water.

Table 3
Rain and outflow components (the sum of the pre-event liquid water content and the snowmelt water represents the pre-event non-rain water outflow).

	Total volume	Rain water volume	Pre-event liquid water content volume	Snowmelt water volume
Rain event (L)	72.7	72.7	0.0	0.0
Outflow (L)	91.7	48.3	29.4	14.0
Fraction of total outflow (%)	100.0	52.7	32.0	15.3

non-rainwater revealed that there were two flow peaks of the pre-event non-rainwater (Fig. 4). The first pre-event non-rainwater flow peak arrived 25 min after the commencement of the artificial rain, and reached a flow rate of 0.54 L min^{-1} (min = 0.44 L min^{-1}, max = 0.67 L min^{-1}). This pre-event non-rainwater discharge represented 56.8% (min = 46.6%, max = 70.2%) of the current total discharge. The second flow peak of the pre-event non-rainwater appeared between the 64th minute and the 67th minute, simultaneously with the event rainwater and the total outflow flow peaks (Table 4). During the second flow peak, the pre-event non-rainwater discharge of 0.44 L min^{-1} (min = 0.36 L min^{-1}, max = 0.55 L min^{-1}) represented 37.6% (min = 30.9%, max = 46.6%) of the current total discharge. Only one significant flow peak of 0.74 L min^{-1} (min = 0.63 L min^{-1}, max = 0.81 L min^{-1}) was identified for the event rainwater (Fig. 4), yielding a contribution of 62.4% (min = 46.6%, max = 69.1%) to the total discharge. The deuterium content in the overall outflow during this flow peak reached a maximum of $\delta^2H = +27.0‰$ V-SMOW. At the end of the experiment, the deuterium content in the outflow reached $\delta^2H = -38.3‰$ V-SMOW, which indicated 21% (min = 2%, max = 35%) of event rainwater in the total outflow.

The total volume of outflow water (91.7 ± 1 L) consisted of 48.3 L of rainwater (min = 47.9 L, max = 48.8 L), which represents 52.7% (min = 52.2%, max = 53.2%) and 43.4 L (min = 42.9 L,

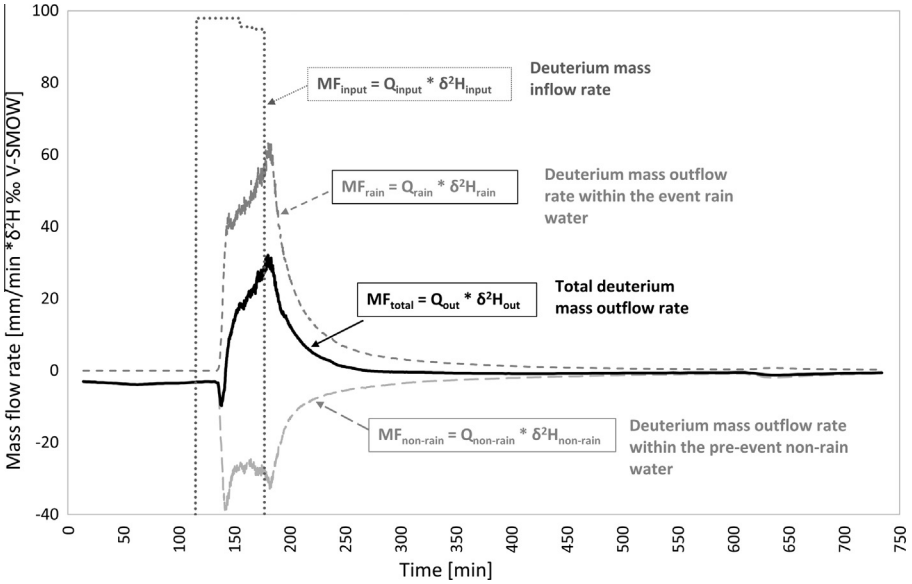

Fig. 5. Comparison of the separated mass flow rates of the outflow components.

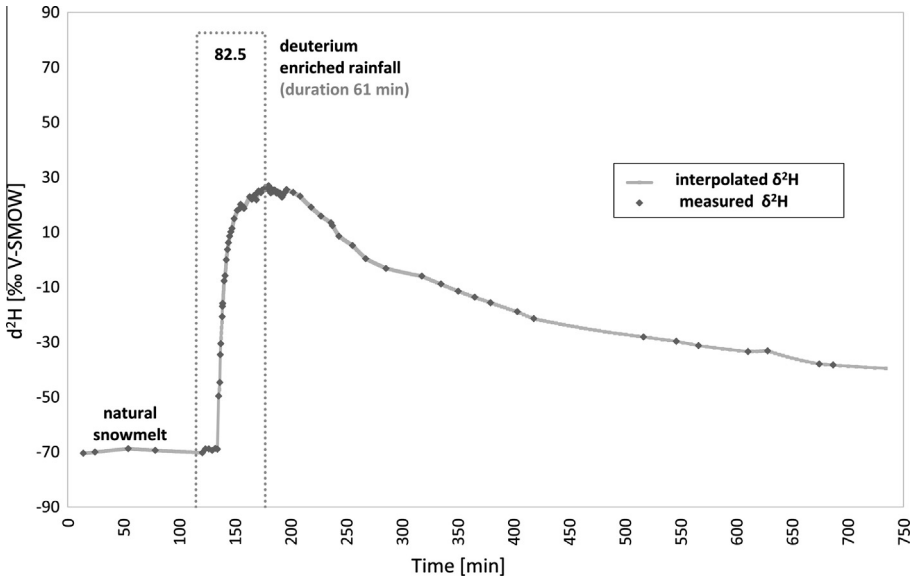

Fig. 6. The deuterium concentration in the total outflow.

Table 4
Data on the flow peaks during the experiment (the first flow peak was observed only in the pre-event non-rain water outflow and total water outflow hydrograph; the second flow peak was observed within the pre-event non-rain water, the event rain water and the total outflow water hydrographs together at the same time).

	First flow peak		Second flow peak
	Pre-event non-rain water	Total outflow water	All water
Time from the commencement of the experiment (min)	25	28	64–67
Deuterium content (‰ V-SMOW)	−4.32	+5.46	+27.0
Total flow rate (L min^{-1})	0.96	1.02	1.18
Rain water flow rate (L min^{-1})	0.40	0.50	0.74
Non-rain water flow rate (L min^{-1})	0.55	0.52	0.44

max = 43.8 L) representing 47.3% (min = 46.8%, max = 47.8%) of the pre-event non-rainwater.

The pre-experimental analysis of the snow profile before the experiment showed that the snowpack was fully ripe and consisted of coarse grains. Two considerable hard layers at 34 cm and at 102 cm were observed in the experimental snow block before the experiment. After the experiment, these two hard layers were visible at 30 cm and at 101 cm. A new significant hard layer was identified at a depth of 91 cm after the experiment.

The event rainwater storage can be indicated through the changes in the vertical distribution of SWE and the deuterium content of the snow block estimated from the 5 cm snow samples taken throughout the experimental snow block before and after the experiment (Fig. 7). During the experiment, the average deuterium content raised from $\delta^2H = -70.0‰$ to $\delta^2H = -47.5‰$ V-SMOW. The analysis of the snow samples indicated the biggest isotopic changes up to 20 cm above the lowest hard layer (30–55 cm of snow depth). Other significant changes in the deuterium compound were observed close to the snow surface. Most of the layers were supplied by the rainwater, but on the other hand four samples under the first hard layer were isotopically depleted. Two snow samples between 63 cm and 73 cm have shown a decrease in SWE, but an increase in deuterium content. This can indicate displacement of pre-event non-rainwater by a small volume of rainwater.

A local increase in SWE and deuterium content also indicates a rainwater retention above the hard layer (Singh et al., 1997). In particular, three samples (43–53 cm) collected above the lower hard layer indicated more than one third of rainwater content stored in the snowpack after the experiment (Fig. 7).

5. Discussion

5.1. Estimation of the mass balance and rainwater dynamics

Snow in the investigated cube was already wet before the artificial ROS. The cube was visibly saturated, releasing melt water from the snowpack. These facts indicated that the storage capacity of the snowpack was exceeded before the experiment and preferential flow paths were mostly developed, so limited new water volume can be stored (Singh and Singh, 2001). Nevertheless the detailed comparison of snow isotopic composition changes (Fig. 7) indicates a volumetric proportion of 14.5% (Eq. (4)) of the event rainwater in the affected experimental snow block volume. For affected area 0.25 m^2, this proportion represents 21.8 L (Eq. (5)) in the snow block with 601 mm of SWE. This result is close to the rainwater storage after the experiment (24.4 L) computed by subtracting the total event rainwater input by the total event rainwater volume in the outflow. This finding indicates that the vertical flow was predominant in the snow cover because the event rainwater storage in the snowpack after the experiment was mainly below the area covered by the artificial rain. A comparison between the ratio of the event rainwater in the outflow and in the snow block after the experiment shows that there is still predominantly event rainwater drainage from the snowpack 9 h after the experiment.

The mass balance revealed that water output was 26% higher than input. This negative mass balance was also supported by a decrease in snow depth and total SWE. The interaction between pre-event non-rainwater and event rainwater showed significant storage of event rainwater in the snowpack. This result is also supported by an increase in mean deuterium content of the snowpack (Fig. 7, Table 5). The event rainwater stored in the snowpack gradually compensated and pushed-out pre-event liquid water content

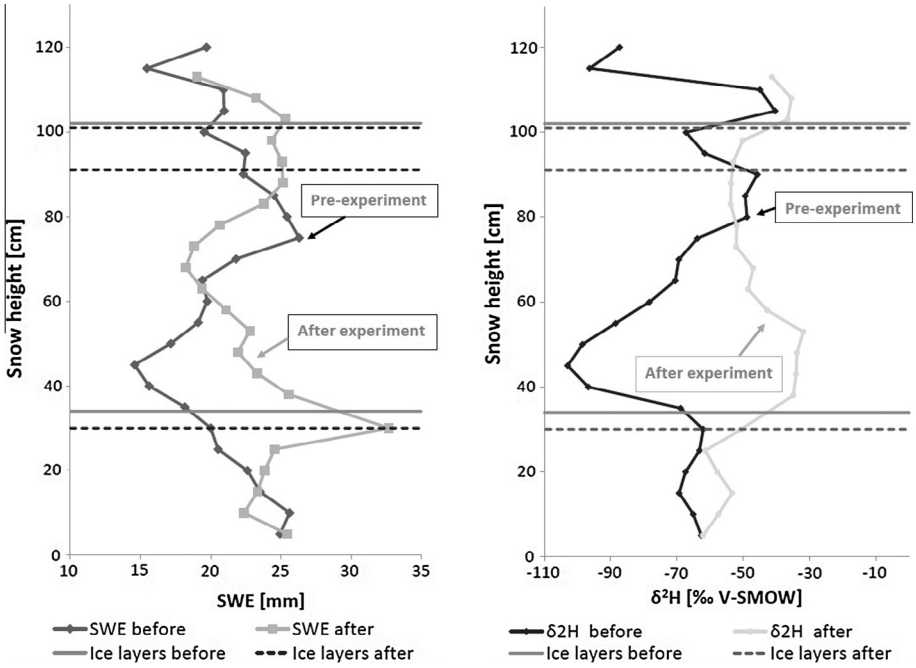

Fig. 7. Comparison of the SWE values (left) and the isotopic composition values (right) in the snowpack before and after the experiment.

Table 5
Overview of isotopic changes in the snowpack (samples taken every 5 cm) and in the outflow water before and after the experiment.

	Pre-experiment (‰ V-SMOW)	Post-experiment (‰ V-SMOW)	Difference (‰ V-SMOW)
Snow – 5 cm samples (mean)	−69.6	−47.5	+22.1
Outflow water (mean)	−70.0	−38.3	+31.1

in the snowpack. This process is further discussed in the next subchapter.

The creation of a new hard layer at 91 cm was probably caused by refreezing of stored liquid water at the interface of the two different snow layers. This interface was not identified as a hard layer before the experiment, but it was probably developed into the hard layer after the artificial ROS. Time between termination of rain event and snow pit investigation was almost 9 h to observe the hydrograph recession. During this time temperature decrease below freezing point, so the hard layer could be the product of refreezing snowpack. The increase in rainwater storage above the hard layers can be caused by two reasons: First, the hard layer acts as a hydraulics barrier and, second, the finer grains above the coarse grains layer causes capillary action and can store more water (Avanzi et al., 2015; Waldner et al., 2004). Although the hard layers were presented in the snowpack, no lateral flow was observed during the experiment. This behaviour can indicate that the flowing water partially moved through the hard layer via developed preferential paths. Although the metal plate acts analogically to the hard layers, it was completely impermeable and forced all leaking water to the outflow channel. The plate changed the flow direction from vertical (typical for unsaturated zone) to horizontal (typical for saturated zone). The metal plate also supports a capillary action when a soaked layer was created above the plate. This slush layer even released water nine hours after the end of the artificial rain.

5.2. Rainwater introduction to the snowpack and first propagation to the runoff

A relatively fast response (a short time lag of runoff generation) of the snowpack to the intensive rain event was observed during the experiment. This response was faster than those reported in other reviewed studies that have applied artificial ROS events (Table 1). The hydrograph separation has revealed that time lag of rainwater was one minute delayed to the total time lag. The authors argue that the time difference is caused by a push-out effect, which was also documented through the propagation of the rain and non-rainwater to the outflow. Rainwater pushed out a significant amount of pre-event non-rainwater, in particular until the first flow peak (Figs. 4 and 5). This explanation is also supported by Maclean et al. (1995), highlighting the wash-out of various ions from the snowpack accompanied by an increase of isotopic concentration in outflow after natural ROS.

The reviewed time lags (Table 1) are very individual, because they are driven mostly by snowpack and precipitation conditions and the infiltration front speed. In particular, rainwater is usually warmer than the isothermal snowpack and causes a higher production of additional snowmelt contrary to a colder snowpack. Therefore, the rainwater has a greater potential to flow downwards (Jones et al., 1989; Maclean et al., 1995). Higher flow rates are also related to high rain intensities introduced on the warm isothermal snowpack. The fast response of the outflow can also be influenced by the experimental setup and applied methods. Kattelmann (1987a) has investigated a subfreezing snowpack under an artificial rain of 30 mm h^{-1} and flow rates of 1.5–9.8 cm min^{-1}. A similar infiltration front speed of 10 cm min^{-1} was also observed by Singh et al. (1997) in isothermal snow under higher rain intensities up to 99.6 mm h^{-1}. The results of Singh et al. (1997) are close to our study because the snowpack hydrological responses in both studies were assessed under similar conditions (Tables 1 and 2). Kattelmann (1987a) summarised the results from several natural ROS studies, and reported infiltration front speeds up to 3 cm min^{-1} in most of the reviewed cases. These values are in

contrast with our experimental data because they reviewed studies carried out at catchment scale under natural conditions.

5.3. Dynamics of individual outflow components

Despite no significant changes in the rain intensity of the event rain during time, two flow peaks were observed within the hydrograph (Fig. 4). This shape of the hydrograph could be caused by increasing snowmelt intensity during the rain event, and by changes in preferential flow paths. No direct investigation of the formation of preferential flow was performed, but we can assume this behaviour on the basis of other studies (Lee et al., 2008; Techel et al., 2011; Zhou et al., 2008).

The amount of the pre-event non-rainwater is also affected by additional melting, which contributed to the outflow during the entire ROS experiment. The amount of additional melting can also be affected by experimental setup in three ways:

(a) The amount of 72.7 mm of relatively warm water was introduced to the isothermal snowpack. It means, that the extra heat from rain was directly used for the melt and not for the snow warming. The temperature of the rain gradually raised from 7.3 °C to 10.7 °C with culmination until the end of the rainwater. The most significant cooling of the incoming rainwater is occurring in top layers. The melt water from the upper layers appeared later in the outflow together with the rainwater. This fact can explain the increase of pre-event non-rainwater during the second flow peak. Calculation of the EB estimated that the amount and temperature of rainwater was probably responsible for a significant portion (56%) of total melt water volume.
(b) Clear sky conditions during the experiment caused the top of the snow cube to receive a high amount of direct short wave radiation, producing additional melt. The investigated snow cube was isolated from the adjacent snowpack by a gap, which partially allowed heat exchange between the air and bare cube sides. The high rainfall intensity caused deeper rainwater percolation through drops-induced holes in the snow. These holes also enabled a more effective income of energy followed by a more intensive snowmelt. On the other hand, the effect of heat exchange between wind and snow was minimized by the wind cover along the simulator construction.
(c) The metal plate could also have a positive effect to the additional melt production, although this effect was not directly measured. The metal plate was continuously cooled by the adjacent snow, but we cannot exclude any extra heating by penetrating solar radiation on the bottom parts on each cube side. Extra heat from the ground can be neglected because metal plate laid on more than 1 m of snow.

Further partitioning of pre-event non-rainwater by energy balance equation revealed that the total snowmelt water volume was 14 L. Neglecting the heat input due to rain yields a natural melt volume of only 5.8 L. This volume is hypothesized to represent the possible natural snowmelt during the experiment. Subsequently, the snowmelt caused by the heat input due to the artificial rain can be estimated to 8.2 L (58.5% of total melt). The difference between the pre-event non-rainwater volume outflow and the computed snowmelt volume represents 29.4 L (min = 28.9 L, max = 29.8 L) (32.1% of the total outflow, min = 31.5%, max = 32.5%) (Table 3). This volume indicates the calculated volume of the pre-event snowpack liquid water content (LWC) in the outflow.

Subtracting the total event rainwater input and the total event rainwater outflow volume shows that 24.4 L (min = 23.9 L, max = 24.8 L) representing 33.6% (min = 32.5%, max = 33.9%) of the event rainwater were still stored in the experimental snow block 9 h after the end of the artificial rain simulation. These findings are presented with respect to some EB input limitations because some components of EB (long wave radiation, albedo, snow emissivity) were only estimated.

The upscaling of the results from point scale to hillslope and catchment scales remains a challenging task, particularly due to larger-scale variations in lateral flow, rainwater and meltwater infiltration, slope, land cover and wind conditions (Walter et al., 2005). The impact of these factors on the partitioning of outflow in heterogeneous environments remains poorly understood.

5.4. Recommendation for future work

The results in this paper support the need to address the hydrological response (time lag of the outflow and the outflow rainwater ratio) of the snowpack under lower rainfall intensities. According to previous studies (Feng et al., 2001; Lee et al., 2010b, 2008; Würzer et al., 2016), the response time increases with decreasing rain intensity, but a substantial gap remains in the knowledge how would the outflow rainwater ratio change with lower rain intensity. The required degree of the deuterium enrichment of the rainwater would be lower, because the rainwater will be also detectable when lower deuterium concentration is used.

Direct measurement of single EB variables (mainly radiation components) should help to build more accurate estimation of the overall EB model. Snowmelt volume calculation should be also supported by independent melt rate monitoring next to the affected block.

For more detailed understanding of rainwater behaviour in various snowpack condition we recommend to carry out more experiments with changing snowpack depth and bulk density.

6. Conclusions

The presented combination of methods of artificial ROS, isotopic hydrograph separation of the event rainwater and the pre-event non-rainwater and energy balance showed a very good applicability for future studies of runoff generation and rainwater interaction with snowpack during ROS. The point scale allows an accurate investigation of dynamics of individual hydrograph components in detailed time resolution. The experimental point scale setup also provides a proper mass balance of rainwater. Although the energy balance has proven adequate for the meltwater calculation, improvements are recommended toward a higher accuracy. As this experiment revealed, rainwater during ROS firstly pushes-out the non-rainwater and then contributes to the outflow. Significant quality changes in the outflowing water quality can therefore be expected during ROS events.

Acknowledgments

This study was funded by the Internal Grant Agency of the Faculty of Environmental Sciences, CULS Prague (projects 20144254, 20124275). Further funding was provided by the Ministry of the Interior of the Czech Republic through the project: Creation of information system for evaluation of avalanche hazard in mountain regions in the Czech Republic (VG 20132015115), and by the Swiss National Foundation (Scopes) project Snow resources and the early prediction of hydrological drought in mountainous streams (SREPDROUGHT) IZ73ZO_152506/CZ. Weather data was kindly provided by the Czech Hydrometeorological Institute, and spatial terrain data was kindly provided by the Krkonoše National

Park Administration. The authors wish to thank Dr. Raelene Sheppard for linguistic correction.

References

Ambach, W., Howorka, F., 1966. Avalanche activity amd free water content of snow at Oberlung (1980 m a.s.l., Spring 1962). In: Symposium at Davos 1965 – Scientific Aspects of Snow and Ice Avalanches. International Association of Scientific Hydrology Publication 69, Davos, pp. 65–72.

Avanzi, F., Hirashima, H., Yamaguchi, S., Katsushima, T., Michele, C.De., 2015. Laboratory-based observations of capillary barriers and preferential flow in layered snow. Cryosph. Discuss. 9 (6), 6627–6659. http://dx.doi.org/10.5194/tcd-9-6627-2015.

Böhm, U., Fiedler, A., Machui-Schwanitz, G., Reich, T., Schneider, G., 2011. Hydrometeorologische Analyse der Schnee- und Tauwettersituation im Dezember 2010/Januar 2011 in Deutschland (in German), Deutscher Wetterdienst (report). Available online at: <http://www.dwd.de/bvbw/generator/DWDWWW/Content/Wasserwirtschaft/Unsere__Leistungen/Schneeschmelzvorhersage/KU4__Tauwetter__2010__11__lang__pdf,templateId=raw,property=publicationFile.pdf/KU4_Tauwetter_2010_11_lang_pdf.pdf> (accessed, Offenbach).

Buttle, J.M., Vonk, A.M., Taylor, C.H., 1995. Applicability of isotopic hydrograph separation in a suburban basin during snowmelt. Hydrol. Process. 9, 197–211. http://dx.doi.org/10.1002/hyp.3360090206.

Carran, W., Hall, S., Kendall, C., Carran, A., Conway, H., 2000. Snow temperature and water outflow during rain and melt; Milford Highway, New Zealand. In: Proceedings of the 2000 International Snow Science Workshop, October 1–6, Big Sky, Montana, pp. 173–177.

Casson, N.J., Eimers, M.C., Watmough, S.a., 2014. Sources of nitrate export during rain-on-snow events at forested catchments. Biogeochemistry 120, 23–36. http://dx.doi.org/10.1007/s10533-013-9850-4.

Colbeck, S.C., 1975. Analysis of hydrologic response to rain-on-snow.

Colbeck, S.C., Davidson, G., 1973. Water percolation through homogeneous snow. In: The Role of Snow and Ice in Hydrology (Proc. Banff Symp., 1972). Unesco-WMO-IAHS. IAHS Publ. 107, pp. 242–257.

Conway, H., 1994. Physical Processes in Snowpacks During Rain or Melt Events. University of Washington, Washington.

Conway, H., Benedict, R., 1994. Infiltration of water into snow. Water Resour. Res. 30, 641–649. http://dx.doi.org/10.1029/93WR03247.

Conway, H., Raymond, C.F., 1993. Snow stability during rain. J. Glaciol. 39, 635–642.

Čekal, R., Ryglewicz, M., Bořiková, L., Suchá, M., Přibyl, J., Kotek, R., 2011. Zpráva o povodni v lednu 2011 (in Czech), Czech Hydrometeorological Institute (report). Available online at: <http://portal.chmi.cz/files/portal/docs/hydro/ohp/povoden_01_2011.pdf>, (accessed 17.10.2014, Prague).

DeWalle, D.R., Rango, A., 2008. Principles of Snow Hydrology. Cambridge University Press, New York.

Dinçer, T., Payne, B.R., Florkowski, T., Martinec, J., Tongiorgi, E., 1970. Snowmelt runoff from measurements of tritium and oxygen-18. Water Resour. Res. 6, 110–124. http://dx.doi.org/10.1029/WR006i001p00110.

Dozier, J., Melack, J.M., Elder, K., Kattelmann, R., Marks, D., Williams, M., 1989. Snow, Snowmelt, Rain, Runoff, and Chemistry in a Sierra Nevada Watershed. Santa Barbara.

Eiriksson, D., Whitson, M., Luce, C.H., Marshall, H.P., Bradford, J., Benner, S.G., Black, T., Hetrick, H., McNamara, J.P., 2013. An evaluation of the hydrologic relevance of lateral flow in snow at hillslope and catchment scales. Hydrol. Process. 27, 640–654. http://dx.doi.org/10.1002/hyp.9666.

Feng, X., Kirchner, J.W., Renshaw, C.E., Osterhuber, R.S., Klaue, B., Taylor, S., 2001. A study of solute transport mechanisms using rare earth element tracers and artificial rainstorms on snow. Water Resour. Res. 37, 1425–1435. http://dx.doi.org/10.1029/2000WR900376.

Ferguson, S.A., 2000. The spatial and temporal variability of rain-on-snow. In: Assessment International Snow Science Workshop, 1–6 October, 2000. American Avalanche Association, Big Sky, Montana, pp. 178–183.

Gude, M., Scherer, D., 1999. Atmospheric triggering and geomorphic significance of fluvial events in high-latitude regions. Z. Geomorphol. Suppl. 115, 87–111.

Herrmann, A., Lehrer, M., Stichler, W., 1981. Isotope input into runoff systems from melting snow covers. Nord. Hydrol. 12, 308–318.

Hestnes, E., Sandersen, F., 1987. Slushflow activity in the Rana district, North Norway. In: Avalanche Formation, Movement and Effect (Proceedings of Davos Symposium, September 1986). IAHS Publ. 162, Davos, pp. 317–330.

HND Bayer, 2011. Gewässerkundlicher Monatsbericht Januar 2011 – Hochwasser (in German), Hochwassernachrichtendienst (report). Available online at: <http://www.hnd.bayern.de/ereignisse/monatsberichte/md_fghw_0111.pdf> (accessed 17.10.2014).

Holko, L., Holzmann, H., De Lima, M.I.P., De Lima, J.L.M.P., 2015. Hydrological research in small catchments – an approach to improve knowledge on hydrological processes and global change impacts. J. Hydrol. Hydromech. 63, 181–182. http://dx.doi.org/10.1515/johh-2015-0032.

Janásková, B., 2006. Ukládání a odbourávání sněhu ve vrcholové oblasti východních Krkonoš (in Czech), Accumulation and ablation of snow cover in the summit parts of the East Giant Mountains. Opera Corcon. 43, 57–80.

Jones, H.G., Tranter, M., Davies, T.D., 1989. The leaching of strong acid anions from snow during rain-on-snow events: evidence for two component mixing. Atmosph. Deposit., 239–250

Juras, R., Pavlásek, J., Děd, P., Tomášek, V., Máca, P., 2013. A portable simulator for investigating rain-on-snow events. Z. Geomorphol. Suppl. Issues 57, 73–89. http://dx.doi.org/10.1127/0372-8854/2012/S-00088.

Kattelmann, R., 1987a. Water release from a forested snowpack during rainfall. In: Forest Hydrology and Watershed Management. IAHS-AISH Publ. 167, Vancouver, pp. 265–272.

Kattelmann, R., 1987b. Some measurements of water movement and storage in snow. In: Avalanche Formation, Movement and Effects. IAHS Publ. 162, Davos, pp. 245–254.

Laudon, H., Hemond, H.F., Krouse, R., Bishop, K.H., 2002. Oxygen 18 fractionation during snowmelt: implications for spring flood hydrograph separation. Water Resour. Res. 38, 1–10. http://dx.doi.org/10.1029/2002WR001510.

Lee, J., Feng, X., Faiia, A., Posmentier, E., Osterhuber, R., Kirchner, J., 2010a. Isotopic evolution of snowmelt: a new model incorporating mobile and immobile water. Water Resour. Res. 46, 1–12. http://dx.doi.org/10.1029/2009WR008306.

Lee, J., Feng, X., Faiia, A.M., Posmentier, E.S., Kirchner, J.W., Osterhuber, R., Taylor, S., 2010b. Isotopic evolution of a seasonal snowcover and its melt by isotopic exchange between liquid water and ice. Chem. Geol. 270, 126–134. http://dx.doi.org/10.1016/j.chemgeo.2009.11.011.

Lee, J., Feng, X., Posmentier, E.S., Faiia, A.M., Osterhuber, R., Kirchner, J.W., 2008. Modeling of solute transport in snow using conservative tracers and artificial rain-on-snow experiments. Water Resour. Res. 44, 1–12. http://dx.doi.org/10.1029/2006WR005477.

Maclean, R.A., English, M.C., Schiff, S.L., 1995. Hydrological and hydrochemical response of a small Canadian Shield catchment to late winter rain-on-snow events. Hydrol. Process. 9, 845–863. http://dx.doi.org/10.1002/hyp.3360090803.

Marshall, H.P., Conway, H., Rasmussen, L.A., 1999. Snow densification during rain. Cold Reg. Sci. Technol. 30, 35–41. http://dx.doi.org/10.1016/S0165-232X(99)00011-7.

Martinec, J., 1987. Meltwater percolation through an alpine snowpack. In: Avalanche Formation, Movement and Effects. IAHS Publ. 162, Davos, pp. 255–264.

Osterhuber, R.S., 1999. Precipitation intensity during rain-on-snow. In: Western Snow Conference. South Lake Tahoe, pp. 153–155.

Penna, D., Stenni, B., Šanda, M., Wrede, S., Bogaard, T.A., Gobbi, A., Borga, M., Fischer, B.M.C., Bonazza, M., Chárová, Z., 2010. On the reproducibility and repeatability of laser absorption spectroscopy measurements for δ^2H and $\delta^{18}O$ isotopic analysis. Hydrol. Earth Syst. Sci. 14, 1551–1566. http://dx.doi.org/10.5194/hess-14-1551-2010.

Singh, P., Singh, V.P., 2001. Snow and Glacier Hydrology, first ed. Kluwer Academic Publishers, Boston.

Singh, V.P., Spitzbart, G., Hübl, H., Weinmeister, H.W., 1997. Hydrological response of snowpack under rain-on-snow events: a field study. J. Hydrol. 202, 1–20. http://dx.doi.org/10.1016/S0022-1694(97)00004-8.

Suecker, J.K., Ryan, J.N., Kendall, C., Jarrett, R.D., 2000. Determination of hydrologic pathways during snowmelt for alpine/subalpine basins, Rocky Mountain National Park, Colorado. Water Resour. Res. 36, 63–75. http://dx.doi.org/10.1029/1999WR900296.

Sui, J., Koehler, G., 2001. Rain-on-snow induced flood events in Southern Germany. J. Hydrol. 252, 205–220. http://dx.doi.org/10.1016/S0022-1694(01)00460-7.

Surfleet, C.G., Tullos, D., 2013. Variability in effect of climate change on rain-on-snow peak flow events in a temperate climate. J. Hydrol. 479, 24–34. http://dx.doi.org/10.1016/j.jhydrol.2012.11.021.

Taylor, S., Feng, X., Kirchner, J.W., Osterhuber, R., Klaue, B., Renshaw, C.E., 2001. Isotopic evolution of a seasonal snowpack and its melt. Water Resour. 37, 759–769. http://dx.doi.org/10.1029/2000WR900341.

Techel, F., Pielmeier, C., Schneebeli, M., 2011. Microstructural resistance of snow following first wetting. Cold Reg. Sci. Technol. 65, 382–391. http://dx.doi.org/10.1016/j.coldregions.2010.12.006.

Tomasson, G.G., Hestnes, E., 2000. Slushflow hazard and mitigation in Vestubyggd, Northwest Iceland. Nord. Hydrol. 31, 399–410.

Tusima, K., 1985. Grain coarsening of snow particles immersed in water and solution. Ann. Glaciol. 6, 126–129.

Viviroli, D., Zappa, M., Gurtz, J., Weingartner, R., 2009. An introduction to the hydrological modelling system PREVAH and its pre- and post-processing-tools. Environ. Model. Softw. 24, 1209–1222. http://dx.doi.org/10.1016/j.envsoft.2009.04.001.

Waldner, P.a., Schneebeli, M., Schultze-Zimmermann, U., Flühler, H., 2004. Effect of snow structure on water flow and solute transport. Hydrol. Process. 18, 1271–1290. http://dx.doi.org/10.1002/hyp.1401.

Walter, M.T., Brooks, E.S., McCool, D.K., King, L.G., Molnau, M., Boll, J., 2005. Process-based snowmelt modeling: does it require more input data than temperature-index modeling? J. Hydrol. 300, 65–75. http://dx.doi.org/10.1016/j.jhydrol.2004.05.002.

Würzer, S., Jonas, T., Wever, N., Lehning, M., 2016. Influence of initial snowpack properties on runoff formation during rain-on-snow events. J. Hydrometeorol. 17, 1801–1815. http://dx.doi.org/10.1175/JHM-D-15-0181.1.

Zhou, S., Nakawo, M., Hashimoto, S., Sakai, A., 2008. Preferential exchange rate effect of isotopic fractionation in a melting snowpack. Hydrol. Process. 22, 3734–3740. http://dx.doi.org/10.1002/hyp.6977.

4.3. Článek III - Rainwater propagation through snowpack during rain-on-snow events under different snow conditions

Roman Juras, Sebastian Würzer, Jirka Pavlásek, Tomáš Vitvar, et Tobias Jonas 2016, Hydrology et Earth System Sciences – Discussion, submited, 2016

Rainwater propagation through snowpack during rain-on-snow events under different snow condition

Roman Juras[1*], Sebastian Würzer[2], Jirka Pavlásek[1], Tomáš Vitvar[1,3], and Tobias Jonas[2]

[1] Faculty of Environmental Sciences, Czech University of Life Sciences Prague, Kamýcká 129, 165 21, Prague, Czech Republic
[2] WSL Institute for Snow and Avalanche Research SLF, Flüelastrasse 11, 7260 Davos Dorf, Switzerland
[3] Faculty of Civil Engineering, Czech Technical University in Prague, Thákurova 7, 166 29 Prague 6, Czech Republic

Correspondence to: Roman Juras (juras@fzp.czu.cz)

Abstract. The mechanisms of rainwater propagation and runoff generation during rain-on-snow (ROS) are still insufficiently known. Understanding the behaviour of liquid water within the natural snowpack is crucial especially for forecasting of natural hazards such as floods and wet snow avalanches. In this study, rainwater percolation through snow was investigated by sprinkling deuterium enriched water on snow and applying an advanced hydrograph separation technique on samples collected from the snowpack runoff. This allowed quantifying the contribution of rainwater and snowmelt in the water released from the snowpack. Four field experiments were carried out during the winter 2015 in the vicinity of Davos, Switzerland. For this purpose, large blocks of natural snow were isolated from the surrounding snowpack to inhibit lateral exchange of water. These blocks were exposed to artificial rainfall with 41 mm of deuterium enriched water. The sprinkling was run in four 30 minutes periods separated by three 30 minutes non-sprinkling periods. The runoff from the snow block was continuously gauged and sampled for the deuterium concentration. At the onset of each experiment initially present liquid water content was first pushed out by the sprinkling water. Hydrographs showed four pronounced peaks corresponding to the four sprinkling bursts. The contribution of rainwater to snowpack runoff consistently increased over the course of the experiment but never exceeded 86 %. An experiment conducted on a cold snowpack suggested the development of preferential flow paths that allowed rainwater to efficiently propagate through the snowpack limiting the time for mass exchange processes to take effect. On the contrary, experiments conducted on ripe isothermal snowpack showed a slower response behaviour and resulted in a total runoff volume which consisted of less than 50 % of the rain input.

Keywords: *hydrograph separation, stable isotopes, sprinkling experiment, preferential flow, flood forecasting*

1 Introduction

Rain-on-snow (ROS) events are a natural phenomenon which has been in the focus of hydrological research in the past decades, particularly because of their high potential to cause natural hazards. ROS initiated severe floods in the past in many European countries such as Germany (HND Bayern, 2011; Sui and Koehler, 2001), Switzerland (Badoux et al., 2013; Rössler et al., 2014), Czech Republic (Čekal et al., 2011) or US (Ferguson, 2000; Kattelmann, 1997; McCabe et al., 2007). Rainwater also affects snowpack stability which can initiate formation of wet snow avalanches (Ambach and Howorka, 1966; Baggi and Schweizer, 2008; Conway and Raymond, 1993) or trigger slushflows (Hestnes and Sandersen, 1987; Nyberg, 1989; Onesti, 1987). In addition to natural hazards, ROS events

are also relevant from a geochemical point of view. Rainwater affects transport of ions (Jones et al., 1989) and solutes (Feng et al., 2001; Harrington and Bales, 1998; Lee et al., 2008; Waldner et al., 2004) through snow which affects the pH and chemical compositions of adjacent streams (Casson et al., 2014; Dozier et al., 1989; MacLean et al., 1995).

Predicting snowpack runoff for an upcoming ROS event requires the understanding of water transport processes through snow. Water input from heavy rainfall flows typically faster through a snowpack than meltwater outside of rain periods, which is why ROS situations may entail an augmented flood risk (Singh et al., 1998). Interactions between the liquid and solid phase of water make the water flow modelling in snow more difficult compared to other porous media like soil or sand where the solid phase is supposed to be stable. Existing water flow models for snow have rarely been specifically tested for ROS scenarios, nevertheless Würzer et al. (2016b) have recently introduced a new approach integrated within the SNOWPACK model (Bartelt and Lehning, 2002; Wever et al., 2015).

Presence of liquid water in snow fastens the metamorphism processes such as snow settling, snowpack warming (Conway and Benedict, 1994) and grain coarsening (Gude and Scherer, 1998; Tusima, 1985). These processes entail a higher hydraulic conductivity and snow permeability which lead to faster water flow (Calonne et al., 2012; Conway and Benedict, 1994). Rainwater introduced to the snowpack during ROS represents an important additional source of liquid water besides snowmelt which can contribute to the generation of snowpack runoff.

There is still a lack of knowledge how rainwater is propagating though snow to generate snowpack runoff and what runoff portion can rainwater represent under various snow conditions. Previous studies have shown that water can flow through snow in two different regimes, matrix flow and preferential flow, which are both governed by specific snow properties (Schneebeli, 1995; Waldner et al., 2004). In the matrix flow regime snow is wetted top down uniformly with all snow being wet above the wetting front (Schneebeli, 1995; Techel et al., 2008). Preferential flow, on the other hand, is characterised by spatially heterogeneous wetting patterns with horizontally isolated wet and dry zones often referred to as flow fingers (e.g. Techel et al., 2008; Waldner et al., 2004). These patterns grow with percolation intensity and grain size (Hirashima et al., 2014). During dye tracer experiments in non-ripe snowpack with temperatures below the freezing point, matrix flow was observed in the uppermost layers of the snowpack whereas preferential flow was observed in deeper layers only (Würzer et al., 2016b, Techel et al., 2008). Concepts of water flow behaviour in snowpack were further investigated in various approaches including rainfall simulation (Conway and Benedict, 1994; Eiriksson et al., 2013; Juras et al., 2013; Singh et al., 1997), artificial wetting (Avanzi et al., 2015; Katsushima et al., 2013; Yamaguchi et al., 2010) or numerical modelling (Hirashima et al., 2010, 2014, Wever et al., 2014, 2015).

The fact that rain and melting snow feature a different isotopic content can be used to differentiate between both components in the snowpack runoff analogically to hydrograph separation, which is a widely used technique especially in watershed hydrology (Buttle et al., 1995; Dinçer et al., 1970; Unnikrishna et al., 2002). Snowpack usually features a heterogeneous vertical isotope composition (Lee et al., 2010; Zhou et al., 2008) which is partially homogenized over the course of the winter season by a combination of moisture exchange, meltwater and rain infiltration (Krouse et al., 1977; Unnikrishna et al., 2002). Isotopically lighter meltwater is produced at the beginning of snowmelt and becomes heavier as melt progresses. This change is augmented by isotopic enrichment of the meltwater through the late spring rainfalls (Unnikrishna et al., 2002). Several authors (Feng et al., 2002;

Hashimoto et al., 2002; Unnikrishna et al., 2002) reported a typical difference of $\delta^{18}O$ around 2‰ between solid snow and liquid water in snow which is mostly caused by the isotopic fractionation. Feng et al. (2002) reported that a difference of 1 ‰ in $\delta^{18}O$ is equivalent of 8 ‰ change in $\delta^{2}H$. Although this discrepancy can lead to some uncertainties in hydrograph separation, only little work has addressed the effects of the time-variant isotopic content of the non-rain water.

Juras et al. (2016) demonstrated in a feasibility study that they could quantify the contribution of rainwater in snowpack runoff during a sprinkling experiment using hydrograph separation techniques. However, their experiment was conducted with very high sprinkling intensities well beyond typical rain intensities. In this paper, we extend their study to investigate the propagation of liquid water through snowpack under conditions representative of natural ROS events and for different types of snowpack. Our data analysis allows answering the following questions:

1. How much does rain water contribute to the total snowpack runoff during ROS?
2. What is the interaction between rain and ripe or cold snowpack?
3. How do initial snowpack conditions of cold and ripe snow influence liquid water transport in snow?

In addition, we present a new approach to deal with isotopic differences within the initial snowpack, and test it against standard procedures.

2 Material and methods

2.1 Study site

Four sprinkling experiments were carried out in the vicinity of Davos, Switzerland. Elevation of the experimental sites ranged between 1850 and 2150 m a.s.l. Details of all sites and experiments are summarised in table 1. All sites were located in open flat terrain. The winter season 2014/2015 was characterized by below-average snowcover and above-average mean air temperatures. Davos climate has a subalpine character with mean air winter temperature of -2.18°C and cumulative winter precipitation of 371 mm (Nov - Apr).

Table 1

2.2 Experimental procedure

Four ROS experiments were conducted in this study. During each experiment deuterium enriched water was sprinkled on an isolated block of snow, consisting of natural and undisturbed snow of 1m² surface area. Each experiment was conducted within three subsequent days: The first day, an experimental snow block of natural snow was prepared. To inhibit lateral exchange of water the snow block was carefully cut out and isolated from adjacent snow using 4 sheets of Ethafoam® of 2cm thickness. A metal tray was pushed through the bottom section of the snow block in a slight angle enabling to collect liquid water from the lowest corner. The tray featured a rim of 5cm height on three of the four sides. The outlet channel was then attached to the fourth side, but only after the tray had been pushed through the snow block. The outlet was connected to a tipping bucket gauge, which also served to sample water for the laboratory analysis. The rainfall simulator was then placed above the snow block

with wind protection cover (Fig. 1) rolled up to ensure ambient thermal conditions. Even if mechanical and thermal disturbances were kept to a minimum the setup was allowed to settle over night before sprinkling experiments commenced the next day.

Figure 1

During the second day, the actual sprinkling onto the snow block was performed. Pre-experimental snow properties were measured in undisturbed snow within a few meters from the experiment at the time that the sprinkling started. We recorded vertical profiles of snow temperature, liquid water content (LWC), grain size and density. LWC was measured using a "Denoth meter" (Denoth, 1994). In addition snow samples were taken to analyse the δ^2H content. Snowpack runoff was recorded from two hours before the first sprinkling burst till five hours after the last sprinkling burst. The snowpack runoff was further sampled for δ^2H content during the entire experiment. The sampling interval varied according to the snowpack runoff rate, ranging from one minute during the peak flow to 20 minutes during periods with marginal flow only. During the sprinkling, the wind protection cover was put in place to enable spatially homogenous sprinkling results. The cover was shortly opened during non-rain period to prevent possible accumulation of warm air. On day 3, approximately 20 hours after the last sprinkling burst, post-experimental snow properties were measured analogously to day 2, with the exception that the sampling was conducted within the snow block that was sprinkled. Again, snow samples were taken to determine how much sprinkling water remained in the snowpack.

2.3 Rainfall simulation and monitoring

An enhanced version of the rainfall simulator described in Juras et al. (2013, 2016) was designed to achieve rain intensities close to observations during natural ROS (Osterhuber, 1999; Rössler et al., 2014; Würzer et al., 2016a). The new device was equipped by a nozzle Lechler 460.368.30.CA which was precisely calibrated in the laboratory and again on site. The nozzle was placed 160 cm above the snow cover ensuring a spatially uniform rainwater distribution for the inner $1m^2$ of the sprinkling area, i.e. over the snow block.

During each experiment about 41 mm of deuterium enriched water was sprinkled in four sprinkling periods of 30 min each, separated by 30 min non-sprinkling periods, resulting in a mean rainfall intensity of 10.25 mm per hour, per burst respectively.

The deuterium content is expressed as a difference relative to Vienna Standard Mean Ocean Water (V-SMOW). For the purposes of an efficient hydrograph separation, tap water was enriched with deuterium to reach a difference of at least δ^2H = 60 ‰ V-SMOW between the snowpack and the sprinkling water. Sprinkling water concentration ranged between δ^2H –23.11 to +22.61 ‰ V-SMOW and initial snowmelt deuterium concentration ranged between δ^2H –132.47 to -88.64 ‰ V-SMOW. The barrels containing the enriched sprinkling water were buried into snow to cool down the water temperature. The mean rain water temperature after pumping varied between 4.3 – 7.5°C (measured over the snow), which is considered representative of temperatures during natural rain on snow events in the area.

2.4 Sampling and laboratory analysis

Water samples collected during the experiments were stored in 10 or 20 ml plastic bottles. To minimize isotopic fractionation, air gaps in the samples were avoided and samples were subsequently frozen until the laboratory analysis. Snow samples were taken along three vertical profiles at 10 cm spacing before and after each experiment. Additionally, three samples of the entire snow profile were taken at the same time. All snow samples were melted at room temperature, filled into 10 ml plastic bottles and frozen until the laboratory analysis.

The analysis were carried out using a laser spectroscopy by LGR Inc. LWIA v2 facility of the Czech Technical University in Prague (Penna et al., 2010). Standard deviation of the results is δ^2H 0.58 ‰ V-SMOW and 95 % confidence interval is δ^2H 0.33 ‰ V-SMOW.

2.5 Data interpretation

The hydrograph separation technique was used to separate rainwater from the non-rain water in the total runoff:

$$Q_{total}(t) \times c_{total}(t) = Q_{rain}(t) \times c_{rain} + Q_{non-rain}(t) \times c_{non-rain}(t) \quad (1)$$

$$Q_{total}(t) = Q_{rain}(t) + Q_{non-rain}(t), \quad (2)$$

where Q [mm· min^{-1}] is the flow rate, c [‰ δ^2H in V-SMOW] is the deuterium concentration and the subscripts *total*, *rain* and *non-rain* represent the total gauged snowpack runoff, the rainwater runoff and water originates from pre-experimental LWC and snowmelt respectively.

The non-rain water was considered as a mixture of two components pre-event liquid water content in the snowpack (pre-LWC) and the additional snowmelt water within the experimental snow block:

$$Q_{non-rain} = Q_{melt} + Q_{pre-LWC}. \quad (3)$$

Q_{melt} represents additional melt water produced during the experiment and $Q_{pre\text{-}LWC}$ represents pre-experimental liquid water content in the snowpack. Since the isotopic content of the snowpack varies within the vertical profile we assume that the reference value of non-rain water is time variant. According to previous investigations (Juras et al., 2016), rainwater appears in the snowpack runoff only after a certain delay. We can therefore assume that at the beginning of runoff the non-rain water consisted mostly of pre-LWC water ($Q_{pre\text{-}LWC}$). After some time contribution of pre-LWC retreats and additional melt water (Q_{melt}) starts to dominate within the non-rain runoff water volume. This water originating instantly from the solid phase has different isotopic content compared to pre-LWC (Feng, 2002; Hashimoto et al., 2002; Unnikrishna et al., 2002). The partitioning of the non-rain water in the snowpack ($c_{non\text{-}rain}$ in eq. 1) can be expressed as:

$$c_{non-rain} = \tan^{-1}\left(\frac{\frac{(T-t)\cdot 20\pi}{S}}{\pi} + 0.5\right) \cdot (c_{solid} - c_{melt}) + c_{melt}, \quad (4)$$

where T is time vector, t [min] is time hypothetically needed to release all pre-LWC water, S is a dimensionless parameter governing the shape of the curve, c_{solid} is deuterium content of solid phase of the entire pre-experimental snowpack, c_{melt} is deuterium content of pre-experimental meltwater. Parameter t was derived as the time when volume of non-rain water equalled pre-LWC (Fig. 2). The temporal smoothing parameter S was set to an arbitrary value of 45, c.f. section 4.4 for a discussion on the sensitivity of alternative approaches regarding eq (4). All fitted parameters are listed in Table 2. An illustration of the mixing curve is displayed in Figure 2

Table 2

The isotopic value of the pre-LWC non-rain water was derived from the sampling of the pre-experiment melt outflow and the isotopic value of the additional melt was derived from the sample of entire snowpack. The isotopic value of the rainwater was derived from the sampling of the water in barrel. In view of the short duration of the experiment, we don't assume any fractionation between solid and liquid phase during the sprinkling.

Rainwater storage in the snow cube was estimated as:

$$Q_{stored} = Q_{rain-} - Q_{rain-out}. \quad (5)$$

We define the LWC deficit as the non-rain water contribution to the snowpack runoff that cannot be satisfied from the initial LWC storage. Hence values above zero indicate the minimal snowmelt that must have occurred to provide LWC for the snowpack runoff. The LWC deficit is calculated as a cumulative deficit from the water balance as:

$$LWC_{deficit}\,(t) = \max\,(\textstyle\sum_0^t V_{non-rain} - LWC_{init}, 0), \quad (6)$$

where LWC_{init} refers to initial total LWC summarised in Table 3 $V_{non\text{-}rain}$ refers to the volume of non-rain water in the runoff. Hydrograph data were analysed for time lag and peak times of each hydrograph component (Fig. 3). We define rainwater time lag as a time when rainwater runoff rate reaches 0.01 mm·h^{-1} (according to Eq. 1, 2). Total water time lag is defined as a time difference between onset of the rain and the first significant increase of total water runoff above the base flow (consisting of melt) (Eq. 2). Peak time is defined as a time difference between onset of the rain and the time of runoff maximum of each hydrograph component.

Uncertainties of rainwater runoff contribution were estimated from using the spread between individual samples from the vertical snow profiles at 10 % and 90 % percentiles.

Figure 3

3 Results

3.1 Snowpack changes

Table 3 shows an overview of the pre-experimental and post-experimental snowpack conditions. The three snow blocks in Ex 2-4 consisted of snow with similar conditions being isothermal, well ripened with bulk densities above 400 kg·m^{-3} and contained considerable initial liquid water. These snowpack conditions are referred to in the text as "ripe snow". Pre-experimental snowpack conditions in Ex1 differed from the other three. Snow temperatures were mostly below the freezing point and the bulk density was around 250 kg·m^{-3}. Despite this, a small amount of pre-experimental LWC was found in the top 5 cm, where the snow temperature was around the freezing point (Ex1). Nevertheless, these snowpack conditions are referred to as "cold snow".

Unlike our expectations, the experiments resulted in greater density changes in ripe snow compared to the changes in cold snow. The total bulk density increased by between 17 and 54 kg·m^{-3} in Ex 2-4 compared to a 4 kg·m^{-3} increase only in Ex 1 (Table 3),. On the contrary, LWC increased in all experiments by very similar values of approx. 2 %.

Table 3

An increased deuterium content of snow, caused by the isotopically enriched sprinkling water, indicate additional storage of rain water. Our results showed a considerable increase in deuterium content (Table 4) only for ex. 2-4 (ripe snow conditions). In comparison, Ex. 1 (cold snow) showed a more ambiguous picture, indicating that only little rainwater volume remained in the snow after the experiment; if at all, the deuterium content even decreased slightly (by -0.88 ‰). Details of the deuterium content of the main components before and after the experiments are listed in Table 4.

Table 4

3.2 Snowpack runoff

All experiments showed a quick response in snowpack runoff within 10 min (Ex1) to 27 min (Ex4) after the start of sprinkling (Fig. 4). However, the first significant increase of deuterium content (signalizing the appearance of the rainwater) was detected in the runoff somewhat later which indicates that rainwater initially pushed out the pre-event LWC and only then started to contribute to the runoff with some delay. Time lags and peak flow times of main hydrograph components are summarised in Table 5. The difference between rainwater time lag and total water time lag indicates the delay with which rainwater appears in the snowpack runoff relative to other source of LWC. Interestingly, this delay was considerable in experiments 2-4 (at least 12 minutes), but only minor (6 minutes) in experiment 1 which was the only one conducted on cold snow.

Also the difference between total runoff and rain runoff demonstrate that water from other sources than rain such as pre-experimental LWC dominated snowpack runoff at the beginning of the sprinkling experiment. Again it is experiment 1 that deviates from the other by featuring a higher rain contribution in the total runoff already during the first sprinkling periods (Fig. 4). Towards the end of the experiment (sprinkling period 4) rain contributed only 27 % in Ex4 but 82 % in Ex1.

The total water time lag was similar between the four sprinkling periods of each experiment, with the exception of Ex1 that featured a considerably longer time lag in the first sprinkling period compared to all subsequent periods, which may hint at the development of preferential flow paths early on during the experiment.

Figure 4

Table 5

3.3 Water balance

All experiments showed a negative snowpack mass balance (Table 6), which is characterized by cumulative total runoff (output) exceeding the cumulative rain input (Fig. 5). This required that additional melt occurred during all experiments. Cumulative event runoff computed according to Eq. 1 and 2 consisted of between 22.0 % (Ex4) and 76.4 % (Ex1) of rainwater (Table 6, Fig. 5). The storage of rainwater was calculated according to Eq. 5 which revealed that averaged over the entire experiment the snowpack retained 21.6 % (Ex1) to 69.6 % (Ex4) of the original rainwater volume. However, the rainwater storage ratio varied over the course of the experiment. After

the first sprinkling period the ratio was always highest and decreased with subsequent sprinkling periods (Table 6), and even depleted almost completely towards the end of Ex1.

Figure 6

The pre-LWC represented an important source of non-rain water in the snowpack runoff, especially during the first sprinkling period. The LWC deficit for each sprinkling period is shown in table 6. For example, in Ex1 only 0.9 mm of pre-LWC was available (Table 3), but 4.1 mm of non-rain water appeared in the outflow after the first sprinkling period (Table 6), resulting in a LWC deficit of 3.17 mm that must have been satisfied by snowmelt. In contrast, the initial snowpack in Ex2-4 contained sufficient pre-LWC to fully explain the non-rain component to the runoff from the first sprinkling period. But also towards the end of these experiments some meltwater is required to explain the observed snowpack runoff.

Table 6

4 Discussion

4.1 Rainwater interaction with the snowpack

Samples from snowpack runoff at the beginning of the sprinkling experiment revealed, that the first water to exfiltrate from the snowpack originated from pre-LWC, and not from the rain. Only with a certain time lag did rain start to appear in the runoff samples. Obviously, rainwater introduced to the snowpack pushed existing pre-LWC water out of the snow block during the onset of the runoff generation. First water samples taken from the runoff featured a similar deuterium content as the pre-LWC, we may thus assume that pre-LWC predominated in the non-rain water at the beginning of the experiment, but as the pre-LWC storage depleted meltwater took over. The process where rainwater shifted the pre-LWC out of the snow matrix has been described as piston flow (Feng et al., 2001; Unnikrishna et al., 2002). The piston flow effect probably played a role not only at the beginning of runoff generation. Time shifts in peak flow times suggest that rainwater pushed non-rain water even beyond the initial phase, although the effect weakened over the course of the experiment (Table 5). A similar behaviour was also described in Juras et al. (2016).

Comparing the volume of retained rainwater within the first sprinkling period with the amount of released non-rain water (Table 6) reveals that in all experiments the initial snowpack had liquid water deficiency. Available pore space in the snowpack was filled after beginning of the sprinkling, which also resulted in relatively little rainwater runoff during the first sprinkling period. The rainwater contribution however increased during subsequent sprinkling periods, as available storage capacity for liquid water depleted and pre-LWC water exfiltrated. During all experiments the ratio of rainwater in total snowpack runoff was well below 100 % at all times (Fig. 4). This indicates that some rainwater is constantly retained in the snowpack (refrozen or as LWC) over the entire course of the sprinkling within both, cold as well as ripe snow.

Differences in the results from Ex1 relative to results from the other experiments demonstrated that the contribution of rainwater to the runoff is influenced by the initial snowpack conditions. Cold snowpack containing low pre-LWC volume allowed high contribution of rainwater to the runoff (Ex1). On the other hand, ripe snowpack with considerable pre-LWC volume showed stronger indication of piston flow, which resulted in mostly non-rain water

to appear in early snowpack runoff. Adding rain, pre-LWC and additional melt resulted in total cumulative runoff volumes exceeding the cumulative rain input on average by 27 % for the experiment with ripe snow (Ex2-4). To the contrary, runoff from the cold snowpack exceeded rain input only by 3 %.

4.2 Hydrological response of snowpack with different snow conditions on ROS

Our results showed that rainwater was transported much faster in cold snow (Table 5) which indicated the presence of preferential flow (Section 3.2). On the other hand, experiment with ripe snow, resulted in a much slower transport of rain water and showed evidence of the matrix flow regime. These findings are in agreement with previous studies of Schneebeli (1995) and Würzer et al. (2016b), but see Colbeck (1975) who reported long time lags to be typical for rain on cold snowpacks. Preferential flow is mostly observed in layered snow, where microstructural transitions can be found in the density profile (Hirashima et al., 2014; Techel et al., 2008). During preferential flow the wetting front is disaggregated into many smaller flow fingers, within which the hydraulic conductivity can be very high (Waldner et al., 2004) allowing water to be transported faster.

The hydraulic conductivity is connected to the intrinsic permeability of snow (Calonne et al., 2012) and varies with the snow grain size and density (Hirashima et al., 2014). The intrinsic permeability increases as the snow density decreases (Calonne et al., 2012), which is in agreement with our results. The snow in Ex1 was characterized by a low density and therefore supported faster generation of snowpack runoff compared to Ex2-Ex4. On the other hand, ripe snow typically features rounded snow grains and initial saturation which are associated with higher hydraulic conductivities. This opposing effect may have led to the findings of Colbeck (1975) cited above. In our experiments however, the distinctly lower density of the snow in Ex1 in combination with the occurrence of preferential flow seem to have prevailed other effects and caused a considerably faster transport of liquid water through the snowpack if compared to the experiments in ripe snow.

Ex1 aside, Ex2-4 showed similar initial snowpack conditions with the exception of snow depth (Table 3). This allowed to verify that rainwater time lags were expectedly sensitive to the transport distance. Time lags recorded during Ex4 were markedly longer than those recorded during Ex2-3, which supports a positive correlation between snow depth and water transport times as also noted by Wever et al. (2014).

4.3 Internal mass exchange

Our results provide an evidence of internal mass and energy exchange processes in the snowpack during the sprinkling experiments. Such processes represent refreezing of rainwater and generation of snowmelt (Avanzi et al., 2015; Wever et al., 2015), whereas mass has additionally been exchanged by the displacement of pre-LWC by rainwater.

After the first sprinkling period the cold snowpack in Ex1 released more non-rain water than can be explained by available pre-experimental LWC. The corresponding LWC deficit even increase over the course of the sprinkling experiment (Table 6). This leads to the conclusion that snowmelt must have occurred as one of the processes involved in runoff generation. Further, rain water retained in the snowpack at the end of the experiment was larger than the final LWC which suggests that at the same time some rain water has been refrozen. Nevertheless, these processes may have been limited to comparably small amounts of water since the LWC deficit as well as the

retained rain water volume were relatively small compared to the runoff volume. This conclusion is also supported by the small difference between the deuterium concentration of the snowpack before and after the experiment (Table 4).

Ex4, to the contrary, started with sufficient LWC to explain the runoff originating from non-rain water until sprinkling period 4. While snowmelt may or may not have happened during the entire experiment, it must at least have occurred during sprinkling period 4. But apparently pre-experimental LWC has dominated the runoff generated early on during the experiment (see discussion on piston flow regime). The same applies to Ex2 and 3, for which snowmelt was evidenced from at least sprinkling period 2 onwards. In all 3 experiments the deuterium concentration differed considerably in snow samples collected before and after the experiment. This suggests that mass exchange processes have had a larger turnover compared to Ex1.

4.4 Using a variable non-rain water reference in eq (4)

The deuterium concentration of pre-experimental melt water and samples taken from the entire snowpack profile differed within all experiments (Table 4). This is caused when snowmelt is not produced over the entire snow profile (Ex 1). Snowmelt prevails in the upper part of the snowpack. And indeed, the deuterium concentration of pre-experimental melt in Ex 1 was very close to values sampled from top level of the snow profile.

We can expect that the pre-experimental melt (sourcing from pre-LWC) is continuously depleted and meltwater is also concurrently produced from the snowpack with different isotopic concentration. This is why we introduced an enhanced approach of hydrograph separation between rainwater and non-rain water by allowing the non-rain water isotopic reference value to be variable in time. This method was compared to the more traditional approach (c.f. Juras et al., 2016) where a constant isotopic value is used from either pre-experimental meltwater or sampled from the entire snowpack. Also different parameters (t, S) in equation 4 were tested. Table 7 summarises rain water time lags, rainwater peak times and cumulative rainwater of all experiments that resulted from our sensitivity tests. While in general the differences between results from different approaches were small, notably different time lags resulted when using a constant isotopic value sampled from the entire snow column.

Especially in Ex1 when the isotopic value from the snowpack is used, the resulting rainwater time lag of 0 is unrealistic. While differences between the approaches are minor, using a time variant non-rainwater reference value seems to be a reasonable approach to arrive at more accurate estimations of rainwater time lags and outflow volumes.

Table 7

5 Conclusion

In this study we investigated liquid water transport behaviour through natural snow by means of sprinkling experiments. Using deuterated water enabled to disentangle the fate of rain water and initial liquid water content. Furthermore, the approach provided evidence of rain water refreezing and meltwater generation to occur together over the course of the sprinkling experiments.

Interestingly, a sprinkling experiment on a cold snowpack resulted in markedly different water transport dynamics in comparison to experiments on melting snow. Snowpack runoff responded comparably quickly to the onset of sprinkling, and rainwater arrived in the runoff with a short delay only. The overall share of rainwater in the runoff was around 80 % indicating that internal mass exchange processes played a minor role. Data from this experiment further suggested the development of preferential flow paths that allowed rainwater to propagate increasingly efficient through the snowpack as the sprinkling continued.

On the other hand, experiments conducted on wet isothermal snowpack, showed a different behaviour. Snowpack runoff was considerably delayed relative to the onset of the sprinkling, and consisted of initial liquid water content only. Rainwater appeared in the runoff only with further delay and with a relatively low share, where the overall contribution of rainwater in the runoff did not exceed 50 %. At the same time, the total runoff volume exceeded rain input plus initial liquid water content which requires that additional water from snowmelt contributed to the runoff. Both findings demonstrate that internal mass exchange processes were important for runoff generation during rain on a melting snowpack.

Data availability

All data are available on request.

Acknowledgement

We would like to thank the scientific exchange program Sciex-NMS^{ch} (project code 14.105), the Swiss Federal Office for the Environment FOEN and Internal Grant Agency of the Faculty of Environmental Sciences, CULS Prague (project 20144254) and the Swiss National Foundation (Scopes) project Snow resources and the early prediction of hydrological drought in mountainous streams (SREPDROUGHT) IZ73ZO_152506/CZ for the funding of the project. Many thanks also belong to Timea Mareková and Pascal Egli for tremendous help and assistance during the field work. We also want to thank the SLF staff for technical support and Martin Šanda for isotope analysis.

References

Ambach, W. and Howorka, F.: Avalanche activity amd free water content of snow at Oberlung (1980 m a.s.l., Spring 1962), in Symposium at Davos 1965 - Scientific Aspects of Snow and Ice Avalanches, vol. 69, pp. 65–72, International Assocciation of Scientific Hydrology Publication 69, Davos., 1966.

Avanzi, F., Yamaguchi, S., Hirashima, H. and De Michele, C.: Bulk volumetric liquid water content in a seasonal snowpack: Modeling its dynamics in different climatic conditions, Adv. Water Resour., 86, 1–13, doi:10.1016/j.advwatres.2015.09.021, 2015.

Badoux, A., Hofer, M. and Jonas, T.: Hydrometeorologische Analyse des Hochwasserereignisses vom 10. Oktober 2011. [online] Available from: http://www.wsl.ch/fe/gebirgshydrologie/wildbaeche/projekte/unwetter2011/Ereignisanalyse_Hochwasser_Oktober_2011.pdf, 2013.

Baggi, S. and Schweizer, J.: Characteristics of wet-snow avalanche activity: 20 years of observations from a high alpine valley (Dischma, Switzerland), Nat. Hazards, 50(1), 97–108, doi:10.1007/s11069-008-9322-7, 2008.

Bartelt, P. and Lehning, M.: A physical SNOWPACK model for the Swiss avalanche warning Part I : numerical model, Cold Reg. Sci. Technol., 35, 123–145, 2002.

Buttle, J. M., Vonk, A. M. and Taylor, C. H.: Applicability of isotopic hydrograph separation in a suburban basin during snowmelt, Hydrol. Process., 9(June 1993), 197–211, doi:10.1002/hyp.3360090206, 1995.

Calonne, N., Geindreau, C., Flin, F., Morin, S., Lesaffre, B., Rolland Du Roscoat, S. and Charrier, P.: 3-D image-based numerical computations of snow permeability: Links to specific surface area, density, and microstructural anisotropy, Cryosphere, 6(5), 939–951, doi:10.5194/tc-6-939-2012, 2012.

Casson, N. J., Eimers, M. C. and Watmough, S. a.: Sources of nitrate export during rain-on-snow events at forested catchments, Biogeochemistry, 120(3), 23–36, doi:10.1007/s10533-013-9850-4, 2014.

Colbeck, S. C.: Analysis of hydrologic response to rain-on-snow, Hanover, New Hampshire. [online] Available from: http://144.3.144.25/uhtbin/cgisirsi.exe/yPf3qH7e6H/0/49, 1975.

Conway, H. and Benedict, R.: Infiltration of water into snow, Water Resour. Res., 30, 641–649, 1994.

Conway, H. and Raymond, C. F.: Snow stability during rain, J. Glaciol., 39(133), 635–642, 1993.

Čekal, R., Ryglewicz, M., Boříková, L., Suchá, M., Přibyl, J. and Kotek, R.: Zpráva o povodni v lednu 2011 (in Czech), Report, Available online at: (http://portal.chmi.cz/files/portal/docs/hydro/ohp/povoden_01_2011.pdf), Accessed 17.10.2014, Prague. [online] Available from: http://portal.chmi.cz/files/portal/docs/hydro/ohp/povoden_01_2011.pdf, 2011.

Denoth, A.: An electronic device for long-terlll snow wetness recording, Ann. Glaciol., 19, 104–106, 1994.

Dinçer, T., Payne, B. R., Florkowski, T., Martinec, J. and Tongiorgi, E.: Snowmelt runoff from measurements of tritium and oxygen-18, Water Resour. Res., 6(1), 110–124, doi:10.1029/WR006i001p00110, 1970.

Dozier, J., Melack, J. M., Elder, K., Kattelmann, R., Marks, D. and Williams, M.: Snow, snowmelt, rain, runoff, and chemistry in a Sierra Nevada watershed, Santa Barbara. [online] Available from: http://o3.arb.ca.gov/research/apr/past/a6-147-32a.pdf, 1989.

Eiriksson, D., Whitson, M., Luce, C. H., Marshall, H. P., Bradford, J., Benner, S. G., Black, T., Hetrick, H. and McNamara, J. P.: An evaluation of the hydrologic relevance of lateral flow in snow at hillslope and catchment scales, Hydrol. Process., 27(5), 640–654, doi:10.1002/hyp.9666, 2013.

Feng, X.: Isotopic evolution of snowmelt 1. A physically based one-dimensional model, Water Resour. Res., 38(10), doi:10.1029/2001WR000814, 2002.

Feng, X., Kirchner, J. W., Renshaw, C. E., Osterhuber, R. S., Klaue, B. and Taylor, S.: A study of solute transport mechanisms using rare earth element tracers and artificial rainstorms on snow, Water Resour. Res., 37(5), 1425–1435, doi:10.1029/2000WR900376, 2001.

Ferguson, S. A.: The spatial and temporal variability of rain-on-snow, in Assessment International Snow Science Workshop, 1-6 October 2000, pp. 178–183, American Avalanche Association, Big Sky, Montana., 2000.

Gude, M. and Scherer, D.: Snowmelt and slushflows: hydrological and hazard implications, J. Glaciol., 26, 381–384, 1998.

Harrington, R. and Bales, R. C.: Modeling ionic solute transport in melting snow, Water Resour. Res., 34(7), 1727–1736, 1998.

Hashimoto, S., Shiqiao, Z., Nakawo, M., Sakai, A., Ageta, Y., Ishikawa, N. and Narita, H.: Isotope studies of inner snow layers in a temperate region, Hydrol. Process., 16(11), 2209–2220, doi:10.1002/hyp.1151, 2002.

Hestnes, E. and Sandersen, F.: Slushflow activity in the Rana district, North Norway, in Avalanche Formation, Movement and Effect (Proceedings of Davos Symposium, September 1986), pp. 317–330, IAHS Publ. 162, Davos., 1987.

Hirashima, H., Yamaguchi, S., Sato, A. and Lehning, M.: Numerical modeling of liquid water movement through layered snow based on new measurements of the water retention curve, Cold Reg. Sci. Technol., 64(2), 94–103, doi:10.1016/j.coldregions.2010.09.003, 2010.

Hirashima, H., Yamaguchi, S. and Katsushima, T.: A multi-dimensional water transport model to reproduce the preferential flow in a snowpack, Cold Reg. Sci. Technol., 108, 31–37, doi:10.1016/j.coldregions.2014.09.004,

2014.

HND Bayern: Gewässerkundlicher Monatsbericht Januar 2011 - Hochwasser (in German), report, Available online at: (http://www.hnd.bayern.de/ereignisse/monatsberichte/md_fghw_0111.pdf), Accessed 17.10.2014. [online] Available from: http://www.hnd.bayern.de/ereignisse/monatsberichte/md_fghw_0111.pdf, 2011.

Jones, H. G., Tranter, M. and Davies, T. D.: The leaching of strong acid anions from snow during rain-on-snow events: evidence for two component mixing, in Atmospheric Deposition, vol. IAHS Publ., pp. 239–250. [online] Available from: http://iahs.info/redbooks/a179/iahs_179_0239.pdf, 1989.

Juras, R., Pavlásek, J., Děd, P., Tomášek, V. and Máca, P.: A portable simulator for investigating rain-on-snow events, Zeitschrift für Geomorphol. Suppl. Issues, 57(1), 73–89, doi:10.1127/0372-8854/2012/S-00088, 2013.

Juras, R., Pavlásek, J., Vitvar, T., Šanda, M., Holub, J., Jankovec, J. and Linda Miloslav: Isotopic tracing of the outflow during artificial rain-on-snow event, J. Hydrol., 1, 1145–1154, doi:http://dx.doi.org/10.1016/j.jhydrol.2016.08.018, 2016.

Katsushima, T., Yamaguchi, S., Kumakura, T. and Sato, A.: Experimental analysis of preferential flow in dry snowpack, Cold Reg. Sci. Technol., 85, 206–216, doi:10.1016/j.coldregions.2012.09.012, 2013.

Kattelmann, R.: Flooding from rain-on-snow events in the Sierra Nevada, in Water-Caused Natural Disasters, their Abatement and Control (Proceedings of the Anaheim Conference, California, June 1996), pp. 59–65, IAHS Publ. 239, Anaheim, California., 1997.

Krouse, R., Hislop, R., Brown, H. M., West, T. and Smith, J. L.: Climatic and spatial dependence of the retention of D/H and 180/160 abundances in snow and ice of North America, in Isotopes and Impurities in Snow and Ice, vol. 1, pp. 242–247., 1977.

Lee, J., Feng, X., Posmentier, E. S., Faiia, A. M., Osterhuber, R. and Kirchner, J. W.: Modeling of solute transport in snow using conservative tracers and artificial rain-on-snow experiments, Water Resour. Res., 44(2), 1–12, doi:10.1029/2006WR005477, 2008.

Lee, J., Feng, X., Faiia, A. M., Posmentier, E. S., Kirchner, J. W., Osterhuber, R. and Taylor, S.: Isotopic evolution of a seasonal snowcover and its melt by isotopic exchange between liquid water and ice, Chem. Geol., 270(1–4), 126–134, doi:10.1016/j.chemgeo.2009.11.011, 2010.

MacLean, R. A., English, M. C. and Schiff, S. L.: Hydrological and hydrochemical response of a small Canadian Shield catchment to late winter rain-on-snow events, Hydrol. Process., 9(April), 845–863, doi:10.1002/hyp.3360090803, 1995.

McCabe, G. J., Hay, L. E. and Clark, M. P.: Rain-on-Snow Events in the Western United States, Bull. Am. Meteorol. Soc., 88(3), 319–328, doi:10.1175/BAMS-88-3-319, 2007.

Nyberg, R.: Observations of slushflows and their geomorphological effects in the Swedish mountain area, Geogr. Ann., 71 A(3), 185–198, 1989.

Onesti, L. J.: Slushflow release mechanism : A first approximation, in Avalanche Formation, Movement and Effect, pp. 331–336, IAHS Publ. 162, Davos., 1987.

Osterhuber, R. S.: Precipitation intensity during rain-on-snow, in Western Snow Conference, pp. 153–155, South Lake Tahoe. [online] Available from: http://www.westernsnowconference.org/sites/westernsnowconference.org/PDFs/1999Osterhuber.pdf (Accessed 9 December 2014), 1999.

Penna, D., Stenni, B., Šanda, M., Wrede, S., Bogaard, T. a., Gobbi, A., Borga, M., Fischer, B. M. C., Bonazza, M. and Chárová, Z.: On the reproducibility and repeatability of laser absorption spectroscopy measurements for δ2H and δ18O isotopic analysis, Hydrol. Earth Syst. Sci., 14(8), 1551–1566, doi:10.5194/hess-14-1551-2010, 2010.

Rössler, O., Froidevaux, P., Börst, U., Rickli, R., Martius, O. and Weingartner, R.: Retrospective analysis of a nonforecasted rain-on-snow flood in the Alps-A matter of model limitations or unpredictable nature?, Hydrol. Earth Syst. Sci., 18(6), 2265–2285, doi:10.5194/hess-18-2265-2014, 2014.

Schneebeli, M.: Development and stability of preferential flow paths in a layered snowpack, IAHS-AIHS Publ., 228(228), 89–95, [online] Available from: http://www.iahs.info/uploads/dms/iahs_228_0089.pdf, 1995.

Singh, P., Spitzbart, G., Hübl, H. and Weinmeister, H. W.: The role of snowpack in producing floods under

heavy rainfall, in Hydrology, Water Resources and Ecology in Headwaters, pp. 89–95, IAHS Publ. 248, Merano., 1998.

Singh, V. P., Spitzbart, G., Hübl, H. and Weinmeister, H. W.: Hydrological response of snowpack under rain-on-snow events: a field study, J. Hydrol., 202(1–4), 1–20, doi:10.1016/S0022-1694(97)00004-8, 1997.

Sui, J. and Koehler, G.: Rain-on-snow induced flood events in Southern Germany, J. Hydrol., 252, 205–220, doi:10.1016/S0022-1694(01)00460-7, 2001.

Techel, F., Pielmeier, C. and Schneebeli, M.: The first wetting of snow: micro-structural hardness measurements using a snow micro penetrometer, in International Snow Science Workshop, vol. 1, pp. 1019–1026, Whistler., 2008.

Tusima, K.: Grain coarsening of snow particles immersed in water and solution, Ann. Glaciol., 6, 126–129, 1985.

Unnikrishna, P. V., McDonnell, J. J. and Kendall, C.: Isotope variations in a Sierra Nevada snowpack and their relation to meltwater, J. Hydrol., 260, 38–57, doi:10.1016/S0022-1694(01)00596-0, 2002.

Waldner, P. a., Schneebeli, M., Schultze-Zimmermann, U. and Flühler, H.: Effect of snow structure on water flow and solute transport, Hydrol. Process., 18, 1271–1290, doi:10.1002/hyp.1401, 2004.

Wever, N., Jonas, T., Fierz, C. and Lehning, M.: Model simulations of the modulating effect of the snow cover in a rain on snow event, Hydrol. Earth Syst. Sci. Discuss., 11(5), 4971–5005, doi:10.5194/hessd-11-4971-2014, 2014.

Wever, N., Schmid, L., Heilig, A., Eisen, O., Fierz, C. and Lehning, M.: Verification of the multi-layer SNOWPACK model with different water transport schemes, Cryosphere, 9(6), 2271–2293, doi:10.5194/tc-9-2271-2015, 2015.

Würzer, S., Jonas, T., Wever, N. and Lehning, M.: Influence of Initial Snowpack Properties on Runoff Formation during Rain-on-Snow Events, J. Hydrometeorol., 17(6), 1801–1815, doi:10.1175/JHM-D-15-0181.1, 2016a.

Würzer, S., Wever, N., Juras, R., Lehning, M. and Jonas, T.: Modeling liquid water transport in snow under rain-on-snow conditions considering preferential flow, Hydrol. Earth Syst. Sci. Discuss., 18(August), 16488, doi:10.5194/hess-2016-351, 2016b.

Yamaguchi, S., Katsushima, T., Sato, A. and Kumakura, T.: Water retention curve of snow with different grain sizes, Cold Reg. Sci. Technol., 64(2), 87–93, doi:10.1016/j.coldregions.2010.05.008, 2010.

Zhou, S., Nakawo, M., Hashimoto, S. and Sakai, A.: The effect of refreezing on the isotopic composition of melting snowpack, Hydrol. Process., 22(June 2007), 873–882, doi:10.1002/hyp, 2008.

Table 1 - Details of the experiments

Site	Latitude	Longitude	Elevation	Label	Date
Sertig 1	46.7227267N	9.8505897E	**1850 m**	Ex1	***17. – 19.3 2015***
Sertig 2	46.7227856N	9.8507236E	**1850 m**	Ex2	***22. – 24.4. 2015***
Dischma	46.7209731N	9.9219625E	**2000 m**	Ex3	**29.4 – 2.5. 2015**
Flüela	46.7436736N	9.9812761E	**2150 m**	Ex4	**7. – 9.5. 2015**

Table 2 – Parameters used in equation 4 for every single experiment.

Experiment	**t [min]**	**S [-]**
Ex1	20	45
Ex2	95	45
Ex3	88	45
Ex4	215	45

Table 3 – Experimental snow block conditions before and after each experiment. Bulk density values were derived from the entire snow profile sample.

Snow properties	Pre-experiment		After-experiment		Difference
	Mean	St. Dev.	Mean	St. Dev.	
	Ex1 – Sertig, Snow pits 17.-19.3.2015				
Bulk density [kg.cm^{-3}]	247	4	251	8	4
Total LWC [%]	0.2	1.1	1.7	0.5	1.6
Total LWC [mm]	0.9	0.3	8.3	2.4	7.4
Snow depth [cm]	54.4	3.7	48.2	3.0	-6.2
Snow temperature [°C]	-1.0	0.6	0.0	0.0	1.0
	Ex2 – Sertig, Snow pits 22.-24.4.2015				
Bulk density [kg.cm^{-3}]	408	18	425	12	17
Total LWC [%]	3.7	0.1	5.3	0.7	1.6
Total LWC [mm]	11.0	0.3	13.9	1.1	2.8
Snow depth [cm]	29.7	2.2	25.8	2.1	-3.9
Snow temperature [°C]	0.0	0.0	0.0	0.0	0.0
	Ex3 – Dischma, Snow pits 29.-1.5.2015				
Bulk density [kg.cm^{-3}]	403	33	457	14	54
Total LWC [%]	3.8	0.3	6.3	0.1	2.6
Total LWC [mm]	10.6	0.8	16.9	0.3	6.3
Snow depth [cm]	28.1	2.5	26.6	2.1	-1.6
Snow temperature [°C]	0.0	0.0	0.0	0.0	0.0
	Ex4 – Fluela, Snow pits 6.-8.5.2015				
Bulk density [kg.cm^{-3}]	477	21	495	9	18
Total LWC [%]	3.5	0.5	5.6	0.3	2.1
Total LWC [mm]	28.7	4.3	45.8	3.7	17.1
Snow depth [cm]	88.4	2.1	81.6	2.4	-6.8
Snow temperature [°C]	0.0	0.0	0.0	0.0	0.0

Table 4 – Overview of deuterium concentration changes within each experiment. Reference values were used in eq. 1 and 4 for hydrograph separation. Snow samples were taken by extracting a vertical core from the entire snow profile.

	Pre-experimental reference value			Reference value after experiment	Difference
	Rainwater	***Melt water***	***Snow sample***	***Snow sample***	***Snow sample***
Ex1	-23.11	-88.64	-138.88	-139.76	-0.88
Ex2	-5.60	-123.49	-120.41	-116.32	4.09
Ex3	22.61	-132.47	-122.00	-105.84	16.16
Ex4	-13.16	-118.66	-127.48	-116.22	11.26

Table 5 – Hydrograph analysis of different artificial rain-on-snow event.

Sprinkling period	Time lag total [min]	Time lag rain [min]	Rainwater velocity [cm.min^{-1}]	Peak time total [min]	Peak time rain [min]
Ex1 - Sertig 17.-19.3.2015 - *snow depth = 54.4 cm*					
1	10	16	3.40	27	33
2	4	4	13.60	22	27
3	4	4	13.60	20	27
4	5	5	10.88	25	25
Ex2 - Sertig 22.-24.4.2015 -*snow depth = 29.7 cm*					
1	15	27	1.10	35	40
2	13	13	2.28	31	36
3	17	17	1.75	28	10
4	13	14	2.12	30	10
Ex3 - Dischma 29.4.-1.5.2015 - *snow depth = 29 cm*					
1	13	26	1.08	33	36
2	9	9	3.12	29	34
3	11	11	2.55	28	31
4	9	9	3.12	27	27
Ex4 - Flüela 6.-8.5.2015 - *snow depth = 88.4 cm*					
1	27	∞*	na*	50	na*
2	27	27	3.27	47	49
3	27	27	3.27	46	53
4	32	32	2.76	47	51

***** rainwater was not recorded in response to the first sprinkling burst

Table 6 – Water balance computed from every outflow peak of the four experiments.

Sprinkling period	Input [mm]	LWC deficit [mm]	Total out [mm]	Rain out [mm]	Rain out [%]	Non-Rain out [mm]	Volume rain stored [mm]	Volume Rain Stored [%]
			Ex1 - Sertig 17.-19.3.2015					
1	10.39	3.17	8.14	4.04	49.65	4.10	6.35	61.10
2	10.39	5.36	11.48	9.29	80.95	2.19	1.10	10.56
3	10.39	6.87	10.52	9.01	85.62	1.51	1.38	13.31
4	10.39	9.15	12.53	10.26	81.85	2.27	0.13	1.29
Total	**41.56**		**42.67**	**32.60**	**76.40**	**10.07**	**8.96**	**21.56**
			Ex2 - Sertig 22.-24.4.2015					
1	10.13	0	8.98	1.76	19.63	7.22	8.37	82.60
2	10.13	4.66	14.00	5.57	39.76	8.43	4.56	45.04
3	10.13	11.55	11.49	4.60	40.04	6.89	5.53	54.59
4	10.13	24.76	20.02	6.81	34.03	13.21	3.32	32.75
Total	**40.52**		**54.49**	**18.74**	**34.40**	**35.75**	**21.78**	**53.74**
			Ex3 - Dischma 29.4.-1.5.2015					
1	10.39	0	7.20	1.58	21.89	5.62	8.81	84.83
2	10.39	0.25	10.44	5.14	49.21	5.30	5.25	50.55
3	10.39	4.98	11.14	6.41	57.55	4.73	3.98	38.30
4	10.39	11.55	16.22	9.64	59.46	6.58	0.75	7.17
Total	**41.56**		**45.00**	**22.77**	**50.60**	**22.23**	**14.25**	**45.21**
			Ex4 – Flüela 6.-8.5.2015					
1	10.39	0	4.62	0.00	0.00	4.62	10.39	100.00
2	10.39	0	12.38	1.89	15.28	10.49	8.50	81.79
3	10.39	0	12.08	3.16	26.14	8.92	7.23	69.61
4	10.39	16.13	28.40	7.60	26.75	20.80	2.79	26.87
Total	**41.56**		**57.48**	**12.65**	**22.00**	**44.83**	**28.91**	**69.57**

Table 7 – Different methods for estimation of reference non-rain water isotopic value were used in this table. 1. Constant value of a) entire snow sample, b) pre-experimental melt water and 2. Different parameters t, S in equation 4, where a) parameter used from Table 2, b) modified parameter from Table 2; t = t/2, S = S, c) modified parameter from Table 2; t = 2t, S = S, d) modified parameter from Table 2; t = t, S/2 = S, e) modified parameter from Table 2; t = t, S = 2S.

	Non-rain reference isotopic source	Time lag rain [min]				Peak time rain [min]				Total rain output [min]			
		Ex1	**Ex2**	**Ex3**	**Ex4**	**Ex1**	**Ex2**	**Ex3**	**Ex4**	**Ex1**	**Ex2**	**Ex3**	**Ex4**
1	**a) Only snow**	0	29	31	39	30	42	38	62	34.2	18.2	21.6	16.2
	b) Only melt	16	27	26	87	33	40	36	-	28.1	19.1	23.2	12.7
2	**a) Mixing - used**	16	27	26	87	33	40	36	-	32.6	18.8	22.8	12.8
	b) Mixing - t/2	15	27	26	87	29	40	36	-	33.8	18.5	22.3	13.8
	c) Mixing - 2 t	16	27	26	87	33	40	36	-	31.4	19.1	23.2	12.8
	d) Mixing - S/2	16	27	26	87	33	40	36	-	32.5	18.8	22.8	12.8
	e) Mixing - 2 S	15	27	26	87	33	40	36	-	32.6	18.8	22.8	12.8

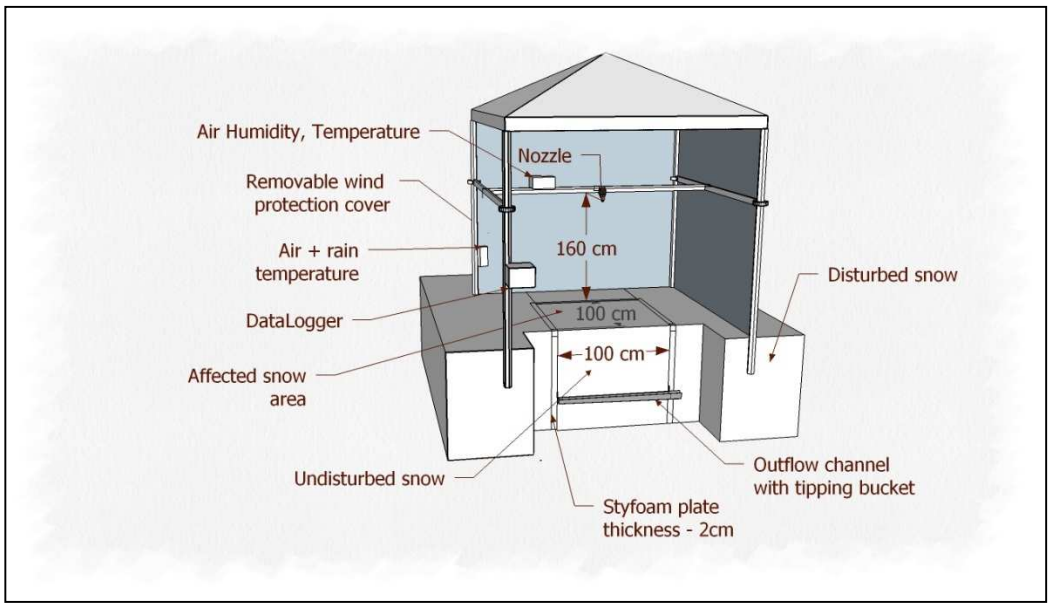

Figure 1 – Experimental setup of rainfall simulator.

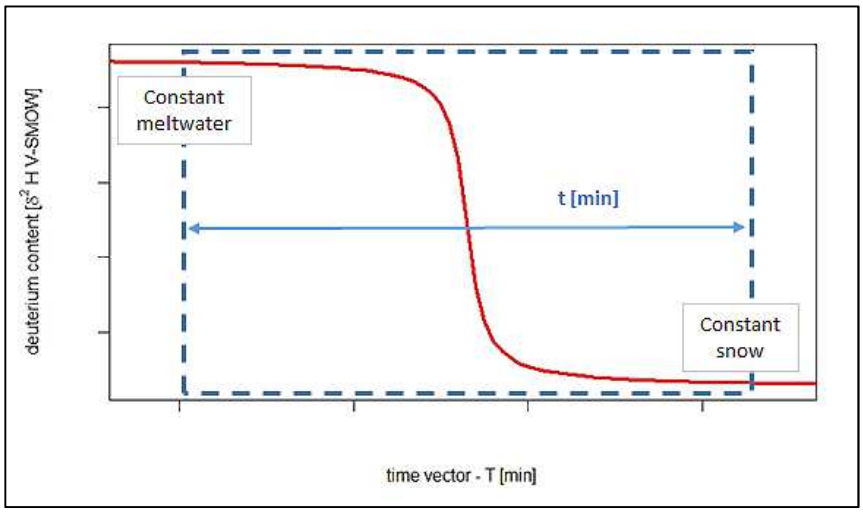

Figure 2 - Generalized mixing curve of non-rain water $c_{non\text{-}rain}(t)$ representing a transition from the deuterium concentration of pre-experimental LWC to a value which is influenced by additional melt.

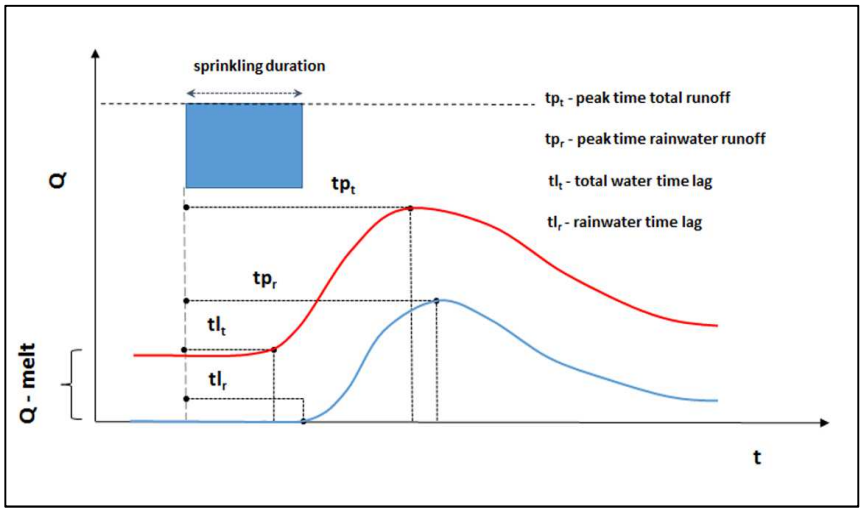

Figure 3 – Graphical definition of peak times and time lags.

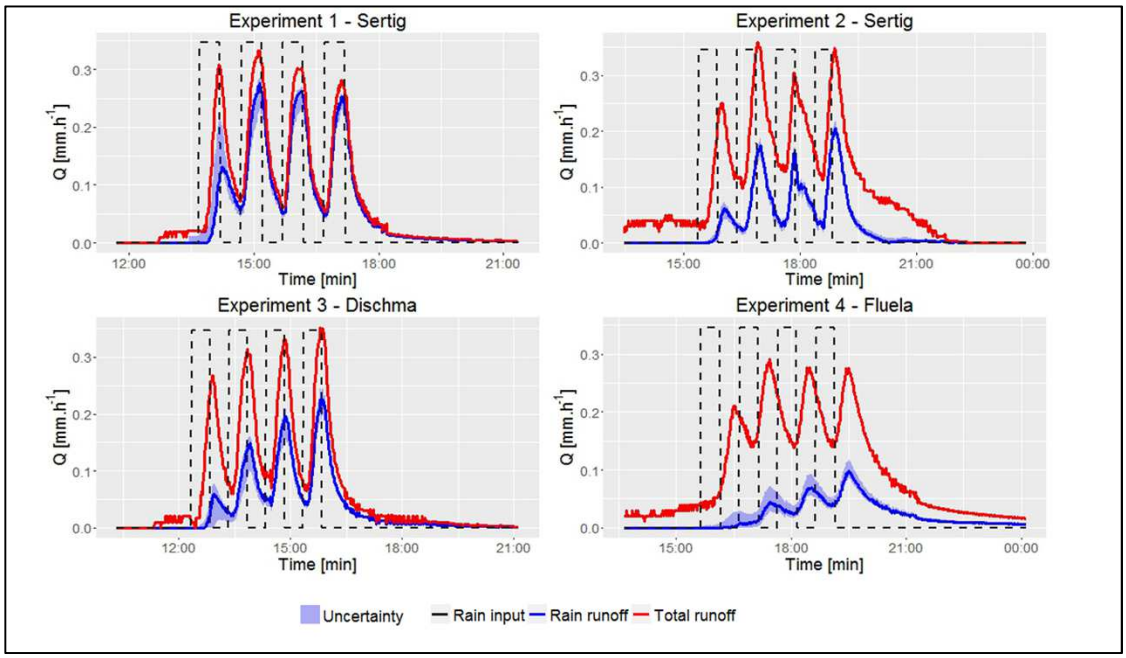

Figure 4 - Runoff from the experimental snow block during all artificial ROS.

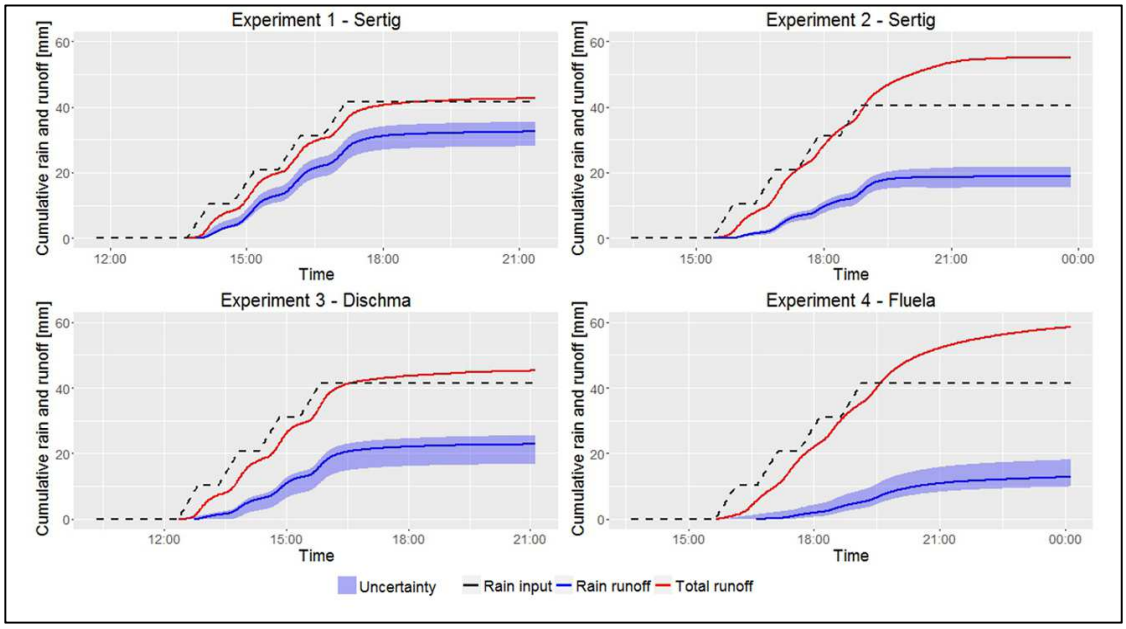

Figure 5 – Cumulative outflow from the investigated snow cube.

4.4. Článek IV - Modeling liquid water transport in snow under rain-on-snow conditions considering preferential flow

Würzer, S., Wever, N., Juras, R., Lehning, M. and Jonas, T.: Modeling liquid water transport in snow under rain-on-snow conditions considering preferential flow, Hydrol. Earth Syst. Sci. Discuss., 18(August), 16488, doi:10.5194/hess-2016-351, 2016

Hydrol. Earth Syst. Sci. Discuss., doi:10.5194/hess-2016-351, 2016
Manuscript under review for journal Hydrol. Earth Syst. Sci.
Published: 3 August 2016

Hydrology and Earth System Sciences
Open Access
Discussions

Modeling liquid water transport in snow under rain-on-snow conditions – considering preferential flow

Sebastian Würzer,[1,2*] Nander Wever,[1,2] Roman Juras,[3] Michael Lehning,[1,2] and Tobias Jonas,[1]

[1]WSL Institute for Snow and Avalanche Research SLF, Flüelastrasse 11, 7260 Davos Dorf, Switzerland
[2]École Polytechnique Fédérale de Lausanne (EPFL), School of Architecture, Civil and Environmental Engineering, Lausanne, Switzerland
[3]Faculty of Environmental Sciences, Czech University of Life Sciences Prague, Kamýcká 129, 165 21, Prague, Czech Republic

Correspondence to: Sebastian Würzer (sebastian.wuerzer@slf.ch)

Abstract. Rain-on-snow (ROS) has the potential to generate severe floods. Thus, precisely predicting the effect of an approaching ROS event on runoff formation is very important. Data analyses from past ROS events have shown that a snowpack experiencing ROS can either release runoff immediately or delay it considerably. This delay is a result of refreeze of liquid water and water transport mechanisms in the snowpack. Water percolation is depending on snow grain properties but also on the presence of structures such as ice layers or capillary barriers. During sprinkling experiments, preferential flow was found to be a process that critically impacted the timing of snowpack runoff. However, current one-dimensional snowpack models are not capable of addressing this phenomenon correctly. For this study, the detailed physics-based snowpack model SNOWPACK is extended with a water transport scheme accounting for preferential flow. The implemented Richards´ Equation solver is modified using a dual-domain approach to simulate water transport under preferential flow conditions. To validate the presented approach, we used an extensive dataset of over 100 ROS events from several locations in the European Alps, comprising meteorological and snowpack measurements as well as snow lysimeter runoff data. The model was tested under a variety of initial snowpack conditions, including cold, ripe, stratified and homogeneous snow. Results show that the model accounting for preferential flow (PF) demonstrated an improved overall and in particular more balanced performance. While the improvements were small for experiments on isothermal wet snow, they were pronounced for experiments on cold snowpacks, where field experiments found preferential flow to be especially prevalent.

Keywords: *snow cover, water transport, snowpack runoff, mountain hydrology, preferential flow, rain-on-snow, one-dimensional snow model*

Hydrol. Earth Syst. Sci. Discuss., doi:10.5194/hess-2016-351, 2016
Manuscript under review for journal Hydrol. Earth Syst. Sci.
Published: 3 August 2016

Hydrology and Earth System Sciences
Discussions

1 Introduction

The flooding potential of Rain-on-snow (ROS) events has been reported for many severe floods in the US (Kattelmann, 1997; Kroczynski, 2004; Leathers et al., 1998; Marks et al., 2001; McCabe et al., 2007), but also in Europe (Badoux et al., 2013; Freudiger et al., 2014; Rössler et al., 2014; Sui and Koehler, 2001; Wever et al., 2014b) where for example up to 70% of peak flow events could be attributed to ROS events for Austria (Merz and Blöschl, 2003). With rising air temperature due to climate change, the frequency of ROS is likely to increase in high elevation areas (Surfleet and Tullos, 2013) as well as in high latitudes (Ye et al., 2008). Besides spatial heterogeneity of the snowpack and uncertainties in meteorological forcing, deficits in process understanding make the consequences of extreme ROS events very difficult to forecast (Badoux et al., 2013; Rössler et al., 2014). For hydro-meteorological forecasters, it is particularly important to know a priori how much and when snowpack runoff is to be expected. Particularly, a correct temporal representation of snowpack processes is crucial to identify whether the presence of a snowpack will attenuate or amplify the generation of catchment-wide snowpack runoff. Most studies investigating ROS only consider the generation of snowpack runoff on a daily or multi-day timescale, where an exact description of water transport processes is less important than for sub-daily time scales (Wever et al., 2014a). Water transport processes are further usually described for snowmelt conditions, but not for ROS conditions, where high rain intensities may fall onto a cold snowpack below the freezing point. In this study however, we particularly focus on snowpack runoff generation at sub-daily scales with special attention to the timing of snowpack runoff which is influenced by preferential flow.

Many studies have shown that flow fingering or preferential flow is an important water transport mechanism in both laboratory experiments (Hirashima et al., 2014; Katsushima et al., 2013; Waldner et al., 2004) as well as under natural conditions, using dye tracer (Gerdel, 1954; Marsh and Woo, 1984; Schneebeli, 1995), temperature investigations (Conway and Benedict, 1994) or by measuring the spatial variability of snowpack runoff (Kattelmann, 1989; Marsh and Pomeroy, 1993, 1999; Marsh and Woo, 1985). The variability of snowpack runoff is defined by the distribution and size of preferential flow paths (PFP), which are dependent on the structure of the snowpack and weather conditions (Schneebeli, 1995). Beyond its importance for hydrological implications, preferential flow may also be crucial for wet snow avalanche formation processes, where snow stability can be depending on the exact location of liquid water ponding (Wever et al., 2016a).

Most snow models describe the water flow in snow as a uniform wetting front, thereby implicitly only considering the matrix flow component. The history of quantitative modeling of water transport in snow starts with Colbeck (1972), who first described a gravity drainage water transport model for isothermal, homogeneous snow. This was done by applying the general theory of Darcian flow of two-fluid phases flowing through porous media, neglecting capillarity. Because water transport is not just occurring in isothermal conditions and snow can therefore not be treated as a classical porous medium, Illangasekare et al. (1990) were the first to introduce a 2D model being able to describe water transport in subfreezing and layered snow. A detailed multi-layer physics based snow model, where water transport was governed by the gravitational part of Richards` Equation described in Colbeck (1972) was introduced by Jordan (1991). With the implementation of the

Hydrol. Earth Syst. Sci. Discuss., doi:10.5194/hess-2016-351, 2016
Manuscript under review for journal Hydrol. Earth Syst. Sci.
Published: 3 August 2016

full Richards` Equation described by (Wever et al., 2014a), the influence of capillary forces on the water flow was firstly represented in an operationally used snowpack model.

A model accounting for liquid water transport through multiple flow paths was developed by Marsh and Woo (1985), but not being able to explicitly account for structures like ice layers and capillary barriers. Recently, multi-dimensional water transport models were developed, which allow for the explicit simulation of PFP (Hirashima et al., 2014). These models are valuable for describing spatial heterogeneities and persistence of PFP, but have not yet been shown to be suitable for hydrological or operational purposes. In general, multi-dimensional models are limited by the fact that they are computationally intensive, thus not thoroughly validated for seasonal snowpacks and yet lack the description of crucial processes such as snow metamorphism and snow settling.

In snowpack models which are used operationally, PFP are not yet considered. The recently introduced Richards' Equation solver for SNOWPACK led to a significant improvement of modelled sub-daily snowpack runoff rates. For this paper, we further modified the transport scheme for liquid water by implementing a dual-domain approach to represent PFP. This new approach is validated against snow lysimeter measurements which were recorded during both natural and artificial ROS events.

The study aims to better describe snowpack runoff processes during ROS events within snowpack models that can be used for operational purposes such as avalanche warning and hydrological forecasting. This requires that the model results remains reliable, i.e. that improvements are not realized on the expense of a decreased model performance during periods without ROS, and that the model must not be too computationally expensive. This is the first study to test a water transport scheme accounting for preferential flow which has been implemented in a snowpack model that meets the above requirements.

Our analysis of simulations of over 100 ROS events targets the following research questions:

- Is snowpack runoff during ROS in a 1D model better reproduced with a dual domain approach to account for preferential flow than with traditional methods considering matrix flow only?
- Are there certain snowpack or meteorological conditions, for which the performance specifically benefits if preferential flow is represented in the model?

This paper is structured as follows: Section 2 describes the snowpack model setup, the water transport models, input data and the event definition. Results of the simulations are shown in Sect. 3. This includes data of sprinkling experiments of ROS (3.1), natural ROS events (3.2) and the validation of the model on a long-term dataset from two alpine snow measurement sites (3.3). The results will be discussed in Sect. 4, followed by the general conclusions found in Sect. 5.

Hydrol. Earth Syst. Sci. Discuss., doi:10.5194/hess-2016-351, 2016
Manuscript under review for journal Hydrol. Earth Syst. Sci.
Published: 3 August 2016

Hydrology and Earth System Sciences Open Access
Discussions

2. Methods

All results in this study are derived from simulations with the one-dimensional physics based snowpack model SNOWPACK (Bartelt and Lehning, 2002; Lehning et al., 2002a; Lehning et al., 2002b; Wever et al., 2014a) using 3 different water transport schemes, described in Sect. 2.2. The model was applied to four experimental sites that were set up for this study in the vicinity of Davos (Sect. 2.3). These sites were maintained over two winter seasons between 2014 and 2016 where data was recorded for several natural ROS events. At the same sites, we conducted a set of 6 sprinkling experiments to simulate ROS events for given rain intensities (Sect. 2.4). Furthermore, we conducted simulations for two extensive datasets from the European Alps: Weissfluhjoch (Switzerland, 46.83° N, 9.81° E, 2540 m MSL, WSL Institute for Snow and Avalanche Research SLF (2015), abbreviated as WFJ in the following) and Col de Porte (France, 45.30° N, 5.77° E, 1325 m MSL, Morin et al. (2012), abbreviated as CDP in the following). These datasets provide meteorological input data for running SNOWPACK as well as validation data, including snowpack runoff. Both datasets have already been used for simulations with SNOWPACK (Wever et al., 2014a) and provide data over more than 10 years each.

Below, the SNOWPACK model and the different water transport models are described first, followed by the description of the field sites for ROS observation in the vicinity of Davos. Then, we detail the setup of the artificial sprinkling experiments. After summarizing the WFJ and CDP dataset, we finally present the definition of ROS events that is used in this study. Most analyses were performed in R 3.3.0 (R Development Core Team, 2016) and figures were created with base graphics or ggplot2 (Wickham, 2009).

2.1 Snowpack model setup

The setup of the SNOWPACK model is similar to the setup used for simulations in Würzer et al. (2016). For all simulations, snow depth was constrained to observed values, which means that the model interprets an increase in observed snow depth at the stations as snowfall (Lehning et al., 1999; Wever et al., 2015). The temperature used to determine whether precipitation should be considered rain (measurements from rain gauges) or snow (from the snow depth sensors) was set to achieve best results for reproducing measured snow height for precipitation driven simulations for the Davos field sites (between 0°C and 1.0°C). For WFJ and CDP, this threshold temperature was set to 1.2°C, where mixed precipitation occurred proportionally between 0.7°C and 1.7°C. Turbulent surface heat fluxes are simulated using a Monin–Obukhov bulk formulation with stability correction functions of Stearns and Weidner (1993), as described in Michlmayr et al. (2008). At the Davos field sites (Sect. 2.3) incoming longwave radiative flux is simulated using the parameterization from Unsworth and Monteith (1975), coupled with a clear sky emissivity following Dilley and O'brien (1998), as described in Schmucki et al. (2014). For the roughness length z0, a value of 0.002m was used for all simulations at the Davos field sites and WFJ, whereas a value of 0.015 was used for CDP. The model was initialized with a soil depth of 1.4, 2.2 and 2.14 m (for WFJ, CDP and Davos field sites, respectively) divided into layers of varying thickness. For soil, typical values for coarse material

Hydrol. Earth Syst. Sci. Discuss., doi:10.5194/hess-2016-351, 2016
Manuscript under review for journal Hydrol. Earth Syst. Sci.
Published: 3 August 2016

Hydrology and Earth System Sciences Discussions

were chosen to avoid ponding inside the snowpack due to soil saturation. Soil heat flux at the lower boundary is set to a constant value of 0.06 W m^{-2}, which is an approximation of the geothermal heat flux.

2.2 Water transport models

The two previously existing methods for simulating vertical liquid water movement within SNOWPACK are either a simple so-called bucket approach (BA) (Bartelt and Lehning, 2002) or solving the Richards' Equation (RE), a recently introduced method for SNOWPACK (Wever et al., 2014a; Wever et al., 2014b).

The bucket approach represents liquid water dynamics by an empirically determined irreducible water content Θ_r which defines if water stays in the corresponding layer or will be transferred to the layer below. This residual water content varies for each layer according to Coléou and Lesaffre (1998). The Richards' Equation represents the movement of water in unsaturated porous media. Its implementation in SNOWPACK and a detailed description can be found in (Wever et al., 2014a).

The preferential flow model presented in this study is based on the RE model, but follows a dual-domain approach, dividing the pore space of the snowpack into a part representing matrix flow and a part representing preferential flow. For both domains Richards' Equation is solved subsequently. The preferential flow model is described by (i) a function for determining the size of the matrix and preferential flow domain, (ii) the initiation of preferential flow (i.e., water movement from matrix flow to preferential flow) and (iii) an return flow condition from preferential flow to matrix flow.

The area of the preferential domain (F) is as a function of grain size (Eq. 1), which has been determined by results of laboratory experiments presented by Katsushima et al. (2013) and field observations with dye tracer:

$$F = 0.0584 r_g^{-1.109} \quad (1)$$

where r_g is grain radius (mm). F is limited between 1% and 90% for reasons of numerical stability. The matrix domain is then accordingly defined as (1-F). Water is transferred from the matrix domain to the preferential domain if the water pressure head for a layer in the matrix domain is higher than the water entry pressure of the layer below, which can, according to Katsushima et al. (2013), also be expressed as a function of grain size. This condition is expected to be met if water is ponding on a microstructural transition (i.e. capillary barriers, ice lenses) inside the snowpack. Additionally, saturation was equalized between the matrix and the preferential domain, in case the saturation of the matrix domain exceeded the one in the preferential domain. To move water back into the matrix part, we apply a threshold in saturation of the preferential flow domain and water will flow back to the matrix domain once this threshold is exceeded. This threshold is used as a tuning parameter in the model.

Refreezing of liquid water in the snowpack is crucial for modeling water transport in subfreezing snow and may also be important for modeling preferential flow. The presented preferential flow model has also been used to simulate ice layer formation under the presence of preferential flow by Wever et al. (2016b). Thereby, a sensitivity study on the role of refreeze in the preferential flow domain and the return flow condition from preferential flow to matrix flow was conducted.

Hydrol. Earth Syst. Sci. Discuss., doi:10.5194/hess-2016-351, 2016
Manuscript under review for journal Hydrol. Earth Syst. Sci.
Published: 3 August 2016

It was found that neglecting refreeze led to the best results for reproducing ice layer formation, but did not significantly affect the performance in reproducing measured hourly snowpack runoff. Therefore, refreeze in the preferential domain is neglected in the presented study. The threshold in saturation for preferential flow (return flow condition) was determined as 0.1. Further details on the implementation of the PF model and its performance can be found in Wever et al. (2016b).

2.3 Davos field sites

Four field sites have been installed within an elevational range of 950 to 1950 m MSL in the vicinity of Davos, Switzerland, with one meteorological station and 3-4 snow lysimeters each (15 in total, 0.45m diameter). The meteorological stations provided most data necessary for running the SNOWPACK model, missing parameters were estimated according to Sect. 2.1. Lysimeters were installed at ground level with an approximate spacing of 10m horizontal distance. The lysimeters consisted of a funnel attached to a precipitation gauge buried in the ground, which monitored snowpack runoff with a tipping bucket. To block lateral inflow at the snow-soil interface, each lysimeter was equipped with a rim of 5 cm height around the inlet. The multiple snow lysimeter setups allowed analyzing the spatial heterogeneity of snowpack runoff. Snowpack properties (SWE, LWC, HS, TS) were manually measured directly before each natural ROS event so that the initial conditions of the snowpack are known in detail. LWC was measured with the "Denoth meter", a device introduced by Denoth (1994). The onset of runoff was defined as the time when cumulative snowpack runoff (measured and simulated, respectively) has reached 1 mm.

2.4 Sprinkling Experiment Description

During winter 2014/15, a total of 6 artificial sprinkling experiments were performed on all four Davos field sites described above to be able to investigate snowpack runoff generation for different snowpack properties. The experiments were conducted with a sprinkling device especially developed for sprinkling on snowpack. The device was a refined version the sprinkling device described in Juras et al. (2013). For each experiment, the device was placed above a snow lysimeter, covered by an undisturbed natural snowpack. The water used for sprinkling was mixed with the dye tracer Brilliant Blue FCF (concentration 0.4 g l^{-1}) to be able to observe PFPs within the snowpack. Sprinkling was performed in 4 bursts of 30 minutes each, interrupted by 30 minutes breaks. Sprinkling was conducted over a 2x2m plot centered above the lysimeters, and with an intensity of 24.7 mm h^{-1}, leading to a total of 49.4 mm artificial rain in each of the experiments. The intensities were determined by calibration experiments on lysimeters not covered by snow and are valid for a certain distance between the nozzle and the sprinkled surface and water pressure at the nozzle. Despite the fact that this value still represents a very intense ROS event, it is within range of natural ROS events and similar or much lower compared to previous studies (19 mm h^{-1}; Eiriksson et al. (2013); 48–100 mm h^{-1}; Singh et al. (1997)). For the sprinkling experiments, the exact timing of rain and intensities are known and the snowpack runoff measured at 1 minute intervals allowed precisely analyzing the performance of model simulations. Figure 1 shows a horizontal cut of a snowpack after the sprinkling experiment and a topview of the

Hydrol. Earth Syst. Sci. Discuss., doi:10.5194/hess-2016-351, 2016
Manuscript under review for journal Hydrol. Earth Syst. Sci.
Published: 3 August 2016

lysimeter after the snowpack was removed for cold and wet conditions, respectively. The blue color indicates where water transport took place and where sprinkled water was held by capillary forces or refrozen.

2.5 Extensive dataset for in-situ validation

Two long-term datasets from two study sites in the European Alps providing snow lysimeter data and high quality meteorological forcing data for running the energy balance model SNOWPACK were chosen to validate the different water transport models systematically. Datasets of both study sites used for the extensive in-situ validation are publicly available. The Col de Porte (CDP) site, located in the Chartreuse range in southeast France has been described in Morin et al. (2012) and the Weissfluhjoch site (WFJ) in the Swiss Alps has been described in Wever et al. (2015). WFJ (46.83° N, 9.81° E) is located at an elevation of 2540 m MSL and CDP (45.30° N, 5.77° E) is located at 1325 m MSL. CDP experiences a warmer climate than WFJ and as a consequence the snowpack produces snowpack runoff more often throughout the entire snow season and ROS events are more frequent than at WFJ. A multi-week snowpack builds up every winter season at CDP, but is, in contrast to WFJ, interrupted by complete melt in some years. The WFJ site is equipped with a 5 m^2 snow lysimeter, which measures the liquid water runoff from the snowpack. It has a 60 cm rim to reduce lateral flow effects near the soil-snow interface (Wever et al., 2014a). CDP is equipped with both a 5 m^2 and a 1 m^2 lysimeter. Here we use data from the 5 m^2 lysimeter, but include data from the 1 m^2 lysimeter to discuss the uncertainty associated with measurements of the snowpack runoff. The studied period for WFJ is from October 1st 1999 to September 30th 2013 (14 hydrological years). Because of possible errors in the lysimeter data in the winter seasons of 1999/00 and 2004/05 as described in (Wever et al., 2014a), these data were excluded from the study. For CDP the studied period is from October 1st 1994 to July 31st 2011 (17 winter seasons) according to the data availability from the 5 m^2 lysimeter.

2.6 CDP+WFJ event definition

As the number and characteristics of ROS events are strongly dependent on the event definition, special care needs to be taken to determine begin and end of a ROS event. Being interested in the temporal characteristics of snowpack runoff during ROS, we need to include the entire period from the onset of rain to the end of ROS induced snowpack runoff. Here we use an event definition according to Würzer et al. (2016) with slightly decreased thresholds to identify ROS events. According to this definition, a ROS event requires a minimum amount of 10 mm rainfall to fall within 24h on a snowpack with a height of at least 25 cm. While the event is defined to begin once the first 1 mm of rain has fallen, the event ends once there is less than 3mm of cumulative snowpack runoff recorded within the following 5h. This definition resulted in a selection of 61 events at CDP and 40 events at WFJ. The model simulations were subsequently evaluated over a time window that extends the event length by 5 and 10 hours at the beginning and end, respectively (Fig. 2). These extended evaluation periods allowed to also investigate a possible temporal mismatch between modelled and observed snowpack runoff.

Hydrol. Earth Syst. Sci. Discuss., doi:10.5194/hess-2016-351, 2016
Manuscript under review for journal Hydrol. Earth Syst. Sci.
Published: 3 August 2016

3 Results

3.1 Experimental sprinkling experiments

During the winter period 2014/15, 6 sprinkling experiments (Ex1-Ex6) were conducted on 4 different sites to be able to investigate snowpack runoff generation for different snowpack properties. With distinct differences in snowpack properties but controlled rain intensities, these experiments were expected to reveal the influence of snow cover properties and differences between the water transport models best. For all experiments, initial snow height (HS), snowpack temperature (TS), and LWC profiles were measured (Table 1). According to these measurements, the snowpack conditions on which the sprinkling experiments were conducted can be separated into two cases: The first 3 experiments were conducted on dry and cold (i.e. below the freezing point) snow and will be called winter experiments. The snowpack of Ex4 and Ex5 was isothermal and in a wet state. At the onset of Ex 6 however, the snowpack was not completely isothermal and had just little LWC. Nevertheless the snowpack already passed peak SWE and was in its ablation phase. Therefore the later 3 experiments (Ex4-Ex6) will be referred to as spring experiments in the following.

For all winter experiments (Fig. 3 and Fig. 4, (a,b,c)), both modeled and observed total event runoff remained below the amount of sprinkling water. During Ex3 no snowpack runoff was observed, because visual inspection afterwards revealed an impermeable ice layer covering both the lysimeter and the adjacent ground. During spring conditions, on the other hand, snowmelt lead to snowpack runoff exceeding total sprinkling input, except for measured snowpack runoff in Ex6 (Fig. 3 and Fig. 4, (d,e,f)).

Additionally, Fig. 4 shows, that just the PF model was capable to reproduce all 4 peaks of observed snowpack runoff for winter conditions (Ex1+2), even if the first peak of Ex1 was strongly underestimated. For spring conditions however, all 3 models managed to represent 4 peaks corresponding to the four sprinkling bursts, but the PF model showed best correspondence with observed snowpack runoff (Fig. 3 and Fig. 4 (d,e,f); Table 1). Regarding the onset of snowpack runoff, the PF model especially led to faster snowpack runoff for the first 2 winter experiments, where the RE and BA models showed delayed snowpack runoff onset. For spring conditions the faster snowpack runoff response of the PF model led to a slightly early snowpack runoff. Maximal snowpack runoff rates for dry and cold conditions were generally overestimated by all models, in case snowpack runoff was measured and snowpack runoff was simulated, whereas wetter conditions led to a minor underestimation.

Regarding the overall correlation between measured and simulated snowpack runoff, PF outperformed the other models (Table 2), in particular during winter conditions. Summarizing, this initial assessment suggests that the PF approach has potential advantages in particular a) as to the timing of snowpack runoff and b) for cold snowpacks which are not yet entirely ripened.

Hydrol. Earth Syst. Sci. Discuss., doi:10.5194/hess-2016-351, 2016
Manuscript under review for journal Hydrol. Earth Syst. Sci.
Published: 3 August 2016

3.2 Natural occurring ROS Events

In January 2015, two ROS events occurred in the vicinity of Davos. They were observed over an elevational range of 950 to 1560 m MSL on the same sites on which also the sprinkling experiments were conducted. Figure 5 shows the course of cumulative rainfall and snowpack runoff for both dates and all sites. Pre-event conditions (HS, LWC, TS) were measured shortly before the onset of rain for both events and are shown together with coefficients of determination (R^2) for hourly snowpack runoff of the different models Table 2.

For the event of 03.01.2015 (Fig. 5, upper row) the lower sites Serneus and Klosters (950 and 1200 m asl) showed a similar snowpack runoff dynamics regarding the delayed onset and the total amount (cumulative sum averaged over the 3 corresponding lysimeters: 20.3 mm and 21.1 mm, respectively). Also the heterogeneity between data from the individual lysimeters was relatively low (Range of 3.1 mm and 3.9 mm, respectively). For the highest located site (Davos), however, the snowpack runoff measured by all 4 lysimeters showed a greater variability in the delayed onset of snowpack runoff (0 to 7 hours) and the total amount of snowpack runoff (mean 24.7 mm; range of 57.9 mm). For the lower sites (Serneus and Klosters), the PF and RE models generated snowpack runoff too early (PF: 2 to 3 hours; RE: 0.3 to 1.4 hours). The BA model generated snowpack runoff rather too late (1.3 to 2 hours), but still within range of the variability of observed snowpack runoff for Serneus. However, the lysimeter snowpack runoff showed good accordance with modelled PF and RE snowpack runoff, whereas the BA always led to underestimation of snowpack runoff. At the higher elevation site Davos, the RE model led to a better representation of mean observed snowpack runoff amount, when compared with BA and PF. The mean observed snowpack runoff onset however was represented best by the PF model (0.3 hours early) if being compared to BA (3.7 hours delay) and RE (1.2 hours delay).

For the event of 09.01.2015 (Fig. 5, bottom row) the lower sites showed again little temporal and spatial heterogeneity in lysimeter runoff (Range of 1 mm and 2.2 mm, respectively), whereas this was more the case for Davos again (Range of 13.3 mm). Observed mean event snowpack runoff was more diverse for all elevations, where Klosters had the highest cumulative snowpack runoff (Serneus 13.3 mm; Klosters 17.7 mm; Davos 7.8 mm). If compared to observed total snowpack runoff, the PF model overestimated snowpack runoff for Serneus and underestimated snowpack runoff for Klosters, whereas the RE and especially the BA model underestimate event snowpack runoff for both sites. For Davos, all models were overestimating event snowpack runoff and led to early snowpack runoff. Except the RE model, which represented onset of snowpack runoff correctly for Serneus, none of the models were able to model snowpack runoff onset correctly for any of the sites.

Hydrol. Earth Syst. Sci. Discuss., doi:10.5194/hess-2016-351, 2016
Manuscript under review for journal Hydrol. Earth Syst. Sci.
Published: 3 August 2016

Hydrology and Earth System Sciences Open Access
Discussions

3.3 Validation on an long-term dataset

3.3.1 Modeled and observed snowpack runoff for the whole dataset

Given the partly contradictory findings on the performance of the three model variants based on the above assessment for artificial ROS simulations under controlled conditions (Sect. 3.1), as well as natural ROS events (Sect. 3.2), further more systematic model test were needed. Therefore we validate the different models based on extensive datasets from the two sites WFJ and CDP, as described in Sect. 2.4.

Before we focus on the specific performance of the PF model for a large number of individual ROS events, we first analyzed the overall model performance throughout the whole study period, i.e. over entire winter seasons. Therefore we analyzed observed and modeled hourly snowpack runoff provided snow heights were above 10 cm to ensure that lysimeter runoff was caused by snowpack runoff and not rainfall. For both sites, R^2 values for PF were slightly higher than for RE (Table 3), which both clearly outperformed the BA. Also the root mean squared errors (RMSE) of the PF model were lower compared to RE and BA. We can therefore conclude that the implementation of the PF approach slightly improves water transport over entire winter seasons.

3.3.2 ROS event characteristics of the extensive dataset

Average characteristics of the individual ROS events at CDP and WFJ are summarized in Fig. 6. The temporal course of rain and snowpack runoff rates averaged over all events at WFJ (40 individual events) and CDP (61 individual events) are shown in Fig. 6 (a). ROS events at WFJ showed, on average, higher maximum rain intensities than at CDP, leading to higher average snowpack runoff intensities in the beginning of the events. Whereas at WFJ, ROS events tended to be short and intense, at CDP the event rainfall extended over a longer period of time. Interestingly, we observed relatively high initial snowpack runoff rates before the actual begin of the ROS event, especially for WFJ, which suggests that many ROS events at this site occurred during the snowmelt period. Averaged over all individual events, snowpack runoff reached a peak after 1 and 4 hours after the onset of rain for WFJ and CDP, respectively. At WFJ snowpack runoff and rain rates in the beginning of the events were generally higher than at CDP. The course of mean temperature during ROS events at both sites is shown in Fig. 6 (b). For both sites, mean air temperature (TA) dropped with the onset of rain. At WFJ, this drop was more distinct and mean TA was higher than at CDP. The mean initial ROS event snow height (HS) for WFJ was 95 cm, which is approximately the average snow height during mid-June (for 70 years of measurements). The mean initial HS for CDP is 67 cm. With a SD of 42 cm, the variability of initial HS for WFJ was higher than for CDP (29 cm).

3.3.3 Modelled and observed snowpack runoff at the event scale

Below we investigate the performance of the three water transport schemes at the event scale. Modeled snowpack runoff was assessed against observations by the coefficient of determination (R^2) and the root mean squared errors (RMSE).

Hydrol. Earth Syst. Sci. Discuss., doi:10.5194/hess-2016-351, 2016
Manuscript under review for journal Hydrol. Earth Syst. Sci.
Published: 3 August 2016

To further analyze the representation of snowpack runoff timing, we defined an absolute time lag error (TLE) as the difference between the onsets of modelled and observed snowpack runoff in hours. The onset of snowpack runoff is defined as the time when cumulative snowpack runoff has reached 10% of total event-snowpack runoff.

Figure 7 shows boxplots of R^2 (a,d), RMSE (d,e) and absolute TLE (c,f) for all 40 ROS events at WFJ (a,b,c) and 61 events at CDP (d,e,f), respectively. For WFJ, R^2 values show that the BA model performance was inferior to the RE model which was in turn outperformed by the PF model. The PF also led to a reduction in RMSE by approximately 50% and 20%, if compared to the BA and RE model, respectively. Whereas the median of TLEs for all models at WFJ was 0 and therefore all models reproduced the onset of snowpack runoff very well, the interquartile range decreased from BA via RE to the PF model. For CDP, a distinct increase in R^2 values could be observed between BA and both RE and PF which showed a similar median R^2. The interquartile range of R^2 values was generally higher than for WFJ and increased from BA to RE, whereas it was decreasing for PF. Also the RMSEs significantly decreased with RE and PF, compared to the BA model. Similarly to WFJ, the median TLE for CDP was zero, except in the case of RE, where negative median TLE indicates that modelled snowpack runoff was on average a bit delayed compared to the observations. Nevertheless, the PF model showed the most consistent results, whereas the BA model showed the largest spread in TLE for individual events. The magnitude of TLE was generally higher for CDP than for WFJ and mostly negative, which means that the modelled snowpack runoff was delayed compared to lysimeter snowpack runoff. For BA and PF, TLE was more often positive (early modelled snowpack runoff), which led to a very good median for BA, but also a larger interquartile range. The PF model led to the same median as the RE model, but showed the smallest interquartile range. As reference we added the comparison between the 1 and 5 m^2 lysimeters installed at CDP (Sect. 2.5) to Fig. 7, referred to as RL. This comparison can be seen as a benchmark performance, as it represents the measurement uncertainty of the validation dataset. As expected, RL shows the highest overall performance measures, but while the results for both PF and RE were reasonably close to those of RL, the BA model performed considerably worse.

The results shown in Fig. 7 may be influenced by both a time lag as well as the degree of reproduction of temporal dynamics. To separate both effects, we conducted a cross-correlation analysis, allowing a shift of up to 3 hours to find the best R^2 value. Figure 8 shows both the time lag, as well as the best R^2 value achieved. Interestingly, the BA model showed best correlations if the modeled snowpack runoff was shifted by 1 or 2 hours (consistently too early compared to observations). The RE model, on the other hand, showed best correlations for a shift in the other direction (consistently too late compared to observations). Neither was the case for PF with lags centered around 0.

The R^2 of the cross correlation analysis gives some indication of how well the temporal dynamics of the observed snowpack runoff can be reproduced, neglecting a possible time lag. The results in Fig. 8 show an improvement in R^2 values for both sites and all models if a time lag is applied. Greatest improvements were observed for the BA model, which even outperformed the RE model at WFJ, albeit not for CDP. The good timing with the PF model is confirmed by almost no lag

Hydrol. Earth Syst. Sci. Discuss., doi:10.5194/hess-2016-351, 2016
Manuscript under review for journal Hydrol. Earth Syst. Sci.
Published: 3 August 2016

for WFJ and only a small lag for CDP needed to maximize R^2. Both RE and PF had maximized R^2 values in range of the lysimeter comparison (RL).

4 Discussion

Even though preferential flow of liquid water through snow is a phenomenon that is known and investigated since a long time, it has not yet been accounted for in 1D snow models that are in use for operational applications. The results of this study show that including this process into the water transport scheme can improve the prediction of snowpack runoff dynamics for individual ROS events as well as for the snowpack runoff of entire snow seasons. Moreover, the representation of the onset of snowpack runoff is improved. This is particularly important at the catchment scale, where a delay of snowpack runoff relative to the start of rain may affect the catchment runoff generation, especially if the time lag varies across a given catchment.

During the sprinkling experiments, sprinkling intensities were higher than average rain intensities during ROS but still within range of peak rain intensities during naturally occurring ROS events in the Swiss Alps (Rössler et al., 2014; Würzer et al., 2016) and the Sierra Nevada, California (Osterhuber, 1999). The use of the PF model clearly led to a better representation of the runoff dynamics for all experiments, including shallow and ripe snowpacks during spring conditions as well as cold and dry snowpacks representing winter conditions. The improvements were strongest for winter conditions, suggesting that under these conditions accounting for preferential flow is most relevant. This is supported by observations of preferential flow paths during winter conditions (Fig. 1 (a)), which were not visible after the spring experiments. During winter conditions just a fraction of the lysimeter area was colored with tracer, indicating preferential flow of the sprinkled water (Fig. 1 (b)), whereas spring conditions left the whole cross section of the lysimeter colored (Fig. 1 (c)). While a fast runoff response can be expected for wet and shallow snowpack and may be easier to handle for all models tested, it is the cold snowpacks that both RE and BA models did not manage to represent well: runoff from these models was more than one hour delayed (Ex1 and Ex2), and missed approx. 10 mm of snowpack runoff within the first hour of observed runoff. This can partly be explained by the fact that BA and RE need to heat up the subfreezing snowpack before they can generate snowpack runoff, whereas refreezing is neglected in the preferential domain of the PF model and runoff can occur even in a not yet isothermal snowpack. Adjusting parameters like the irreducible water content Θ_r for the BA model could probably lead to earlier runoff under these conditions, but thereby lead to earlier runoff, for example for WFJ events, where TLE already is positive for several events.

Despite the improved representation of the temporal runoff dynamics of the PF model (Table 1), the total event runoff of both RE and PF models is very similar for most conditions. Notably, the total event runoff for dry snowpacks is mostly overestimated by all models, suggesting underestimation of water held in the capillarities. In cold snowpacks, dendricity of snow grains may still be high, such that water retention curves developed with rounded grains underestimate

Hydrol. Earth Syst. Sci. Discuss., doi:10.5194/hess-2016-351, 2016
Manuscript under review for journal Hydrol. Earth Syst. Sci.
Published: 3 August 2016

the suction. Additionaly, high lateral flow was observed during the experiment for those conditions (Fig. 1a). This leads to an effective loss of sprinkling water per surface area of the lysimeter, which of course cannot be reproduced by the models. Therefore, observed snowpack runoff likely underestimates the snowpack runoff that would have resulted from an equivalent natural ROS event and we assume that the performance of the PF and RE models to capture the event runoff is probably better than reported in Table 1.

Interestingly, despite having the coldest snowpack, time lag for the 1st natural ROS event at Davos was shorter than for the other 2 sites. This relationship where a cold and non-ripe snowpack led to smaller lag times was also found during sprinkling experiments conducted by Juras and Würzer (unpublished data). We assume that this is an indication for the presence of pronounced preferential flow paths under those conditions, which is also supported by the high spatial variability of snowpack runoff. Glass et al. (1989) state that the fraction of preferential flow per area is decreasing with increasing permeability, which itself has found to be increasing with porosity (Calonne et al., 2012). Therefore, with a decreasing preferential flow area due to lower densities, the cold content of a snowpack loses importance, but saturated hydraulic conductivity is reached faster within the preferential flow paths. The combination of those effects then is suspected to lead to earlier runoff. This behavior should be ideally reproduced by the PF model and indeed the onset of runoff is caught well for this event.

The PF model led to improvements for hourly runoff rates at CDP and WFJ for a dataset comprising several years of runoff measurements. This is an important finding, demonstrating that the new water transport scheme aimed at a better representation of preferential flow during ROS events, did not negatively impact on the overall robustness of the model. To the contrary, the overall performance over entire seasons could even be improved. Whereas all models represent the overall seasonal runoff better for WFJ (Table 3), this was not found on the event scale (Fig. 7). However, the CDP simulations exhibit a larger interquartile range in R^2 values and are therefore generally less reliable. The observed differences in model performance between both sites may either be caused by differences in snowpack or meteorological conditions or by issues with the observational data. Despite an obvious contrast in the elevation of both sites, the average conditions during ROS events seem to vary. Figure 6 suggests that at WFJ short and rather intense rain events dominate. The higher maximum rain intensities at WFJ, compared to CDP, are probably due to the later occurrence of ROS at this site (May-June), where air temperatures and therefore rain intensities are usually higher than earlier in the season (Molnar et al., 2015). Regarding mean intensities over the event scale, data shown in Fig. 6 further imply that short and intense ROS events typically attenuate the rain input (ratio runoff to rain < 1), whereas long ROS event rather lead to additional runoff from snowmelt, which is in line with results presented in Würzer et al. (2016).

Snow height is generally higher at WFJ where the average initial snow height for the ROS events analyzed was 30 cm higher than at CDP. Ideally, the performance of the water transport scheme in the snowpack should not be affected by the snow depth. At both sites, the snowpack undergoing a ROS event is mostly isothermal with a mean initial LWC of 1.9 vol% (CDP) and 3.3 vol% (WFJ). The initial snowpack densities at both sites were quite different. At WFJ, densities for all ROS

Hydrol. Earth Syst. Sci. Discuss., doi:10.5194/hess-2016-351, 2016
Manuscript under review for journal Hydrol. Earth Syst. Sci.
Published: 3 August 2016

events are around 450-500 kg m^{-3}, whereas for CDP densities are spread from below 200 kg m^{-3} up to 500 kg m^{-3}. This suggests that the variable performance of all models at CDP (Fig. 7d) may be associated with early season ROS events. A linear regression fit suggests a positive, albeit weak correlation of snowpack bulk densities and event-R^2 for the RE and PF model at CDP, but not for the BA model. For WFJ on the other hand, a clear correlation between R^2 and HS was found for the BA model (R^2 =0.44), but not for RE and PF model. This leads to the assumption that performance of RE and PF model is slightly better for higher densities, whereas the BA performance is primarily dependent on snow height.

5 Conclusions

A new water transport model is presented that accounts for preferential flow of liquid water within a snowpack. The model deploys a dual-domain approach based on solving the Richards‘ Equation for each domain separately (matrix and preferential flow). It has been implemented as part of the physics based snowpack model SNOWPACK which enables for the first time to account for preferential flow paths within a model framework that is used operationally for avalanche warning purposes and snow melt forecasting.

The new model was tested for sprinkling experiments over a natural snowpack, dedicated measurements during natural ROS events, and an extensive evaluation over 101 historic ROS events recorded at 2 different alpine long-term research sites. This assessment led to the following main conclusions:

Compared to alternative approaches, the model accounting for preferential flow (PF) demonstrated an improved overall and in particular more balanced performance, by showing smallest interquartile ranges for R^2 values for a set of more than 100 ROS events. When evaluated over entire winter seasons, the performance statistics were superior to those of a single domain approach (RE), even if the differences were small. Both PF and RE models, however, outperformed the model using a bucket approach (BA) by a large margin (increasing median R^2 by 0.23 and 0.39 for WFJ and 0.47 and 0.46 for CDP). In sprinkling experiments with 30-min bursts of rain at high intensity the PF model showed a substantially improved temporal correspondence to the observed snowpack runoff, in direct comparison to the RE and BA models. While the improvements were small for experiments on isothermal wet snow, they were pronounced for experiments on cold snowpacks.

Model assessments for over 100 ROS events recorded at two long-term research sites in the European Alps revealed rather variable performance measures on an event-by-event basis between the three models tested. The BA model tended to predict too early onset of snowpack runoff for wet snowpacks and a delayed onset of runoff for cold snowpacks, whereas RE was generally too late. Combined with results from a separate cross correlation analysis, results suggested the PF model to provide the most balanced performance concerning the timing of the predicted runoff.

While there is certainly room for improvements of our approach to account for preferential flow of liquid water through a snowpack, this study provides a first implementation within a model framework that is used for operational

applications. Adding complexity to the water transport module did not negatively impact on the overall performance and could be done without compromising the robustness of the model results.

Improving the capabilities of a snowmelt model to accurately predict the onset of snowpack runoff during a ROS event is particularly relevant in the context of flood forecasting. In mountainous watersheds with variable snowpack conditions, it may be decisive if snowpack runoff occurs synchronously across the entire catchment, or if the delay between onset of rain and snowpack runoff is spatially variable e.g. with elevation. In this regard, accounting for preferential flow is a necessary step to improve snowmelt models, as shown in this study.

Acknowledgements

We thank the Swiss Federal Office for the Environment FOEN and the scientific exchange program Sciex-NMSch (project code 14.105) for the funding of the project. Special thanks belong to Jiri Pavlasek for making it possible to conduct the sprinkling experiments, the extensive work and valuable exchange of ideas during the experiments. We also would like to thank Timea Mareková and Pascal Egli for their help during the experiments.

References

Badoux, A., Hofer, M., and Jonas, T.: Hydrometeorologische Analyse des Hochwasserereignisses vom 10. Oktober 2011 (in German), Tech. Rep., WSL/SLF/MeteoSwiss, 92 pp. [Available online at http://www.wsl.ch/fe/gebirgshydrologie/wildbaeche/projekte/unwetter2011/Ereignisanalyse_Hochwasser_Oktober_2011.pdf], 2013.

Bartelt, P., and Lehning, M.: A physical SNOWPACK model for the Swiss avalanche warning Part I: numerical model, Cold Reg. Sci. Technol., 35, 123-145, doi: 10.1016/S0165-232x(02)00074-5, 2002.

Calonne, N., Geindreau, C., Flin, F., Morin, S., Lesaffre, B., Rolland du Roscoat, S., and Charrier, P.: 3-D image-based numerical computations of snow permeability: links to specific surface area, density, and microstructural anisotropy, Cryosphere, 6, 939-951, doi: 10.5194/tc-6-939-2012, 2012.

Colbeck, S. C.: A theory of water percolation in snow, J. Glaciol., 11, 369-385, 1972.

Coléou, C., and Lesaffre, B.: Irreducible water saturation in snow: experimental results in a cold laboratory, Ann. Glaciol., 26, 64-68, 1998.

Conway, H., and Benedict, R.: Infiltration of water into snow, Water Resour. Res., 30, 641-649, doi: 10.1029/93WR03247, 1994.

Denoth, A.: An electronic device for long-term snow wetness recording, Ann. Glaciol., 19, 104-106, 1994.

Dilley, A., and O'brien, D.: Estimating downward clear sky long-wave irradiance at the surface from screen temperature and precipitable water, Q. J. R. Meteorol. Soc., 124, 1391-1401, doi: 10.1002/qj.49712454903, 1998.

Eiriksson, D., Whitson, M., Luce, C. H., Marshall, H. P., Bradford, J., Benner, S. G., Black, T., Hetrick, H., and McNamara, J. P.: An evaluation of the hydrologic relevance of lateral flow in snow at hillslope and catchment scales, Hydrol. Process., 27, 640-654, doi: 10.1002/hyp.9666, 2013.

Freudiger, D., Kohn, I., Stahl, K., and Weiler, M.: Large-scale analysis of changing frequencies of rain-on-snow events with flood-generation potential, Hydrol. Earth Syst. Sci., 18, 2695-2709, doi:10.5194/hess-18-2695-2014, 2014.

Gerdel, R. W.: The transmission of water through snow, Eos Trans. AGU, 35, 475-485, 1954.

Glass, R., Steenhuis, T., and Parlange, J.: Wetting Front Instability, 2, Experimental Determination of Relationships Between System Parameters and Two-Dimensional Unstable Flow Field Behavior in Initially Dry Porous Media, Water Resour. Res., 25, 1195-1207, doi: 10.1029/WR025i006p01195, 1989.

Hirashima, H., Yamaguchi, S., and Katsushima, T.: A multi-dimensional water transport model to reproduce preferential flow in the snowpack, Cold. Reg. Sci. Technol., 108, 80-90, doi:10.1016/j.coldregions.2014.09.004, 2014.

Illangasekare, T. H., Walter, R. J., Meier, M. F., and Pfeffer, W. T.: Modeling of meltwater infiltration in subfreezing snow, Water Resour. Res., 26, 1001-1012, 1990.

Jordan, R.: A one-dimensional temperature model for a snow cover: Technical documentation for SNTHERM. 89, DTIC Document, 1991.

Juras, R., Pavlásek, J., Děd, P., Tomášek, V., and Máca, P.: A portable simulator for investigating rain-on-snow events, Z. Geomorphol., Supplementary Issues, 57, 73-89, 2013.

Katsushima, T., Yamaguchi, S., Kumakura, T., and Sato, A.: Experimental analysis of preferential flow in dry snowpack, Cold Reg. Sci. Technol., 85, 206-216, doi:10.1016/j.coldregions.2012.09.012, 2013.

Kattelmann, R.: Spatial Variability of Snow-Pack Outflow at a Site in Sierra Nevada, U.S.A., Ann. Glaciol., 13, 1989.

Kattelmann, R.: Flooding from rain-on-snow events in the Sierra Nevada, IAHS Publ., 239, 59-66, 1997.

Kroczynski, S.: A comparison of two rain-on-snow events and the subsequent hydrologic responses in three small river basins in Central Pennsylvania, Eastern Region Technical Attachment, 4, 1-21, 2004.

Leathers, D. J., Kluck, D. R., and Kroczynski, S.: The severe flooding event of January 1996 across north-central Pennsylvania, Bull. Am. Meteorol. Soc., 79, 785-797, doi:10.1175/1520-0477(1998)079<0785:TSFEOJ>2.0.CO;2, 1998.

Lehning, M., Bartelt, P., Brown, B., Russi, T., Stockli, U., and Zimmerli, M.: SNOWPACK model calculations for avalanche warning based upon a new network of weather and snow stations, Cold Reg. Sci. Tech., 30, 145-157, doi:10.1016/S0165-232X(99)00022-1, 1999.

Lehning, M., Bartelt, P., Brown, B., and Fierz, C.: A physical SNOWPACK model for the Swiss avalanche warning Part III: Meteorological forcing, thin layer formation and evaluation, Cold Reg. Sci. Tech., 35, 169-184, doi: 10.1016/S0165-232x(02)00072-1, 2002a.

Lehning, M., Bartelt, P., Brown, B., Fierz, C., and Satyawali, P.: A physical SNOWPACK model for the Swiss avalanche warning Part II: Snow microstructure, Cold Reg. Sci. Tech., 35, 147-167, doi: 10.1016/S0165-232x(02)00073-3, 2002b.

Marks, D., Link, T., Winstral, A., and Garen, D.: Simulating snowmelt processes during rain-on-snow over a semi-arid mountain basin, Ann. Glaciol., 32, 195-202, doi:10.3189/172756401781819751, 2001.

Marsh, P., and Woo, M.-K.: Wetting Front Advance and Freezing of Meltwater Within a Snow Cover 1. Observations in the Canadian Arctic, Water Resour. Res., 20, 1853-1864, 1984.

Marsh, P., and Woo, M. K.: Meltwater movement in natural heterogeneous snow covers, Water Resour. Res., 21, 1710-1716, 1985.

Marsh, P., and Pomeroy, J.: The impact of heterogeneous flow paths on snowmelt runoff chemistry, Proc. East. Snow. Conf, 1993, 231-238, 1993.

Marsh, P., and Pomeroy, J.: Spatial and temporal variations in snowmelt runoff chemistry, Northwest Territories, Canada, Water Resour. Res., 35, 1559-1567, 1999.

McCabe, G. J., Clark, M. P., and Hay, L. E.: Rain-on-Snow Events in the Western United States, Bull. Am. Meteorol. Soc., 88, 319-328, doi:10.1175/bams-88-3-319, 2007.

Merz, R., and Blöschl, G.: A process typology of regional floods, Water Resour. Res., 39, doi:10.1029/2002wr001952, 2003.

Michlmayr, G., Lehning, M., Koboltschnig, G., Holzmann, H., Zappa, M., Mott, R., and Schöner, W.: Application of the Alpine 3D model for glacier mass balance and glacier runoff studies at Goldbergkees, Austria, Hydrol. Process., 22, 3941-3949, doi:10.1002/hyp.7102, 2008.

Molnar, P., Fatichi, S., Gaál, L., Szolgay, J., and Burlando, P.: Storm type effects on super Clausius–Clapeyron scaling of intense rainstorm properties with air temperature, Hydrol. Earth Syst. Sci., 19, 1753-1766, doi: 10.5194/hess-19-1753-2015, 2015.

Morin, S., Lejeune, Y., Lesaffre, B., Panel, J. M., Poncet, D., David, P., and Sudul, M.: An 18-yr long (1993-2011) snow and meteorological dataset from a mid-altitude mountain site (Col de Porte, France, 1325m alt.) for driving and evaluating snowpack models, Earth Syst. Sci. Data, 4, 13-21, doi: 10.5194/essd-4-13-2012, 2012.

Osterhuber, R.: Precipitation intensity during rain-on-snow, in: Proceedings of the 67th Annual Western Snow Conference, 67th Annual Western Snow Conference, South Lake Tahoe California, 1999, 153–155, 1999.

R Development Core Team: R: A Language and Environment for Statistical Computing, Vienna, Austria. R Foundation for Statistical Computing, Retrieved from http://www.R-project.org/, 2016.

Rössler, O., Froidevaux, P., Börst, U., Rickli, R., Martius, O., and Weingartner, R.: Retrospective analysis of a nonforecasted rain-on-snow flood in the Alps-a matter of model limitations or unpredictable nature?, Hydrol. Earth Syst. Sci., 18, 2265-2285, doi:10.5194/hess-18-2265-2014, 2014.

Schmucki, E., Marty, C., Fierz, C., and Lehning, M.: Evaluation of modelled snow depth and snow water equivalent at three contrasting sites in Switzerland using SNOWPACK simulations driven by different meteorological data input, Cold Reg. Sci. Technol., 99, 27-37, doi:10.1016/j.coldregions.2013.12.004, 2014.

Schneebeli, M.: Development and stability of preferential flow paths in a layered snowpack, in: Biogeochemistry of Seasonally Snow-Covered Catchments (Proceedings of a Boulder Symposium July 1995), edited by Tonnessen, K., Williams, M., and Tranter, M., 1995, 89-96, 1995.

Singh, P., Spitzbart, G., Hübl, H., and Weinmeister, H.: Hydrological response of snowpack under rain-on-snow events: a field study, J. Hydrol., 202, 1-20, doi:10.1016/S0022-1694(97)00004-8, 1997.

Stearns, C. R., and Weidner, G. A.: Sensible and Latent Heat Flux Estimates in Antarctica, in: Antarctic Meteorology and Climatology: Studies Based on Automatic Weather Stations, edited by: Bromwich, D. H., and Stearns, C. R., Antarctic Research Series, Vol. 61, American Geophysical Union, 109-138, 1993.

Sui, J., and Koehler, G.: Rain-on-snow induced flood events in Southern Germany, J. Hydrol., 252, 205-220, doi:10.1016/S0022-1694(01)00460-7, 2001.

Surfleet, C. G., and Tullos, D.: Variability in effect of climate change on rain-on-snow peak flow events in a temperate climate, J. Hydrol., 479, 24-34, doi:10.1016/j.jhydrol.2012.11.021, 2013.

Unsworth, M. H., and Monteith, J.: Long-wave radiation at the ground I. Angular distribution of incoming radiation, Q. J. R. Meteorol. Soc., 101, 13-24, doi:10.1002/qj.49710142703, 1975.

Waldner, P. A., Schneebeli, M., Schultze-Zimmermann, U., and Flühler, H.: Effect of snow structure on water flow and solute transport, Hydrol. Process., 18, 1271-1290, doi: 10.1002/hyp.1401, 2004.

Wever, N., Fierz, C., Mitterer, C., Hirashima, H., and Lehning, M.: Solving Richards Equation for snow improves snowpack meltwater runoff estimations in detailed multi-layer snowpack model, Cryosphere, 8, 257-274, doi:10.5194/tc-8-257-2014, 2014a.

Wever, N., Jonas, T., Fierz, C., and Lehning, M.: Model simulations of the modulating effect of the snow cover in a rain-on-snow event, Hydrol. Earth. Sys. Sci., 18, 4657-4669, doi:10.5194/hess-18-4657-2014, 2014b.

Wever, N., Schmid, L., Heilig, A., Eisen, O., Fierz, C., and Lehning, M.: Verification of the multi-layer SNOWPACK model with different water transport schemes, Cryosphere, 9, 2271-2293, doi: 10.5194/tc-9-2271-2015, 2015.

Wever, N., Vera Valero, C., and Fierz, C.: Assessing wet snow avalanche activity using detailed physics based snowpack simulations, Geophys. Res. Lett., doi:10.1002/2016GL068428, 2016a.

Wever, N., Würzer, S., Fierz, C., and Lehning, M.: Simulating ice layer formation under the presence of preferential flow in layered snow covers, Submitted to Cryosphere Discuss., doi: 10.5194/tc-2016-185, 2016b.

Wickham, H.: ggplot2: Elegant Graphics for Data Analysis, Use R!, Springer-Verlag New York, VIII, 213 pp., 2009.

WSL Institute for Snow and Avalanche Research SLF: Meteorological and snowpack measurements from Weissfluhjoch, Davos, Switzerland, doi:10.16904/1 2015. dataset

Würzer, S., Jonas, T., Wever, N., and Lehning, M.: Influence of initial snowpack properties on runoff formation during rain-on-snow events, J. Hydrometeorol., 17, 1801-1815, doi: 10.1175/JHM-D-15-0181.1, 2016.

Ye, H., Yang, D., and Robinson, D.: Winter rain on snow and its association with air temperature in northern Eurasia, Hydrol. Process., 22, 2728-2736, doi:10.1002/hyp.7094, 2008.

Hydrol. Earth Syst. Sci. Discuss., doi:10.5194/hess-2016-351, 2016
Manuscript under review for journal Hydrol. Earth Syst. Sci.
Published: 3 August 2016

Hydrology and Earth System Sciences
Open Access
Discussions

Table 1: Snowpack pre-conditions and execution dates for the sprinkling experiments as well as R^2 values for the different model simulations. Measured values are snow height (HS), bulk liquid water content (LWC), bulk snow temperature (TS).

Initial snowpack conditions					R^2 of hourly runoff of the simulations		
Experiment	HS [cm]	LWC [vol%]	TS [°C]	DATE	RE	PF	BA
Serneus (Ex1)	48.5	0.1	-1.3	26-Feb-15	0.22	0.45	0.09
Davos (Ex2)	54.5	0.4	-2.5	27-Feb-15	0.25	0.6	0.08
Sertig (Ex3)	71.5	0	-1.6	28-Feb-15	NA	NA	NA
Klosters (Ex4)	15.7	6.9	0	26-Mar-15	0.78	0.96	0.86
Klosters (Ex5)	7	4.9	0	8-Apr-15	0.71	0.84	0.88
Davos (Ex6)	39.3	0.9	-0.6	10-Apr-15	0.52	0.82	0.37

Hydrol. Earth Syst. Sci. Discuss., doi:10.5194/hess-2016-351, 2016
Manuscript under review for journal Hydrol. Earth Syst. Sci.
Published: 3 August 2016

Hydrology and Earth System Sciences
Open Access
Discussions

Table 2: Snowpack pre-conditions and R^2 for hourly snowpack runoff for natural events Jan 03 + Jan 09

	Site	Pre-event snowpack conditions			R^2 for hourly snowpack runoff		
		HS (cm)	LWC (vol%)	TS (°C)	RE	PF	BA
03.01.2015	Serneus	19	0	0	0.61	0.35	0.83
	Klosters	24	0	-0.1	0.73	0.66	0.79
	Davos	20	0	-0.4	0.28	0.30	0.13
09.01.205	Serneus	14.5	0.1	-0.2	0.94	0.56	0.79
	Klosters	18	0.1	-0.2	0.84	0.66	0.70
	Davos	19.5	0.1	-0.6	0.00	0.04	0.01

Hydrol. Earth Syst. Sci. Discuss., doi:10.5194/hess-2016-351, 2016
Manuscript under review for journal Hydrol. Earth Syst. Sci.
Published: 3 August 2016

Hydrology and Earth System Sciences
Discussions

Table 3: R^2 and mean absolute errors for hourly snowpack runoff for 17 and 14 years, for CDP and WFJ, respectively.

	R^2 hourly snowpack runoff			RMSE of snowpackrunoff ($mm\ h^{-1}$)		
	BA	RE	PF	BA	RE	PF
CDP	0.33	0.50	0.52	0.57	0.45	0.41
WFJ	0.5	0.7	0.75	0.53	0.34	0.30

Hydrol. Earth Syst. Sci. Discuss., doi:10.5194/hess-2016-351, 2016
Manuscript under review for journal Hydrol. Earth Syst. Sci.
Published: 3 August 2016

Hydrology and Earth System Sciences
Open Access
Discussions

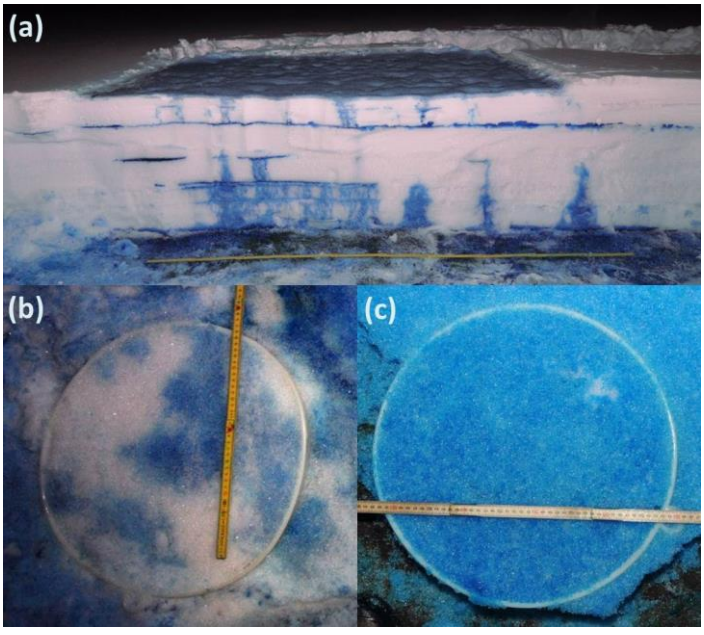

Figure 1: (a) Horizontal cut of a snowpack after the sprinkling experiment Sertig Ex1. Lateral flow and the presence of PFP were observed. PFP were generated at regions with rain water ponding at ice layers and layer boundaries with a change in grain size (creating capillary barriers). (b) Lysimeter area after sprinkling during winter conditions: Colored areas indicate the area where water percolated due to preferential flow. (c) Lysimeter area after sprinkling during spring conditions: Colored area shows that water percolated uniformly, indicating dominating matrix flow.

Hydrol. Earth Syst. Sci. Discuss., doi:10.5194/hess-2016-351, 2016
Manuscript under review for journal Hydrol. Earth Syst. Sci.
Published: 3 August 2016

Hydrology and Earth System Sciences
Open Access
Discussions

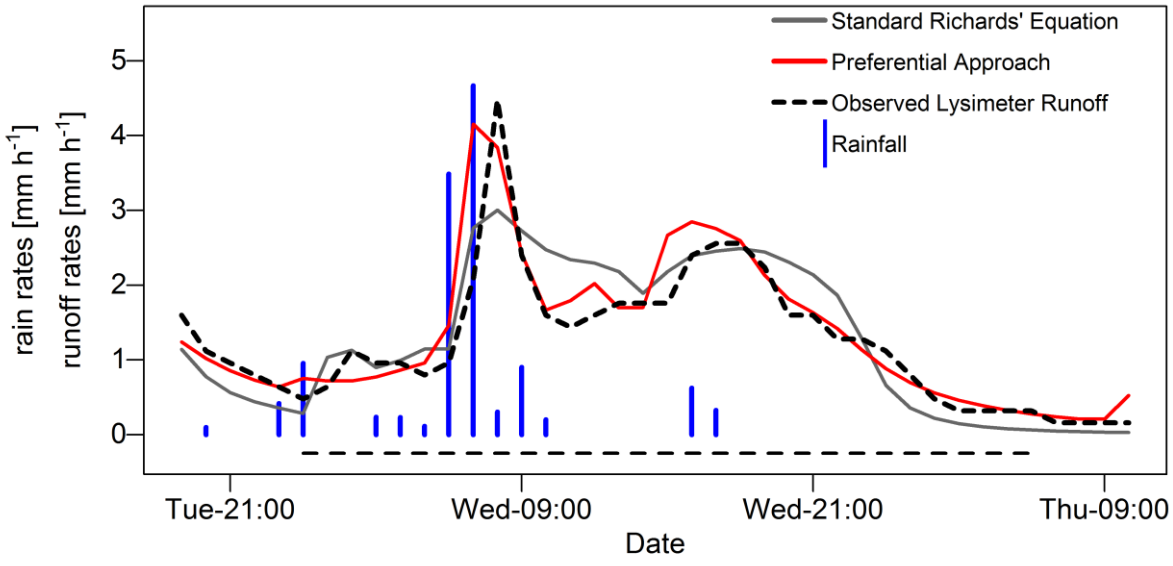

Figure 2: Example of a ROS event occurring at WFJ. The entire extent of the x-axis refers to the evaluation period; the bar below the x-axis refers to the event length.

Hydrol. Earth Syst. Sci. Discuss., doi:10.5194/hess-2016-351, 2016
Manuscript under review for journal Hydrol. Earth Syst. Sci.
Published: 3 August 2016

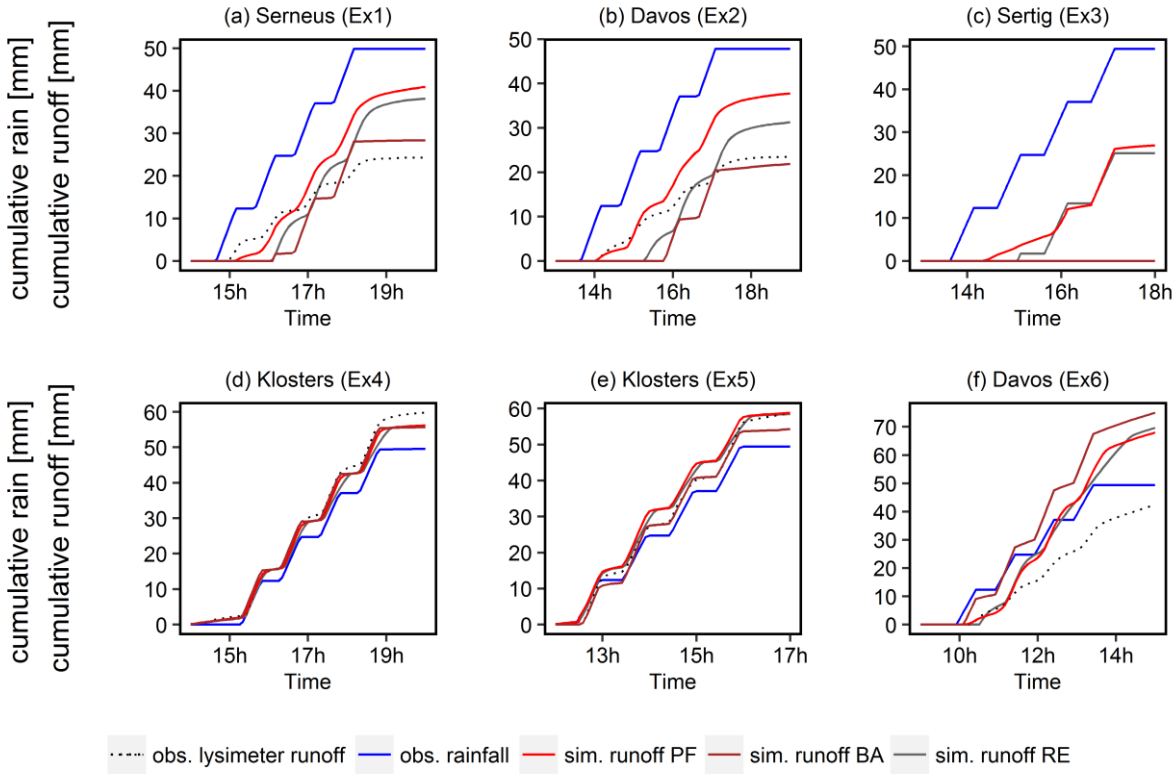

Figure 3: Cumulative rain and snowpack runoff displayed for the six sprinkling events. Ex1 (a) - Ex3 (c) were conducted during winter conditions, Ex4 (d) – Ex6 (f) were conducted during spring conditions.

Hydrol. Earth Syst. Sci. Discuss., doi:10.5194/hess-2016-351, 2016
Manuscript under review for journal Hydrol. Earth Syst. Sci.
Published: 3 August 2016

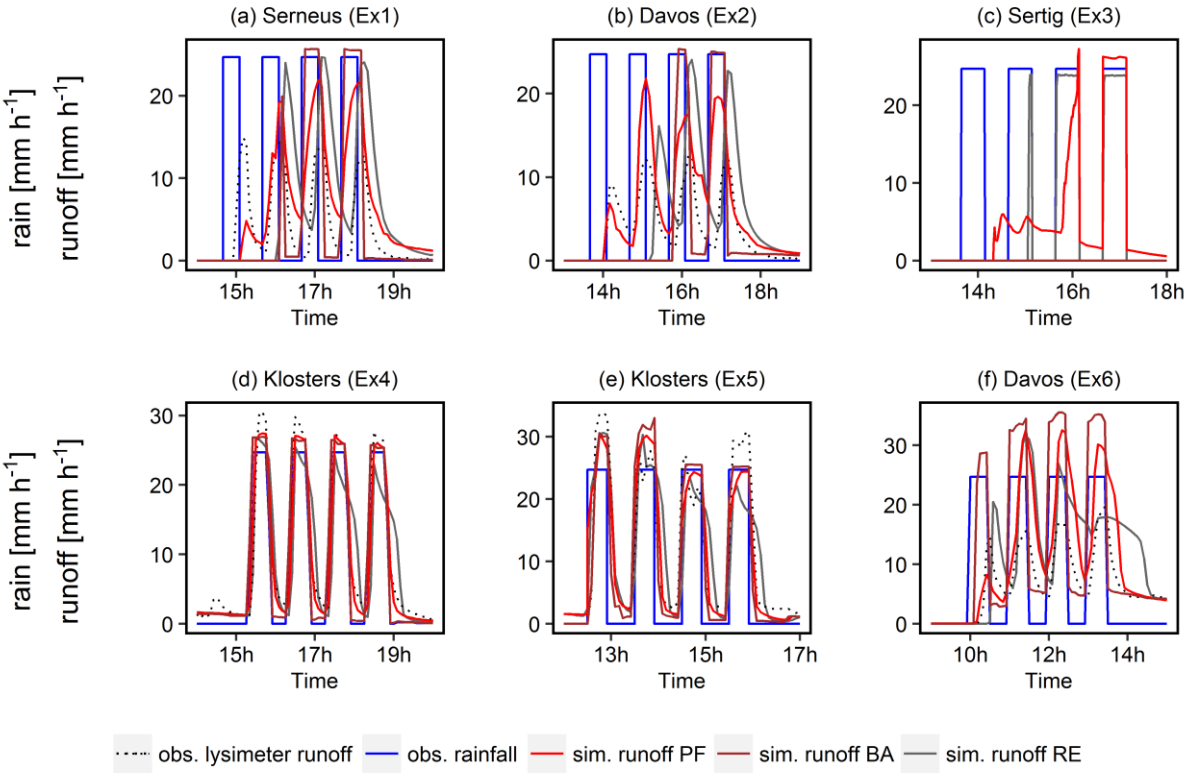

Figure 4: Rain and snowpack runoff displayed as hydrographs for the six sprinkling events. Ex1 (a) - Ex3 (c) were conducted during winter conditions, Ex4 (d) – Ex6 (f) were conducted during spring conditions.

Hydrol. Earth Syst. Sci. Discuss., doi:10.5194/hess-2016-351, 2016
Manuscript under review for journal Hydrol. Earth Syst. Sci.
Published: 3 August 2016

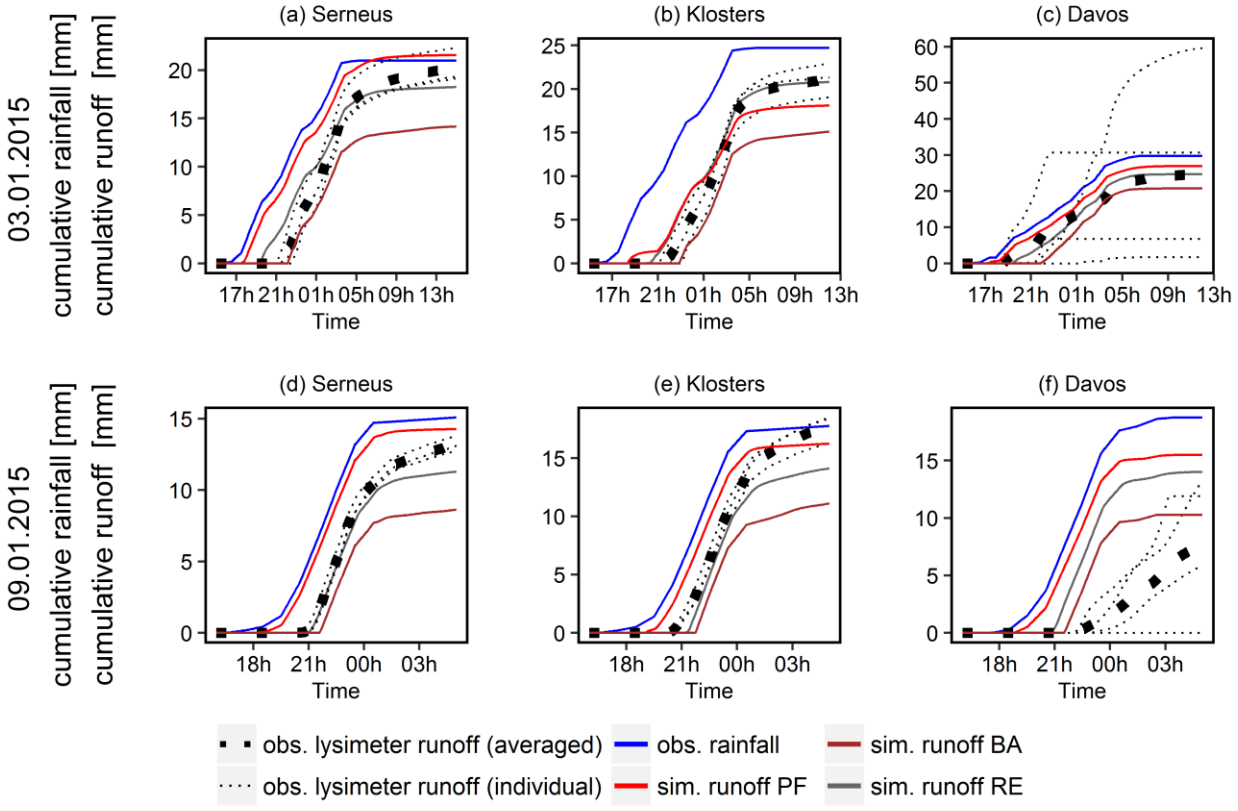

Figure 5: Natural ROS events at 3rd and 9th of January 2015 in (a) Serneus, (b) Klosters and (c) Davos

Hydrol. Earth Syst. Sci. Discuss., doi:10.5194/hess-2016-351, 2016
Manuscript under review for journal Hydrol. Earth Syst. Sci.
Published: 3 August 2016

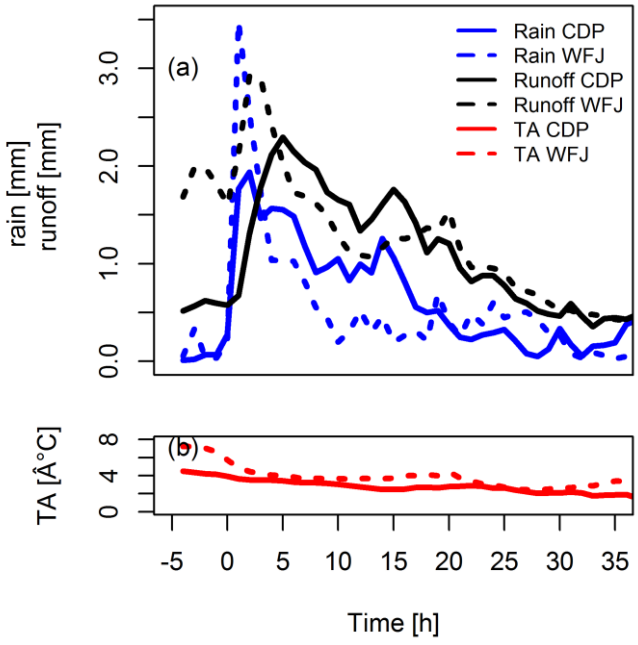

Figure 6: (a) Course of mean rain (blue) and measured snowpack runoff (red) for WFJ (dotted) and CDP (solid) for all 40 and 61 events respectively. (b) Mean air temperature for WFJ (dotted) and CDP (solid). The displayed period is extended by 5 hours prior to event beginning according to the event definition (0 h).

Hydrol. Earth Syst. Sci. Discuss., doi:10.5194/hess-2016-351, 2016
Manuscript under review for journal Hydrol. Earth Syst. Sci.
Published: 3 August 2016

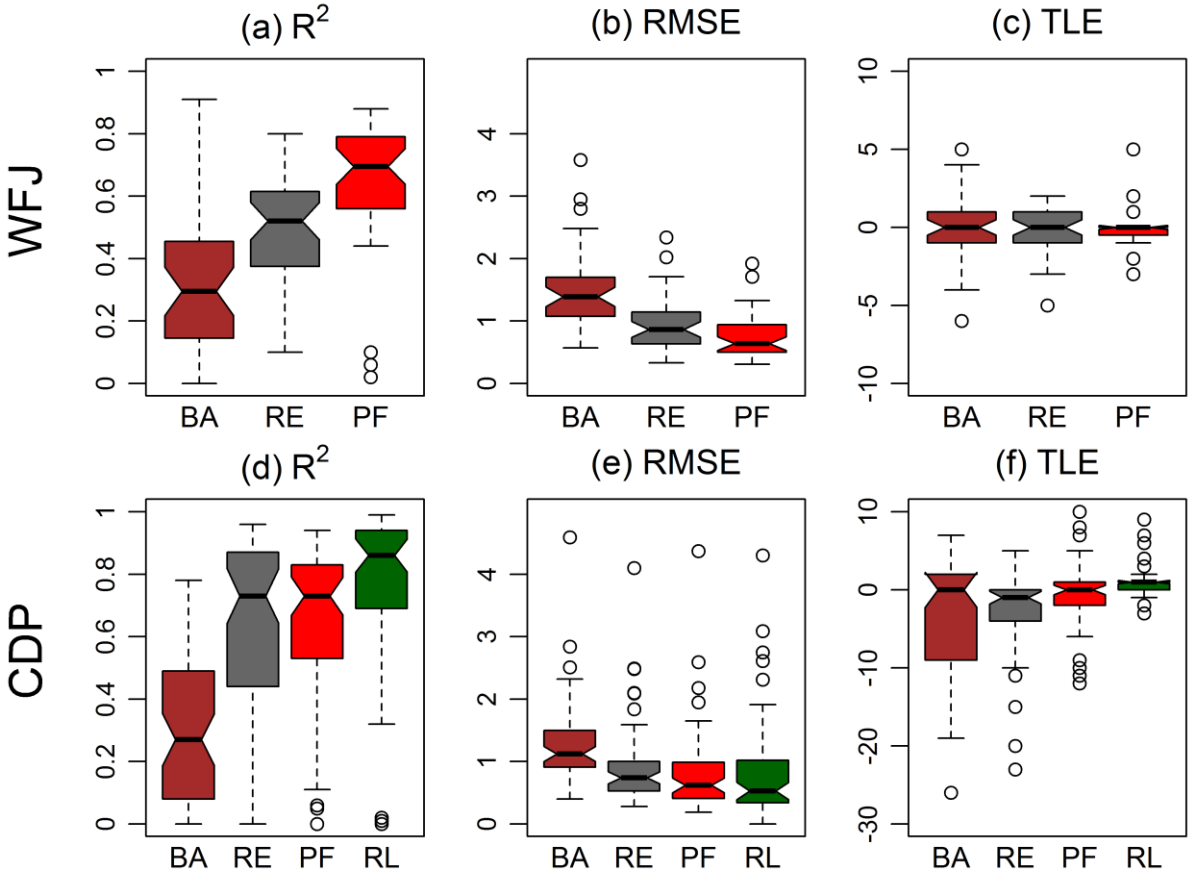

Figure 7: RMSE, R^2 and TLE for simulations of 61 ROS events at the CDP site and of 40 ROS events at the WFJ site for all models (BA, RE, PF) and the reference lysimeter (RL) available only for CDP.

Hydrol. Earth Syst. Sci. Discuss., doi:10.5194/hess-2016-351, 2016
Manuscript under review for journal Hydrol. Earth Syst. Sci.
Published: 3 August 2016

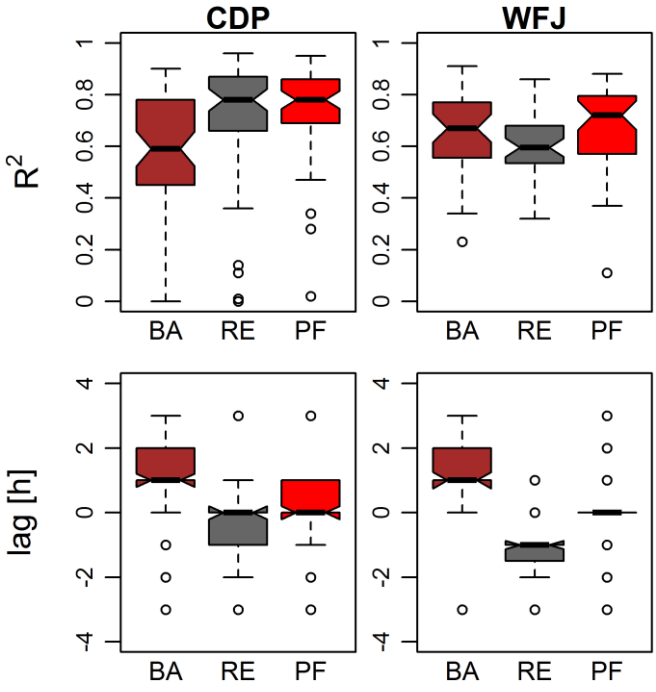

Figure 8: Best R^2 values and corresponding lags using a cross-correlation function allowing a time shift (lag) of max -/+ 3 hours.

5. Komentář k výsledkům

V této kapitole jsou shrnuty všechny dosažené výsledky, které byly prezentovány v jednotlivých článcích v kapitole výsledky. Dále jsou přidána některá doplňková měření, která nebyla v článcích prezentována a vzájemné porovnání dosažených výsledků ze všech článků. Tyto dodatečné informace tak přispívají k ucelenějším vědeckým poznatkům ke studované problematice.

5.1. Data a lokality

Data ze zadešťovacích experimentů byla získána v horském prostředí v České republice, Německu a Švýcarsku v nadmořské výšce od 950 do 2150 m n. m. Jelikož v uvedených článcích někdy chybí konkrétní specifikace experimentálních lokalit, tak pro přehlednost jsou všechny lokality uvedeny v tabulce 1. Kromě dat prezentovaných v jednotlivých článcích byla ještě získána data během počátečního testování zadešťovací metodiky, která byla pouze částečně prezentována v článku I. V kapitole 8.3.2 (Obr. 23) jsou však výsledky z těchto experimentů využity pro doplnění datové sady popisujících závislost rychlosti propagace vody ve sněhové pokrývce na intenzitě deště. Pro lepší orientaci v následujících kapitolách je nově zavedeno také přehledné označení každého experimentu nezávislé na označení v publikovaných článcích.

5.2. Využití zadešťovacích simulátorů

V předložené práci byly představeny dva základní koncepty simulace deště na sněhovou pokrývku in situ. Každý z obou typů experimentů umožňuje zaměřit se na různé aspekty chování dešťové vody ve sněhové pokrývce. Pro simulaci ROS byl vyvinut speciální zadešťovací simulátor, jehož specifikace je popsána v článku I. Tento simulátor byl následně testován v článku I a poté byla testována i metoda separace hydrogramu během ROS v článku II. Simulátor i metodika byly po získaných zkušenostech upraveny a následně použity pro další experimenty popisující články III a IV.

Jednotlivé typy experimentů byly uzpůsobené podle účelu studia daných charakteristik proudění a odtoku dešťové vody. Tato kapitola shrnuje a komentuje základní principy použité metodiky simulace deště na sněhovou pokrývku.

Tab. 1 – Přehledné informace o všech lokalitách. Tabulka také ukazuje, v jakém článku byla data z daných experimentů použita.

Datum	Lokalita	Typ	Souřadnice	Nadm. výška (m n. m.)	Stát	Označení	Článek
26.2.2015	Serneus	Lysimetr	46.89308N, 9.83636E	950	Švýcarsko	L1	IV
27.2.2015	Davos	Lysimetr	46.81278N, 9.84840E	1550	Švýcarsko	L2	IV
28.2.2015	Sertig	Lysimetr	46.72278N, 9.85074E	1850	Švýcarsko	L3	IV
26.3.2015	Klosters	Lysimetr	46.86247N, 9.89806E	1200	Švýcarsko	L4	IV
8.4.2015	Klosters	Lysimetr	46.86247N, 9.89806E	1200	Švýcarsko	L5	IV
10.4.2015	Davos	Lysimetr	46.81277N, 9.84837E	1550	Švýcarsko	L6	IV
18.3.2015	Sertig	Izotopy	46.72273N, 9.85059E	1850	Švýcarsko	ID1	III
23.4.2015	Sertig	Izotopy	46.72279N, 9.85072E	1850	Švýcarsko	ID2	III
1.5.2015	Dischma	Izotopy	46.72097N, 9.92196E	2000	Švýcarsko	ID3	III
7.5.2015	Flüela	Izotopy	46.74367N, 9.98128E	2150	Švýcarsko	ID4	III
14.4.2012	Labská	Izotopy	50.77119N, 15.54590E	1300	Česká republika	IL1	II
7.3.2011	Spitzingsee	Testování	47.66759N, 11.85611E	1265	Německo	T1	-
8.3.2011	Spitzingsee	Testování	47.66760N, 11.85641E	1265	Německo	T2	-
20.3.2011	Kvilda	Testování	49.00524N, 13.56306E	1185	Česká republika	T3	-
21.3.2011	Kvilda	Testování	49.00533N, 13.56330E	1185	Česká republika	T4	I
22.3.2011	Kvilda	Testování	49.00522N, 13.56329E	1185	Česká republika	T5	-
24.3.2011	Kvilda	Testování	49.00509N, 13.56368E	1185	Česká republika	T6	-
31.3.2011	Kvilda	Testování	49.00513N, 13.56398E	1185	Česká republika	T7	-
2.4.2011	Kvilda	Testování	49.00506N, 13.56419E	1185	Česká republika	T8	-

5.2.1. Souvislá sněhová pokrývka – Lysimetr

Během tohoto typu experimentu byla zadešťována souvislá sněhová pokrývka, kde byl na rozhraní půda/sníh umístěn lysimetr s dataloggerem. Jako stopovač bylo použito barvivo brilliant blue FCF (BB), které umožnilo vizualizovat místa proudění dešťové vody a následně i charakter proudění. Kromě simulací ROS byly lysimetry využity také ke sledování přírodních ROS. Využití lysimetrů při přírodních a umělých dešťových událostech je popsáno v článku IV. Na Obr 12a, b je znázorněna sestava lysimetru s dataloggerem před instalací a po instalaci v terénu.

Na základě získaných zkušeností můžeme shrnout základní výhody a nevýhody tohoto typu experimentů:

+ Neporušená sněhová pokrývka poskytuje přírodě blízké podmínky. Dochází k minimálnímu ovlivnění termálních a mechanických vlastností sněhové pokrývky vlivem manipulace.
+ Je možné určit typ proudění (matricové, preferenční) ale i rozhraní dvou vrstev, kde často dochází ke vzniku laterárního toku.
+ Minimalizace okrajového efektu kvůli velkému rozstřiku do okolí lysimetru.
+ Je možné studovat i přírodní dešťové události, protože lysimetr je možné mít instalovaný po celou sezónu. Simulaci můžeme provézt až na konci sezóny, kdy již máme k dispozici většinu dat odtoku.
- Není možné určit hmotnostní bilanci kvůli neizolované experimentální doméně a častému rozlivu vody do stran.
- Není možné kontinuálně měřit vlastnosti (teplotu, vlhkost) zasažené sněhové pokrývky, aniž by došlo k výraznému porušení původních přirozených podmínek.
- Není možné provádět separaci hydrogramu vzhledem k nemožnosti odebírat vzorky vody na výtoku.

Obr. 12 – A) Lysimetr spojený s člunkovým průtokoměrem – celkový pohled před instalací. B) Instalace lysimetru a dataloggeru v terénu před zimní sezónou (foto: autor).

5.2.2. Izolovaná sněhová pokrývka - izotopové experimenty

V práci jsou uvedeny dva typy experimentů s izolovanou sněhovou pokrývkou od okolí. V prvním typu byla izolovaná experimentální kostka 1x1 m ponechána obnažená během celé simulace deště (článek II). V druhém případě byly izolované experimentální sněhové kostky následně opatřeny izolační vrstvou, která byla fixována váhou okolního sněhu. Experimentální kostka tak obsahovala pouze přírodní neporušený sníh (článek III). Celkový pohled a srovnání všech typů experimentů je na Obr. 13.

Praxe ukázala výhody a nevýhody tohoto experimentálního přístupu:

+ Izolace umožňuje přesnou hmotnostní bilanci.

Komentář k výsledkům

+ Možnost sledování změny vlastností (především teploty) sněhu během experimentu. Umístění (teplotních) čidel však může částečně narušit strukturu sněhové pokrývky a tím ovlivnit dráhu preferenčních cest.
+ Možno provádět separaci hydrogramu na základě vzorkování vody na odtoku. Velkou výhodou je také přizpůsobení intenzity vzorkování podle jednotlivých fází odtoku (Obr. 14).
- Samotný proces izolace experimentální sněhové kostky od okolí může částečně ovlivnit její termální a mechanické vlastnosti (lokální zhutnění), což může mít za následek zrychlené zrání sněhu v kostce oproti okolí.
- Nebylo možné použít barvivo v kombinaci s deuteriem. Analýza obarvené vody by mohla způsobit poškození laboratorních přístrojů.
- Větší časová a personální náročnost (potřeba alespoň 3 dny a 4 lidi).

Obr. 13 – Srovnání zadešťovacích experimentů A) Izolovaná sněhová pokrývka – nezakrytá (článek I, II), B) Souvislá sněhová pokrývka (článek IV) a C) Izolovaná sněhová pokrývky zakrytá (článek III) (foto: autor).

Obr. 14 – A) Odběr vzorku vody na odtoku B) Rozpuštěné vzorky odebraného sněhu v 10 ml lahvičkách (foto: autor).

5.2.3. Monitoring fyzikálních veličin

Prováděné experimenty měly za cíl kromě studia odtoku ze sněhové pokrývky také sledovat změny sněhové pokrývky způsobené následkem deště. Z toho důvodu byly vždy před a po experimentu podle technických možností analyzovány základní charakteristiky sněhové pokrývky jako: výška, hustota, teplota, LWC a základní stratifikace vrstev (Obr. 15). Při experimentech, kde byly použity izotopy, se navíc ve sněhové pokrývce analyzovala také koncentrace deuteria před a po experimentu (článek II, III).

Obr. 15 – Analýza vlastností sněhové pokrývky po experimentu. A) Měření vlhkosti sněhu v profilu, B) Měření celkové hustoty a odkrytá teplotní čidla na měření teploty sněhové pokrývky během experimentu (foto: autor).

Kromě výše uvedených analýz byla využívána i dodatečná meteorologická měření z přilehlých meteorologických stanic (Obr. 16a). Meteorologická data byla využita především jako vstupy do modelu energetické bilance (článek II). Nastavení experimentů však komplikuje využití těchto dat a přináší oproti přírodním ROS několik problémů. Zadešťovací simulátor je koncipován tak, že je jeho konstrukce chráněna před větrem, který výrazně ovlivňuje trajektorii dešťových kapek. Vítr se však běžně provází

přírodní ROS a je významným hybatelem turbulentní výměny tepla, která způsobuje tání pokrývky. Druhá generace zadešťovacího simulátoru (článek III, IV) využívá jako ochranu před větrem stan. Zadešťovaná pokrývka je tak kvůli střeše stanu krytá ze všech stran. Toto zakrytí tak výrazně ovlivní bilanci krátkovlnného i dlouhovlnného záření, ale i teplotu vzduchu a relativní vlhkost vzduchu uvnitř stanu (Obr. 16b). Pro přesné výstupy z EB je tedy nutné měřit všechny veličiny uvnitř stanu. Z technických důvodů však bylo možné měřit pouze teplotu a relativní vlhkost vzduchu (článek III). Data z radiace mohla být použita u experimentu IL1, kde simulátor nebyl zakryt střechou a na zasaženou pokrývku tak dopadalo sluneční záření.

Z hlediska energetické bilance je také důležité měřit teplotu vstupní dešťové vody, která také významně ovlivňuje dodatečné tání (rce 10). Zde ovšem také nastává problém, na jakém místě v hydraulickém systému simulátoru teplotu měřit. Během dopravy vody z barelu do trysky, potažmo při rozstřiku na sněhovou pokrývku se může teplota vody změnit vlivem vnějších faktorů (tření v potrubí, ohřívání potrubí vlivem radiace, atd.). Teplota deště byla pak ještě doplňkově měřena 30 cm nad sněhovou pokrývkou, tak aby bylo teplotní čidlo zasaženo dešťovými kapkami (L1-L6, ID1-ID4). Teplotu vody na výstupu není třeba měřit, protože pokud se voda ve sněhové pokrývce vyskytuje v kapalném stavu, tak je vždy ochlazena na 0°C. Tento fakt využili např. Conway et Benedict (1994) při sledování čela zvlhčení pomocí lokálního oteplení sněhu na 0°C. Během testování metodiky byla tato skutečnost potvrzena.

Pro reálnou simulaci deště je nutné skrápět sníh vodou o teplotě podobné teplotě vzduchu. Během experimentů se však voda v barelech ohřívala vlivem radiace. Z toho důvodu je nutné zásobní barely s vodou ochlazovat sněhem kolem barelů.

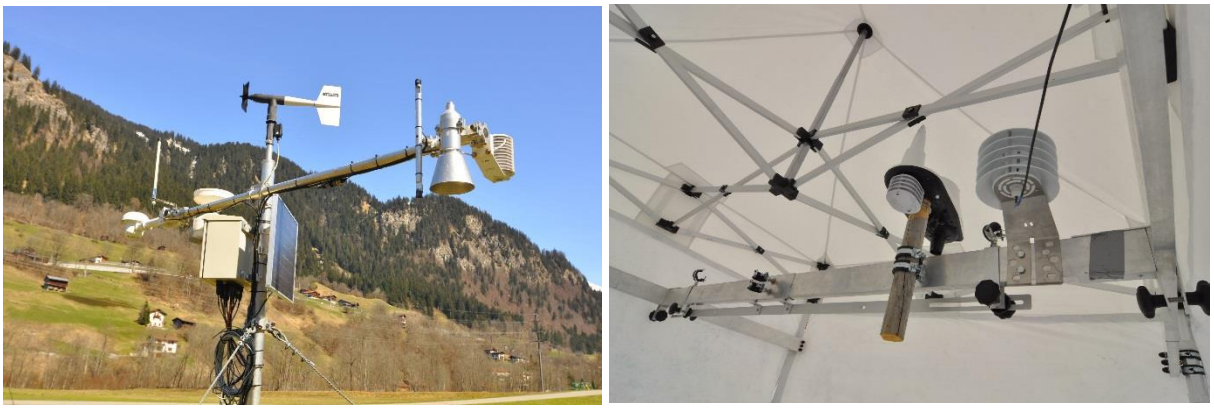

Obr. 16 – Měření meteorologických veličin A) Profesionální meteorologická stanice umístěná na lokalitě, B) Dodatečné měření teploty a relativní vlhkosti vzduchu uvnitř stanu umístěné na konstrukci zadešťovacího simulátoru (foto: autor).

5.2.4. Kalibrace

Celý zadešťovací systém bylo nutné před nasazením v terénu důkladně testovat a kalibrovat. Nejdůležitější byl výběr trysky, která při vhodném tlaku dokáže produkovat dostatečně malou, přírodě blízkou intenzitu srážky s rovnoměrným rozložením. Ukázalo se, že tyto požadavky je velmi těžké splnit. Především pokud zadešťovaná plocha má rozměry pouze 1x1 m. Na druhou stranu zadešťování v terénu větší plochy je velmi technicky náročné. Kalibrace trysek byla prováděna in situ i v laboratoři. Průtok tryskou byl kalibrován především v závislosti na tlaku a na výšce trysky nad zadešťovanou plochou. Rozložení umělé srážky na ploše bylo kalibrováno pomocí sítě měrných nádob rozložených na ploše. Ukázky procesu kalibrace v terénu a získaných výsledků jsou uvedeny na Obr. 17.

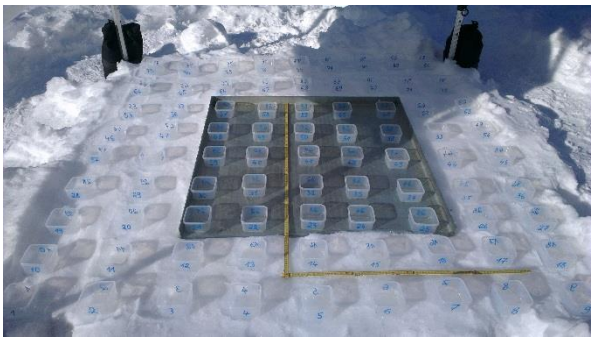

Lechler 430.368.CA						Pressure (bar):		2
Rain intensity (mm.h^{-1})						Height (cm):		160
1.07	3.68	6.11	6.55	5.47	4.32	2.89	1.77	0.62
2.11	5.69	9.43	10.90	9.33	7.61	5.37	3.65	1.69
3.22	7.71	12.33	16.70	14.93	11.17	7.85	5.66	2.98
3.42	8.60	18.02	29.23	25.79	20.54	15.16	9.33	4.53
3.14	8.45	18.97	29.93	23.32	24.25	29.05	16.70	5.82
2.16	6.35	11.58	19.13	23.62	23.72	30.99	15.09	5.82
1.33	3.57	7.33	11.70	15.49	20.64	17.69	9.91	4.71
0.69	2.39	5.06	7.51	9.10	11.68	9.76	6.12	2.82
0.20	0.95	2.79	4.23	5.54	6.43	5.21	3.35	1.58
Plate	MIN	7.33	MEAN	19.17	MAX	30.99	STDEV	6.88
All	MIN	0.20	MEAN	9.65	MAX	30.99	STDEV	7.98

Obr. 17 – Kalibrace rozložení srážky na ploše A) ukázka provedení in situ (foto: autor), B) ukázka výsledků.

Kromě trysek byl kalibrován i člunkový průtokoměr a to staticky a dynamicky. Detaily kalibrace průtokoměru jsou shrnuty v článku I.

Pro tuto studii byla vyvinuta speciální teplotní čidla, která umožnují kontinuálně zaznamenávat teplotu sněhové pokrývky. Tato čidla byla také kalibrovaná a porovnávána vzhledem ke rtuťovému teploměru při ponoření do lázně tvořenou ledem a vodou, která měla 0°C (Obr. 18).

Obr. 18 – Laboratorní kalibrace teplotních čidel (foto: autor).

5.3. Dynamika odtoku během ROS

Experimenty byly prováděny na dva typy sněhové pokrývky. **Nevyzrálá** sněhová pokrývka se vyznačovala malou hustotou do 250 kg.m^{-3} a průměrnou teplotou pod bodem mrazu. Tato pokrývka neobsahovala kapalnou vodu nebo pouze velmi malé množství v horních vrstvách. **Vyzrálá** sněhová pokrývka byla charakteristická hustotou nad 330 kg.m^{-3} a průměrnou teplotou kolem 0°C. Vyzrálá sněhová pokrývka obsahovala kapalnou vodu v celém profilu.

5.3.1. Charakteristiky proudění a odtoku ze sněhové pokrývky

Na základě výsledků z 6 experimentů na souvislou sněhovou pokrývku bylo zjištěno, že v **nevyzrálé** (studené) sněhové pokrývce dominovalo především **preferenční proudění** (L1 – L3) **a ve vyzrálé** sněhové pokrývce dominovalo **matricové proudění** (L4 – L6). Charakter proudění byl určen pomocí vizualizace preferenčních cest pomocí barviva BB (Obr. 19-21).

Preferenční proudění v nevyzrálé pokrývce bylo charakteristické jak vertikálním, tak horizontálním pohybem (laterární tok). Tento fakt byl již dříve popisován jinými autory (Katsushima et al., 2013; Waldner et al., 2004). Na rozhraní dvou vrstev, kdy jemnozrnná vrstva leží na vrstvě hrubozrnné, dochází ke vzlínání (kapilárnímu sání) a k lokálnímu nasycení nad tímto rozhraním. Bylo pozorováno, že toto nasycení může dosahovat hodnot LWC > 10% (např. L3), ale v okolí této nasycené vrstvy byla měřena nulová vlhkost. Zároveň vzrostla teplota sněhu v této nasycené vrstvě na 0°C (Obr. 19). Po nasycení této vrstvy a oslabení kapilárního sacího tlaku dochází k následnému pohybu vody směrem dolů, kdy se tvoří nové preferenční cesty (Katsushima et al., 2013).

V některých případech se charakter proudění měnil, kdy v horních vrstvách nebo nad rozhraním vrstev se vyskytlo matricové proudění, které se postupně změnilo na preferenční proudění. Preferenční proudění vzniká nejčastěji v heterogenním sněhu, kde se často mění velikost a tvar sněhových krystalů (Hirashima et al., 2014). Tento aspekt byl také uvažován v novém modulu modelu SNOWPACK (článek IV), kdy je celá sněhová pokrývka rozdělena na zóny preferenčního toku a zóny matricového toku a tyto zóny spolu navzájem komunikují.

Ve vyzrálé sněhové pokrývce převažovalo matricové proudění**.** Sněhová pokrývka byla obarvená v celém svém objemu, protože většinou pórů proudila dešťová voda (Obr. 22). Na základě podobných vlastností sněhu (LWC, hustota, T_s) předpokládáme, že matricové proudění nastalo i během izotopových experimentů na vyzrálé sněhové pokrývce, přestože dráhy toku nebyly vizualizovány (ID2 – ID4 a IL1).

U vyzrálého sněhu můžeme uvažovat převažující vliv vertikálního proudění a minimální výskyt laterárního proudění ze dvou důvodů: 1) Sníh byl obarven pouze v ploše dosahu trysky a byl pozorován minimální pohyb vody do stran. 2) U experimentů na vyzrálou pokrývku (L4, L5) byl zaznamenán vyšší kumulativní odtok, než u experimentů na nevyzrálou sněhovou pokrývku (L1, L2). Voda tak proudila sněhovou pokrývkou přímo směrem dolů. Pouze experiment L6 vykazoval výsledky mezi oběma

uvedenými charakteristikami. Vlastnosti sněhové pokrývky by se však daly charakterizovat mezi vyzrálou a nevyzrálou sněhovou pokrývkou (T_S = -0.6, hustota = 355, LWC = 0.9%).

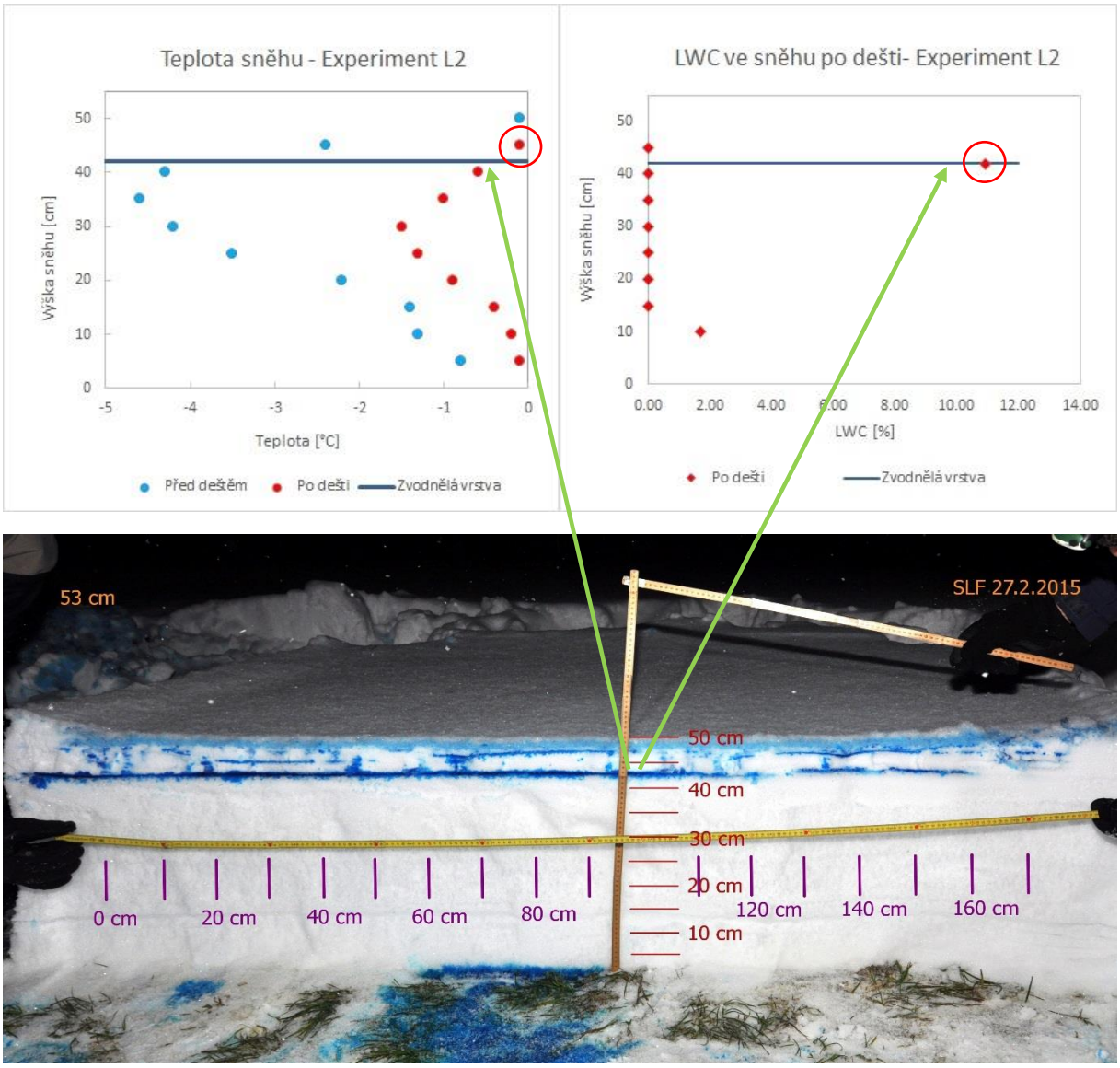

Obr. 19 – Horizontální řez sněhovou pokrývku znázorňující zvodnělou vrstvu (42 cm), která vznikla na rozhraní dvou sněhových vrstev s různou zrnitostí. Grafy v horní části obrázku ukazují vykreslenou teplotu a LWC před a po experimentu. Zakroužkovány jsou hodnoty měřené ve zvodnělé vrstvě (foto: autor).

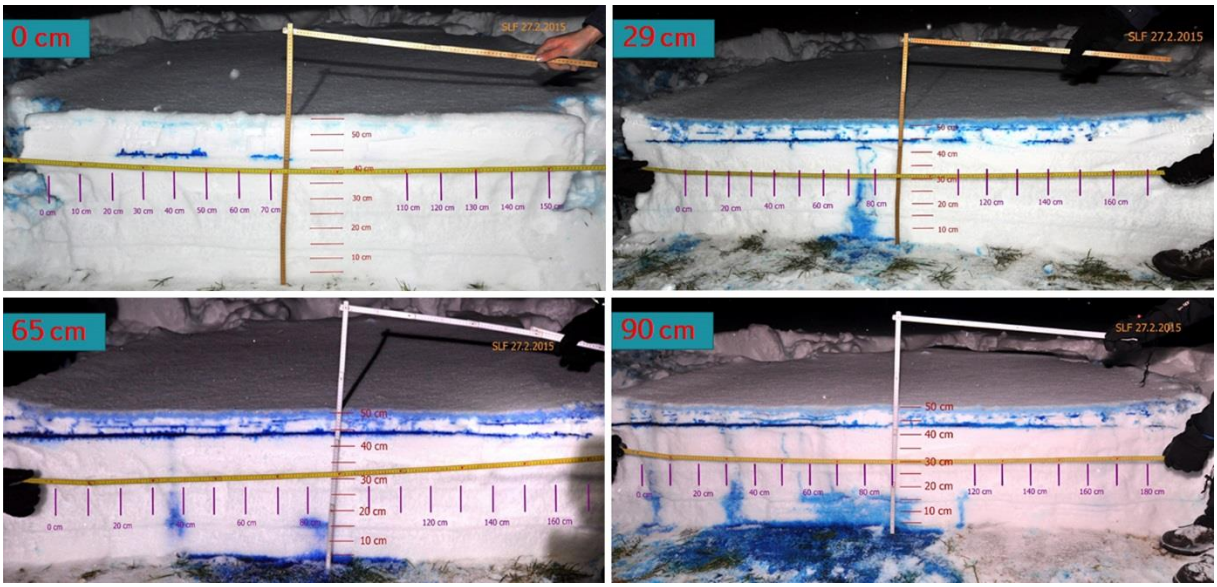

Obr. 20 – Řezy nevyzrálou sněhovou pokrývkou po experimentu L2 znázorňující proměnlivost preferenčních cest v horizontální ose.

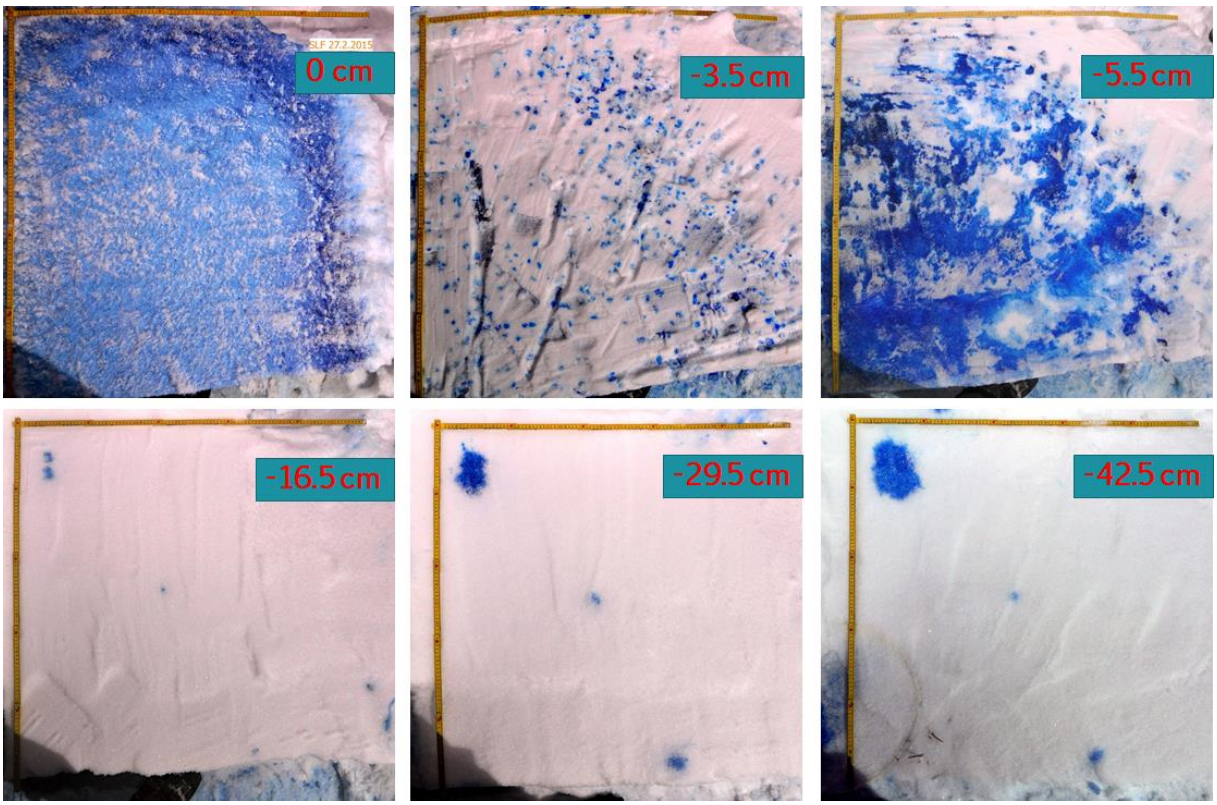

Obr. 21 – Řezy nevyzrálou sněhovou pokrývkou po experimentu L2 znázorňující proměnlivost preferenčních cest ve vertikální ose.

Obr. 22 – Řezy vyzrálou sněhovou pokrývkou po experimentu L4 znázorňují rovnoměrný tok celou pokrývkou.

5.3.2. Rychlost odezvy

Izotopové experimenty ukázaly, že se doba zdržení celkového odtoku a odtoku dešťové vody na výtoku liší. Dešťová voda se objevila vždy později jak u pilotního experimentu (IL1), tak u dalších experimentů (ID1 – ID4). Bylo sice provedeno malé množství experimentů, ale přesto můžeme při porovnání výsledků vyvodit několik závěrů.

V článku III jsou analyzovány 4 experimenty, kdy jeden z experimentů byl prováděn na nevyzrálou sněhovou pokrývku. Z výsledků jednoznačně vyplývá, že nevyzrálá pokrývka (ID1) měla při stejné intenzitě deště rychlejší hydrologickou reakci, než vyzrálá sněhová pokrývka (ID2-ID4). Na druhou stranu na při experimentu IL1 byla skrápěna vyzrálá pokrývka a rychlost propagace obou složek odtoku byla naměřena ještě rychlejší, než při ID1. Zároveň při IL1 byl naměřen nejmenší rozdíl mezi dobou zdržení celkové a dešťové vody na výtoku (pouze 1 min). LWC zde bohužel nebyla z technických důvodů měřena. Můžeme ale předpokládat že LWC byla vysoká, vzhledem k měřenému pre-experimentálnímu tání a manuálnímu určení vlhkosti sněhové pokrývky jako mokré, tj. *pendulární režim 3-8 %* (Fierz et al., 2009). Manuální test byl proveden pouze pro získání orientační hodnoty LWC, absolutní hodnotu LWC takto odhadovat nelze (Techel et al., 2011). Rychlost propagace při experimentu IL1 byla pravděpodobně způsobena cca 7x vyšší intenzitou srážky, než u experimentu ID1. To potvrzuje také Würzer et al. (2016), který uvádí, že intenzita odtoku závisí na intenzitě srážky.

Tento fakt byl ještě podpořen porovnáním rychlostí propagace kombinovaného odtoku ze sněhové pokrývky v závislosti na intenzitě deště v rámci všech 18ti experimentů (Tab. 1). Z výsledků lineární regrese vykreslených na Obr. 23 vyplývá, že rychlost propagace roste s intenzitou deště ($r^2 = 0.6015$, $p = 2.54 \times 10^{-4}$). Slabší vazba byla zjištěna mezi rychlostí propagace a počáteční hustotou ($r^2 = 0.2518$, $p = 0.03385$) nebo počáteční LWC ($r^2 = 0.1709$, $p = 0.2687$). Při vyhodnocení všech experimentů s různou intenzitou deště roste rychlost propagace na hustotě sněhu. Pokud ale hodnotíme pouze experimenty se

stejnou intenzitou, tak rychlost propagace klesá s hustotou sněhu (Obr. 23b). Tato závislost je sice těsnější, ale vzhledem k malému počtu měření málo průkazná. Z výsledků je patrné, že rychlost propagace je více závislá na počáteční LWC, než na hustotě. Data z experimentů ze zapojené sněhové pokrývky sice ukazují neprůkaznou vazbu ($r^2 = 0.217$, $p = 0.427$), ale pokud vyloučíme nejodlehlejší naměřenou hodnotu LWC (L4), tak závislost výrazně stoupne ($r^2 = 0.977$, $p = 0.012$). Z těchto výsledků můžeme předpokládat, že rychlost propagace dešťové vody primárně závisí na intenzitě deště a v druhé řadě na vlastnostech sněhové pokrývky. Pokud porovnáváme podobné intenzity deště, tak rychlost propagace celkové vody negativně nejvíce závisela na počáteční vlhkosti sněhu (tj. rychlost klesá s rostoucí vlhkostí). To je poměrně překvapivý výsledek, protože např. Jordan (1983) popisuje u rychlosti propagace tavné vody pravý opak, tj. že rychlost proudění tavné vody závisí na počáteční LWC (saturaci) pozitivně (tj. rychlost roste se zvyšující se vlhkostí). Zjištěná negativní závislost rychlosti propagace celkové vody na počáteční LWC může být spojená s popisovaným pístovým efektem (článek II, III), kdy je pohyb dešťové vody „brzděn“ vytlačováním kapalné vody z pokrývky. Výsledky z L3 však ukazují, že od určitého stupně nasycení by mohla být závislost na počáteční LWC pozitivní. Pro toto tvrzení však provedená měření poskytují jen velmi málo dat a jde tak pouze o hypotézu, kterou je třeba ověřit dalším výzkumem.

Závislost rychlosti propagace vody na odtoku během ROS by měla být vyhodnocena na experimentech prováděných za stejných podmínek, tj. stejné nastavení podmínek experimentů a stejná intenzita srážky.

Pokud hodnotíme rychlost propagace u zapojené sněhové pokrývky, tak musíme vzít v úvahu, že měření bylo omezeno plochou lysimetru. Z fotografií je zřejmé, že preferenční cesty se objevovaly i mimo lysimetr (Obr. 20). První voda se tak teoreticky objevila na sněhové bázi dříve, ale vlivem preferenčního proudění mohla odtéct mimo lysimeter. Tento fakt může podhodnocovat skutečnou rychlost propagace vody skrze sněhovou pokrývku a může tak vysvětlit přibližně 2.5x menší rychlost u experimentů se souvislou pokrývkou, než u experimentu s izolovanou pokrývkou. Na druhou stranu vzhledem k rozlévání dešťové vody do stran v nevyzrálé sněhové pokrývce, můžeme předpokládat zpomalení propagace dešťové vody i z tohoto důvodu.

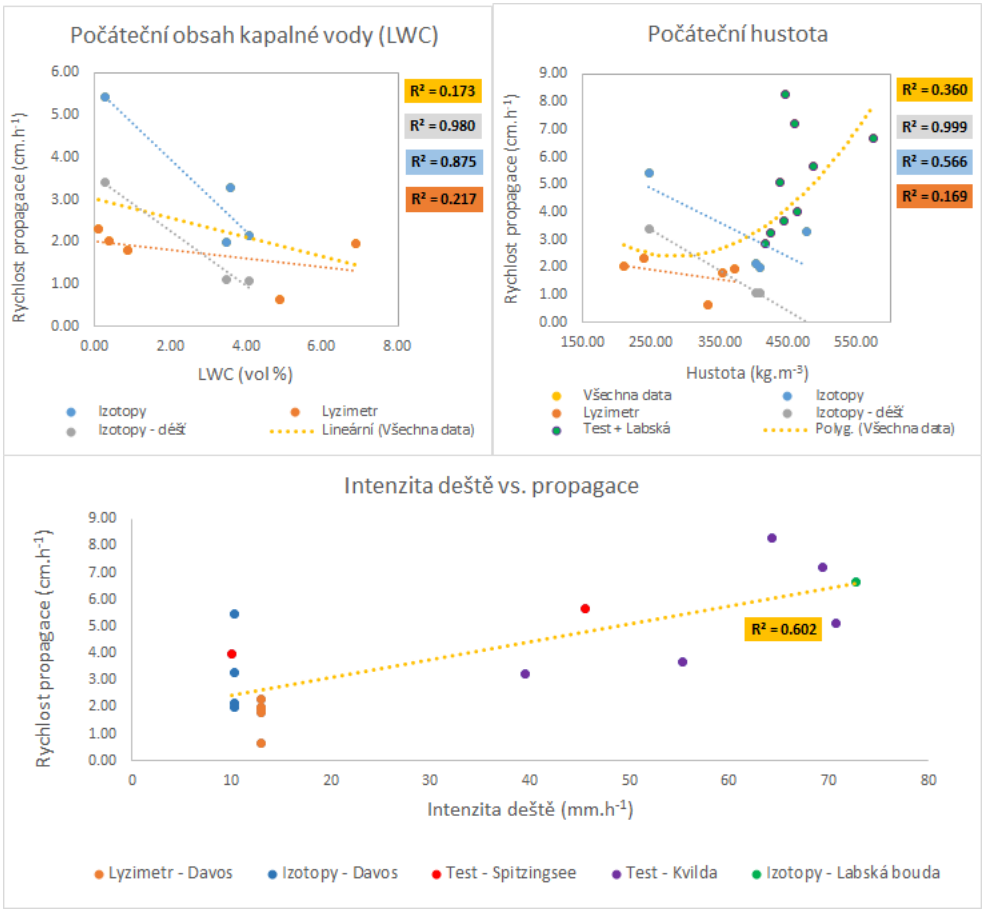

Obr. 23 – Závislost rychlosti propagace vody do odtoku během deště na charakteristikách sněhové pokrývky A) LWC a B) hustotě a na C) intenzitě deště.

5.3.3. Složení a velikost celkového odtoku

Během simulovaných ROS se odtok skládal z dešťové a nedešťové vody. Tyto dvě složky odtoku lze od sebe oddělit pomocí separace hydrogramu popsané v kapitole 2.9. Tato metoda je založena na rozdílném izotopickém složení dešťové vody a tavné vody, respektive sněhové pokrývky. Jedná se tedy o přímou metodu stanovení jednotlivých složek odtoku a je využita v článcích II a III. Nedešťová voda se skládá z kapalné vody, která je přítomna ve sněhové pokrývce před deštěm (LWC) a vody vzniklé z dodatečného tání, jehož množství lze vypočítat pomocí rovnice energetické bilance (rce 13). Tato nepřímá metoda separace složek nedešťové vody byla použita v článku II. Přesnost tohoto výpočtu je však náročná na vstupy, které nejsou vždy k dispozici.

Ze získaných výsledků je zřejmé, že množství dešťové vody na odtoku závisí na vlastnostech sněhové pokrývky, potažmo na režimu proudění. Odtok z nevyzrálé sněhové pokrývky byl z velké části tvořen dešťovou vodou (ID1), zatímco z vyzrálé sněhové pokrývky byla dešťová voda zastoupena maximálně z poloviny (ID2 – ID4, IL1).

Pomocí izotopové analýzy bylo zjištěno, že dešťová voda nejdříve vytlačuje kapalnou vodu (LWC) ze sněhové pokrývky, která zpočátku tvořila naprostou většinu odtoku. Dešťová voda se propagovala do

odtoku až později. Jakmile se ale začala propagovat, tak její podíl na odtoku velmi rychle stoupnul. Tento jev označujeme jako pístový efekt a byl popsán u výtoku jak z nevyzrálé, tak z vyzrálé sněhové pokrývky v článku II a III.

Při experimentech na izolovanou sněhovou pokrývku vždy převyšoval kumulativní odtok nad celkovým kumulativním přítokem. U vyzrálé sněhové pokrývky (IL1, ID2-ID4) byla tato převaha větší, než u nevyzrálé pokrývky (ID1). Toto může být v měřítku povodí potenciálně důležitý faktor z hlediska vzniku zvýšených průtoků následkem ROS, respektive vzniku povodní.

Nevyzrálá sněhová pokrývka reagovala relativně malým kumulativním odtokem, v porovnání s celkovým přítokem. Malý odtok byl pozorován jak u experimentů se zapojenou sněhovou pokrývkou (L1, L2), tak s izolovanou sněhovou pokrývkou (ID1).

Velikost celkového kumulativního odtoku byla ovlivněna vlastnostmi sněhové pokrývky, což můžeme shrnout do následujících bodů:

1) Během preferenčního proudění v **souvislé nevyzrálé** pokrývce se voda často rozlévala do stran (laterární proudění) a tím pádem se nedostala do lysimetru (L1, L2).
2) Dešťová voda velmi rychle protekla **izolovanou nevyzrálou** sněhovou pokrývkou a odtok tak byl složen převážně z dešťové vody a minimálně z tavné vody (ID1).
3) V **souvislé vyzrálé** sněhové pokrývce výrazně převažovalo vertikální proudění nad horizontálním, z toho důvodu bylo více vody zaznamenáno na lysimetru (L4 – L6).
4) Ve **vyzrálé izolované** sněhové pokrývce byl odtok z velké části tvořen nedešťovou vodou, což navyšovalo celkový vyteklý objem. Takto velké množství nedešťové vody v odtoku mělo několik příčin. Vyzrálá sněhová pokrývka obsahovala před deštěm poměrně velké množství kapalné vody (LWV > 3.5%), která byla vlivem deště transformována do odtoku. Můžeme také předpokládat intenzivní tání, protože sněhová pokrývka již byla izotermální a tak se dodané teplo spotřebovalo přímo na fázovou přeměnu a ne na ohřev sněhu.

Použití modelu SNOWPACK s využitím RE ukázalo, že celkový modelovaný kumulativní odtok z vyzrálé sněhové pokrývky je v dobré shodě s pozorovaným celkovým odtokem (L4, L5). U nevyzrálé pokrývky (L1, L2) dochází ke značnému nadhodnocení modelovaného odtoku nad pozorovaným. Přesto použití modelu preferenčního proudění (PF) přináší lepší výsledky v porovnání s modely RE a „Bucket approach“ (BA - viz tab. 1, článek IV). Výzvou pro další výzkum je použití těchto modelů i na experimenty s izolovanou sněhovou pokrývkou.

5.3.4. Změna sněhové pokrývky

Déšť dopadající na sněhovou pokrývku měl vliv na změnu jejích vlastností a to jak u vyzrálé, tak u nevyzrálé sněhové pokrývky. U vyzrálé sněhové pokrývky byly tyto změny výraznější. Konkrétně byly

ve sněhové pokrývce sledovány změny ve výšce, teplotě, obsahu kapalné vody, hustotě, případně obsahu deuteria.

Výška sněhové pokrývky vlivem sesedání a částečnému odtávání očekávaně klesla a to v rámci všech provedených experimentů.

Teplota se měnila podle předpokladů pouze u nevyzrálé sněhové pokrývky, u vyzrálé izotermální pokrývky zůstala teplota stejná. Nevyzrálá sněhová pokrývka se vlivem teplejšího deště vždy ohřála, což se projevilo na konečném zvýšení teploty. Vnitřní zvýšení teploty mohlo být také způsobeno částečným přemrzáním dešťové vody v pokrývce, kdy se do okolí uvolňuje latentní teplo.

Obsah kapalné vody (LWC) se zvýšil ve všech případech, kdy byla tato hodnota měřena (ID1 – ID4, L1 – L6). Zvýšení LWC bylo zapříčiněno zadrženým objemem dešťové vody, ale pravděpodobně i objemem vody, vzniklé dodatečným táním. Zadržení dešťové vody ve sněhové pokrývce lze dokumentovat na zvýšení obsahu deuteria ve sněhu (článek II, III). Obr. 24 doplňuje výsledky z článku III a ukazuje, že zadržení dešťové vody, dokumentované na zvýšení obsahu deuteria, není ve vertikálním profilu rovnoměrné a v některých vrstvách došlo dokonce ke snížení obsahu deuteria. Toto izotopické ochuzení (vylehčení) může být způsobeno transportem lehčí vody z vyšších vrstev, která se následně zadržela v níže položených vrstvách. Vyzrálá sněhová pokrývka vykazovala vždy výrazné zvýšení obsahu deuteria ve sněhové pokrývce (ID2 – ID4, IL1). U nevyzrálé sněhové pokrývky došlo dokonce k mírnému poklesu průměrné koncentrace deuteria. Tento pokles se dá však považovat spíše za chybu měření. Vzhledem k nárůstu vlhkosti u experimentu ID1 můžeme očekávat, že kromě tavné vody se ve sněhu zadržela i nějaká dešťová voda. Minimální měřená změna v obsahu deuteria tak může být způsobena geometrií preferenčních cest, v nichž se dešťová voda mohla zadržet. Analyzované vzorky sněhu tak mohly být odebrány mimo tyto preferenční cesty a to mohlo způsobit zkreslení výsledků.

Změny v hustotě sněhové pokrývky nemůžeme hodnotit tak jednoznačně. U experimentů s vyzrálou pokrývkou hustota v některých případech stoupla (ID2 – ID4, L6), ale v některých zase klesla (L4, L5, IL1). Na druhou stranu u nevyzrálé pokrývky (L1-L3, ID1) hustota vždy stoupla. Pro pokles hustoty u tří experimentů nebylo nalezeno žádné objektivní vysvětlení, snad jen chyba v měření. Obecný předpoklad je, že hustota sněhové pokrývky se následkem ROS zvýší (Marshall et al., 1999). Toto zvýšení nastává vlivem sesedání a zadržení dešťové vody.

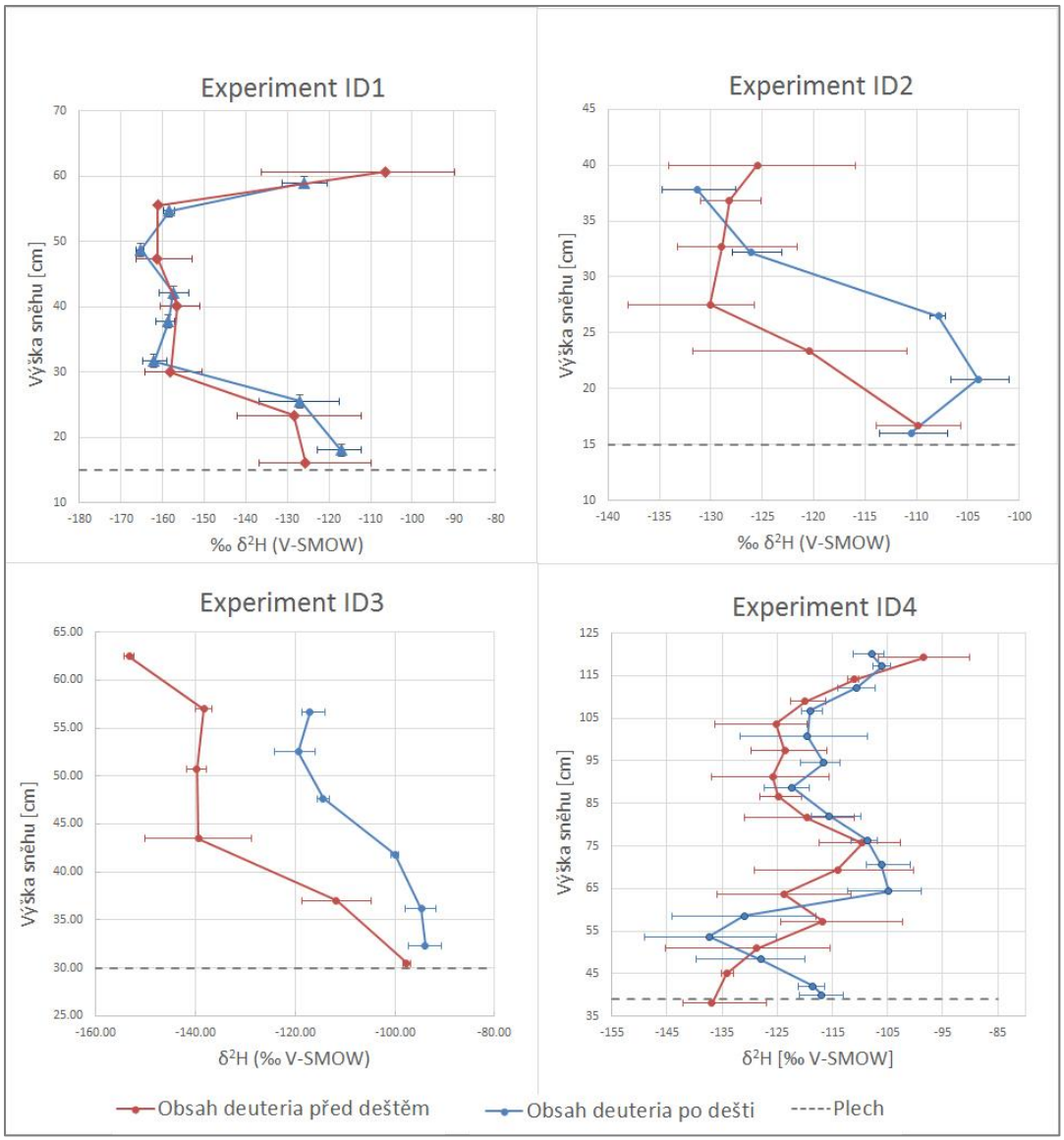

Obr. 24 – Vertikální profily ze 4 experimentů na izolovanou sněhovou pokrývku, které znázorňují změnu obsahu deuteria následkem umělého deště.

5.4. Nejistoty

Z předchozích podkapitol vyplývá, že při vyhodnocení výsledků ze zadešťování sněhové pokrývky je třeba brát v úvahu řadu nejistot, které jsou způsobeny měřicí technikou nebo použitou metodikou výpočtu. Pro přehlednost jsou tyto nejistoty uvedeny v následujícím seznamu:

- Nejistoty na vstupu a určení přesné intenzity a množství deště.
- Nehomogenní distribuce deště na plochu.
- Nejistota na člunkovém průtokoměru.
- Nejistoty při výpočtu tání – problematické měření a použití veličin rovnice energetické bilance.
- Nejistoty při separaci – problém s určením referenční hodnoty nedešťové vody. Předpokládáme, že se tato hodnota mění podle toho, jak se mění zásoba kapalné vody ve sněhové pokrývce.

- Při experimentech měla dešťová voda stálou koncentraci deuteria, ale koncentrace přírodního deště se často mění (McDonnell et al., 1990).
- Z důvodu proveditelnosti byly experimenty často prováděny v podmínkách, kdy se ROS běžně nevyskytují (slunečno – vysoká radiace, bezvětří – malá turbulentní výměna tepla, vysoká teplota deště, malá velikost kapek). Z toho mohou plynout další nejistoty při srovnání výsledků experimentů s reálnými přírodními událostmi.

5.5. Doporučení pro další studium

Během experimentů se stále vyvíjela metodika umožňující komplexní výzkum proudění vody ve sněhové pokrývce. Prezentovanou metodiku však nepovažuji jako konečnou a pro další výzkum by bylo vhodné zvážit několik vylepšení.

1) Spojení vizualizačních technik pomocí barviva a metody separace hydrogramu během stejného experimentu by umožnilo komplexnější studium režimu proudění a zároveň dynamiku jednotlivých složek na výtoku. Nabízí se tak možnost využití i jiných v hydrologii běžných stopovačů, např. nitráty – NO_3-N (Casson et al., 2014) nebo využití luminiscence přidáním uraninu (Gerke et al., 2013). Nevýhodou deuteria je především cena, která limituje počet opakování (na každý experiment je třeba analyzovat cca 200 vzorků vody).
2) Zadešťovaná plocha 1x1 m může být v některých případech limitující, především při dosahování malých intenzit deště a při studiu laterálního toku. Z toho důvodu by bylo vhodné zadešťovat větší plochu. Stávající sněhové polštáře v síti ČHMÚ umožňují kontinuální monitoring odtoku a po úpravě i možnost pravidelného vzorkování odtokové vody. Mírnou modifikací metodiky se může monitoring odtoku ze sněhových polštářů rozšířit i na studium přírodních ROS. Spojily by se tak částečně výhody zadešťování izolované a souvislé sněhové pokrývky.
3) Pro stanovení některých závislostí s větší jistotou je třeba provést více experimentů s aplikací separace složek odtoku, zejména na nevyzrálou sněhovou pokrývku. Výsledky těchto experimentů by bylo vhodné srovnat s výsledky modelu SNOWPACK využívající RE a PF. Jak bylo ukázáno v článku IV, tak model má největší problémy stanovit odtok především v nevyzrálé pokrývce. Pro přesné modelování je však třeba provést důkladnou zrnitostní analýzu sněhové pokrývky a detailní popis jednotlivých vrstev.

6. Závěr

Nově vyvinutá metodika umožňuje simulovat dešťové srážky na sněhovou pokrývku. V rámci této metodiky je možné stopovat dešťovou vodu jak ve sněhu pomocí vizualizace preferenčních cest, tak na odtoku ze sněhové pokrývky pomocí separace hydrogramu. Přestože simulace přirozených podmínek je omezená, tak metodika poskytuje relevantní výsledky při sledování dynamiky dešťové vody ve sněhu. Hlavní výhodou je především možnost nastavení počátečních podmínek a kontrola procesů během simulace.

Podle původního předpokladu bylo potvrzeno, že dešťová voda se chová ve vyzrálé sněhové pokrývce rozdílně, než v nevyzrálé pokrývce. Předpoklad, že dešťová voda proudí rychleji ve vyzrálé sněhové pokrývce, však potvrzen nebyl. Vlivem pístového efektu nejdříve vytlačila dešťová voda z pokrývky kapalnou vodu a částečně byla pokrývkou zadržena, což zpozdilo její odtok. Vyzrálá sněhová pokrývka transformovala dešťovou srážku mnohem více, než byl původní předpoklad. To mělo také za následek, že kumulovaný kombinovaný odtok z vyzrálé sněhové pokrývky obsahoval maximálně 50 % dešťové vody, ale celkově převyšoval celkový vstup deště. Tento fakt může být velmi důležitý z hlediska potenciálních povodní, především pokud bychom podobné chování očekávali i v měřítku povodí.

Na druhou stranu nevyzrálá sněhová pokrývka transformovala dešťovou vodu pouze omezeně, protože většina vstupní dešťové vody se objevila také na odtoku. Počáteční předpoklad, že dešťová voda bude intenzivně interagovat s nevyzrálou pokrývkou a většina vody se v ní zadrží, se také nepotvrdil. Vyzrálá pokrývka zadržela dešťovou vodu především vlivem rozlivu do stran a následnému přemrznutí. Lokálně docházelo na rozhraní dvou vrstev k výrazné akumulaci, která je ale vzhledem k celkovému dodanému objemu výrazně nižší. Pokud bylo rozlivu zamezeno, tak voda sněhem rychle protekla a byla pouze minimálně transformována.

Přítomnost dešťové vody ve sněhové pokrývce působila také změny v jejích vlastnostech. Změny nastaly jak ve vyzrálé, tak v nevyzrálé sněhové pokrývce. Ve vyzrálé pokrývce byly však tyto změny větší, především díky větší interakci dešťové vody se sněhem.

Zároveň bylo potvrzeno, že rychlost hydrologické odpovědi sněhové pokrývky závisí především na intenzitě deště a v druhé řadě na počátečních vlastnostech sněhu.

7. Seznam symbolů a zkratek

Zkratka	česky	anglicky
^{18}O	izotop kyslíku	oxygen isotope
^{2}H	deuterium	deuterium
^{3}H	tritium	tritium
BA	Bucket approach	Bucket approach
BB	brilliant blue FCF	
C	oblačnost (%)	cloudiness (%)
Ca	tepelná kapacita vzduchu (1,29 $kJ.m^{-3}.°C^{-1}$)	specific heat capacity of air (1,29 $kJ.m^{-3}.°C^{-1}$)
CDP	Col de Porte	Col de Porte
$c_{non-rain}$	koncentrace deuteria nedešťové vody (δ^2H ‰ V-SMOW)	deuterium concentration of non-rain water (δ^2H ‰ V-SMOW)
c_{rain}	koncentrace deuteria deště (δ^2H ‰ V-SMOW)	rain water deuterium concentration (δ^2H ‰ V-SMOW)
c_{total}	koncentrace deuteria v celkovém vzorku (δ^2H ‰ V-SMOW)	deuterium concentration in total sample (δ^2H ‰ V-SMOW)
C_w	specifické teplo vody (4.2 $kJ.kg^{-1}.°C^{-1}$)	specific heat of water (4.2 kJ.kg-1.°C-1)
d	průměr sněhového/ledového zrna (mm)	snow/ice grain diameter (mm)
e	emisivita sněhu	emissivity of snowpack surface
EB	model energetické bilance	energy balance model
E_v	latentní teplo výparu ($J.kg^{-1}$)	latent heat of vaporization ($J.kg^{-1}$)
F	celková plocha preferenčních cest v řezu (m^2)	the area of preferential domain (m^2)
g	gravitační zrychlení ($m.s^{-2}$)	Gravitational acceleration ($m.s^{-2}$)
h	hydraulická výška (m)	hydraulic head (m)
HS	výška sněhu (cm)	snow height (cm)
C_h	přenosový koeficient pro zjevné teplo	sensible heat transmission coefficient
K	nenasycená hydraulická vodivost ($m.s^{-1}$)	unsaturated hydraulic conductivity ($m.s^{-1}$)
k	propustnost (m^2)	intrinsic permeability (m^2)

Seznam symbolů a zkratek

k_g	tepelná vodivost půdy ($W.m^{-2}$)	thermal conductivity of soil ($W.m^{-2}$)
L_f	latentní teplo fázové přeměny ($J.kg^{-1}$)	latent heat of fusion $J.kg^{-1}$)
L_n	dlouhovlnná radiace (μm)	long wave radiation (μm)
LWC	obsah kapalné vody ve sněhu (%)	liquid water content (%)
M_d	množství tavné vody za den ($mm.d^{-1}$)	melt water column produced per day ($mm.d^{-1}$)
MF	hmotnostní tok ($mm.min^{-1}.\delta^2H$ ‰ V-SMOW)	mass flow ($mm.min^{-1}.\delta^2H$ ‰ V-SMOW)
M_s	množství tavné vody za sekundu ($mm.s^{-1}$)	melt water column produced per second ($mm.s^{-1}$)
P_c	kapilární tlak ($N.m^{-2}$)	capillary pressure ($N.m^{-2}$)
PF	preferenční proudění	preferential flow
PFP	preferenční cesta	preferential flow path
PI	průměrná intenzita deště ($m.h^{-1}$)	mean rain intensity ($m.h^{-1}$)
pre-LWC	kapalný podíl vody ve sněhu před deštěm (%)	liquid water content of snow before rain (%)
q	rychlost proudění ve sněhové pokrývce ($m.s^{-1}$)	water flux in snowpack ($m.s^{-1}$)
Q_E	tok latentního tepla evaporace, kondenzace nebo sublimace ($kJ.m^{-2}$)	latent heat flux of evaporation, condensation or sublimation ($kJ.m^{-2}$)
Q_G	tepelný tok z půdy ($kJ.m^{-2}$)	ground heat flux ($kJ.m^{-2}$)
Q_H	tok zjevného tepla konvektivního tepla získaného ze vzduchu ($kJ.m^{-2}$)	sensible heat flux ($kJ.m^{-2}$)
Q_I	změny vnitřní energie sněhu ($kJ.m^{-2}$)	internal snowpack energy changes ($kJ.m^{-2}$)
Q_{IK}	vnitřní energie kapaliny ($W.m^{-2}$)	internal changes of liquid phase ($kJ.m^{-2}$)
Q_{IL}	vnitřní energie ledu ($W.m^{-2}$)	internal changes of solid phase ($kJ.m^{-2}$)
Q_{IV}	vnitřní energie výparu ($W.m^{-2}$)	internal changes of vapour ($kJ.m^{-2}$)
Q_{ln}	tepelný tok dlouhovlnné radiace ($kJ.m^{-2}$)	heat flux of longwave radiation ($kJ.m^{-2}$)
Q_M	celková energie získaná sněhovou pokrývkou ($kJ.m^{-2}$)	Total gained energy of snowpack ($kJ.m^{-2}$)
Q_{melt}	průtok tavné vody ($mm.h^{-1}$)	melt water flux ($mm.h^{-1}$)
$Q_{non\text{-}rain}$	průtok nedešťové vody ($mm.h^{-1}$)	non-rain water flux ($mm.h^{-1}$)
Q_{NR}	bilance záření ($kJ.m^{-2}$)	net radiation, ($kJ.m^{-2}$)

Seznam symbolů a zkratek

Q_P	tepelný tok, způsobený deštěm ($kJ.m^{-2}$)	heat flux caused by rain ($kJ.m^{-2}$)
Q_{rain}	průtok dešťové vody ($mm.h^{-1}$)	rain water flux ($mm.h^{-1}$)
Q_{sn}	tepelný tok krátkovlnné radiace ($kJ.m^{-2}$)	short wave radiation flux ($kJ.m^{-2}$)
Q_{total}	celkový průtok vody ($mm.h^{-1}$)	total water runoff ($mm.h^{-1}$)
R^2	koeficient determinace	coefficient of determinartion
RE	Richardsova rovnice	Richard's equation
r_g	poloměr sněhového/ledového zrna (mm)	snow grain radius (mm)
RMSE	střední kvadratická chyba	root mean square error
ROS	déšť na sníh	rain-on-snow
R_p	množství dešťové srážky (m)	total column of rain water (m)
Sn	krátkovlnná radiace	short wave radiation
SWE	vodní hodnota sněhu	snow water equivalent
T_A	průměrná teplota vzduchu	mean air temperature
TDR	-	time domain refractometry
TLE	absolutní chyba doby zpoždění	absolut time lag error
T_r	teplota deště (°C)	rain water temperature (°C)
T_s	teplota sněhu (°C)	snow temperature (°C)
t_z	doba zpoždění celkového odtoku (min)	time lag of total runoff (min)
tz	čas zpoždění (min)	time lag (min)
Vs	objem vzorku sněhu (m^3)	volume of snow sample (m^3)
V-SMOW		Vienna standard mean ocean water
V_w	podíl kapalné vody ve sněhu (L)	fraction of liquid water in snowpack (L)
WFJ	Weissfluhjoch	Weissfluhjoch
z	geodetická výška (m)	geodetic head (m)
α	albedo sněhu	snow albedo
β	tepelná kvalita sněhové pokrývky	thermal quality of snow
δ^2H	deficit deuteria vůči V-SMOW (‰)	deuterium deficit to V-SMOW (‰)
ε	permitivita	permitivity
θ	vlhkost sněhu (%)	snow wetness (%)
λ	vlnová délka (μm)	wavelength (μm)
μ	dynamická vizkozita vody ($m^2.s^{-1}$)	dynamic viscosity of water ($m^2.s^{-1}$)
ρa	hustota vzduchu ($kg.m^{-3}$)	density of air ($kg.m^{-3}$)
ρi	hustota ledu ($kg.m^{-3}$)	density of ice ($kg.m^{-3}$)
ρs	hustota sněhu ($kg.m^{-3}$)	bulk density of snow ($kg.m^{-3}$)
ρw	hustota vody ($kg.m-^3$)	density of water ($kg.m^{-3}$)
σ	Stefan-Boltzmannova konstanta (5.67×10^{-11} $kW.m^{-2}.K^{-4}$)	Stefan-Boltzmann constant (5.67×10^{-11} $kW.m^{-2}.K^{-4}$)
φ	pórovistost	porosity

8. Seznam literatury

Akitaya, E.: A calorimeter for measuring free water content of wet snow, Ann. Glaciol., 6, 246–247, 1985.

Ambach, W. and Howorka, F.: Avalanche activity amd free water content of snow at Oberlung (1980 m a.s.l., Spring 1962), in Symposium at Davos 1965 - Scientific Aspects of Snow and Ice Avalanches, vol. 69, pp. 65–72, International Assocciation of Scientific Hydrology Publication 69, Davos., 1966.

Avanzi, F., Hirashima, H., Yamaguchi, S., Katsushima, T. and Michele, C. De: Laboratory-based observations of capillary barriers and preferential flow in layered snow, Cryosph. Discuss., 9 (6), 6627–6659, doi:10.5194/tcd-9-6627-2015, 2015.

Badoux, A., Hofer, M. and Jonas, T.: Hydrometeorologische Analyse des Hochwasserereignisses vom 10. Oktober 2011. [online] Available from: http://www.wsl.ch/fe/gebirgshydrologie/wildbaeche/projekte/unwetter2011/Ereignisanalyse_Hochwasser_Oktober_2011.pdf, 2013.

Böhm, U., Fiedler, A., Machui-Schwanitz, G., Reich, T. and Schneider, G.: Hydrometeorologische Analyse der Schnee- und Tauwettersituation im Dezember 2010 / Januar 2011 in Deutschland (in German), report, Available online at: (http://www.dwd.de/bvbw/generator/DWDWWW/Content/Wasserwirtschaft/Unsere__Leistungen/Schneeschmelzvorhersage/KU4__Tauwetter__2010__11__lang__pdf,templateId=raw,property=publicationFile.pdf/KU4_Tauwetter_2010_11_lang_pdf.pdf). Accessed, Offenbach. [online] Available from: http://www.dwd.de/bvbw/generator/DWDWWW/Content/Wasserwirtschaft/Unsere__Leistungen/Schneeschmelzvorhersage/KU4__Tauwetter__2010__11__lang__pdf,templateId=raw,property=publicationFile.pdf/KU4_Tauwetter_2010_11_lang_pdf.pdf, 2011.

Brun, E., Martin, E., Simon, V., Brun, B. E., Martin, E., Simon, V. and Gendre, C.: An energy and mass model of snow cover sidtable for operational avalanche forecasting, J. Glaciol., 35(12), 333–342 [online] Available from: http://www.igsoc.org/journal.old/35/121/igs_journal_vol35_issue121_pg333-342.pdf\nhttp://www.researchgate.net/profile/Eric_Martin12/publication/200472476_An_energy_and_mass_model_of_snow_cover_suitable_for_operational_avalanche_forecasting/links/5422c9b60, 1989.

Calonne, N., Geindreau, C., Flin, F., Morin, S., Lesaffre, B., Rolland Du Roscoat, S. and Charrier, P.: 3-D image-based numerical computations of snow permeability: Links to specific surface area, density, and microstructural anisotropy, Cryosphere, 6(5), 939–951, doi:10.5194/tc-6-939-2012, 2012.

Casson, N. J., Eimers, M. C. and Watmough, S. a.: Sources of nitrate export during rain-on-snow events at forested catchments, Biogeochemistry, 120(3), 23–36, doi:10.1007/s10533-013-9850-4, 2014.

Colbeck, S. C.: One-dimensional water flow through snow, CRREL, Honover, New Hampshire. [online] Available from: http://www.amazon.com/One-dimensional-water-through-Research-report/dp/B0006WKP7K (Accessed 6 July 2013), 1971.

Colbeck, S. C.: The capillary effects on water percolation in homogeneous snow, J. Glaciol., 67, 143–151, 1974.

Conway, H.: Physical processes in snowpacks during rain or melt events, University of Washington, Washington. [online] Available from: http://www.ntis.gov/search/product.aspx?ABBR=ADA275445 (Accessed 7 July 2013), 1994.

Conway, H. and Benedict, R.: Infiltration of water into snow, Water Resour. Res., 30(3), 641–649, doi:10.1029/93WR03247, 1994.

Conway, H. and Raymond, C. F.: Snow stability during rain, J. Glaciol., 39(133), 635–642, 1993.

Čekal, R., Ryglewicz, M., Bořiková, L., Suchá, M., Přibyl, J. and Kotek, R.: Zpráva o povodni v lednu 2011 (in Czech), Report, Available online at:

(http://portal.chmi.cz/files/portal/docs/hydro/ohp/povoden_01_2011.pdf), Accessed 17.10.2014, Prague. [online] Available from: http://portal.chmi.cz/files/portal/docs/hydro/ohp/povoden_01_2011.pdf, 2011.

Davis, R. E., Dozier, J. and Lachapelle, R.: Field and Laboratory Measurements of Snow Liquid Waterby Dilution, Water Resour. Res., 21(9), 1415–1420, 1985.

Denoth, A.: An electronic device for long-terlll snow wetness recording, Ann. Glaciol., 19, 104–106, 1994.

DeWalle, D. R. and Rango, A.: Principles of snow hydrology, Cambridge University Press, New York., 2008.

Dinçer, T., Payne, B. R., Florkowski, T., Martinec, J. and Tongiorgi, E.: Snowmelt runoff from measurements of tritium and oxygen-18, Water Resour. Res., 6(1), 110–124, doi:10.1029/WR006i001p00110, 1970.

Dozier, J., Melack, J. M., Elder, K., Kattelmann, R., Marks, D. and Williams, M.: Snow, snowmelt, rain, runoff, and chemistry in a Sierra Nevada watershed, Santa Barbara. [online] Available from: http://o3.arb.ca.gov/research/apr/past/a6-147-32a.pdf, 1989.

Eiriksson, D., Whitson, M., Luce, C. H., Marshall, H. P., Bradford, J., Benner, S. G., Black, T., Hetrick, H. and McNamara, J. P.: An evaluation of the hydrologic relevance of lateral flow in snow at hillslope and catchment scales, Hydrol. Process., 27(5), 640–654, doi:10.1002/hyp.9666, 2013.

Engineers, U. A. C. of: Runoff from snowmelt, Washington., 1998.

Feng, X., Kirchner, J. W., Renshaw, C. E., Osterhuber, R. S., Klaue, B. and Taylor, S.: A study of solute transport mechanisms using rare earth element tracers and artificial rainstorms on snow, Water Resour. Res., 37(5), 1425–1435, doi:10.1029/2000WR900376, 2001a.

Feng, X., Kirchner, J. W., Renshaw, C. E., Osterhuber, R. S., Klaue, B. and Taylor, S.: A study of solute transport mechanisms using rare earth element tracers and artificial rainstorms on snow, Water Resour. Res., 37(5), 1425–1435, doi:10.1029/2000WR900376, 2001b.

Feng, X., Taylor, S., Renshaw, C. E. and Kirchner, J. W.: Isotopic evolution of snowmelt 1. A physically based one-dimensional model, Water Resour. Res., 38(10), 35-1-35–8, doi:10.1029/2001WR000814, 2002.

Ferguson, S. A.: The spatial and temporal variability of rain-on-snow, in Assessment International Snow Science Workshop, 1-6 October 2000, pp. 178–183, American Avalanche Association, Big Sky, Montana., 2000.

Fierz, C., Armstrong, R. L., Durand, Y., Etchevers, P., Greene, E., Mcclung, D. M., Nishimura, K., Satyawali, P. K. and Sokratov, S. A.: The International Classification for Seasonal Snow on the Ground, 1st ed., IHP-VII Technical Documents in Hydrology N°83, IACS, Paris., 2009.

Fisk, D.: Method of measuring liquid water mass fraction of snow by alcohol solution, J. Glaciol., 32(112), 538–539, 1986.

Freudiger, D., Kohn, I., Stahl, K. and Weiler, M.: Large-scale analysis of changing frequencies of rain-on-snow events with flood-generation potential, Hydrol. Earth Syst. Sci., 18(7), 2695–2709, doi:10.5194/hess-18-2695-2014, 2014.

Garvelmann, J., Pohl, S. and Weiler, M.: Variability of Observed Energy Fluxes during Rain-on-Snow and Clear Sky Snowmelt in a Midlatitude Mountain Environment, J. Hydrometeorol., 15(3), 1220–1237, doi:10.1175/JHM-D-13-0187.1, 2014.

Gerke, K. M., Sidle, R. C. and Mallants, D.: Criteria for selecting fluorescent dye tracers for soil hydrological applications using Uranine as an example, J. Hydrol. Hydromechanics, 61(4), 313–325, doi:10.2478/johh-2013-0040, 2013.

Gude, M. and Scherer, D.: Atmospheric triggering and geomorphic significance of fluvial events in high-latitude regions, Zeitschrift für Geomorphol. Suppl. Issues, 115, 87–111 [online] Available from: http://dx.doi.org/10.1127/zfgsuppl/115/1999/87, 1999.

Harrington, R. and Bales, R. C.: Modeling ionic solute transport in melting snow, Water Resour. Res., 34(7), 1727–1736, 1998.

Hashimoto, S., Shiqiao, Z., Nakawo, M., Sakai, A., Ageta, Y., Ishikawa, N. and Narita, H.: Isotope studies of inner snow layers in a temperate region, Hydrol. Process., 16(11), 2209–2220, doi:10.1002/hyp.1151, 2002.

Herrmann, A., Lehrer, M. and Stichler, W.: Isotope input into runoff systems from melting snow covers, Nord. Hydrol., 12, 308–318, 1981.

Hestnes, E. and Sandersen, F.: Slushflow activity in the Rana district, North Norway, in Avalanche Formation, Movement and Effect (Proceedings of Davos Symposium, September 1986), pp. 317–330, IAHS Publ. 162, Davos., 1987.

Hirashima, H., Yamaguchi, S., Sato, A. and Lehning, M.: Numerical modeling of liquid water movement through layered snow based on new measurements of the water retention curve, Cold Reg. Sci. Technol., 64(2), 94–103, doi:10.1016/j.coldregions.2010.09.003, 2010.

Hirashima, H., Yamaguchi, S. and Katsushima, T.: A multi-dimensional water transport model to reproduce the preferential flow in a snowpack, Cold Reg. Sci. Technol., 108, 31–37, doi:10.1016/j.coldregions.2014.09.004, 2014.

HND Bayern: Gewässerkundlicher Monatsbericht Januar 2011 - Hochwasser (in German), report, Available online at: (http://www.hnd.bayern.de/ereignisse/monatsberichte/md_fghw_0111.pdf), Accessed 17.10.2014. [online] Available from: http://www.hnd.bayern.de/ereignisse/monatsberichte/md_fghw_0111.pdf, 2011.

Jones, E. B., Rango, A. and Howell, S. M.: Snowpack Liquid Water Determinations Using Freezing Calorimetry, Nord. Hydrol., 14(3), 113–126, doi:10.2166/nh.1983.010, 1983.

Jordan, P.: Meltwater movement in a deep snowpack: 1. Field observations, Water Resour. Res., 19(4), 971–978, doi:10.1029/WR019i004p00971, 1983.

Jordan, R.: A One-Dimensional Temperature Model for a Snow Cover: Technical Documentation for SNTHERM.89, U.S.Army Corps Eng. Cold Reg. Res. Eng. Lab., (Special Report 91-16), 49, doi:No. CRREL-SR-91-16, 1991.

Jordan, R.: Effects of capillary discontinuities on water flow and water retention in layered snowcovers, Def. Sci. J., 45(2), 79–91 [online] Available from: http://scholar.google.com/scholar?hl=en&btnG=Search&q=intitle:Effects+of+capillary+discontinuities+on+water+flow+and+water+retention+in+layered+snowcovers#0, 1995.

Katsushima, T., Yamaguchi, S., Kumakura, T. and Sato, A.: Experimental analysis of preferential flow in dry snowpack, Cold Reg. Sci. Technol., 85, 206–216, doi:10.1016/j.coldregions.2012.09.012, 2013.

Kattelmann, R.: Some measurements of water movement and storage in snow, in Avalanche Formation, Movement and Effects, pp. 245–254, IAHS Publ. 162, Davos., 1987a.

Kattelmann, R.: Water release from a forested snowpack during rainfall, in Forest Hydrology and Watershed Management, vol. 167, pp. 265–272, IAHS-AISH Publ. 167, Vancouver., 1987b.

Kattelmann, R.: Flooding from rain-on-snow events in the Sierra Nevada, in Water-Caused Natural Disasters, their Abatement and Control (Proceedings of the Anaheim Conference, California, June 1996), pp. 59–65, IAHS Publ. 239, Anaheim, California., 1997.

Kociánová, M. and Štursová, H.: Phenomena connected with thawing of snow cover in tundra zone in the Krkonoše Mts . (in Czech), Opera Corcon., 45, 13–34, 2008.

Kuroiwa, D.: Liquid permeability of snow, in General Assembly, pp. 380–391, International Association of Hydrological Sciences Publication. Vol. 79, Bern., 1968.

Laudon, H., Seibert, J., Köhler, S. and Bishop, K.: Hydrological flow paths during snowmelt: Congruence between hydrometric measurements and oxygen 18 in meltwater, soil water, and runoff, Water Resour. Res., 40(3), n/a--n/a, doi:10.1029/2003WR002455, 2004.

Lee, J., Feng, X., Posmentier, E. S., Faiia, A. M., Osterhuber, R. and Kirchner, J. W.: Modeling of solute transport in snow using conservative tracers and artificial rain-on-snow experiments, Water Resour. Res., 44(2), 1–12, doi:10.1029/2006WR005477, 2008.

Lee, J., Feng, X., Faiia, A. M., Posmentier, E. S., Kirchner, J. W., Osterhuber, R. and Taylor, S.: Isotopic evolution of a seasonal snowcover and its melt by isotopic exchange between liquid water and ice, Chem. Geol., 270(1–4), 126–134, doi:10.1016/j.chemgeo.2009.11.011, 2010a.

Lee, J., Feng, X., Faiia, A., Posmentier, E., Osterhuber, R. and Kirchner, J.: Isotopic evolution of snowmelt: A new model incorporating mobile and immobile water, Water Resour. Res., 46(11), 1–12, doi:10.1029/2009WR008306, 2010b.

Lehning, M., Bartelt, P., Brown, B., Russi, T., Stockli, U. and Zimmerli, M.: SNOWPACK model calculations for avalanche warning based upon a new network of weather and snow stations, Cold Reg. Sci. Technol., 30(February 1998), 145–157, 1999.

Levia, D. F. and Leathers, D. J.: Rain-induced Snowmelt, in Encyclopedia of Snow, Ice and Glaciers, edited by V. P. Singh, P. Singh, and U. K. Haritashia, pp. 915–917, Springer, Dordrecht., 2011.

MacLean, R. A., English, M. C. and Schiff, S. L.: Hydrological and hydrochemical response of a small Canadian Shield catchment to late winter rain-on-snow events, Hydrol. Process., 9(April), 845–863, doi:10.1002/hyp.3360090803, 1995.

Marshall, H. P., Conway, H. and Rasmussen, L. A.: Snow densification during rain, Cold Reg. Sci. Technol., 30(1–3), 35–41, doi:http://dx.doi.org/10.1016/S0165-232X(99)00011-7, 1999.

McCabe, G. J., Hay, L. E. and Clark, M. P.: Rain-on-Snow Events in the Western United States, Bull. Am. Meteorol. Soc., 88(3), 319–328, doi:10.1175/BAMS-88-3-319, 2007.

McClung, D. and Schaerer, P.: The Avalanche Handbook, 3rd ed., edited by U. C. Holster, Cordee, Seattle., 2006.

McDonnell, J. J., Bonell, M., Stewart, M. K. and Pearce, A. J.: Deuterium variations in storm rainfall: implications for stream hydrograph separation, Water Resour. Res., 26, 455–458, 1990.

Nobles, H. L.: Slush avalanches in northern Greenland and the classification of rapid mass movements, Int. Assocciation Sci. Hydrol., 69, 267–272, 1966.

Pomeroy, J., Fang, X. and Marks, D. G.: The cold rain-on-snow event of June 2013 in the Canadian Rockies - characteristics and diagnosis, Hydrol. Process., 30(17), 2899–2914, doi:10.1002/hyp.10905, 2016.

Qu, S., Liu, H., Cui, Y. and Shi, P.: Test of newly developed conceptual hydrological model for simulation of rain-on-snow events in forested watershed, Water Sci. Eng., 6(20090094120008), 31–43, doi:10.3882/j.issn.1674-2370.2013.01.003, 2013.

Rice, K. C. and Hornberger, G. M.: Comparison of hydrochemical tracers to estimate source contributions to peak flow in a small, forested, headwater catchment, Water Resour. Res., 34(7), 1755–1766, doi:10.1029/98WR00917, 1998.

Rössler, O., Froidevaux, P., Börst, U., Rickli, R., Martius, O. and Weingartner, R.: Retrospective analysis of a nonforecasted rain-on-snow flood in the Alps-A matter of model limitations or unpredictable nature?, Hydrol. Earth Syst. Sci., 18(6), 2265–2285, doi:10.5194/hess-18-2265-2014, 2014.

Safeeq, M., Shukla, S., Arismendi, I., Grant, G. E., Lewis, S. L. and Nolin, A.: Influence of winter season climate variability on snow???precipitation ratio in the western United States, Int. J. Climatol., 36(9), 3175–3190, doi:10.1002/joc.4545, 2016.

Shimizu, H.: Air permeability of deposited snow, Low Temp. Sci. Ser. A, 22, 1–32, 1970.

Sihvola, A. and Tiuri, M.: Sihvola_1986_SnowFork for field determination of the density and wetness profiles of a snow pack.pdf, IEEE Trans. Geosci. Remote Sens., GE-24, 1986.

Singh, P. and Singh, V. P.: Snow and Glacier Hydrology, 1st ed., edited by V. P. Singh, Kluwer Academic Publishers, Boston., 2001.

Singh, V. P., Spitzbart, G., Hübl, H. and Weinmeister, H. W.: Hydrological response of snowpack under rain-on-snow events: a field study, J. Hydrol., 202(1–4), 1–20, doi:10.1016/S0022-1694(97)00004-8, 1997.

Spusta, V. and Kociánová, M.: Lavinový katastr české části Krkonoš v období 1961/62 – 1997/98, Opera Corcon., 35, 3–205, 1998.

Suecker, J. K., Ryan, J. N., Kendall, C. and Jarrett, R. D.: Determination of hydrologic pathways during snowmelt for alpine/subalpine basins, Rocky Mountain National Park, Colorado, Water Resour. Res., 36(1), 63–75, doi:10.1029/1999WR900296, 2000.

Sui, J. and Koehler, G.: Rain-on-snow induced flood events in Southern Germany, J. Hydrol., 252, 205–220, doi:10.1016/S0022-1694(01)00460-7, 2001.

Taylor, S., Feng, X., Kirchner, J. W., Osterhuber, R., Klaue, B. and Renshaw, C. E.: Isotopic evolution of a seasonal snowpack and its melt, Water Resour., 37(3), 759–769, doi:10.1029/2000WR900341, 2001.

Taylor, S., Feng, X., Williams, M. and McNamara, J.: How isotopic fractionation of snowmelt affects hydrograph separation, Hydrol. Process., 16(18), 3683–3690, doi:10.1002/hyp.1232, 2002.

Techel, F. and Pielmeier, C.: Point observations of liquid water content in wet snow – investigating methodical, spatial and temporal aspects, Cryosph., 5(1), 1–11, doi:10.5194/tc-5-1-2011, 2011.

Techel, F., Pielmeier, C. and Schneebeli, M.: The first wetting of snow: micro-structural hardness measurements using a snow micro penetrometer, in International Snow Science Workshop, vol. 1, pp. 1019–1026, Whistler., 2008.

Techel, F., Pielmeier, C. and Schneebeli, M.: Microstructural resistance of snow following first wetting, Cold Reg. Sci. Technol., 65(3), 382–391, doi:10.1016/j.coldregions.2010.12.006, 2011.

Tomasson, G. G. and Hestnes, E.: Slushflow hazard and mitigation in Vestubyggd, Northwest Iceland, Nord. Hydrol., 31(4/5), 399–410, 2000.

Uhlenbrook, S. and Hoeg, S.: Quantifying uncertainties in tracer-based hydrograph separations: a case study for two-, three- and five-component hydrograph separations in a mountainous catchment, Hydrol. Process., 17(2), 431–453, doi:10.1002/hyp.1134, 2003.

Unnikrishna, P. V., McDonnell, J. J. and Kendall, C.: Isotope variations in a Sierra Nevada snowpack and their relation to meltwater, J. Hydrol., 260, 38–57, doi:10.1016/S0022-1694(01)00596-0, 2002.

Waldner, P. a.: Water and Solute Release from a Subalpine Snow Cover, Swiss federal institute of technology Zürich., 2002.

Waldner, P. a., Schneebeli, M., Schultze-Zimmermann, U. and Flühler, H.: Effect of snow structure on water flow and solute transport, Hydrol. Process., 18, 1271–1290, doi:10.1002/hyp.1401, 2004.

Walter, M. T., Brooks, E. S., McCool, D. K., King, L. G., Molnau, M. and Boll, J.: Process-based snowmelt modeling: does it require more input data than temperature-index modeling?, J. Hydrol., 300,

65–75, doi:10.1016/j.jhydrol.2004.05.002, 2005.

Wever, N., Jonas, T., Fierz, C. and Lehning, M.: Model simulations of the modulating effect of the snow cover in a rain on snow event, Hydrol. Earth Syst. Sci. Discuss., 11(5), 4971–5005, doi:10.5194/hessd-11-4971-2014, 2014a.

Wever, N., Fierz, C., Mitterer, C., Hirashima, H. and Lehning, M.: Solving Richards Equation for snow improves snowpack meltwater runoff estimations in detailed multi-layer snowpack model, Cryosphere, 8(1), 257–274, doi:10.5194/tc-8-257-2014, 2014b.

Wever, N., Würzer, S., Fierz, C. and Lehning, M.: Simulating ice layer formation under the presence of preferential flow in layered snowpacks, Cryosph. Discuss., 3(August), 1–24, doi:10.5194/tc-2016-185, 2016.

Würzer, S., Jonas, T., Wever, N. and Lehning, M.: Influence of Initial Snowpack Properties on Runoff Formation during Rain-on-Snow Events, J. Hydrometeorol., 1801–1815, doi:10.1175/JHM-D-15-0181.1, 2016.

Ye, H., Yang, D. and Robinson, D.: Winter rain on snow and its association with air temperature in northern Eurasia, Hydrol. Process., 2736(June), 2728–2736, doi:10.1002/hyp, 2008.